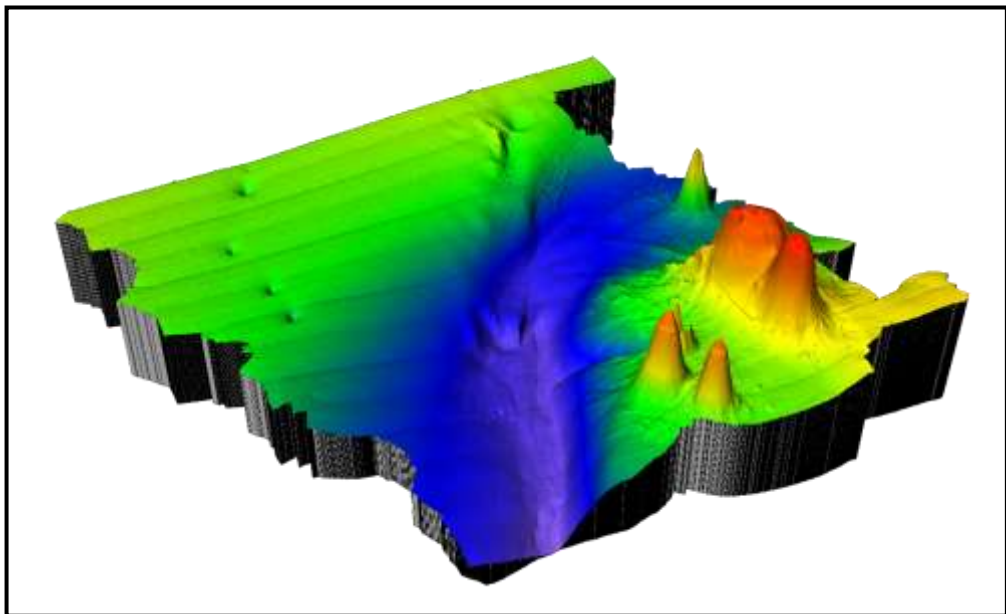




UNIVERSITY OF PALERMO
Department of Earth and Marine Sciences (DiSTeM)
Ph.D. in Earth and Marine Sciences

**NEOTECTONIC ACTIVITY AND EMISSION OF FLUIDS IN THE
NORTHWEST SICILY CHANNEL**

Scientific Sector Geo/02



Ph.D. Candidate **Spatola Daniele**

COORDINATOR of Ph.D.

Prof Alessandro Aiuppa

SUPERVISORS

Prof Attilio Sulli

Dr Aaron Micallef

XXIX CICLO
A.A. 2014-2016

NEOTECTONIC ACTIVITY AND EMISSION OF FLUIDS IN
THE NORTHWEST SICILY CHANNEL

DOTTORATO



Ph.D. thesis in Earth and Marine Sciences

Department of Earth and Marine Sciences

University of Palermo

Italy

SUPERVISORS

Prof Attilio Sulli, Department of Earth and Marine Sciences, University of Palermo, Italy

Dr Aaron Micallef, Department of Geoscience, University of Malta, Msida, Malta

REVIEWERS

Dr Alessandra Savini, Department of Earth and Environmental Sciences, University of Milano-Bicocca Milano, Italy

Dr Claudio Lo Iacono, National Oceanography Centre, Southampton, United Kingdom

LIST OF CONTENTS

<i>ACKNOWLEDGMENTS</i>	<i>1</i>
<i>ABSTRACT</i>	<i>2</i>
<i>RIASSUNTO</i>	<i>6</i>
<i>COLLABORATION AND PROPERTY DATA</i>	<i>10</i>
<i>TALK AND POSTER PRESENTATIONS OF THE PRELIMINARY RESULTS AT INTERNATIONAL CONFERENCES</i>	<i>13</i>
<i>1 CHAPTER 1- INTRODUCTION TO TOPIC</i>	<i>14</i>
1.1 Specific motivation and aims of the project	14
1.2 Seafloor fluid and gas seepage	16
1.3 Methane seafloor seepage	19
1.4 Fluid escape structures	20
1.4.1 Pockmarks	22
1.4.2 Mud Volcanoes	29
1.5 Gas hydrates	32
1.6 Submarine landslide and sediment mass movements	35
<i>2 CHAPTER 2 - REGIONAL SETTING OF THE STUDY AREA</i>	<i>39</i>
2.1 Geographic and Geomorphological setting	39
2.2 Geological Setting	43
2.3 Stratigraphy	46
2.4 Volcanism	49
2.5 Seismicity	52
2.6 Oceanographic setting	54

3	CHAPTER 3 - DATA AND METHODS	57
3.1	Multibeam Data	57
1	Acquisition	60
2	Processing	63
3.2	Chirp Data	65
1	Acquisition	65
2	Processing	66
3.3	Multichannel Seismic profiles	68
4	CHAPTER 4 - THESIS OUTLINE	71
	4.1 Geomorphology of the volcanic sector around the Graham Bank (Sicily Channel, central Mediterranean Sea)	
	Abstract	72
1.	Introduction	73
2.	Geological Setting	75
3.	Materials and Methods	78
4.	Results	79
	4.1 Geomorphological characterisation	79
	4.1.1 Western sector	80
	4.1.2 Central sector	81
	4.1.3 Eastern sector	81
	4.2 Seismic characteristics	89
5.	Discussion and Conclusions	91
	5.1 Tectonic control	91
	5.2 Morphological interpretation of the seamounts	92

4.2 Fluid Escape Structures in the Graham Bank (Sicily Channel, central Mediterranean) triggered by volcanism and tectonics

Abstract	96
1. Introduction	97
2. Geological Setting	101
3. Data and methods	104
4. Results	105
4.1 Geomorphological characterisation	105
4.2 Seismostratigraphic analysis	113
4.2.1 High-resolution data	113
4.2.2 High-penetration data	117
4.3 Isopach Maps	120
5. Discussion	121
5.1 Seafloor morphology controlled by tectonic, volcanic and sedimentary processes	121
5.2 Fluid escape structures	123
5.3 Controlling factors of fluid flow	124
6. Conclusions	127

4.3 Submarine Gravity Driven Deposits in the volcanic Graham Bank (central Mediterranean Sea): an interaction among tectonic and volcanic triggering mechanisms

Abstract	128
1 Introduction	129
2 Regional Setting	132
2.1 Geological setting	132
2.2 Morphology and Oceanography	133
3 Materials and Methods	134
4 Results	135

4.1	Geomorphological outline	135
4.2	Gravity driven deposits	138
4.3	Seismostratigraphic analysis	142
4.3.1	Seismostratigraphic features of the Gravity driven deposits	144
5	Discussion	146
5.1	Types of gravity driven deposits	147
5.1.1	Soft-sediment deformation structures, SSDs	147
5.1.2	Rock Falls	148
5.1.3	Debris avalanches	148
5.2	Driving forces and trigger mechanisms	149
5.2.1	Tectonic trigger mechanisms	149
5.2.2	Volcanic trigger mechanisms	150
5.2.3	Sedimentary/oceanographic trigger mechanisms	151
6	Conclusions	151
5	<i>CHAPTER 5 – SYNTHESIS AND CONCLUSIONS</i>	<i>153</i>
	REFERENCES	158
	ATTACHMENT	181

ACKNOWLEDGEMENTS

First and foremost, I would like to thank Prof Attilio Sulli for giving me the opportunity to work on this diverse and wonderful topic.

I sincerely thank Prof A. Sulli and Dr A. Micallef, my supervisors, for their very useful and indispensable suggestions, which have improved all my studies and research for my Ph.D. Their very important advice and ideas helped me greatly in getting to grips with the complex scientific issue and the large amount of data available. Thanks to them, I had several opportunities to work on the scientific marine geology field participating in different oceanographic cruises. This helped me to develop my expertise with acoustic and seismic methods. It has been a great experience to know and to work with people of different countries and in different working groups facing the same challenges in their projects. It has been an honor to be their Ph.D. student.

I thank Dr Alessandra Savini and Dr Claudio Lo Iacono for agreeing to be the reviewers of my Ph.D. thesis.

Many thanks also goes to the whole Marine Geology group of the University of Palermo, which provided a great working environment. I am grateful to Dr L. Basilone and to Prof A. Aiuppa (coordinator of Ph.D.) of the University of Palermo.

Special thanks are due to Dr P. Galea, head of the Department of Geosciences as well as the University of Malta for their skilled help during the last year of my Ph.D. studies.

I am grateful to Dr G. Basilone (IAMC of Capo Granitola); P. Guida, Master of the R/V Minerva UNO and all his crew for their help during the data acquisition and the on-board operations. The oceanographic cruise that was fundamental for this Ph.D. project was benefited from funding and ship-time through the RITMARE project (CNR Mazara del Vallo, Capo Granitola section). Thank you also for the great times we had on research cruises together.

My family, David and Daniel supported me throughout my studies and always encouraged me to pursue this project. I want to thank them for that.

ABSTRACT

The southern Sicilian coast represents an important contribution to Italian tourism, the Sicily Channel is an important communication path because at the top of its seafloor there are many pipelines, and submarine communication cables which are laid to carry signals, and which are very important to the minor islands.

In this work, we are presenting results of the detailed geomorphological and seismostratigraphic analysis based on new very high-resolution dataset (multibeam and CHIRP) acquired during the ACUSCAL 2015 Cruise. We also used low resolution bathymetric and seismic data provided from online database (ViDEPI, GEBCO, EMODnet).

This study allows us to reconstruct the tectonic volcanic mass movement and bottom current processes and to identify and map several relative geological elements (e.g. fluid escape structures, gravity driven deposits, volcanic morphologies) which were used to describe the geological setting of the study area. The latter is a small area (approx 100 km²) located in a shallow sector of the north-western Sicily Channel, at a distance of 45 km from the Sicilian coastline, where seven seamounts (M1-M7) have been identified and studied between 10 and 350 m in depth.

In the study area, the interaction of the sedimentary multilayer (e.g. Holocene sedimentary body, Messinian Evaporites) and the volcanic context (i.e. Graham Bank) with the tectonic activity (shallow and deep) creates a complex and highly geological framework hosting seafloor seepage.

The main focus is the description of the fluid escape structures suggesting a possible model for the origin of the fluid and the mechanisms by which it is transferred to the seafloor. Another important aim is the reconstruction of the relationship between the deep tectonic structures and the fluid escape structures in the north-west Sicily Channel.

Seafloor seepage is a widespread phenomenon in the global ocean forming important seafloor morphologies. It affects the global carbon cycle and provides the basis for abundant chemosynthetic organisms living in and on the seafloor.

In this Ph.D. project, detailed investigation about the geological setting of such sites and the controlling factors for spatial and temporal distribution of the fluid escape structures were indispensable to understand the “fluid flow system functions”

This work is a prime example of these interactions and their influence on seafloor seepage in the Western part of the Sicily Channel.

Many pockmarks, mounds and some active seafloor seepages (i.e. hydro acoustic anomalies) have been identified and investigated using both stratigraphic information provided by AGIP/ENI Wells in conjunction with various geophysical data primarily multibeam and Chirp and secondarily multichannel seismic profiles and low resolution bathymetric data.

The accurate bathymetric surveying by multibeam instruments allowed us to recognise several positive (mounds) and negative morphologies (pockmarks) linked at the fluid escape phenomena. The bathymetric data revealed an increase in size of the pockmarks with increasing distance to the elongated channel located in the central part of the study area and also that both pockmarks and mounds are isolated, aligned or clustered.

CHIRP profiles imaged the presence of several recent faults affecting the Holocene sedimentary body and the occurrence of hydro-acoustic anomalies in the water column, located mainly at the top of the recognised volcanoes.

The Multichannel seismic profiles that were correlated with the Agip/Eni wells, showed several acoustic anomalies (often from the Messinian Evaporites) and sub vertical normal fault systems, which affect gas migration in the sub-seafloor.

In the western part of the study area, the Messinian Evaporites rise up to the seafloor with a jagged seafloor topography of the MES deforming the complete geological succession. Additionally, the volcanic context supplies large volumes of material to the seafloor, which are distributed as seamounts. The uplift of Messinian deposits concurrently with the formation of sub vertical normal faults leads to gases/fluids migration towards the seafloor forming a field at pockmarks of different sizes. In the eastern part, the rise up of volcanic material through the sub vertical normal faults leads to gases/fluids migration towards the top of the seamounts forming vertical plumes. The first study case of this work revealed a strong tectonic control on the development and distribution of the seepage features in the study area.

The aim of the second study case of this work was the identification, description and classification of different examples of gravity driven deposits.

The recognised gravity driven deposits in the study area using CHIRP and Multibeam data are: (i) soft-sediment depositional structures (SSDSs), (ii) rock falls and (iii) large debris avalanches.

We however estimated the main pre-conditioning geomorphological factor, which could have induced sediment instability and the trigger mechanisms often linked to different geological processes.

This second study case revealed that these geomorphological structures are characterised by a genesis probably linked to elevate slopes of the seabed as well as trigger different factors.

Finally, mainly using the multibeam data and secondarily the CHIRP data, a cluster of seamounts that was recognised within the study area have been investigated and studied in detail. Their main dimensions and relative physical parameters have been measured and tabulated, allowing a morphometric and morphologic classification on the basis of their shapes.

Several restrictive criteria were applied in order to be certain of their volcanic origin (conical shape with maximum height, basal ratio, aspect ratio) obtaining finally what can be classified as volcanic seamounts. These structures are very similar to submarine volcanoes described elsewhere on the seafloor. Some show at the top plain morphologies interpreted as marine terraces, others show a typical cone shape of the volcanoes one of which is characterised by a complex shape. On the basis of their morphological features these have been subdivided into three categories.

RIASSUNTO

Le coste della Sicilia meridionali rappresentano un importante contributo per il turismo italiano. Il Canale di Sicilia è la principale via di comunicazione fra la Sicilia e le isole minori e Malta perché sul suo fondo mare nel corso degli ultimi cinquant'anni sono stati installati numerosi cavi di comunicazione sottomarini.

In questo lavoro di dottorato, stiamo presentando i risultati ottenuti dall'analisi geomorfologica e sismostratigrafica di nuovi di dati geofisici ad altissima risoluzione (multibeam e CHIRP) acquisiti durante la campagna scientifica "ACUSCAL 2015". Questo studio ha permesso di ricostruire le principali caratteristiche geologiche del settore nord occidentale del Canale di Sicilia, afferenti la tettonica, il vulcanesimo, le geomorfologia e le correnti oceanografiche al fine di identificare e mappare diversi elementi morfologici (strutture da risalita di fluidi, frane sottomarine, morfologie vulcaniche).

L'area di studio è una piccola area localizzata in un settore marino poco profondo del Canale di Sicilia nord-occidentale ad una distanza di 45 km dalla costa siciliana. Essa è estesa circa 100 km² ed è dalla presenza di sette vulcani sottomarini (denominate come M1-M7) localizzati in un range batimetrico compreso tra i 10 e 350 m.

Il fenomeno di risalita di fuori uscita di fluidi e/o gas dal fondo mare è estremamente diffuso a livello globale, esso forma importanti morfologie sottomarine, inoltre influenza il ciclo globale del carbonio e la vita la base di molti organismi chemiosintetici che vivono sia sul fondo mare o all'interno del sedimento che

Al fine di capire il regime di funzionamento dei "sistemi di risalita dei fluidi", indagini dettagliate della struttura geologica di siti da essi caratterizzati e dei fattori che regolano la distribuzione spaziale e temporale di queste strutture risultano essere indispensabili.

Nel settore NW del Canale di Sicilia l'interazione del multistrato sedimentario (ad esempio con le evaporiti del Messiniano) e del contesto vulcanico (Banco Graham) con l'attività tettonica (sia superficiale che profonda) ha generato un ambiente geologico molto complesso che ospita numerose manifestazioni di risalita di fluidi.

Questo progetto di dottorato nasce con lo scopo di studiare queste interazioni e influenza delle risalite di fluidi sul fondo marino nella parte occidentale del Canale di Sicilia.

Le evaporiti del Messiniano che a tratti risalgono fino al fondo del mare in corrispondenza dei luoghi dove la copertura Plio-Pleistocenica ha i minimi valori sono caratterizzati da una superficie del messiniano (ricostruita tramite l'analisi sismostratigrafica di profili multicanale) si presenta molto irregolare e spesso deforma profondamente la successione geologica completa.

Il contesto vulcanica invece fornisce grandi volumi di materiale sul fondo del mare, che sono palesati dalla presenza delle montagne sottomarine.

L'obiettivo principale di questo studio è stato il riconoscimento e la descrizione delle strutture da risalita di fluidi suggerendo la possibile origine degli stessi e i principali meccanismi attraverso i quali si è trasferito dei fluidi fino al fondo mare. Altro importante obiettivo è stato la ricostruzione delle principali relazioni esistenti tra le strutture tettoniche profonde con le strutture da risalita di fluidi riconosciute nel settore nord occidentale del Canale di Sicilia.

Le strutture da risalita di fluidi quali pockmark, mound e plume sono stati identificati e studiati utilizzando sia le informazioni stratigrafiche fornite dai pozzi AGIP / ENI che vari dati geofisici come dati morfobatimetrici (multibeam), Chirp e profili sismici multicanale in associazione con dati batimetrici a bassa risoluzione.

Lo studio dei dati morfobatimetrici ci ha permesso di riconoscere le diverse morfologie positive e negative quali pockmark e mound legate alle emissioni di fluidi. I profili CHIRP invece ci hanno

permesso di identificare l'insorgenza di alcune anomalie idro acustiche nella colonna d'acqua in cima dei vulcani e la presenza di numerose faglie recenti che dislocano il corpo sedimentario Olocenico. Infine i profili sismici multicanale che sono stati correlati con i pozzi Agip hanno mostrato diverse anomalie acustiche all'interno del multistrato sedimentario e numerose faglie normali sub-verticale che influenzano la migrazione del gas attraverso il multilayer sedimentario. Nella parte occidentale dell'area di studio, i depositi messiniani superficiali e la presenza di faglie sub-verticali favorisce la migrazione dei gas e/o fluidi verso fondale marino formando un'area caratterizzata da numerosi pockmark mostrandoti dimensioni diverse. Lo studio morfobatimetrico dei questi siti ha mostrato che le dimensioni dei pockmark crescono con l'aumentare della distanza dal canale a controllo tettonico situato nella parte centrale dell'area di studio. Nella parte orientale invece la risalita di materiale vulcanico attraverso lo stesso sistema di faglie sub-verticali porta con se grandi volumi di gas e/o fluidi che vengono rilasciati nella colonna d'acqua sotto forma di plume verticali in corrispondenza della sommità dei vulcani. Questa prima parte del dottorato ha mostrato come nell'area di indagine lo sviluppo e la distribuzione delle emissioni di fluidi è strettamente legato all'evoluzione strutturale dell'area evidenziando un forte controllo tettonico.

La seconda parte del lavoro ha avuto come obiettivo l'identificazione, la descrizione e la classificazione dei diversi esempi di frane sottomarine che hanno come fattore predisponente l'elevata pendenza del fondale marino e differente causa di innesco.

Queste frane sottomarine controllate dalla forza di gravità hanno portato alla formazione di diversi tipi di depositi che sono stati riconosciuti nell'area di studio. Questi sono stati suddivisi in: (i) soft-sediment depositional structures (SSDSs), (ii) rock falls and (iii) large debris avalanches.

Abbiamo valutato il principale fattore predisponente che potrebbe aver indotto l'instabilità dei sedimenti e i principali meccanismi di innesco spesso legati ai principali processi geologici che influenzano l'area di studio.

Infine, come ultimo punto di questo Ph.D., utilizzando i dati multibeam, le montagne sottomarine riconosciute all'interno dell'area di studio sono state analizzate e studiate in dettaglio attraverso un approccio morfologico-quantitativo, al fine di ricostruire la loro origine ed evoluzione. Per adempiere a questo obiettivo è stata usata una metodologie usata in altri contesti marini come esempio nelle isole Canarie.

Le principali dimensioni e altri i parametri fisici ricavati sono stati misurati, calcolati e inseriti in diverse tabelle, permettendo una loro classificazione morfometrica e morfologica basata sulla loro forma. Inoltre, per essere certi della loro origine vulcanica sono stati applicati diversi criteri restrittivi (forma conica con altezza massima, rapporto basale, aspect ratio) ottenendo infine, che possono essere senza alcun dubbio classificati come vulcani sottomarini. Queste strutture infatti sono molto simili ai principali vulcani sottomarini descritti in altri settori marini. Particolarità di alcuni di loro è che mostrano alla loro sommità delle morfologie pianeggianti con inclinazione di uno o due gradi che sono state interpretate come terrazzi marini.

COLLABORATION AND PROPERTY OF THE NEW DATA

The new and unpublished very high-resolution geophysical data used in this Ph.D. project are both CHIRP and Multibeam data that was acquired in collaboration with researchers of the CNR during the oceanographic cruise ACUSCAL 2015, performed between 18 to 28 May 2015.

The above-mentioned research project involved the definition of the biological context of the Sicily Channel. In the same project, some researchers of the marine geology group of the University of Palermo were also involved to identify and to describe the geological features of the Sicily Channel.

During the second year of this Ph.D. project, Prof Sulli A., Dr Basilone L., Dr Basilone G. and myself organised the part of the ACUSCAL 2015 cruises concerning the geological acquisition. Furthermore, in May 2015, we have been a part of the scientific crew (geology group) during the oceanographic survey ACUSCAL that was carried out on board the R/V “Minerva Uno” (Fig. 1).



Figure 1 R/V Minerva uno used for the acquisition of the new dataset consulted in this Ph.D. project.

In detail: the geological activities of this oceanographic cruise were (Fig. 2):

- Acquisition of very high-resolution multibeam data to mapping the morpho-bathymetric elements, aimed at identifying areas where there are fluid escape structures and the main active geological features of the seafloor;
- Acquisition of water column data using the Multibeam instrument (Reson 7160) to identify the seepage plumes and the possible acoustic anomalies;
- Acquisition of very high-resolution seismic data (CHIRP profiles) to reconstruct a detailed stratigraphic and structural reconstruction of the sub-seafloor (i.e. Holocene Sedimentary Body);
- Collection of samples of water or fluids and acquisition of the physical parameters of the water column using a multiparameter probe (e.g. CTD) and rosette multi-sampler and associated collection of water by Niskin bottles to obtain the vertical profiles of temperature, pH, electrical conductivity and dissolved oxygen, and a detailed geochemical characterisation of the samples;
- Measurement of the concentration of the CO₂ in the water column using the Contros Hydro C sampler to obtain the vertical profiles of CO₂ flux in the water column;
- Collection of samples of the bottom of the substrate using box corer to make a distribution sediment map.

TALK AND POSTER PRESENTATIONS OF THE PRELIMINARY RESULTS AT INTERNATIONAL CONFERENCES

During these three years of my Ph.D., course some of the preliminary results of the project were presented as talks as well as presentation of nd posters at the international congresses.

Società Geologica Italiana Assembly 2016, Napoli, Italy - Poster session:

Spatola D., et al. (2016). Fluid escape structures revealing volcanic and tectonic activity in the Graham Bank (Sicily Channel).

Spatola D., et al. (2016). Volcano and Neotectonic related slope failures in the north-western Sicily Channel (central Mediterranean Sea): Implications for understanding and assessing geohazard risk. (this was valuated to be the best poster of the session).

Società Geologica Italiana Assembly 2016, Napoli, Italia - Talk session:

Spatola D., et al. (2016). Fluid escape structures revealing volcanic and tectonic activity in the Graham Bank (Sicily Channel).

European Geosciences Union General Assembly 2016, Vienna, Austria - Poster session:

Spatola D., et al. (2016). Neotectonic and volcanic activity revealed by fluid escape structures in the Graham Bank region (Sicily Channel, central Mediterranean Sea).

European Geosciences Union General Assembly 2016, Vienna, Austria - Talk session:

Spatola D., et al. (2016). Neotectonic and volcanic activity revealed by fluid escape structures in the Graham Bank region (Sicily Channel, central Mediterranean Sea).

Chapter 1

1. INTRODUCTION TO TOPIC

1.1 SPECIFIC MOTIVATION AND AIMS OF THE PROJECT

This doctoral project focused on the use of geophysical data such as low and very high-resolution bathymetric data, in combination with CHIRP seismic data and multichannel profiles, to investigate the northwestern Sicily Channel and to elucidate the principal control drivers on the fluid escape systems characterising the submarine sector around the active volcanic area known as Graham Bank.

The study area (sector around the Graham Bank) in this Ph.D. project some times was named “Sector of Banks”. It is located in the northwestern Sicily Channel, which is characterised by a complex geological framework resulting from the tectono-sedimentary evolution of various morphological elements: the Adventure Bank, Graham Bank, Nerita Bank, Terrible Bank, Nameless Bank and numerous minor sedimentary and volcanic banks (formed by several submarine volcanoes).

The main scientific aim is to identify and to map the fluid escape structures (pockmarks and mounds) as also to infer the fluid flow systems in order to understand the role of the tectonics in the migration (rise up) mechanisms of fluids from the deeper crustal sector and the consequent spill-out from the seabed.

We used several specific objectives in this work to accomplish this goal such as:

- To define the stratigraphy and the structural mechanisms of buried geological structures in the study area.

- To identify the role of geological features, such as “active fault systems”, in regulating the fluid flow systems and the fluid escape processes.
- To describe the several fluid escape structures and to suggest a possible model for the origin of the fluid and the mechanisms by which it is transferred to the seafloor;
- To reconstruct the relationships between the deep tectonic structures and fluids escape structures in the north-west Sicily Channel.
- To propose a geological model for the northwest Sicily Channel and its key evolutionary phases during the Quaternary.
- To assess the submarine geohazard associated with these geological features.

1.2 SEAFLOOR FLUIDS AND GAS SEEPAGE

Fluid seepage is a widely recognised global phenomenon (Skarke et al. 2014) and evidence of fluid escape from the seabed into the water column are well documented in the world's oceans (Figs. 3, 4; Suess, 2010).

This geological phenomenon is characterised by two different categories of seafloor seepage such as Hot Vents and Cold Seeps, often associated with different geological contexts (Fig. 3).

- **Hot Vents** are mostly places along ocean spreading centres where fluids of high temperature escape from the seafloor. These fluids have been heated in the close vicinity of magma chambers within the spreading centres and carry a load of dissolved elements from the surrounding rocks (Edmond et al., 1982).
- **Cold Seeps** are defined as localities of low temperature fluid and gas escape from the seafloor (Talukder, 2012). They usually show a lower emission rate than Hot Vents. Low temperature seeping fluids and gases comprise groundwater, brine, fluid hydrocarbon and a range of gases such as methane, ethane and carbon dioxide.

A great portion of the fluid emitted at cold seeps consists of CO₂ or/and CH₄.

These gases are usually generated into the sedimentary basins either at shallow depths/low temperatures (microbial gas) or at greater depths/higher temperatures (thermogenic gas), reaching the seafloor via diffused or focused fluid flow systems.

Minor amounts are attributed to other hydrocarbon gases that usually occur in conjunction especially with thermogenic gases, methane (Judd and Hovland, 2007) and CO₂ (McGinnis et al., 2011) and which can be linked to the volcanic contexts and to the rise up of magma.

Fluid seepages have a great economic importance as they are often linked to the large accumulations of sub-seafloor hydrocarbon deposits and often are the main topic of the preliminary study in Oil and Gas exploration.

However, seeping fluids also have direct implications for the biosphere (e.g. growth and development of coral mounds and chemosynthetic communities), the hydrosphere (e.g. ocean acidification), and the atmosphere (e.g. contributing CH_4 and CO_2).

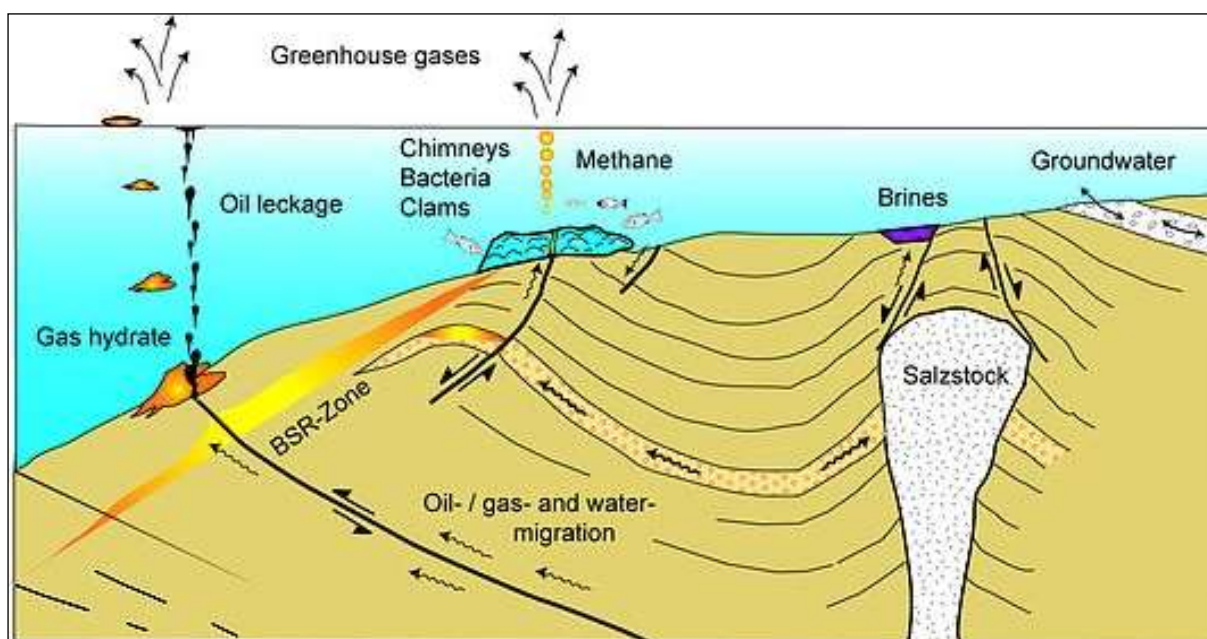


Figure 3 A diagrammatic representation of the formation of brine pools in pockmarks, mud volcanoes and carbonate chimneys through the movement of gases in the sediment. Diagram from IFM-GEOMAR

Methane is the biggest contributor to seeping gases by volume with regards to the escape of fluids or/and gases from the seafloor, (Claypool and Kvenvolden, 1983; Floodgate and Judd, 1992; Hovland et al., 1993; Judd and Hovland, 2007). Seepage of methane from continental margins into the atmosphere was recently estimated at 0.05 Gt of carbon annually, accounting for up to 5% of global methane emissions to the atmosphere (Judd et al. 2007; Reeburgh 2007; McGinnis et al. 2006).

In many petroliferous basins, such as The Gulf of Mexico (Macdonald et al., 1993; Ding et al., 2008), the North Sea as well as the Sicily Channel, fluid hydrocarbons from oil to asphalt can be observed in various forms. Small pools probably linked to the genesis or to the evolution of mega pockmarks are commonly found in the seafloor in areas of active tectonics (Charlou et al., 2003).

The Sicily Channel is a well-known fluid flow province and an important hydrocarbon region of the Mediterranean Sea.

In the eastern Sicily Channel, microbial and thermogenic fluid flow systems, and related fluid escape features (pockmarks, plumes, pipes, methane anomalies, carbonate crusts, domes and ridges (attributed to mud volcanism)) have been reported across a wide depth range. (Cangemi et al., 2010; Foglini et al., 2011; Holland et al., 2003; Holland et al., 2006; Max et al., 1993; Micallef et al., 2011; Prior, 2005; Savini et al., 2009; Taviani et al., 2013). Vulnerable marine ecosystems (e.g. *Callogorgia verticillata*) associated with gas seepage are known to occur in the same region (Savini et al., 2009).

In the western Sicily Channel, fluid flow systems and their geochemistry have only been investigated for Pantelleria Island and other small areas. An active degassing of probable mantle-derived fluids has been recognised in the thermal waters of the south-western part of Sicily along the coast of Agrigento (i.e. Sciacca area). The main hypothesis is that the degassing of fluids in this region is rooted in depth, either aligned to the main trends of fault systems or linked to the neotectonic activity. This would corroborate a tectonic control on the transfer process from the mantle towards the surface of both magmatic bodies and related degassing fluids.

1.3 METHANE SEAFLOOR SEEPAGE AND METHANE FORMATION

Methane seafloor seepage is a common type of cold seepage phenomena, which occurs on the seabed forming a great variety of structures.

These morphologies recognised at different ranges of bathymetry are mainly:

- (i) pockmarks (Hovland, 1981; Pilcher and Argent, 2007; Sahling et al., 2008),
- (ii) mud volcanoes (Milkov, 2000; Kopf, 2002; Milkov et al., 2004; Feseker et al., 2008; Wagner-Friedrichs et al., 2008; Perez-Garcia et al., 2009).

The escape of methane from the seafloor is a consistent feature throughout geological times as documented by seismic surveys (Andresen et al., 2011; Ho et al., 2012) and seepage outcrops (Campbell et al., 2002, 2006; De Boever et al., 2009).

An indispensable prerequisite for the formation of seafloor methane seepage is the presence of abundant organic matter to form methane and to facilitate its migration towards the seafloor.

Methane in marine sediments can be formed through two processes: microbially and thermogenically. Both processes lead to the alteration of buried organic matter and the formation of different hydrocarbons. The combination of: (i) thick sedimentary successions, (ii) continuous burial and (iii) pathways for the migration of the gas through various processes explains the widespread occurrence of methane seepage in this setting.

Abiogenic methane could be of volcanic or hydrothermal origin and is usually not observed on passive continental margins (e.g. Gulf of Mexico and western African margin). Gas fronts in mud-rich sediments are a result of the widespread formation of methane in the sub-seafloor for example in the Baltic Sea (Laier and Jensen, 2007). These very shallow occurrences contrast with methane formation at great depths in sedimentary basins (Judd et al., 2002; Figueiredo et al., 2010).

1.4 FLUID ESCAPE STRUCTURES

Fluid seepage can significantly shape the seafloor across continental margins, giving rise to a range of morphologies known as fluid escape structures (Fig. 4). Their main physical features are strongly dependent on the type of fluid involved and the sedimentary setting in which they occur.

The presence of fluid escape structures has been well documented in different part of the world in both active and passive continental margins (Fader, 1991; Judd and Hovland, 2007; Micallef et al., 2011; Solheim and Elverhøi, 1985).

The fluid escape phenomena characterise compressional and extensional geodynamic contexts, producing diverse positive relief (mounds and mud volcanoes) or negative relief (e.g. pockmarks) morphologies (Berndt, 2005; Brothers et al., 2013; Etiope, 2015; Judd et al., 2002; Kvenvolden and Rogers, 2005; Skarke et al., 2014).

Other indicators of gas seepage on the seafloor include focussed or diffused plumes (Sauter et al. (2006), mud and carbonate mounds (Milkov et al. 2004), carbonate crusts and slabs (Lewis and Cochrane 1990), near-seafloor gas hydrate (MacDonald et al. 1994), and chemosynthetic communities (Lewis and Cochrane 1990).

Their spatial distribution can be random, clustered or elongated parallel to geological structures (Hasiotis et al. 2002; Forwick et al. 2010).

Evidence of fluid escape structures occurs predominantly in coastal and shallow environments and may lead to the destabilization of marine slopes (e.g. Bussmann and Suess, 1998; Stegmann et al., 2011; Pennino et al. 2014), since the gases can also influence geotechnical properties of sediments as well as promote slope instability (Hovland et al. 1985, Davis, 1992).

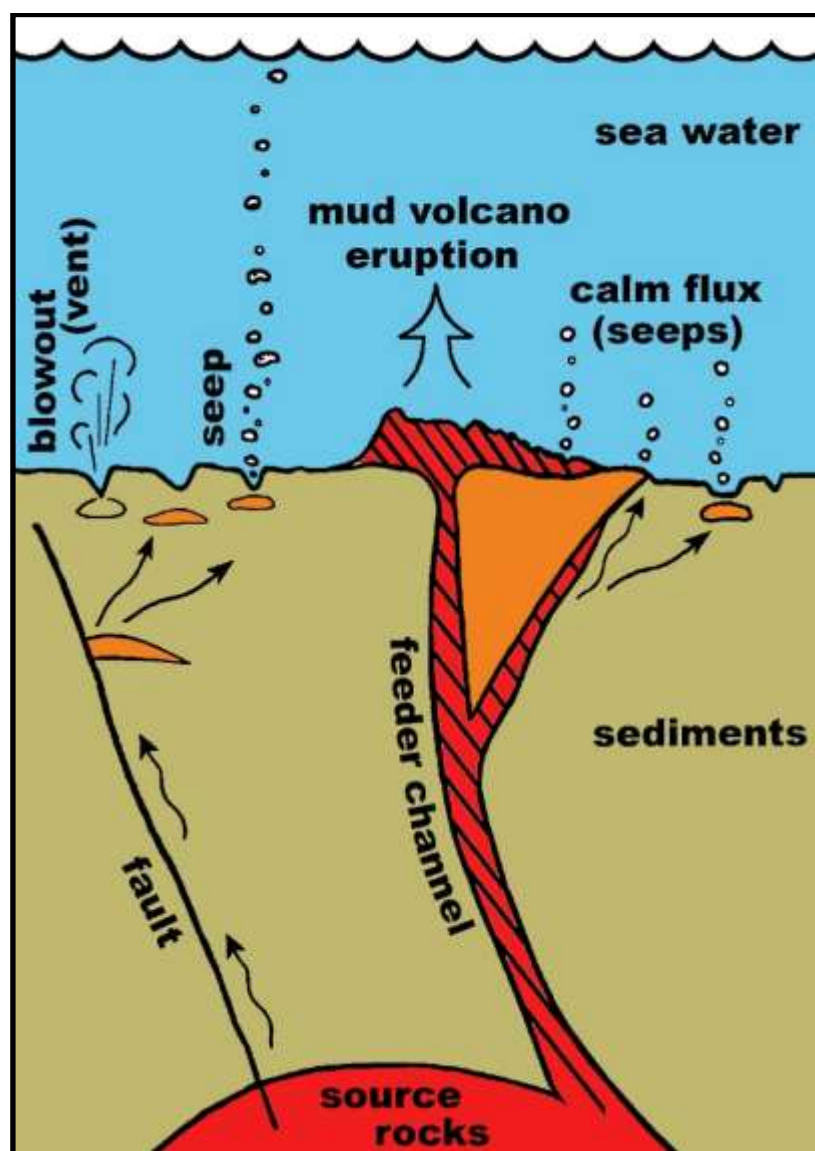


Figure 4 A sketch schematically showing the pathways for sediment degassing (modified from Dimitrov and Woodside, 2003).

1.4.1 POCKMARKS

Pockmarks are circular to elongated depressions (Figs. 5, 6), discovered in the 1960s (King et al. 1970), with steep flanks and flat to cone shaped bottoms (Solheim et al. 1985; Judd and Hovland, 2007), caused by the escape of fluids through the seabed (Judd and Hovland, 1992).

Their discovery and first study were possible thanks to the new and high resolution technology mapping of the seafloor (e.g. Side Scan sonar, Multibeam, Sub-bottom profiles and ROV).

Pockmarks have been recognised at the top of the seabed affected by fluid migration and seepage through the seafloor (King and MacLean, 1970; Hovland et al., 1985; Hovland et al. 1987; Hovland and Judd 1988). They can occur both in very shallow waters and in water depths down to 4800 m, having diameters of up to 1.5 km wide and depths of 150 m.

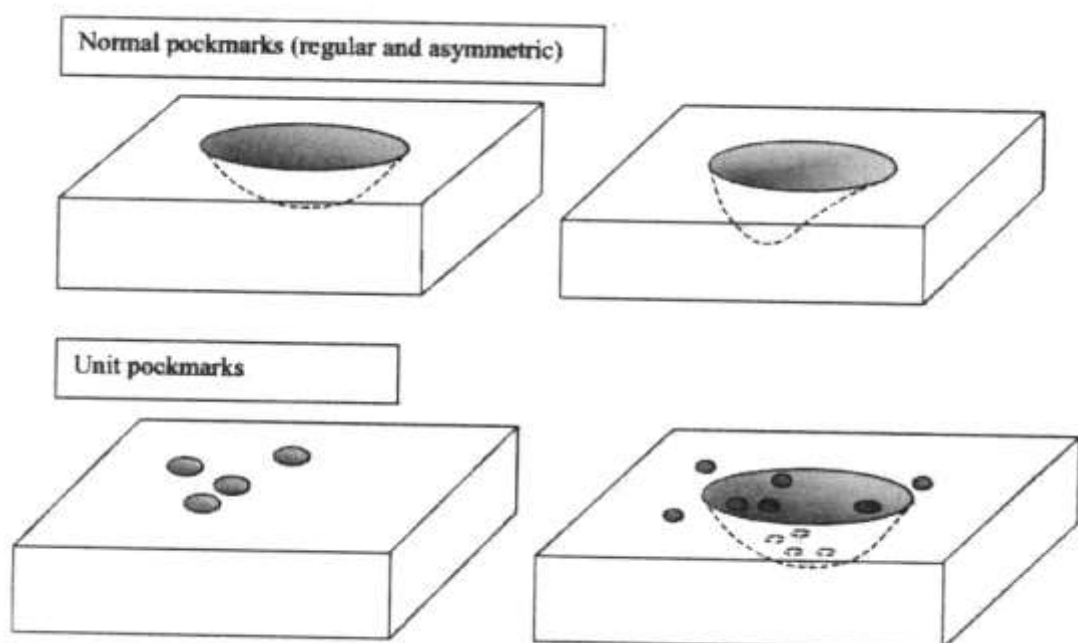


Figure 5 Illustration of the main classes of pockmarks, regular and asymmetric in shape; unit pockmarks, with and without “parental” normal pockmark (Hovland et al. 2002).

At the present time, any circular depressions (regular or asymmetric) recognised through the interpretation of the morphological and bathymetric data can be interpreted as pockmarks. Many authors use the word pockmark to describe the depressions of the seafloor characterised by a great variety of shape and size, such as axis starting from a few meters varying up to 800 meters and depths of between 0.5 m and 50 m showing different shapes (Fig. 6).

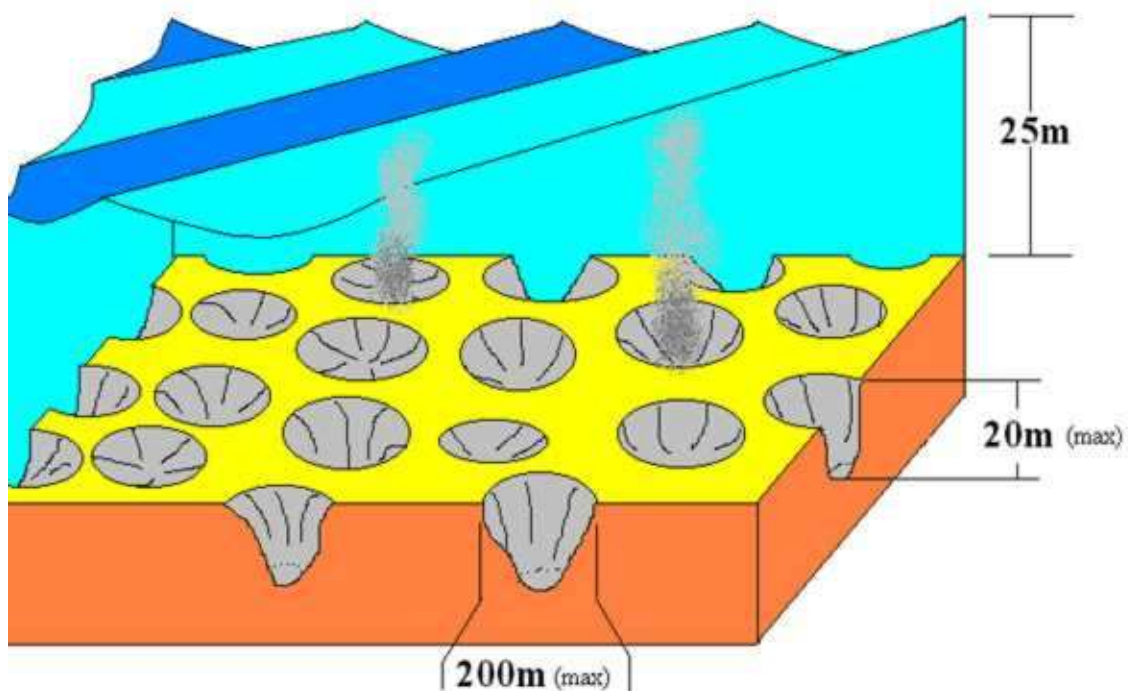


Figure 6 Schematic representation of the pockmarks field in Patras Bay (from <http://patrasoceanography.tripod.com/Gas%20in%20Marine%20Sediments.htm>).

The active seepage from pockmarks does not help the sedimentation from the water column. The infill of pockmarks by sediments is known in those cases during periods of inactive seepage.

The pockmarks, once formed, are not necessarily active but may be inactive and could be buried by rapid sedimentation associated with large quantities of gas, which may be emitted from the seafloor in relatively short periods.

Buried pockmarks are however well documented, which can be up to 4 km in diameter, which provide evidence of past fluid flow activity on palaeo-seafloors (Cartwright et al. 2011).

Pockmarks spatial distribution can be clustered - linked to underlying geological structures such as faults, folds, channels and mud diapirs (Hasiotis et al. 2002),- or random. They have been found forming aligned morphologies along the direction of system faults, which act as the preferential way for the ascent of the fluids (Fig. 7; Fader, 1991; Soter, 1999; Hovland and Judd, 1988, Etiope et al. 2008).

Futhermore, pockmarks are often located adjacent to submarine landslide scars and have been proposed as earthquake precursors (Hasiotis, T. et al.. 1996). Knowledge on the spatio-temporal behaviour of pockmarks can be crucial for the assessment of geohazards on continental slopes as well as elucidate the stress history of continental margins (Micallef et al. 2007).



Figure 7 Bathymetric data from MAREANO shows ridges and craters (green=deepest, orange=shallowest) in the Barents Sea. Thousands of pockmarks, shown as dark dots, are seabed craters formed when gas or liquid erupts and streams through the seabed surface (<https://www.ngu.no/en/topic/marine-landforms>).

Many authors proposed different mechanisms for the genesis and evolution of pockmarks such as, seepage of freshwater, venting of interstitial gas, and pore water escape during sediment compaction, sediment rafting by methane gas hydrates, and others.

The most used mechanism to describe the formation of these structures is fluids migration from the bottom, water and / or gas. The rise of a gas column in the sub-seafloor is expected to lead to the liquefaction of sediment (Cathles et al., 2010). The invasion of pressurized gas into an overlying seal can already destabilize the sediment cohesion at the surface if the gas chimney reaches halfway from the gas reservoir to the surface (Cathles et al., 2010; Fig. 8).

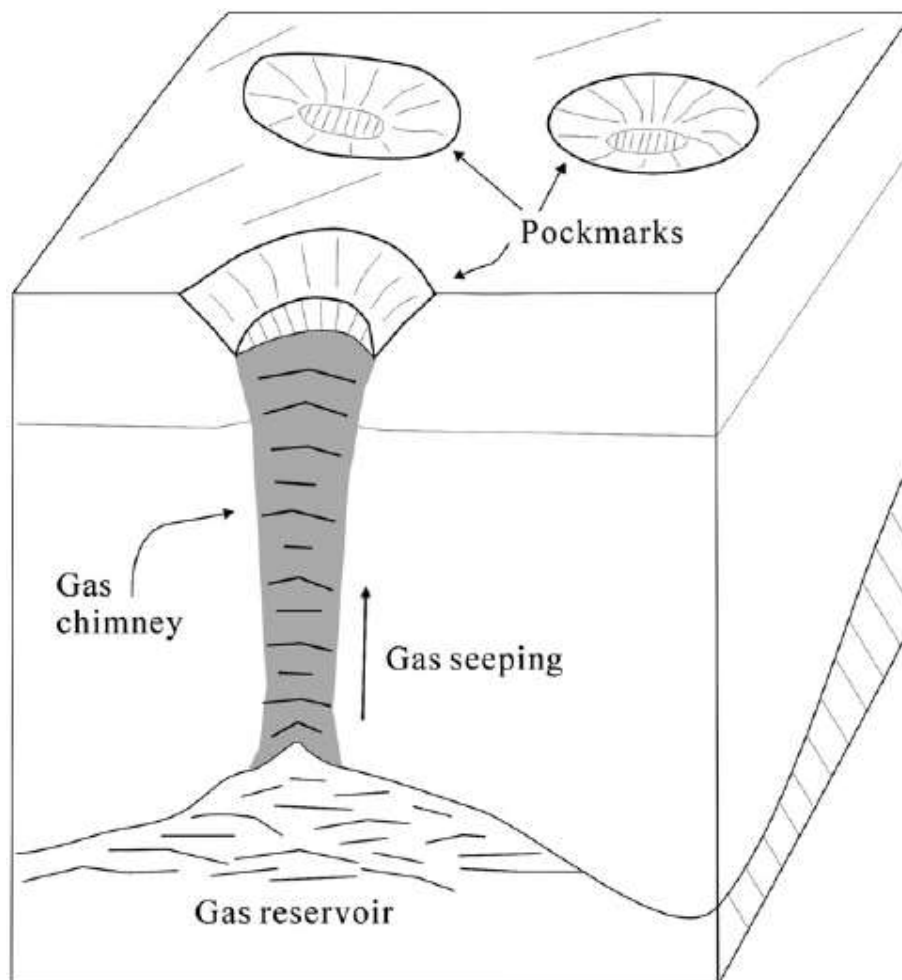


Figure 8 Pockmarks are frequently located atop gas chimneys. Slow, continued gas leakage through the chimneys sustains vent communities, which produce carbonate mounds in the pockmarks. Figure modified from Hovland (1989).

The most popular model based on laboratory experiments, theoretical models and detailed field studies of active and fossil pockmarks, proposes that pockmarks form abruptly when pockets of local over-pressured gas erupts through the seafloor sediments, where they are maintained by sustained gas seepage and bottom current activity that prevent fine-grained particles from settling.

The study of pockmarks and relative fluids is very complicated because the presence of gas within the sediments is often deduced through the recognition of areas acoustically turbid (Schubel 1974) or associated with the wipe-out zone on high-resolution seismic profiles (Hovland, 1991; Hovland et al 1984, 1987; Solheim and Elverhoi 1993; Kelley et al 1994) (Fig. 9).

In the seismic reflection profiles, pockmarks often exhibit evidence of truncated reflectors showing sectional reflectors (at high amplitude) with the typical V shape, which are maintained in depth of up to 300-400 m (about 500 ms, TWTT) and a good lateral continuity. However, the seismic investigations (in particular high-resolution) of areas at pockmarks show the occurrence of a wide abundance of buried pockmarks, illustrating continued and alternated seepage activity (Andresen et al., 2011; Ho et al., 2012).

In some works, the pockmarks are identified and described as structures associated with interstitial gas (methane), which was directly collected in the sediments (Whiticar and Werner 1981).

The presence of free gas within sediments produces a strong impedance contrast, which makes a seismic unit characterised by a transparent seismic facies delimited by very high amplitude horizon bottom-simulating reflection (BSR).

Volumes of free gas below the BSR are assumed to be most influential in the formation of BSRs (MacKay et al., 1994; Haacke et al., 2007). The BSR was often detected in sites where there are pockmarks associated with an acoustic backscatter in the water column above (Hovland and

Judd 1988; Kelley et al 1994; Paull et al 1995), which is often interpreted as a plume from the seabed (Sauter et al 2006).

The bottom-simulating reflector (BSR) is also produced by the negative impedance contrast between gas hydrate filled pore space above and gas filled pore space below the bottom of the Gas hydrates (Figs. 11, 12).

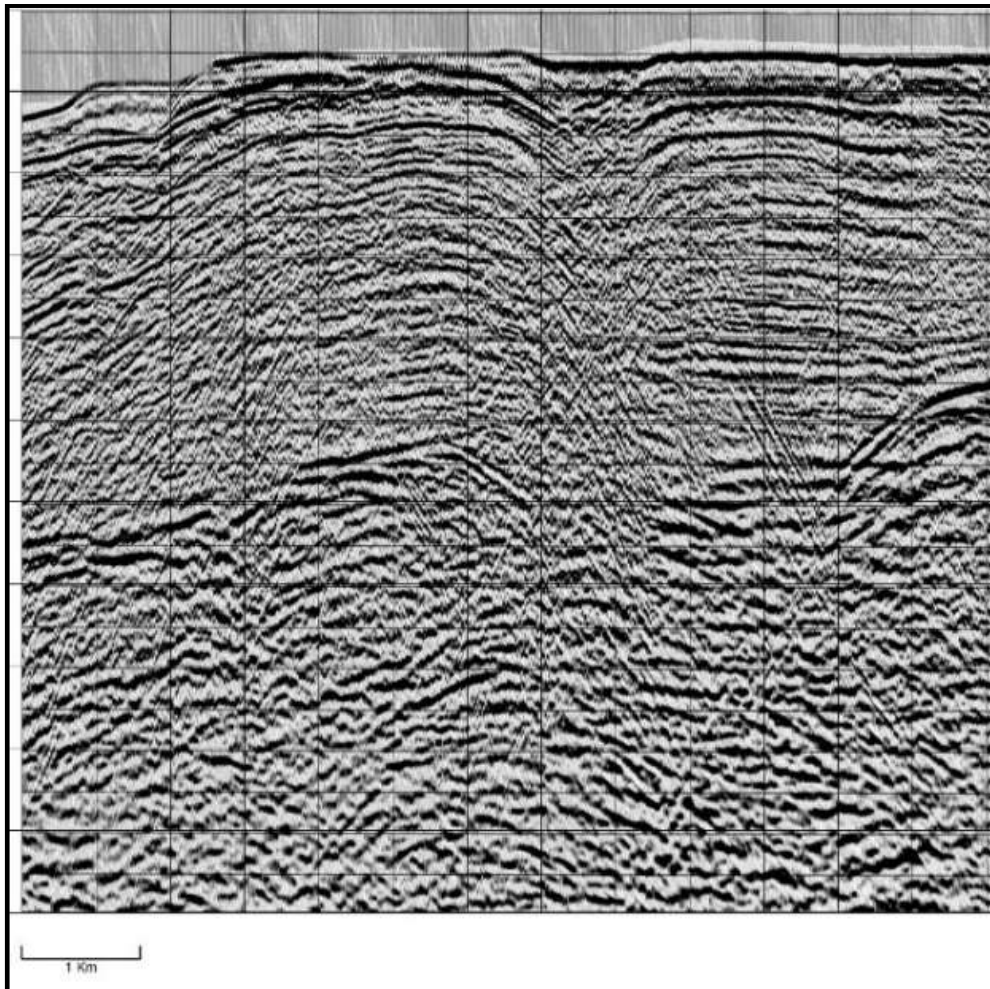


Figure 9 Detail of a multichannel seismic profile (from ViDEPI) acquired in the Sicily Channel showing a big pockmark with above an acoustic anomaly.

Seepage of ancient hydrocarbon gases is also recognised as a significant natural source of methane and global climate change in the past (Kennett, J.P. and Stott, L.D., 1990). Pockmarks comprise key evidence of such releases (Judd et al. 2002). Understanding the temporal dynamics

of pockmark formation is thus fundamental to an accurate reconstruction of past and future climate changes (Dickens 2003).

Pockmarks also affect the ecology characterising a dense accumulations of chemosynthetic-based and microbial benthic communities of the seabed, sustaining unique oasis-type ecosystems (Kennett, J.P. and Stott, L.D., 1990).

Apart from showing high biomass and productivity, these little studied communities play an important role in controlling greenhouse gases, which may be key breeding grounds for fish populations (Sibeut et al. 2003). Pockmarks do not only increase habitat structure and complexity, but they may also provide refuges from trawling activity and other anthropogenic disturbances.

Pockmarks can form in any marine or lake environment, if the sediments are suitable for their formation (Hovland & Judd, 1988).

They are documented in different marine contexts including the oil-rich regions (Hovland et al. 1984; Rise et al., 1999, Micallef et al., 2011), regions with shallower crystalline basement (Papatheodorou et al. 2001), estuaries and coastal areas (Hill et al. 1992; Garcia-Garcia et al.1999), lakes and sectors with hydrothermal activity (Pickrill 1993).

Several fields of pockmarks have been recognised in most of the Mediterranean Sea. The most important examples are across the offshore of Greece, in all the Tyrrhenian Sea (Pennino et al., 2014 and references therein) as well as in the Sicily Channel, in particular near the Iblean Maltese Plateau (Savini et al., 2009; Micallef et al. 2011).

1.4.2 MUD VOLCANOES

The mud volcanoes are positive dome-shaped seafloor structures extremely variable in size, ranging up to 4 km in diameter, and 500 m in height (e.g. Henry et al.,1990; Le Pichon et al.,1990; Kopf, 2002; Hovland et al., 2005, Savini et al. 2009). They have generally been described in the literature as “mud-cones”, “mud lumps”, “outcrop or cratered mounds”, “mud diapirs”, “mud pies”. These are recognised in the entire world and in different sedimentary contexts at all water depths (Fig. 10).

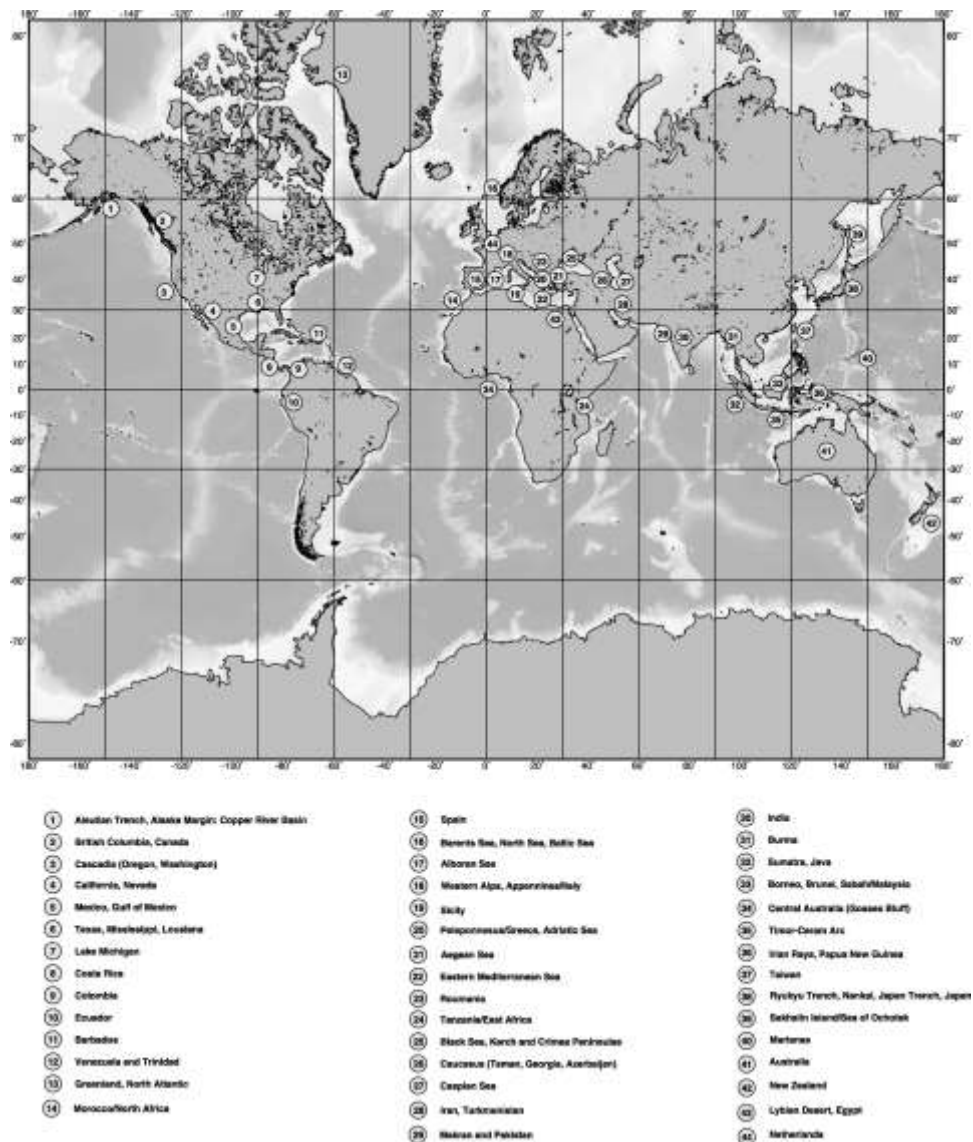


Figure 10 Location map of the main mud volcanoes on Earth (Kopf et al. 2002).

Mud volcanoes are mainly described as episodic expulsions, both in submarine or subaerial environments of a mixture of water, gas and solid products from deeper parts of the sedimentary cover (Guliev, 1992). The material that is emitted is referred to as "Mud Breccia" and is mainly responsible for the shapes of the mud volcanoes which are characterised by circular or elongated positive seafloor relieves of different sizes (Milkov, 2000; Dimitrov, 2002; Kopf, 2002).

Mud Volcano features (e.g. height and areal limits) are linked to the physical properties of the material erupted and also to the environment where the rash occurs.

In other words, the mud volcanoes are extrusion points showing positive topography at the seafloor (Milkov, 2000; Kopf, 2002), which periodically and continuously emit a mix consisting mainly of mud and other sedimentary components associated with gas, water or oil. In Holland et al. (2003), the gas was reported to vent from most of the structures, and subsequently in Holland et al. (2006), the authors documented important methane anomalies in seawater with concentrations above 200 nmol/l.

Mud volcanoes generally occur in areas where there are thick sedimentary sequences with soft and fine-grained sediments at great depths where the sediments are moved upwards together with ascending gas and are expelled at the seafloor (Judd and Hovland, 2007; Talukder, 2012).

In the last years, through high resolution morpho-bathymetric data, the presence of mud volcanism has been well documented in many parts of the world.

Examples of such features are the Håkon Mosby mud volcano in the SW Barents Sea (Milkov et al., 2004; Feseker et al., 2008; Perez-Garcia et al., 2009) and the mud volcanoes of the Black Sea (Wagner-Friedrichs et al., 2008).

The occurrence of deep submarine mud volcanoes have been well documented to exist in many parts of the Mediterranean Sea (Camerlenghi and Pini, 2009), in the eastern Mediterranean

ridge (Cita et al., 1996), in the Alboran Sea (Sautkin et al., 2003) and in the Ionian Sea (Ceramicola et al., 2007). Shallow mud volcanoes were reported in the central Mediterranean and in particular along the continental shelf of the Iblean-Maltese Plateau (Holland et al., 2003, Savini et al. 2009).

1.5 GAS HYDRATES

A type of fluid escape structure linked to the instability of the Gas Hydrates (Fig. 11) is called a gas hydrate mound (MacDonald et al., 2003; Van Dover et al., 2003).

Gas hydrates are natural solid compounds (mainly clathrates) composed of water and natural gases (often methane) with low weight molecular “Gas Hydrates” which can be formed in environments characterised by low temperature, high pressure and sufficient concentration of gas.



Figure 11 Example of Natural Gas Hydrates collected in Indian Ocean (<http://science.howstuffworks.com/environmental/energy/natural-gas-hydrates.htm>).

Gas hydrates are made up of a rigid crystal lattice of water cages with atoms of gases. They are essentially water clathrates of natural gas where water crystallizes in the isometric crystallographic system and held together by weak van der Waals (Kvenvolden, 1993).

During the 1950s many chemical and geochemical studies were carried out regarding the crystallographic interpretation of these hydrates which led to the determination of the sI and sII structure (Sloan, 2003), while the hexagonal structure, sH, was successively discovered by Ripmeester et al. (1987). All the above-mentioned structures differ in the number and size of cavities as well as their unit cell. Gas hydrates consists of about 85% water on a molecular basis and the number of guest molecules can be trapped within the cavities depending on the structure lattice.

The presence of small amounts of gas hydrates in sediments is not easily recognisable using seismic data, while large volume of them are very clearly identifiable in the seismic data since their presence alters the geophysical properties of the marine sediments. Gas hydrates are generally recognised on the basis of a particular seismic reflector named “Bottom Simulating Reflectors” in deep ocean contexts (BSR; Lu and McMehan, 2002).

Lu and McMehan (2002) described the BSR as a negative strong reflection, which is approximately parallel to the sea-floor reflection and is thought to mark the base of gas hydrate stability zone (Fig. 12). This acoustic impedance contrast creates a reflector with high amplitude that cuts across the bedding plan. The acoustic velocity of the area above the BSR contrasts well with the BSR itself due to an increase in sediment velocity because the presence of free gas below the stability zone of the gas hydrates influences the physical characteristics of the sediment.

The mapping of the gas-hydrate associated BSR has been a favourite method of gas hydrate exploration in the past as well as up to the present day. The BSR is easily recognisable because it is parallel to the seabed (Thakur and Rajput, 2011) and this makes it easier to recognise the free gas within the sediments.

Gas hydrates have been documented in places where bottom simulating reflectors (BSRs) are absent (Wood and Ruppel, 2000). While the identification of a BSR does not necessarily lead to the discovery of gas hydrates (CSIRO, Sydney Basin Technical Report 2009).

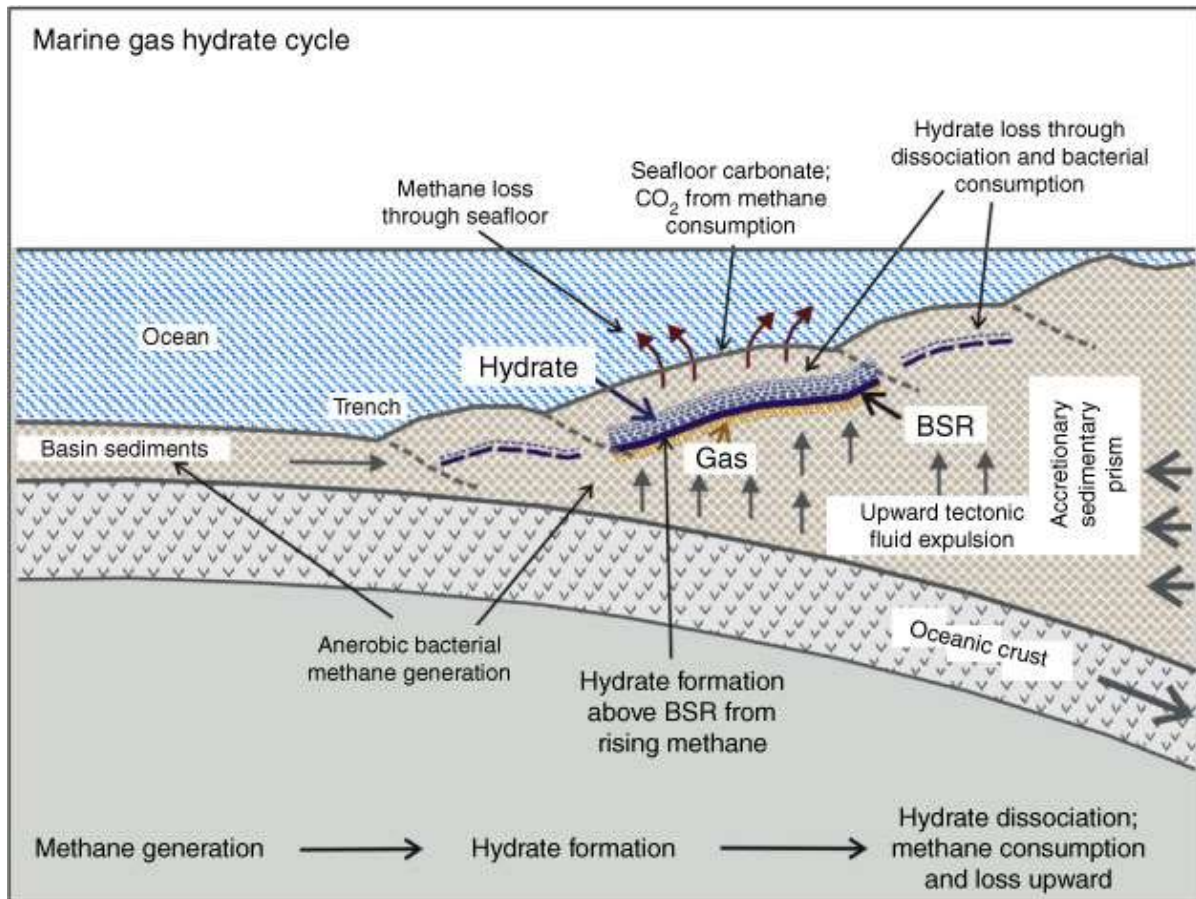


Figure 12 Marine gas hydrate cycle (after Hyndman and Davis, 1992). BSR = bottom-simulating reflector.

1.6 SUBMARINE MASS MOVEMENTS

Mass movements indicate all the phenomena of falling material (e.g. rocks, debris or mud) controlled by the force of gravity (Fig. 13; Varnes, 1958; Skempton & Hutchinson, 1969).

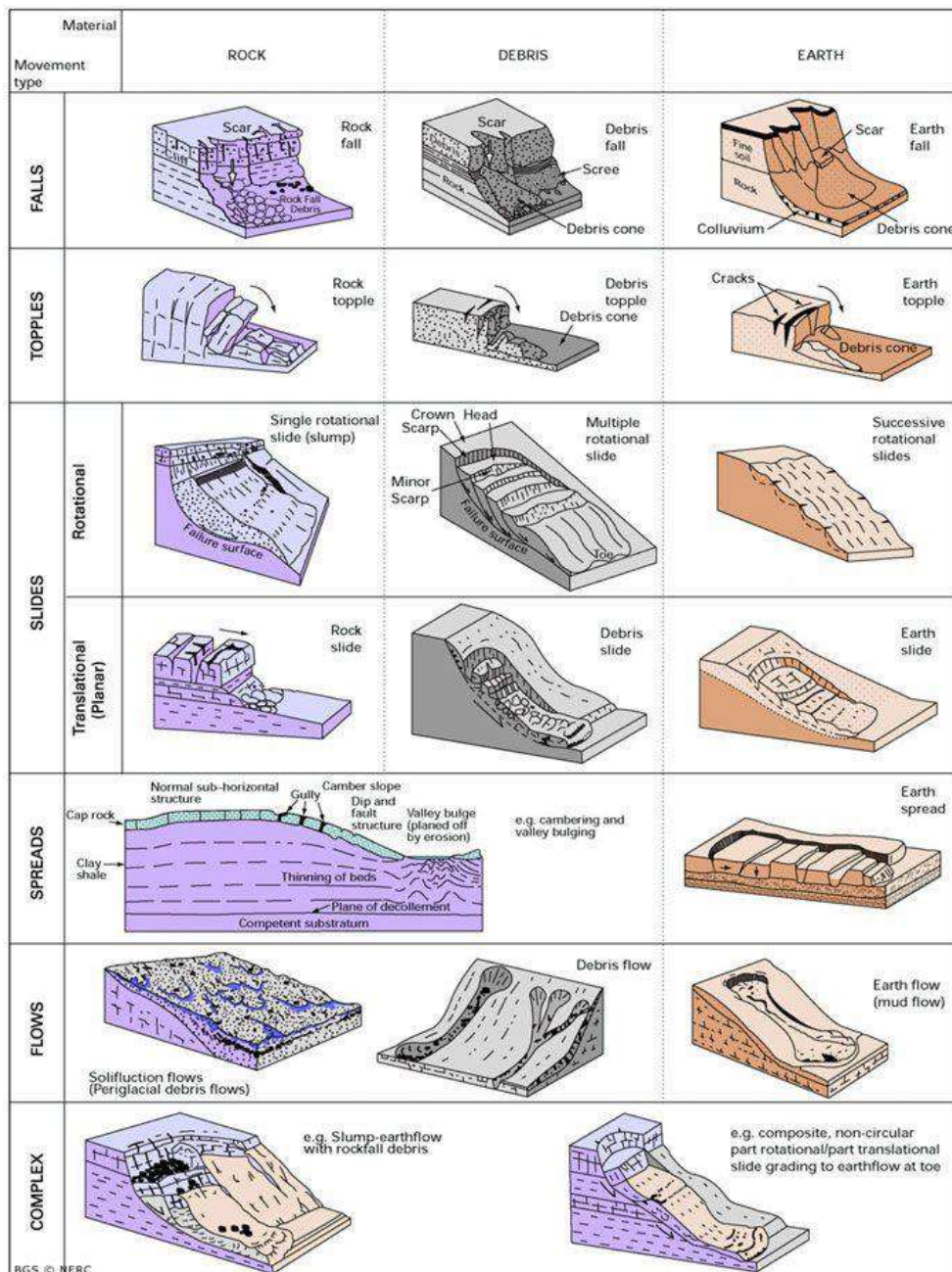


Figure 13 Landslide classification after Cruden and Varnes, 1996 (Taken from the web page of British Geological Survey).

In the submarine context, the mass movements are the most important phenomena for the modelling of the seafloor morphology producing important structures such as canyons, erosional channels, landslides and other structures.

The “submarine mass movements” consist of all the movements of rock or loose materials, along a sliding surface representing the main mass transport processes of material along the continental margins (Haflidason et al. 2004) while submarine landslides are one of the main agents through which sediments are transferred across the continental slope to the deep ocean. The latter mainly occurs in sectors with jagged morphology with elevated slopes on the seabed, for example in proximity with the seamounts, canyons or gullies and slopes.

The mass movements can also however be associated with seafloor seepage and can be formed in proximity with fluid escape structures.

High-resolution bathymetric imaging with advanced geotechnical methods are providing very significant advances in this geological field.

Recent works have been made to improve a complete understanding of:

- (i) The relation between tectonics and mass movement occurrence (Moore and Strasser 2016);
- (ii) The role that fluids plays in pre-conditioning slope instability.

Submarine landslides are classified on the basis of the type of movement and on the geotechnical features of the relative deposits (Fig. 13).

The controlling factors of the landslides are mainly linked to the physical features of the slope.

The most common causes of the submarine landslides are rapid sedimentation, retrogressive evolution (Hampton et al., 1996), the oceanographic activity, the tectonic and seismic activity (Hampton et al., 1996; Biscontin et al., 2004; Coulter, 2005), volcanic activity, fluid escape phenomena and wave action.

The complexity and variety of physical mechanism that are involved in submarine landslides and in submarine mass movement is still up for debate.

At the present time, the main approach to the study of submarine landslides is based on the:

- Morphological characterisation (morphology, geometry, structure);
- Preconditioning factors that are those related to the geology, morphology, hydrology of the sector. Examples are sedimentology, fluid flow regime, tectonic setting, shape and size of the geological bodies, lithology, and stratigraphy, status of fracturing and alteration of the rocks, permeability, and gradient of the morphology.
- Trigger mechanisms which are an external stimulus to initiate the instability process determining the rapid alteration of the natural equilibrium (e. g. increase of the specific weight, increase of the gradient of the slope, geological load increase, increase in the groundwater, decreased cohesion, and seismic stress),
- Transport mechanism (flow mechanics),
- Frequency of the process (stratigraphic analysis and isotopic dating).

Geo-Hazards related to such submarine landslides range from the destruction of offshore infrastructures to the collapse of coastal facilities and the generation of tsunamis. The main consequences of submarine landslide and sediment mass movements on infrastructure and coastal communities is well known, thanks to a few notorious events that made global headlines. Some

landslides were described to be the cause of tsunamis and had ruptured a series of submarine cables.

Scientific researches on this geological topic remains highly topical, irrespective of whether it focuses on the consequences that such events may have on human and natural environments. The geo-hazards and risks associated with submarine mass movements remain a fundamentally important focus in several scientific researches.

This marine area is geographically considered an important area for geological knowledge of the Mediterranean, and also has a high potential in economic productivity for extraction of oil and gas and of natural resources (fisheries). With regards to its economic importance in recent decades, it has been the object of numerous geological-oceanographic studies (Colantoni, 1975; Millot, 1999; Civile et al., 2008; 2010; Corti et al., 2003, 2006), which showed the presence of different types of submarine morphologies (such as areas of submarine volcanic activity, mud volcanoes, seamounts, mounds, pockmarks and others).

In the Sicily Channel the morphology of the seafloor is very jagged and is characterised by continuous alternations of high, and low morphologies (Fig. 16). Morphologically, the Sicily Channel is a marine sector comprising (i) the wide continental shelves such as the Tunisian, the Iblean-Maltese Plateau and the Adventure Bank (ii) the steep continental slope, (iii) furrowed by deep basins, (iv) volcanic seamounts and (v) submarine banks (Colantoni, 1975).

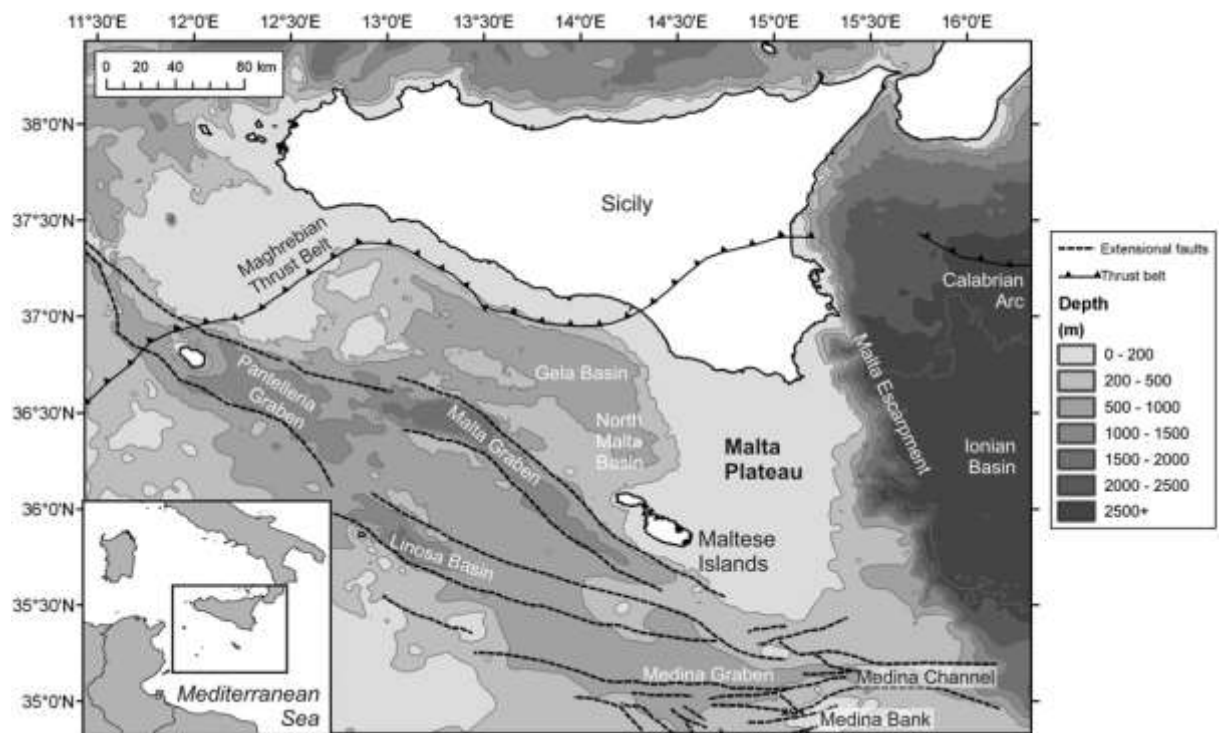


Figure 15 Bathymetric map of the northern section of the Pelagian Platform in the Central Mediterranean, showing the Malta Plateau and the principal morphological and structural features in the region (Micallef et al. 2011).

It is possible to distinguish the following morphologies in the Sicily Channel in detail:

- The wide and steep continental shelves (up to 170 km and 2.5° respectively) and steep continental slopes (up to 14°) ranging in waters from about 140 to 1000 m in depth often affected by gullies, channels and mounds;
- Four deep basins at a depth of up to 1750 m (e.g., Gela Basin, Pantelleria, Malta and Linosa Grabens);
- Several volcanic seamounts and submarine banks (e.g., Adventure, Nerita, Terribile, Graham, and Nameless).

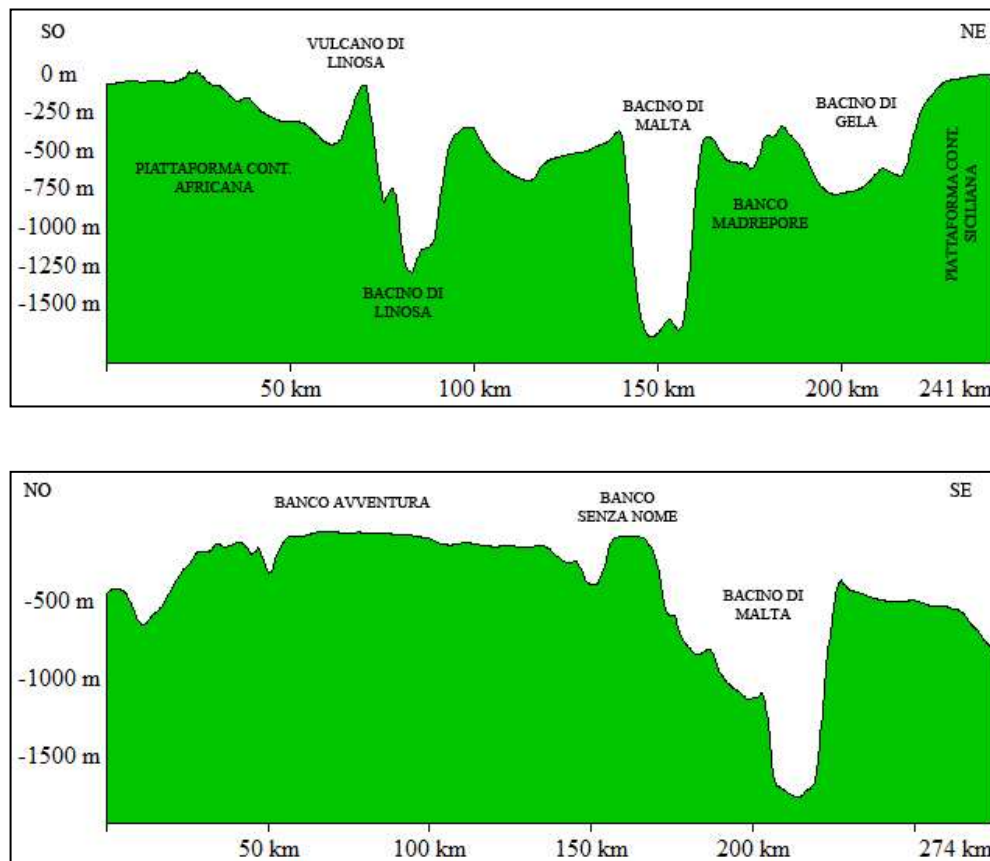


Figure 16 Bathymetric profiles of the Sicily Channel from low resolution bathymetric data (GEBCO project).

This complicated morphological setting is the result of its complex geology because the latter is the external part of the Siculo-Maghrebian collisional complex (Handy et al., 2010; Catalano et al., 2013 cum bibliography) known as the Tunisian-Pelagian foreland.

The real distribution of the bathymetry is shown through the hypsometric curve and the bathymetric map obtained using the low resolution bathymetric dataset provided by GEBCO Project (Fig. 17). The main range of bathymetry comprises between 0 and 200 m in depth and is represented by the continental shelf and upper slope.

The bathymetry increases towards the central sector where there are three morpho-structural depressions (with NW-SE trend) known as Pantelleria, Linosa and Malta-Medina Grabens. The latter is the deepest with a depth of over 1700 m (Figs. 15, 16, 17; Colantoni, 1975; Finetti, 1984).

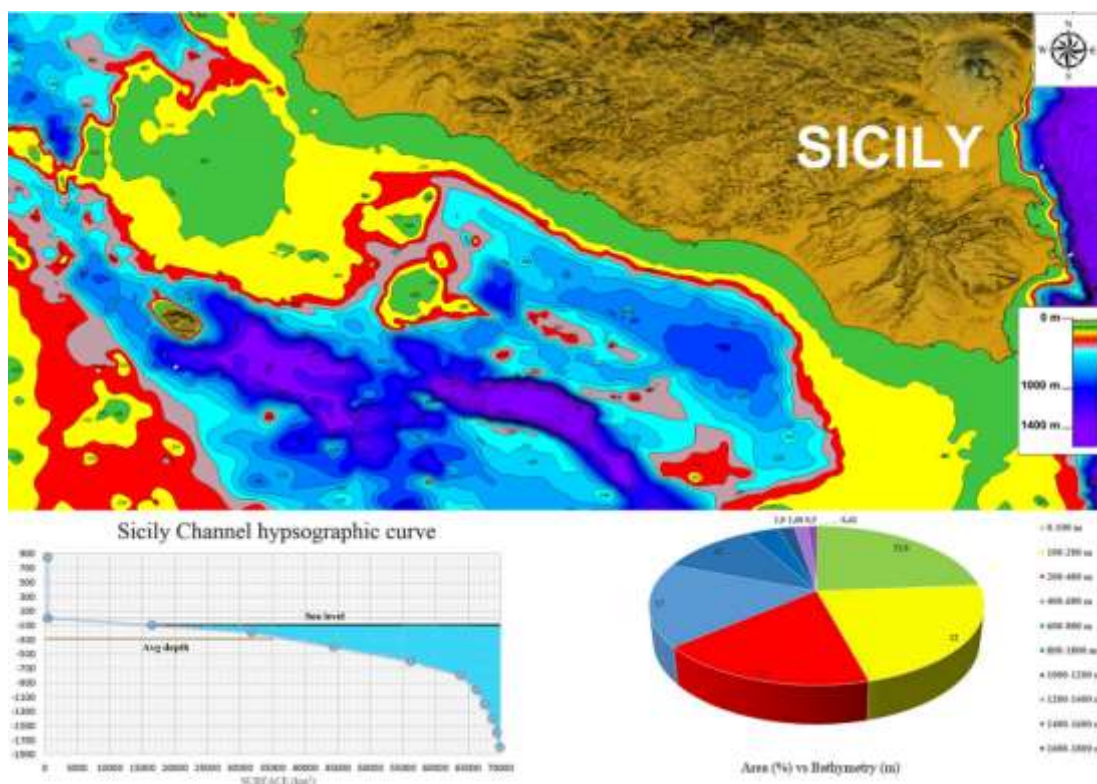


Figure 17 The map shows the distribution of the bathymetry in the Sicily Channel. In the bottom left corner one finds the hypsographic curve, while in the right corner one has the cake chart showing the relationship between areas and bathymetry in the Sicily Channel.

2.2 GEOLOGICAL SETTING

The Sicily Channel is a continental domain known as Pelagian block (Burolet et al., 1978). It comprises the seafloor between the southern coast of Sicily, the eastern coast of Tunisia and the Malta Escarpment (central Mediterranean Sea, Fig. 18), which forms part of the central Mediterranean orogenic region, that links the African Maghrebides with the Southern Apennines across the Calabrian accretionary wedge (inset in Fig. 18). The Sicily Channel is an almost rectangular prong of the North African passive continental margin that is a major geodynamic sub-province undergoing tectonic extension and crustal thinning (Max and Colonatoni, 1992). It is characterised by thinned continental lithosphere (60-70 km), shallow Moho depth (20-25 km), and high heat density flow density, positive Bouguer anomaly and significant volcanic activity often associated with magnetic anomalies (Della Vedova et al. 1989).

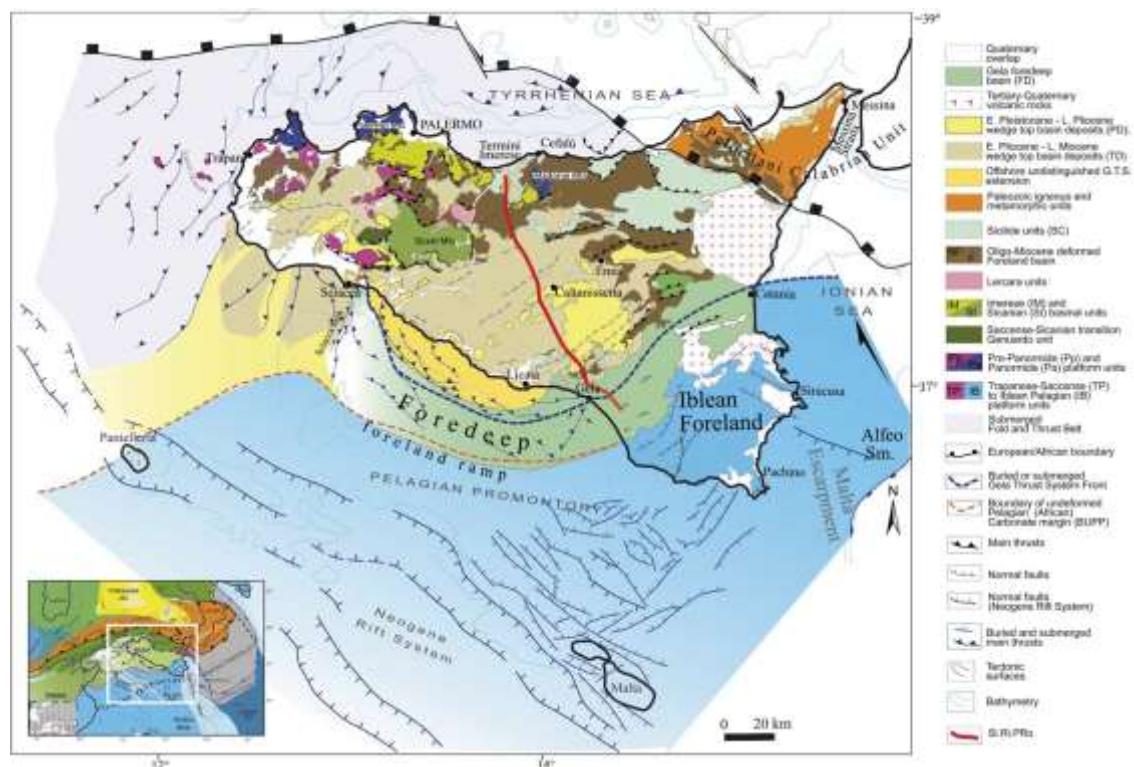


Figure 18 Geological structural map of Sicily, the inset shows the structural map of the Central Mediterranean. (Modified after Catalano & D'Argenio, 1982; Catalano et al., 2013).

In many previous works, the region was described as a result of transtensional tectonics (Finetti & Del Ben, 1986; Argnani et al. 1989; Boccaletti et al. 1987) or of rifting processes (Colantoni, 1975; Illies, 1981; Finetti & Del Ben, 1986). The central part of the Sicily Channel is believed to be both a tectonic trough linked to the transtensional deformation, which has generated the pull-apart basins involving deep crustal levels (Finetti, 1984; Corti et al. 2003; Civile et al., 2010) or an effect of the mantle convections developed during the roll-back of the African lithosphere slab beneath the Tyrrhenian plate (Argnani, 1990).

At the present time, the Sicily Channel is believed to be the result of the interaction of two different tectonic processes, the Sicilian-Maghrebian collision (Catalano and D'Argenio, 1978, 1982; Roure et al., 1990; Casero and Roure, 1994; Lentini et al., 1994; Catalano et al., 1996, 2000, 2013a; Bello et al., 2000;; Granath and Casero, 2004; Finetti et al., 2005; Sulli 2000; Corti et al. 2003; Accaino et al., 2011; Albanese and Sulli, 2012), and the Sicily Channel rifting, which have coexisted contemporaneously at least since the Pliocene (Corti et al., 2006).

The orogenic region is represented by the Sicilian Fold and Thrust Belt (FTB) and its submerged prolongation and is considered to be a segment of the Alpine collisional belt, resulting from both post-collisional convergence between Africa and Europe (Bonardi et al., 2003) as well as roll-back of the subduction hinge of the African crust (Catalano et al., 1996; Casero and Roure, 1994; Lentini et al., 1994).

The Sicilian FTB is a roughly south vergent thin-skinned imbricated wedge, progressively emplaced since the early-middle Miocene. It originated from the piling-up of tectonic bodies, derived from the deformation of the paleogeographic domains developed during the Mesozoic in the African rifted continental margin. It grows above a northwest dipping regional monocline consisting of Mesozoic carbonate platform deposits of the Iblean foreland, covering the stretched African continental crust (Figs.18, 19, 20; Catalano et al., 2013).

The foreland area, outcropping in south-eastern Sicily and submerged in the Sicily Channel (Iblean-Maltese Plateau), is affected by several Neogene–Quaternary NW-SE normal faults which are related to the Sicily Channel Rift active during the Neogene-Quaternary and to the Pantelleria, Malta, Linosa grabens (Finetti, 1984).

2.3 STRATIGRAPHY

Several previous studies identified the stratigraphic configuration in the Sicilian Fold and Thrust Belt (FTB; Catalano & D'Argenio, 1982; Montanari, 1987) and are recognised in the adjacent submarine area (Catalano, 1987; Catalano et al. 1989; Torelli et al. 1991). Detailed multichannel seismic profiles acquired across the Sicily Channel were correlated with many AGIP/ENI wells to display the real stratigraphic/structural setting of the area (Fig. 19).

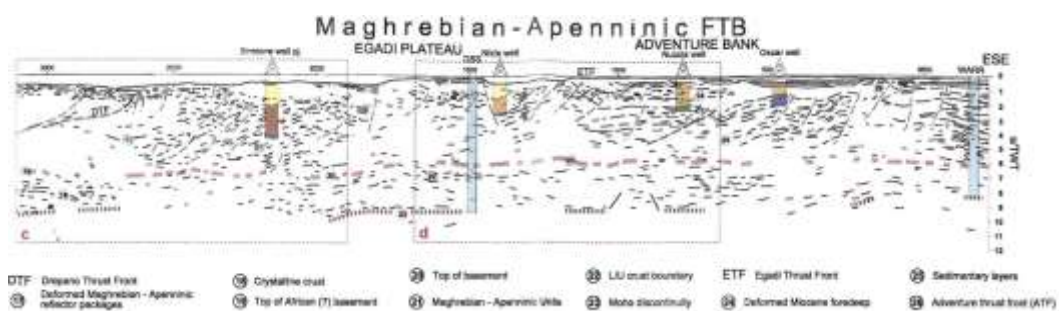


Figure 19 Line drawing of the deep seismic profile CROP_M23 (Catalano et al. 2000).

Type litho-tectonic assemblages and the stratigraphy is strongly related to the Africa margin domains (Fig. 20).

The Sicily Channel is composed of the submerged carbonate stack complex of the Mazara-Sciacca and the Gela Thrust System (Figs. 19, 20, 21).

The Gela Thrust System is an accretionary prism of NE-SW-verging imbricated tectonic layers of Upper Cretaceous-Lower Pleistocene deposits formed of various lithologies, which are over thrusting the Iblean-Pelagian foreland units.

The carbonate stack units, recognised for example in the Adventure Bank (Argnani, 1993; Sulli, 2000), comprise a 6-7 km thick Meso-Cenozoic carbonate succession formed of carbonate platform and pelagic deposits (Figs. 20, 21).

This Mesozoic carbonate succession displays strong lateral variations in facies as a result of the NNW-SSE oriented syn-sedimentary fault systems active during the lowermost Jurassic extensional regime (e.g. Streppenosa basin, Patacca et al. 1979; Frixia et al. 2000).

The succession includes several volcanic (mostly basalts) intercalations, covered by 2-2.5 km of Miocene-Pliocene clastic, evaporitic and carbonate deposits (Gasparo Morticelli et al., 2015 and references therein), is coeval to the Late Neogene thrust stacking as described above.

The succession also includes the Upper Triassic peritidal dolostones of the Sciacca Fm (Gela and Ragusa Oil Fields reservoir), the Lower Jurassic peritidal limestone, Inici Formation (Vega Oil Field reservoir), and the deep-water organic-rich limestone (intraplatform Streppenosa basin).

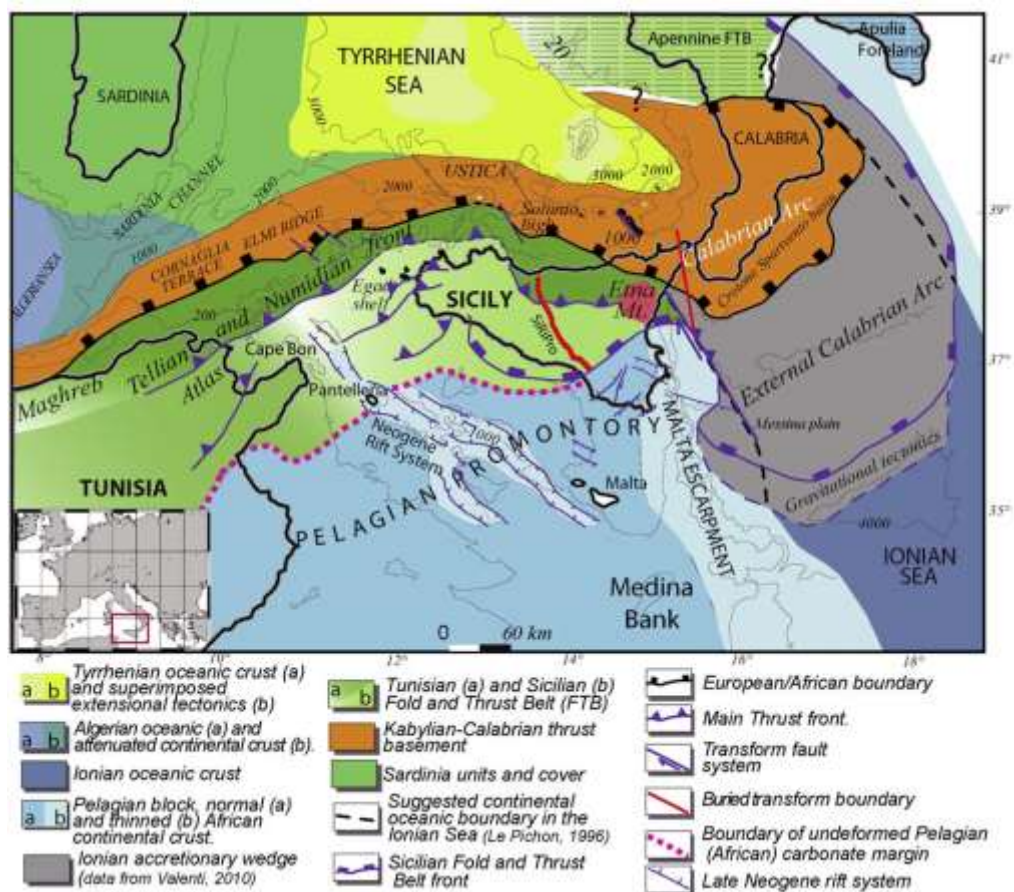


Figure 20 Main elements characterising the collisional complex of Sicily (modified after Catalano et al., 2000).

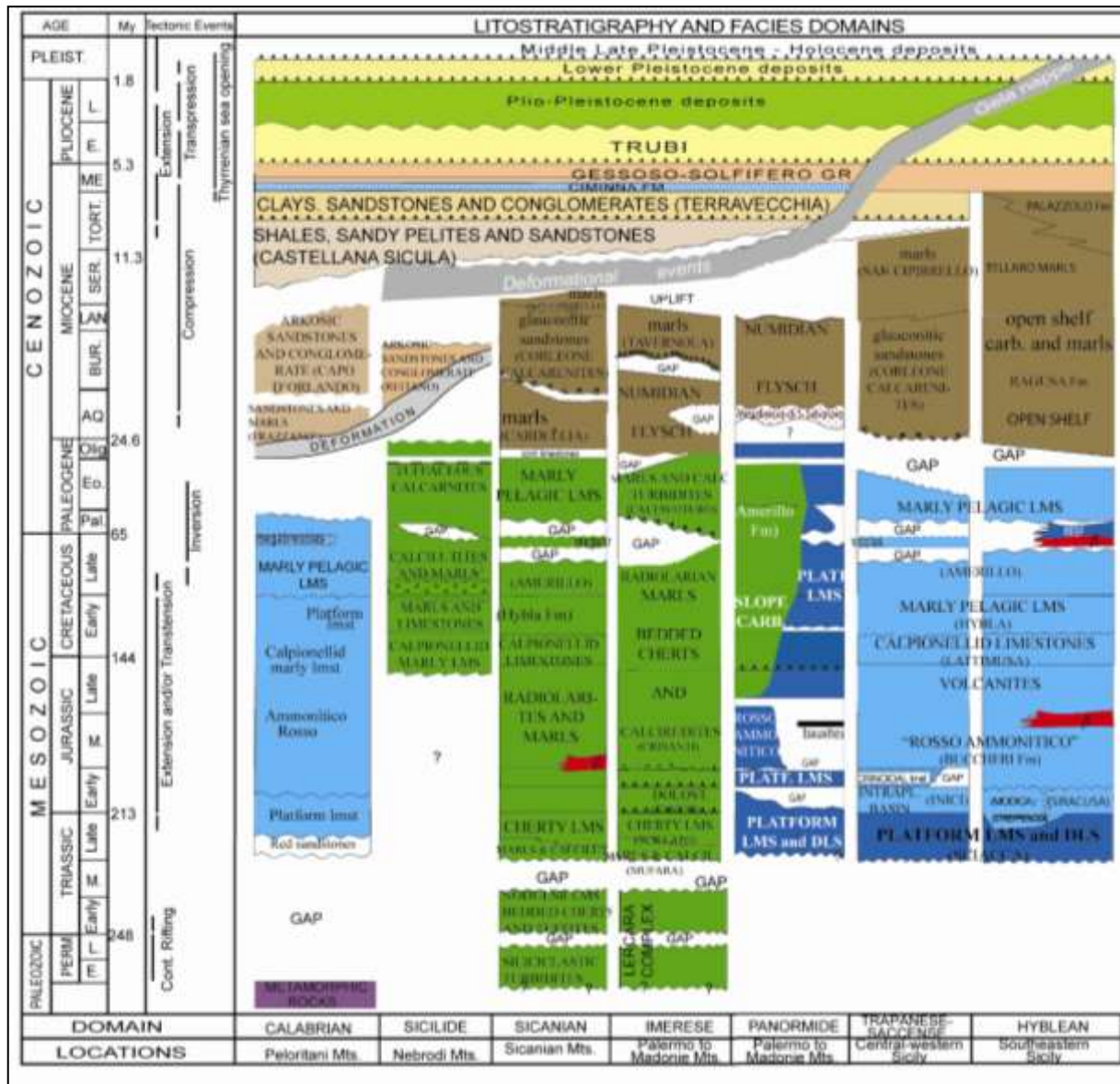


Figure 21 Stratigraphy and facies domain of the Sicilian sedimentary successions (modified from Catalano et al. 2000).

2.5 VOLCANISM

The “Sicily Channel Continental Rifting” produced the main volcanic islands (Pantelleria and Linosa) and submarine volcanic structures located at the top of the Adventure Plateau, Graham and Nameless banks (Peccerillo, 2005; Rotolo et al., 2006).

The volcanism took place during the Pliocene–Pleistocene (Calanchi et al. 1989; Peccerillo, 2005; Rotolo et al., 2006) and is mainly concentrated in the Pantelleria and Linosa islands and in many submarines banks (e.g. part of the Adventure Bank, Graham Bank, Nameless Bank and other minor banks; Fig. 22).

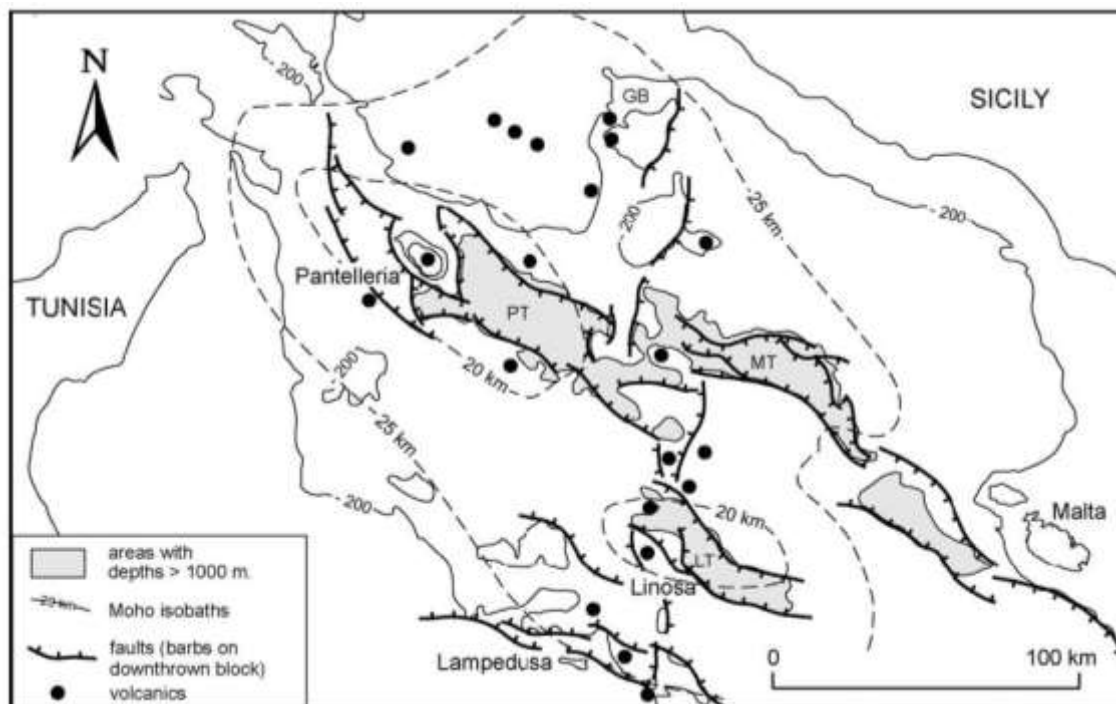


Figure 22 Schematic structural map of the Sicily Channel. PT: Pantelleria trough; MT: Malta trough; LT: Linosa trough; GB: Graham bank. Location of volcanic centres are from Calanchi et al. (1989), CNR (1991), Grasso et al. (1993), Rotolo et al. (2006) and Civile et al. (2008); Moho isobaths are from Finetti and Del Ben (2005).

The erupted volcanic products of the Sicily Channel have an alkaline to peralkaline affinity, and consist mainly of alkali basalts and hawaiites (Corti et al., 2006; Rotolo et al., 2006). These

general petrological features were considered similar to the typical anorogenic magmatism that characterises the extensional areas (continental rifting; Corti et al., 2003; 2006).

The oldest magmatic products of the Sicily Channel have been found in a seamount located in the Nameless Bank where some dredged samples were collected and successively dated with the K-Ar method to 9.5 - 0.4 Ma (Beccaluva et al., 1981).

The volcanic activity of Pantelleria and Linosa Islands and submarine Banks is younger and has been active since Plio-Pleistocene (Calanchi et al., 1989). The nineteenth century historic volcanic activity took place near Pantelleria, Linosa, Graham Bank and Nameless Bank. Some of these historical volcanic events have occurred with the submarine Foerstner 'volcano' (A.D. 1891; Washington 1909) and the emergence of the Ferdinanda Island (A.D. 1831; Colantoni et al. 1975) that is part of the Graham Bank (Fig. 23).

Pantelleria Island is a "layer-volcano", which emerges above sea level for about half of its body and has a surface area of 83 km². It is the biggest onshore volcanic edifice of the Sicily Channel. Its volcanic products show an alkaline-peralkaline affinity and are formed mainly of alkaline basalts, hawaiites, trachytes and 94% of peralkaline trachytes and rhyolites peralkaline (Pantelleriti, Barberi et al., 1969; Villari, 1974; Carapezza et al., 1979; Beccaluva et al., 1981; Civetta et al., 1998; Flournoy et al., 2000; Parello et. al, 2000).

The Linosa Island was formed through three main volcanic phases between 1.06 and 0.53 million years ago (Lanzafame et al., 1994).

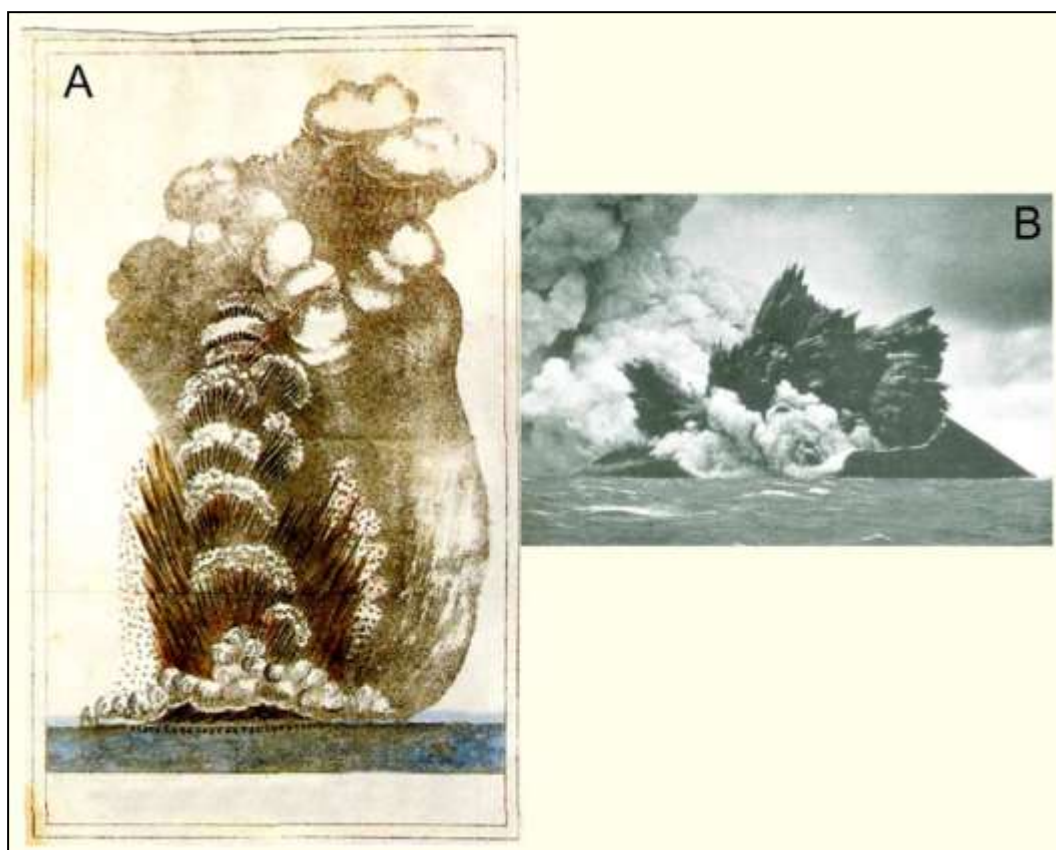


Figure 23 The eruption of “Ferdinandea Island” in 1831, of Surtseyan type with cypressoids clouds (from C. Gemellaro / INGV).

2.6 SEISMICITY

The Central Mediterranean is highly seismic due to its complicated geodynamic context.

The seismic activity of the Sicily Channel is related to the Rift Zone and Siculo-Maghrebian collisional context. It mainly generates shallow earthquakes with low-intensity (Ferruggia et al., 1987) that can be subdivided into two phases using the historical information, which are tabulated into the INGV catalogues (Fig. 24).

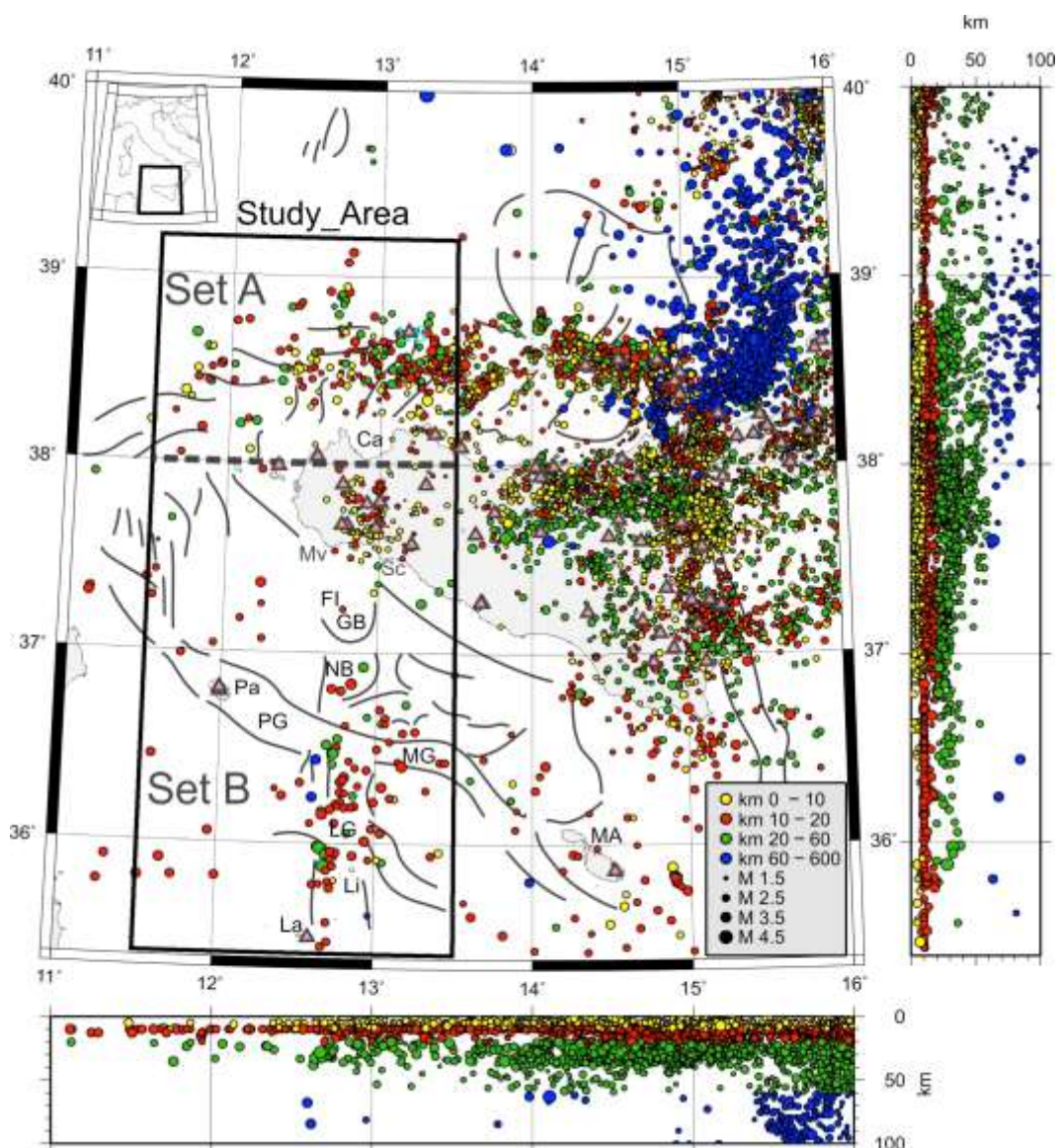


Figure 24 Instrumental seismicity of the Sicily area from 1981 to 2012. Black lines report the main morphological structure of the area. Black rectangle encloses the seismicity used in this work. Set A and B are subsets used to

calculate the Gutenberg-Richter distributions discussed in the text. Ca, Castellammare del Golfo; FI, Ferdinandea Island; GB, Graham Bank; La, Lampedusa; LG, Linosa Graben; Li, Linosa; Ma, Malta; MG, Malta Graben; Mv, Mazara del Vallo; NB, Nameless Bank; Pa, Pantelleria; PG, Pantelleria Graben; SC, Sciacca; US, Ustica (Calo and Parisi 2016).

➤ The first phase is a typical example of seismic swarm generating shocks, which range from weak to strong and is often preceded or accompanied by strong thunderous rumbles coming from underground. Despite these events the strong and abiding shaking, did not have catastrophic effects on the affected sites and their genesis could be attributed to the presence of numerous volcanic structures present in the Sicily Channel. This theory appears to be confirmed by the seismic events, which have occurred during the historical eruptions of the Ferdinandea Island in 1831 as well as during the eruption in the offshore area of Pantelleria in 1891.

➤ The second phase begins roughly with the advent of instrumental observations and the first monitoring networks to the present day. It is characterised by events with high intensity of magnitude and also characterised by important catastrophic effects. One example of these is the “Earthquake of the Valle del Belice” (1968), where part of the most important buildings were severely damaged (Rigano et al., 1998). This group of seismic activity involves up to 10–20 km deep hypocentres spread over the strait with local magnitude up to 3.5 (Chiarabba et al. 2005; Galea 2007).

The seismicity is weak in proximity to the southcentral coast of Sicily whereas it is higher along the Pantelleria depression and the Malta and Lampedusa ones. Earthquakes in this area can occur to a depth of up to 60 km and in a few cases with magnitude reaching up to 5 (Calo and Parisi, 2014).

2.7 OCEANOGRAPHIC SETTING

The Sicily Channel plays a primary role in the dynamics of the Mediterranean circulation connecting the sub-basins of the eastern and western Mediterranean Sea. The geographic position of the Sicily Channel as well as its jagged morphology of the seabed (Fig. 25) form a complex oceanographic circulation that represents the main communication pathway between the occidental and oriental basins of the Mediterranean.

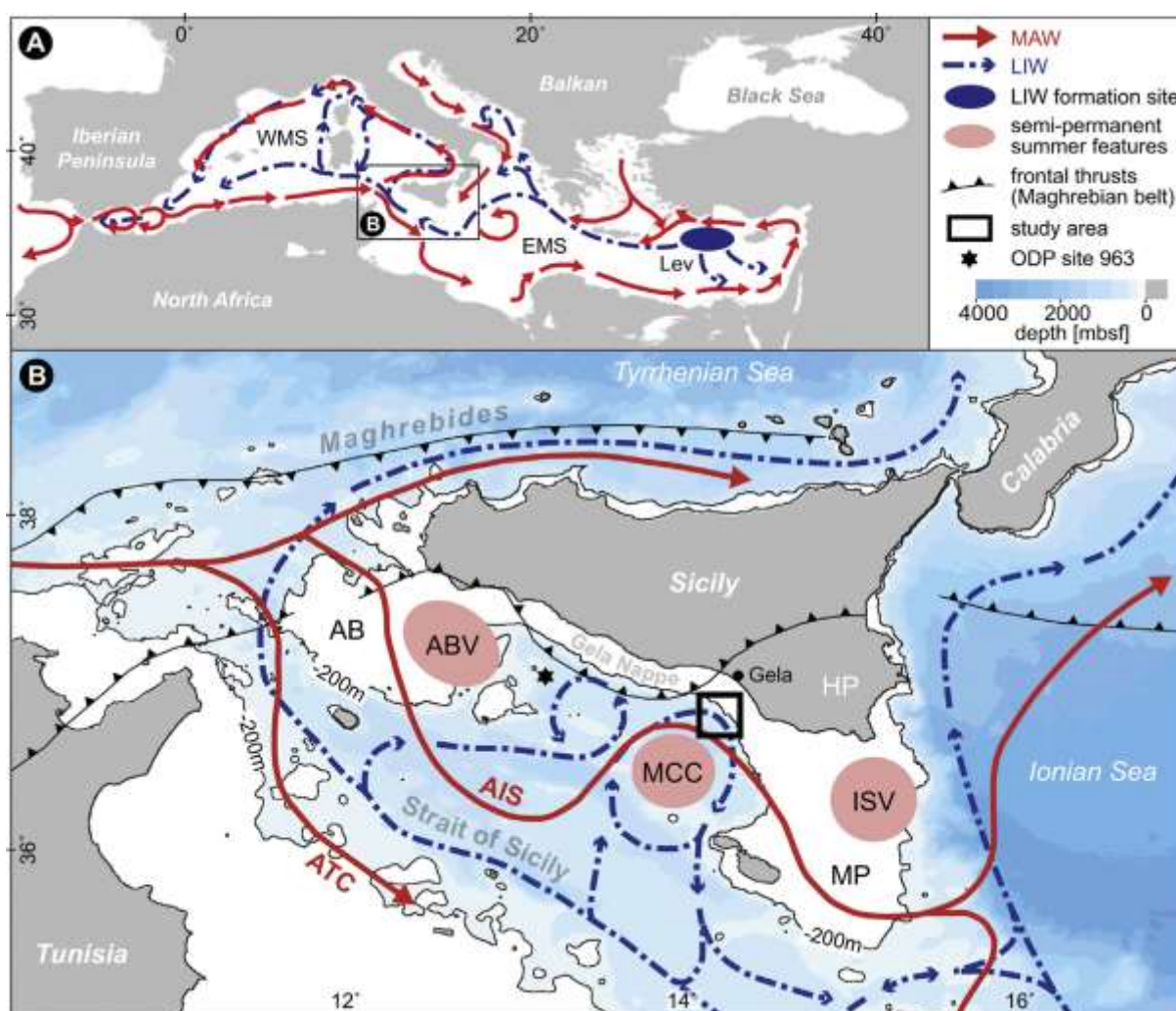


Figure 25 Main pathways of surface (Modified Atlantic Water, MAW) and intermediate (Levantine Intermediate Water, LIW) waters in the Mediterranean Sea showing formation area of the LIW (after Millot, 1999; Hernandez-Molina et al., 2006). WMS 1/4 Western Mediterranean Sea; EMS 1/4 Eastern Mediterranean Sea; Lev 1/4 Levantine Sea. B) Scheme of two-layer exchange circulation in the Strait of Sicily (SoS), modified from Lermusiaux and Robinson (2001), Beranger et al. (2004) and Ciappa (2009). Fresh surface waters from the Atlantic Ocean meander along the Tunisian and Sicilian shelf (red arrows, between 0 and 200 m), accompanied by a concurrent subsurface

outflow of relatively more saline Mediterranean waters (blue arrows, between 200 and 600 m). Main water masses: MAW 1/4 Modified Atlantic Water, LIW 1/4 Levantine Intermediate Water; surface water branches: AIS 1/4 Atlantic Ionian Stream, ATC 1/4 Atlantic Tunisian Current; mesoscale summer features: ABV 1/4 Adventure Bank Vortex (cyclonic); MCC 1/4 Maltese Channel Crest (anticyclonic); ISV 1/4 Ionian Shelfbreak Vortex (cyclonic); AB 1/4 Adventure Bank; HP 1/4 Iblean Plateau; MP 1/4 Malta Plateau. Main tectonic elements are redrawn according to Jenny et al. (2006). (Kuhlmann et al. 2015).

In Millot, (1999), the author proposed a mathematical model about the oceanic circulation for the Sicily Channel, which provides the presence of:

- Shallow cold waters, coming from the Atlantic Ocean (Modified Atlantic Water, MAW) flowing from west to east,
- Deep and heavily salted warm waters coming from the Levantine basin (Leventine Intermediate Water, LIW), which flow to the western Mediterranean basin (Millot, 1999; Lafuente et al. 2002).

The Modified Atlantic Water (MAW) in the proximity of the Strait of Sicily undergoes a bifurcation giving rise to the Atlantic Tunisian Current (ATC) (Lemursiaux & Robinson, 2001) and the Atlantic Ionian Stream (AIS), which flows, into the Ionian basin (Lermusiaux, 1999; Robinson et al., 1999; Lermusiaux and Robinson, 2001; Gaberšek et al., 2007).

Recent studies show that the amount of water carried by AIS current depends on the incidence angle that the water masses form with the Sicilian coast. The AIS current is a feature occurring during summer that together with the Atlantic Tunisian Current flow along the Tunisian-Libyan shelf break (Beranger et al., 2004; Sorgente et al., 2003). It flows along the southern platform of Sicily and generates a vortex current known as the Adventure Bank Vortex (ABV) across the homonym Bank (Lemursiaux & Robinson, 2001; Gaberšek et al., 2007) and towards the southeast coast of Sicily and then runs towards the Maltese Platform, where they form another bifurcation, in front to “Capo Passero” and towards the Ionian Sea (Lafuente et al., 2002).

Normally the water of the Mediterranean Sea is warmer than the air above it in the winter and cooler in the summer period (approximately 2 ° difference), while in the Sicily Channel, the waters are warmer and with salinity content comprising between 35 and 37 ‰.

In July, the water temperature reaches between 24° and 26 °, with a surplus of heat of about 10° in comparison with the Atlantic Ocean. In winter, the average temperature remains about 14°-15°. The temperature of the waters does not show significant changes below the 300 m depth, where the masses of water are stable and the isotherm is of 13°.

The above information is provided by the online database of the Istituto Superiore per la Protezione e la Ricerca Ambientale (ISPRA, <http://www.isprambiente.gov.it/en>) together with some oceanographic works (Kuhlmann et al. (2015; Astraldi et al., 2002).

Chapter 3

3. DATA AND METHODS

3.1 MULTIBEAM DATA

A classic echosounder or single beam is a geophysical instrument for the marine exploration, which emits an acoustic wave that expands with a spherical front along the column of water, dispersing the acoustic energy equally in all directions (Fig. 26).

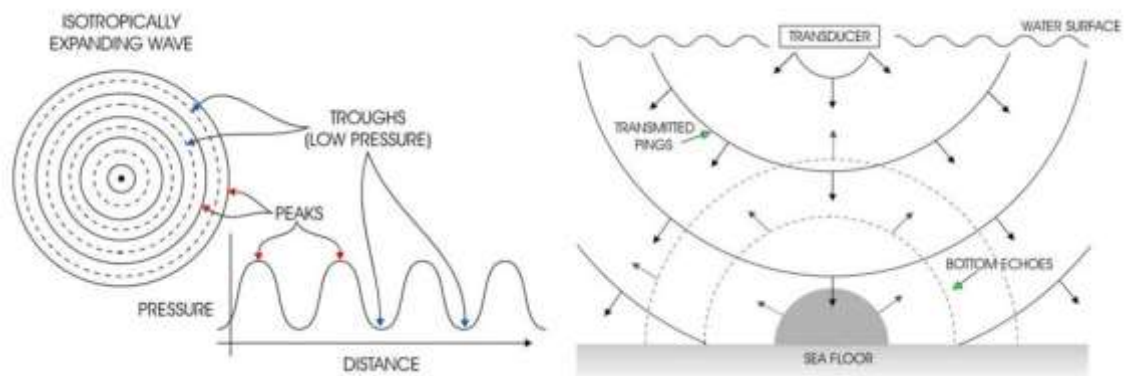


Figure 26 Sketch of the single beam: a signal pulse emitted from a classic echo sounder expands spherically with an amplitude and uniform energy in all directions.

MultiBeam echosounder (MBES) is the most recent system that allows the bathymetric surveying of the seabed, river and lake obtaining a digital model of the seabed with high quality and precision.

The modern echo-sounder systems for bathymetric surveys (Multibeam) enable a moving vehicle to get high spatial and vertical resolution of sweeps (swath) with a width of 3-5 times the water depth below the transducer.

The instrument allocated on the boat emits a pulse to sound frequencies, which are very tight in the direction of advancement and very wide laterally, with a fan-shaped geometry. It is formed by an array of receivers perpendicular to the array of projectors. The intersection between the transmitted pulses and the received pulses form a series of elliptical areas on the seabed named

footprint (Figs. 27, 29). The footprint in correspondence with the centre of the array (nadir of the MB) has a circular shape and becomes increasingly elliptical towards the outer parts of the beam. The size of the footprint varies with the depth of the water column and it is strongly linked to the angle of the beam.

The size of the footprint can be calculated at the Nadir of the Multibeam using a specific algorithm:

$$X_f = \tan(\alpha) * P;$$

Where α is the angle of the beams and P is the depth of the water column.

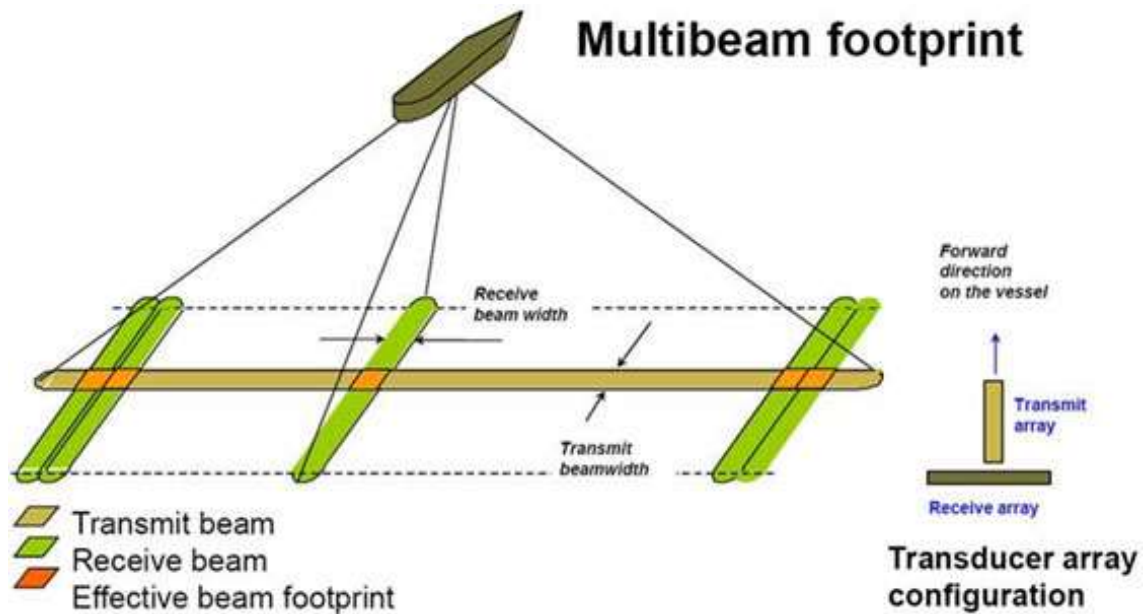


Figure 27 The figure shows the multibeam sonar footprint below the ship. The transmitted acoustic beam is narrow along the track and wide across the track (area in yellow). One received beam is highlighted in green. The intersection of the transmitted beam area and the individual received beam area provides the footprint for that beam, shown in orange. The depth is the average depth within the intersecting area.

At present, there are different MultiBeam instruments that are characterise by different technical features such as frequency, number of beams and angles (Fig. 28).

The operating frequency of the Multibeam is the main feature to distinguish the different types of MBES. It allows to estimate the maximum operating depth as well as the vertical and lateral resolution of the instrument (Fig. 28).

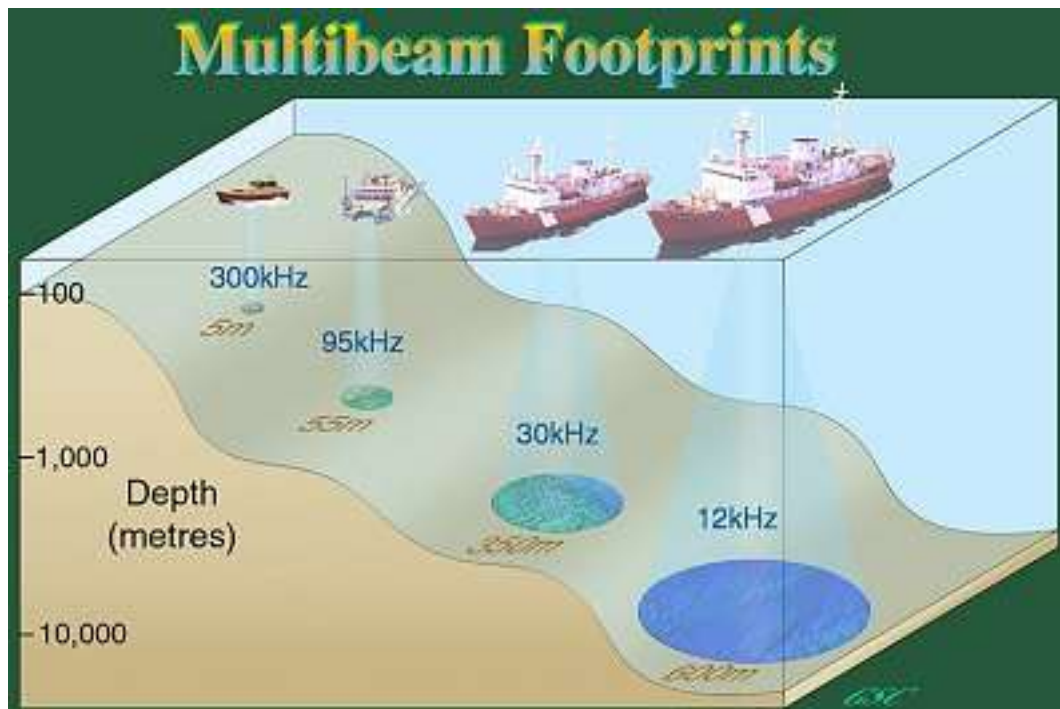


Figure 28 The figure shows different examples of the multibeam sonar footprint below the ship.

The measurements performed with a Multibeam system allow to obtain total coverage of the areas as well as to obtain a digital terrain model (DTM) with elevated resolution that can be used to reconstruct a final three-dimensional representation of the seabed.

The speed of the boat during the survey, for a good acquisition, should be between 3 knots and 5 knots.

The analysis of the returning echoes, on the front of the Multibeam plate and the measurement of time from the pulse output provides the data for the assignment of the correct spatial coordinates at each point on the ground illuminated by the beam (footprint).

The travel times are converted to distances using the sound speed gradients in the water column that is usually measured by probe, taking into account any effects of ray-bending due to the path of the signal in water layers with different propagation velocity.

The recognition via amplitude is generally valid in areas not too far apart laterally, where the return angles are high, and a good part of the emitted signal is reflected, while in the most remote areas of the sweep (swath), the signals return to lower and lower corners of the boat with decreasing intensity.

Each single beam (beam) has been assigned a corner and return time, a real-time processing or post-processing system, which recognises the position of the transducer at each instant, and is able to calculate each point on the ground illuminated by the beam of the respective spatial coordinates. Since this is a moving platform in the water, and therefore subject to changes in position over time, the systems are coupled to a reference unit (Motion Reference Unit, MRU).

A gyrocompass is used to measure the bearing of the navigation. The measured data is recorded in the reference of the transducer system. The positions of the return signals are assigned converting distances in the timing and correcting the angles of the measures provided by the MRU.

This data must be further filtered successively and corrected, generally for the elimination of spurious or unreliable data, for the tide, for positioning errors, to errors in the calculation of the speed of sound in water.

Furthermore, after accurate processing, the bathymetric data can be used to obtain Digital Terrain Models (DTM).

3.1.1 ACQUISITION

The multibeam data used in this Ph.D. project have been acquired during the ACUSCAL 2015 oceanographic cruise carried out in May 2015, within of the RITMARE Project. It is the new generation of the hull-mounted system Reson SeaBat 7160 (Fig. 30).

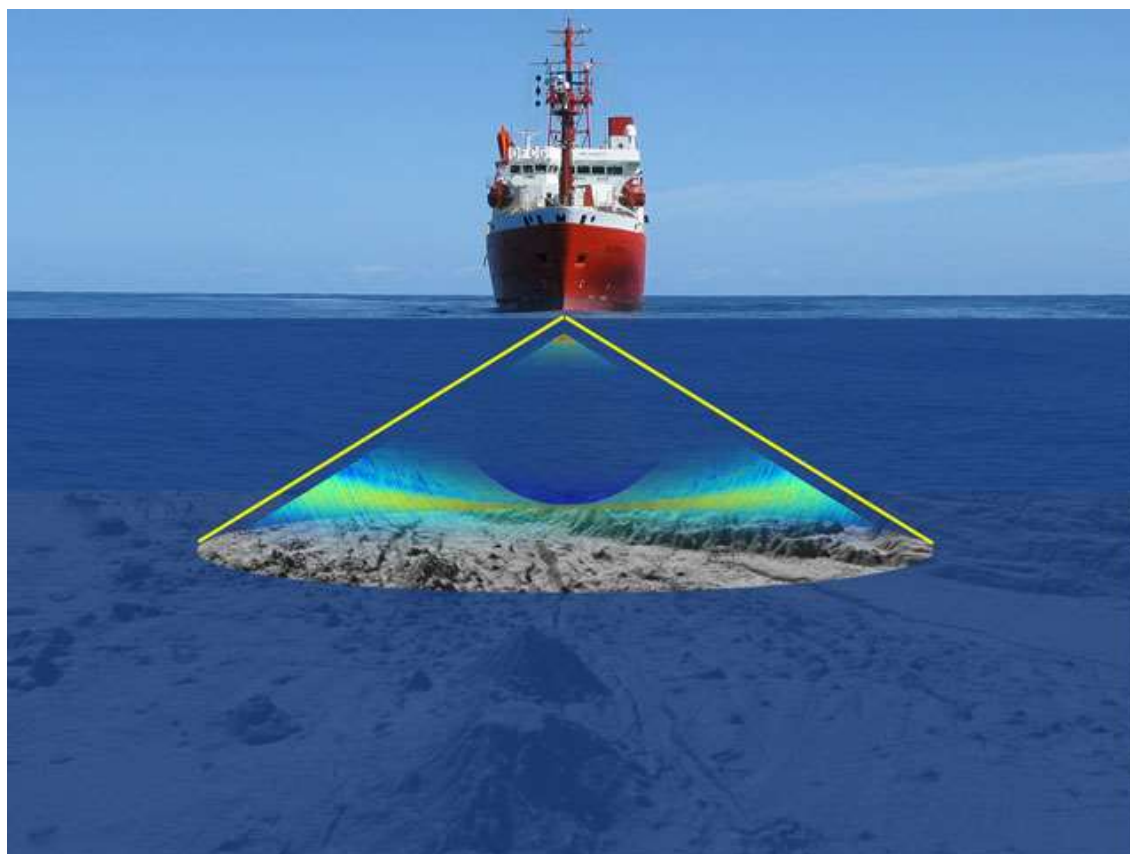


Figure 29 Sketch of multibeam surveying with a hull mounted hydro acoustic device.



Figure 30 Multibeam Reason SeaBat 7160 equipment.

The Reson system employs 59 pre-formed beams over a swath width of 90° . The frequency used by this system is 15.5 kHz. The EM120 system on the other hand employs a frequency of 12 kHz and uses 191 beams at a maximum opening angle of 140° .

The echosounder systems are corrected for ships motion and opening angles were set depending on the sea state, water depth and expected seafloor topography.

The Multibeam instrument, during the acquisition, was interfaced with software platform PDS2000, which operated the navigation, the acquisition and the subsequently processing (Fig. 31).

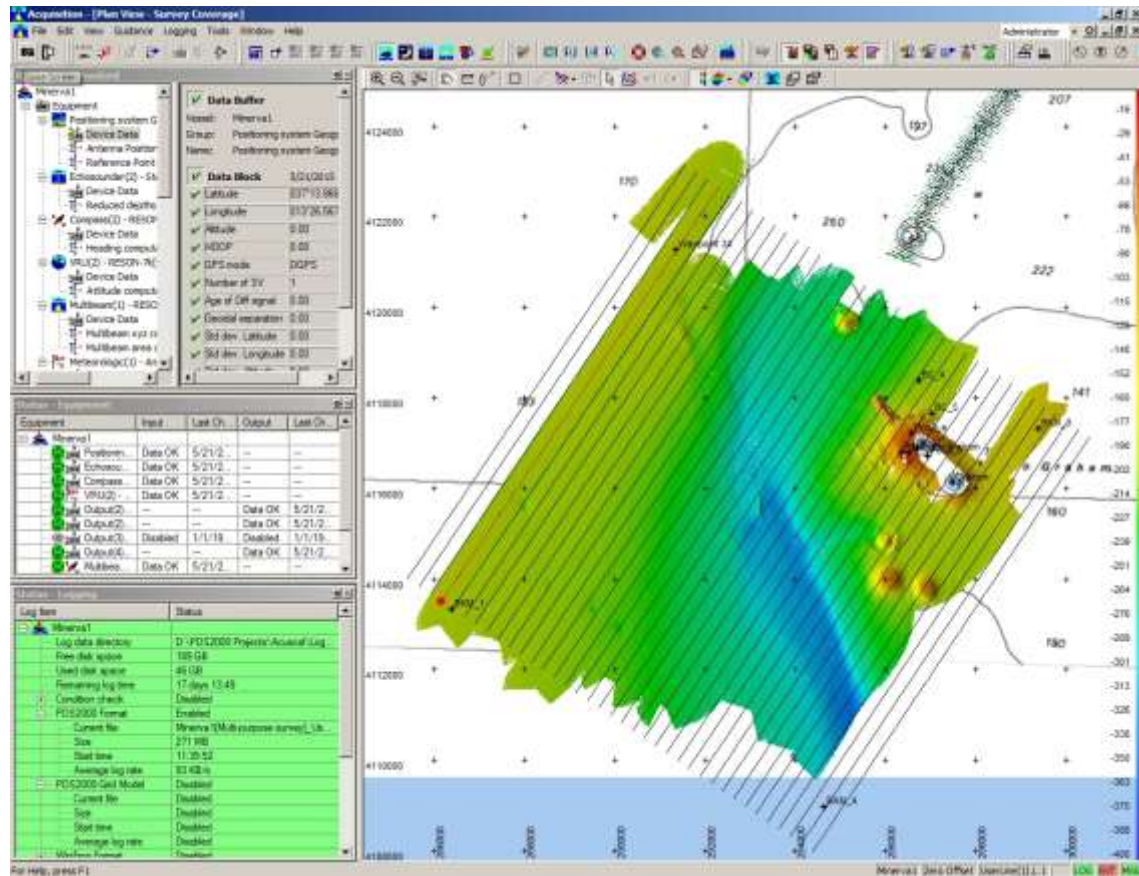


Figure 31 Screenshot of PDS2000 during the acquisition of the multibeam data.

The radiolocation was based on the DGPS Satellite methodology (by Fugro) and was used to ensure sufficient accuracy and reliability in the location of the bathymetric data, during the acquisition.

The survey was conducted using the system WGS 84, with UTM, zone 33 N as geodetic reference.

3.1.2 PROCESSING

The bathymetric data was processed at the Marine Geology Laboratory of the Department of Earth and Marine Sciences of the University of Palermo by PDS2000 software (Reason) and

successively was reprocessed at the Department of Geosciences of the University of Malta using Caris Hips and Sips 9.0 (Fig. 32).

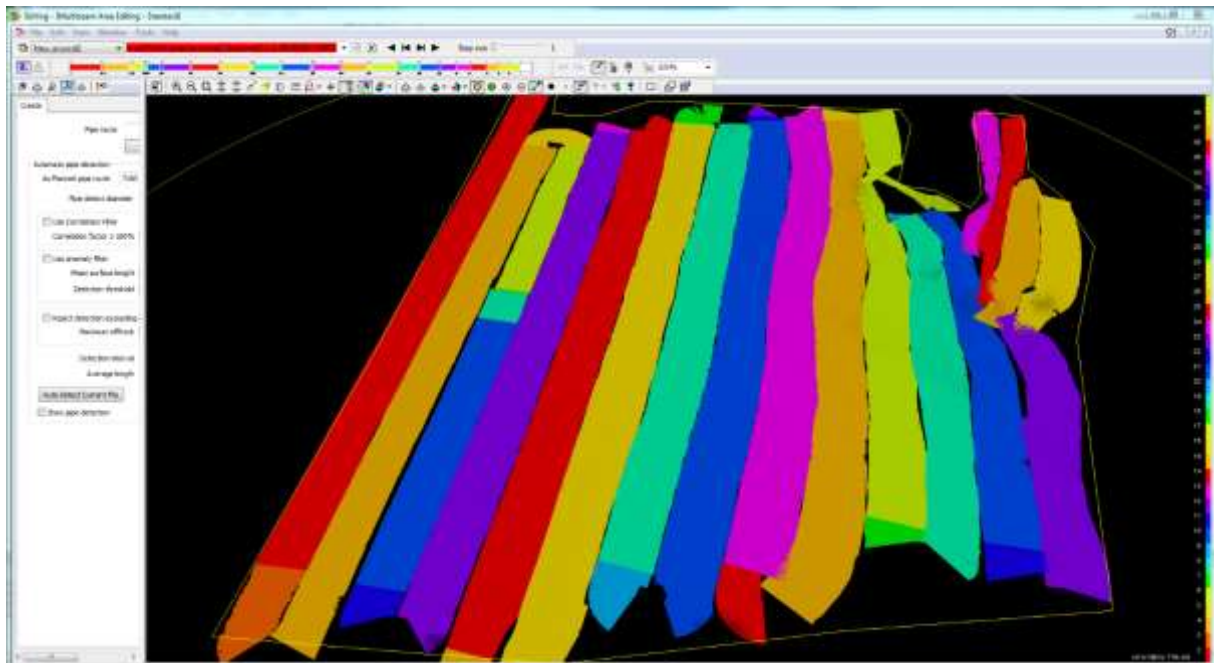


Figure 32 Screenshot of PDS200 during the processing of the multibeam data.

These two software packages, that are the most important software about the acquisition and processing of multibeam data, have many functions such as programming, survey design, navigation and data acquisition, filtering, processing and graphical representation of the data.

A general processing strategy was carried out including an initial automatic removal of outliers followed by an interactive manual elimination of false pings and errors in the raw data were corrected through tools and filters.

This technique allowed us to eliminate unreal data.

The filters and tools mainly used were:

1. *Depth and Range filters;*

2. *Nadir filter;*
3. *Editor del multibeam;*
4. *Editor del DTM (Digital Terrain Model; Fig. 33).*

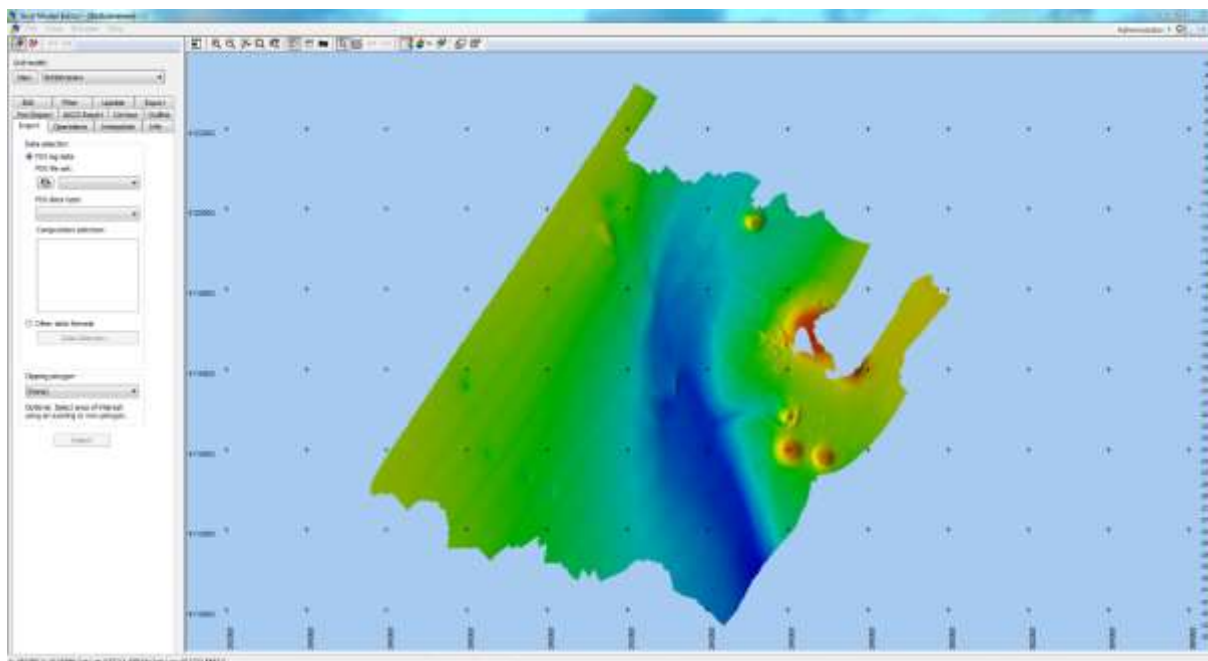


Figure 33 Screenshot of PDS200 during the editing of the multibeam data.

3.2 VERY HIGH RESOLUTION SEISMIC DATA (CHIRP)

The Sub-Bottom Profiler Chirp is a type of very high resolution geophysical technology which allows to obtain a good reconstruction of the sub-seafloor (in the order of few centimetres).

This technology generates an acoustic wave with frequencies between 2 and 7 kHz that are quickly sampled by Analog-to-Digital and that are converted and processed in real time.

3.2.1 ACQUISITION

The very high resolution seismic lines (single-channel) have been recorded using a hull mounted 16 transducer Teledyne/Benthos CHIRP III. The instrument was mounted below the oceanographic ship MINERVA UNO (Fig. 34).



Figure 34 Teledyne/Benthos CHIRP III equipment.

Data acquisition was performed using frequencies ranging 162 between 2 and 7 kHz and a ping rate between 250 and 750 ms, Tx power between 5 and 7, pulse 163 length of 10 ms and 30-42 db of gain.

The “Communication Technology SWANPRO” software recorded the seismic reflection data (Fig. 35).

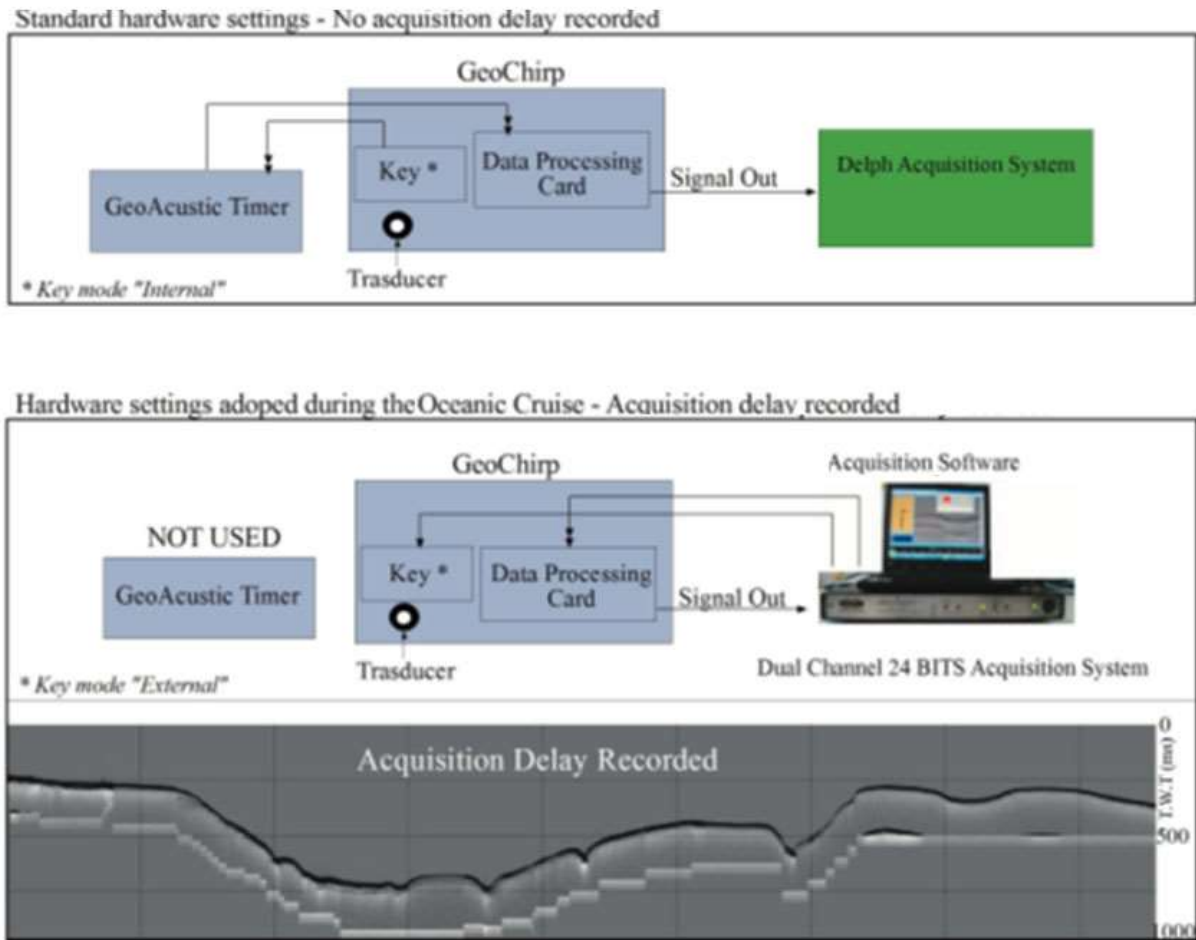


Figure 35 Hardware settings adopted during the Oceanographic Cruise.

3.2.2 PROCESSING

The seismic profiles were processed and interpreted using Kingdom and GeoSuite Work software packages.

Data processing included Automatic Gain Control, Swell Filter and Muting, and Time Variant Gain.

- **Automatic Gain Control, AGC:** This tool is based on a self-adapted amplification function that typically improves the filtered data. All the data is amplified to a

specific level of mV, within a window with variable time. This mathematical operator adjusts the gain of the reflectors.

- **Swell filter and muting:** The Swell filter and muting are mathematical functions that are based on different algorithms in the same plan.
 - The first one being an automatic function of the fund picking which allows to eliminate anomalies linked to abnormal oscillation of the boat such as due to strong waves or other effects linked to the instrument displacement.
 - The second is a function known as muting which is usually used after the filter previously described. It allow to eliminate the noise of the water column highlighting only the seismic data from the seabed, also eliminating the presence of gases plumes in the water column.
- **Time Variant Gain:** This filter is a statistic function of amplification of the signal. It may be constant for predetermined value in the time domain or can be variable in time choosing the time range in which to apply it. The signal grows linearly between two prefixed data values.

These operators are needed to overcome the limitations of these types of investigation, linked to the fact that acoustic waves generated from a point source propagate with a front spherical wave. In fact, the acoustic impulse decreases geometrically on the way from the source causing a loss of energy, which produces an attenuation of the reflectors in depth.

3.3 MULTICHANNEL SEISMIC PROFILES

The multichannel data used was acquired in many research cruises during the reconnaissance seismic campaigns progressively acquired by Agip, on behalf of the State, accordingly to Law July 21th 1967, n. 613.

The off-shore areas that were investigated for the petroleum exploration are marked by a capital letter from A to G. The documentation concerns expired, and therefore public, mining permits and concessions, filed since 1957 with UNMIG, National Mining Office for hydrocarbon and geothermal energy of the Ministry for Economic Development.



Figure 36 Location Map of the Zone C and G.

The main advantage of multichannel seismic systems compared to the single channel systems is that the same point of the seafloor and of the sub-seafloor, during the acquisition, is investigated by the acoustic wave many times. This skill that is named Common Mid-Point (CMP), with the redundancy investigation of the seabed, allows the stacking of the recorded traces which are assigned to the same location on the seafloor. This stacking greatly increases the Signal-to-Noise ratio (S/N) of the data, facilitating the processing of the raw data as well as the differentiation

of true signal returns from random noise (Yilmaz, 2001). The Common Mid Point stacking is based and always associated with other processing steps such as the geo-referencing of shots, receivers and mid-points, CMP-binning, velocity analysis and Normal Move-Out (NMO) correction.

In this work, seismic lines acquired in the “Zona C and Zona G” by the Department of Industry of the Italian Government (Figs. 36, 37) were used which are published and can be downloaded by ViDEPI Project website. The data was acquired using watergun and airgun instruments coupled with a 2400 m long multichannel streamer equipped with 96 groups, 15 geophones per group, a group interval of 25 m and an active section length of 50 m.

The profiles have low vertical resolution (between 10 and 80 m) and high penetration power (about 6 s TWTT).

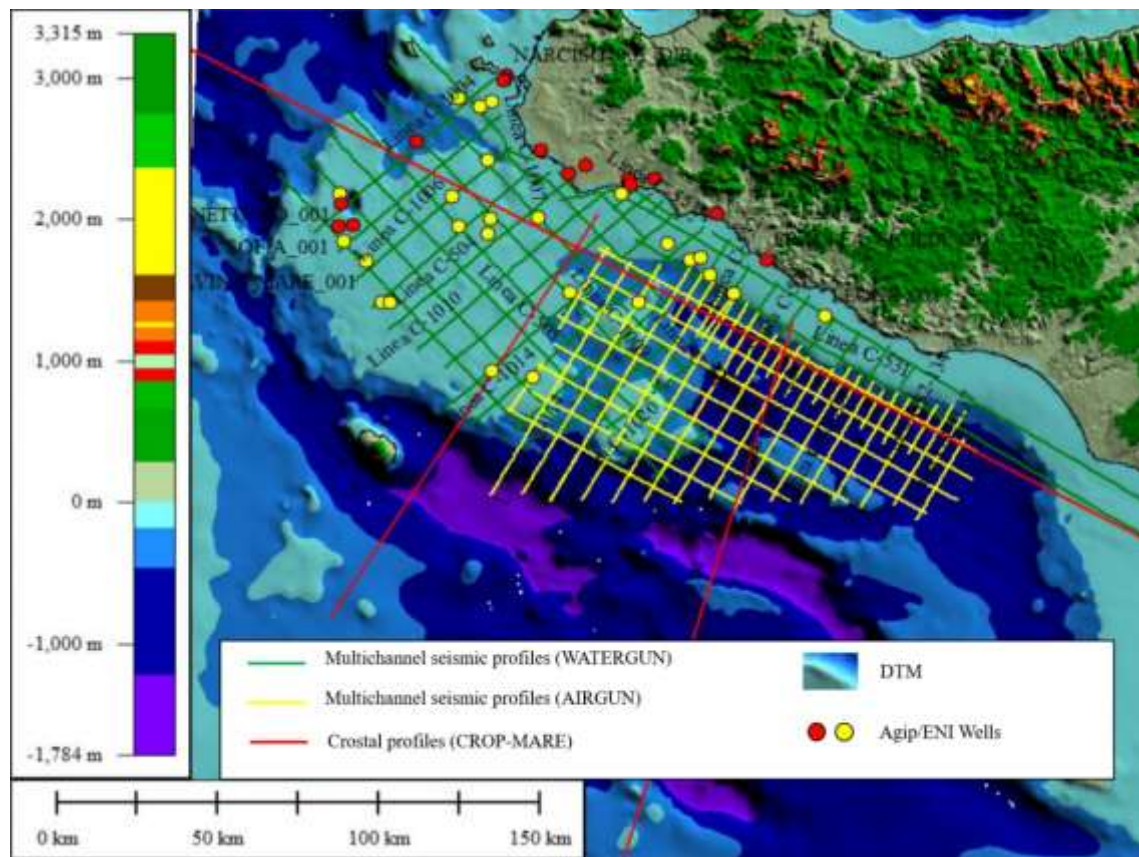


Figure 37 Multichannel seismic grid and shaded relief bathymetric map of the Sicily Channel based on data provided from ViDEPI and GEBCO projects. In green the water-gun multichannel seismic profiles, in yellow airgun multichannel seismic profiles and in red CROP profiles.

In the ViDEPI database, the multichannel seismic profiles are available in raster format (PDF). We converted the raster files to SEG-Y format files before any seismostratigraphic interpretation was carried out, (Fig. 38).

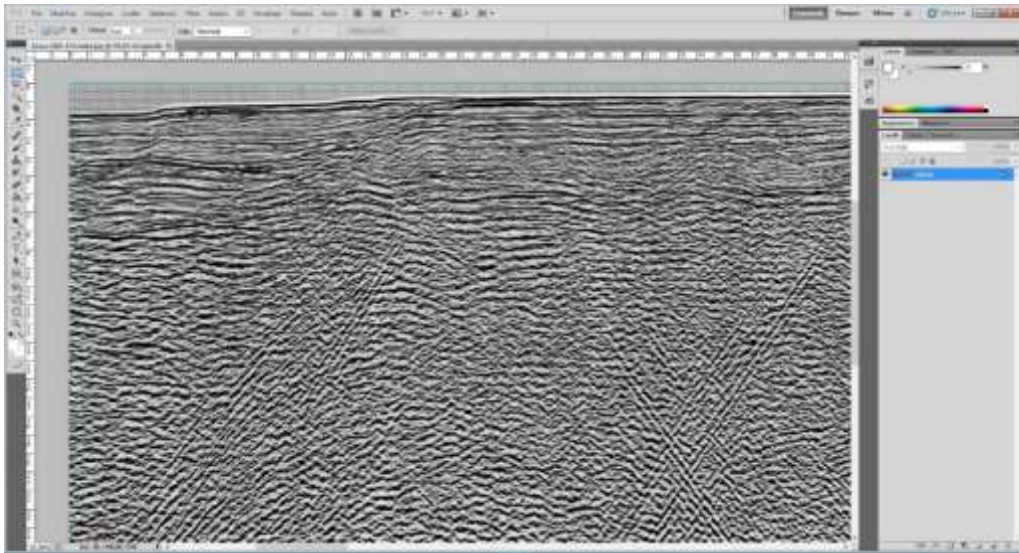


Figure 38 Editing of seismic profiles in raster format using Adobe Suite.

This involved merging all files in one seismic profile, geo-referencing them (Datum WGS84, UTM33) using a GIS software, and converting to SEG-Y format using a Matlab script (image2segy) (Fig. 39).

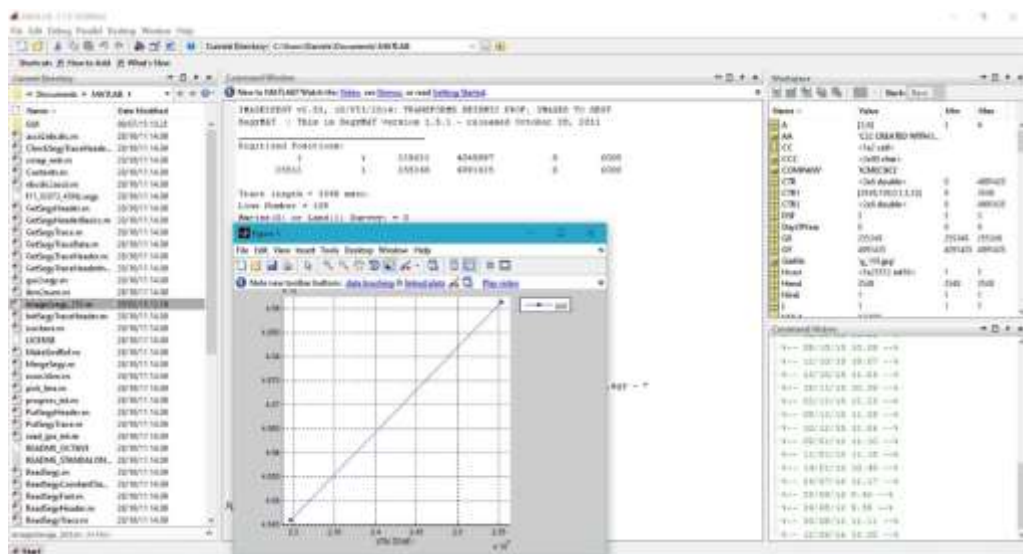


Figure 39 Conversion of the raster format to SEG-Y format using Matlab.

Chapter 4

4. THESIS OUTLINE

After an introduction into the topic, data & methods of the project and the regional setting of the Sicily Channel and in detail of the study area, the chapters 4 with the paragraphs 4.1, 4.2 and 4.3 represent main case studies, which were based on the main aims of the project.

They summarize the main results obtained in this Ph.D. project (such as the detailed description of the fluid escape structures, gravity driven deposits and volcanic seamounts), done on available geophysical data (CHIRP and Multichannel seismic profiles and Multibeam data) in the marine context of the sector around the Graham Bank.

These three individual works have been conducted for publication purposes and are given and drafted here in manuscript form.

4.1. Geomorphology of the volcanic sector around the Graham Bank (Sicily channel, central Mediterranean Sea)

Abstract

In this work, we are presenting the results of the geomorphological, quantitative analysis of the high-resolution bathymetric data (multibeam) associated with the seismostratigraphic of CHIRP profiles acquired during the ACUSCAL 2015 Cruise.

The study area is a small volcanic active area located in a shallow sector of the north-western Sicily Channel, at a distance of 45 km from the Sicilian coastline, where a cluster of seamounts (M1-M7) occur between 10 and 350 m in depth. They have been identified and studied in detail. Their main dimensions and associated parameters have been measured and tabulated allowing a morphometric and morphologic classification on a shape basis. In order to be certain of their volcanic origin, several restrictive criteria were applied (conical shape with maximum height, basal ratio, aspect ratio) to the initial tally, obtaining finally that can be identified and classified as volcanic seamounts. They are in shape and in size very similar to submarine volcanoes described on the seafloor in the earth.

The volcanoes are 115-180 m high and 500-1500 m wide showing at the top of some of them big flat morphology, and also they are characterised by steep flanks with an average slope of 30°. Their morphometric parameters allowed us to classify and to subdivide them in three different populations of seamounts based on their shape. M2 and M3 form the Graham Bank (3.5 km X 2.8 km) that was affected in the last 100 years, by many eruptions (Colantoni et al. 1975). Some of them show at the top plain morphologies interpreted as marine terraces.

Furthermore, the geomorphological and seismostratigraphic analysis permitted a better knowledge of the study area and to infer the tectonic control of the genesis and the growth of the cluster of volcanoes since the Last glacial Maximum. The volcanic seamounts are aligned along

two trends (NW-SE and N-S), parallel to the main tectonic structures of the Sicily Channel following the main tectonic trends of the Sicily Channel indicating that the growth of the Graham Bank sector had an important development (both with submarine and aerial events) into the genesis and evolution of the Sicily Channel.

Keywords: Graham Bank, seamounts, mound, active tectonics, submarine volcanic edifice, fluid escape.

1. Introduction

In the Sicily Channel, the volcanic activity is mainly concentrated in the islands Pantelleria and Linosa and in the group of submarines banks (Adventure Bank, Graham Bank, Nameless Bank and many other minor submarine banks). The volcanic activity of Pantelleria and Linosa Islands and submarine Banks is active since Plio-Pleistocene (Calanchi et al., 1989).

Seamount volcanism is a common characteristic in the marine environment and represents an important proportion of the world's sea floor (e.g. Pacific Ocean: Rappaport et al. 1997; Indian Ocean: Magde and Smith, 1995; Hillier and Watts, 2007; Atlantic Ocean: C.R. Ruiz et al. 2000; M.J.R. Gee et al. 2001; J. Dóniz et al. 2008; Mediterranean Sea: Favalli et al. 2005;).

Most of Earth's volcanic activity occurs beneath the sea, at water depths exceeding 1000 m (Carey and Sigurdsson, 2007; Rivera et al., 2013). One of the main controls of submarine eruptions is water depth that together with magma supply, its composition and volatile content control the submarine volcanic manifestations (McBirney, 1963; Head, J.W.I., and Wilson, L., 2003). Volcanic activity in shallow water may result in explosive eruptions (Kokelaar, B.P., and Durant, G.P., 1983) Tracking the depth of an eruption, of how it evolves together at a precise morphobathymetric reconstruct are essential for risk analysis. Tracking the depth of an eruption,

of how it evolves together at a precise morphobathymetric reconstruct are essential for risk analysis.

In recent years, the acquisition of multibeam swath bathymetry associated often with CHIRP (very-high resolution seismic profiles) has enhanced the knowledge of submarine volcanic areas all over the world (Gee et al., 2001; Hürlimann et al., 2001; Masson et al. 2002; Mitchell et al. 2002; Le Friant et al. 2004; Sigurdsson et al. 2006; Wright et al. 2006, 2008; Oehler et al. 2008; Llanes et al. 2009; Sakellariou et al. 2010; Casalbore et al., 2011; Conte et al., 2014).

Two main approaches can be distinguished in the development of morphometric analysis of submarine volcanoes. However, in the last decade they have become more quantitative conducted on statistical study and have different objectives including morphological definition of the seamount (e.g. Jordan et al. 1983; Smith and Jordan, 1987; 1988), determination of the volcano size (Favalli et al. 2005), establishment of correlations between volcanoes parameters such as height, volume, diameter max, diameter minimum and other (Rappaport et al. 1997; C. R. Ruiz et al. 2000).

In all the Sicily Channel, the seabed shows evident presence of submarine volcanism and in particular in proximity of the Pantelleria and Lipari Islands, and in the northwestern sector such as around the Sector of Banks (e.g. Adventure, Graham, Nerita, Terribile, Nameless), which is a great volcanic sector known as “Campi Flegrei of the Sicily Channel”. It is characterised by a shallow continental shelf, less than 180 m deep on average with low inclination, often less than 1-2° with a big shelf break is located at depth between 90 m (central sector) and 135 m (western and eastern part). The above-mentioned volcanic banks (peaks at 7 m above sea level), are often composed of several volcanic seamounts, located at depths often less than 250 m. These submarine banks are characterised by different typology of volcanic activity often associated a many morphology elements both positive both negative, such as dykes, neck, hummocky surface or individual

hummocks but also seabed morphologies likely associated to escaping of fluid such as pockmark and mound). Some of them often display sub-flat surfaces often showing traces of marine abrasion and some-times subaerial erosion.

Global sea-level changes can be determined by several factors, including large-scale geological processes (plate tectonic movements which produce variations in the capacity of sedimentary basins), astronomical and sub-Milankovian cycles (Schulz, 2002; Caputo, 2007).

In this paper, using a very high resolution dataset both multibeam and CHIRP, we for first time, wanted to investigate the morphology and quantitatively describe and classify the seamounts in different groups with different evolution. In order to define the morphological variability of the volcanoes. We measured and estimated many parameters such as basal shape, basal diameter max, basal diameter minimum, summit diameter, basal depth, summit depth, height, volume, flatness, flank slope. This mathematical study associated to morpho-bathymetric and stratigraphic analysis allows a detailed characterization of recognised seamounts. In conclusion, on the basis of an integrated morphological and seismostratigraphic reconstruction with the geological background, the main aims of the paper are to report of evidence of the principal structures on the genesis and to infer the evolution of the Graham Bank.

2. Geological setting

The Sicily Channel (central Mediterranean Sea) is a structural element of the African continent, between the southern coast of Sicily, the northern coast of Africa and the Malta Escarpment (Fig. 1). It is a part of the foreland Sicilian-Maghrebian Fold and Thrust Belt (FTB) and is often described as a result of both the post-collisional convergence between Africa and Europe (Bonardi et al., 2003), and the roll-back of the subduction hinge of the African-Ionian crust (Catalano et al., 1996; 2000a; Granath and Roure, 2004; Finetti et al., 2005).

The Sicilian FTB is a roughly S-vergent thin-skinned imbricated wedge, progressively emplaced since the Miocene. The FTB originated from the piling-up of tectonic bodies, deriving from the deformation of the paleo-geographic domains developed during the Mesozoic in the African rifted continental margin. It grows above a northwest dipping regional monocline consisting of Mesozoic carbonate platform deposits of the Iblean foreland, covering the stretched African continental crust (Handy et al., 2010; Catalano et al., 2013 and references therein).

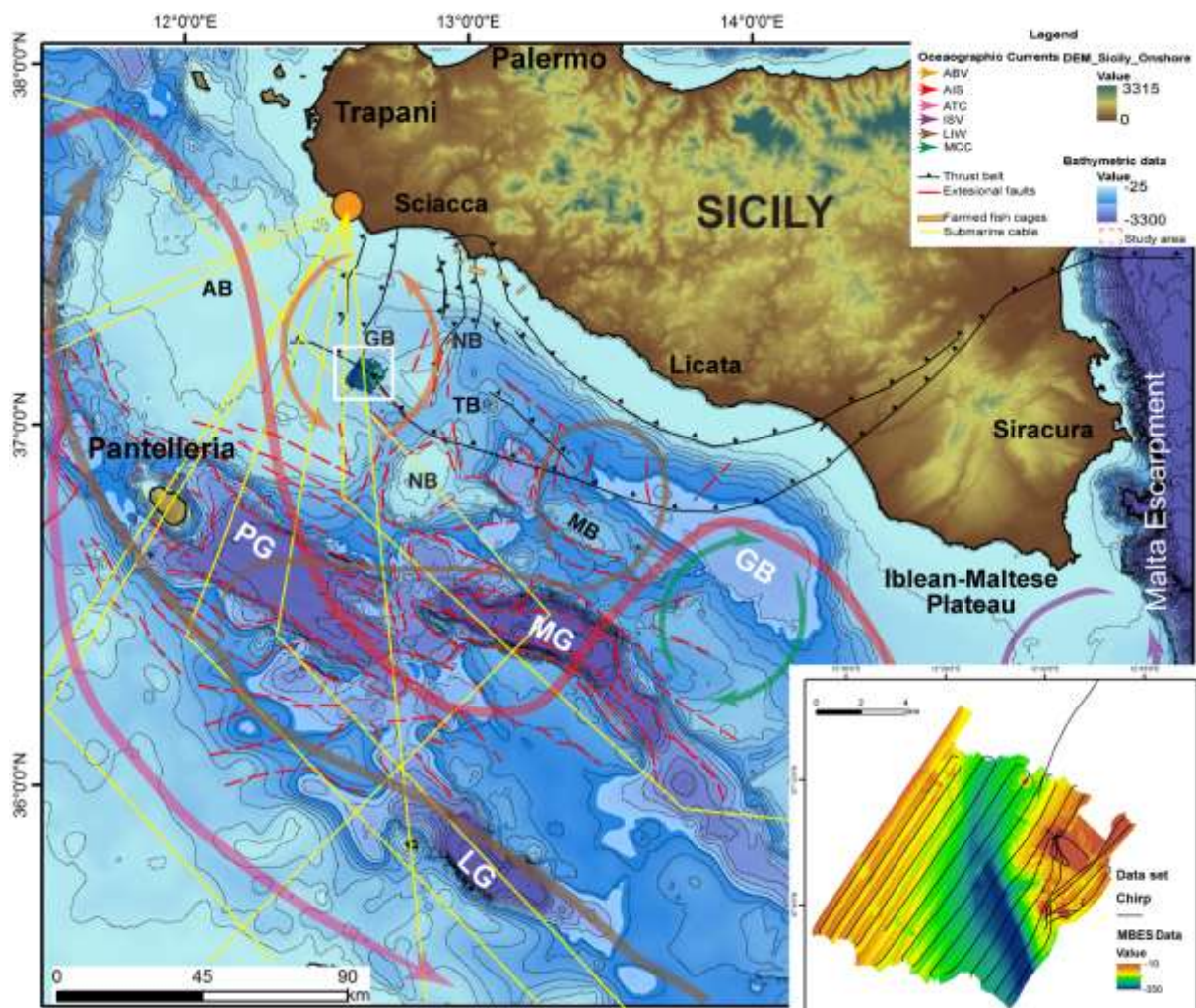


Figure 1 Bathymetric map of the Sicily Channel (Central Mediterranean), showing the main physiography, Plio-Pleistocene graben systems, and distribution of main pathways Main water masses: MAW (Modified Atlantic Water), LIW (Levantine Intermediate Water); AIS (Atlantic Ionian Stream), ATC (Atlantic Tunisian Current); ABV (Adventure Bank Vortex); MCC (Maltese Channel Crest); ISV (Ionian Shelfbreak Vortex); ABV (Adventure Bank Vortex) and in yellow indicated the submarine cables. The inset shows morphobathymetric and seismic reflection data set.

The foreland area, cropping out in south-eastern Sicily (Iblean-Maltese Plateau) and submerged in the Sicily Channel (Pelagian Block), is the result of the interaction of both the Sicilian-Maghrebian collision and the Sicily Channel rifting (Fig. 1, Argnani, 1990; Catalano et al., 1996; Sulli, 2000; Finetti et al., 2005). The Pelagian carbonate platform—consists of 6-7 km thick Mesozoic carbonate platform and pelagic deposits, with several volcanic (mostly basalts) intercalations. They display lateral facies variations as a result of the syn-sedimentary fault systems active during the Jurassic extensional rifting tectonics (e.g., Streppenosa basin; Patacca et al. 1979; Frixia et al. 2000). The carbonate succession is covered by 2-2.5 km of Miocene-Pliocene clastic, evaporitic and carbonate deposits (Antonelli et al., 1991; Catalano et al., 1996).

The present day structural setting of the Sicily Channel is characterised by NW-SE -oriented sub-vertical Neogene-Quaternary normal faults controlled the horst-and-graben structural setting of the “Sicily Channel Rift Zone” (Pantelleria, Malta and Linosa grabens and Adventure Bank, Fig. 1, Finetti, 1984; Argnani, 1990; Corti et al., 2003 and references therein).

Three bathymetric depressions, Pantelleria, Malta, and Linosa grabens (Fig. 1) that are the morphological expression of a continental rifting episode affecting the northern African lithosphere since the Neogene-Quaternary (Finetti, 1984; Argnani, 2009) dominate the Sicily Channel. The rifting thinned the continental crust to 15–18 km since the Early Pliocene (Argnani 1990; Civile et al. 2008) and opened the above-mentioned grabens controlled by NW-SE subvertical normal faults (Fig. 1, Finetti 1984; Torelli et al. 1991; Catalano et al., 1993; Finetti & Del Ben 2005; Civile et al. 2010).

The rifting process was often accompanied by widespread subaerial and submarine volcanic activity (i.e., Pantelleria and Linosa volcanic islands, Graham and Nameless banks, Fig. 1). This volcanism, with alkaline to peralkaline affinity related to anorogenic magmatism (Corti et al., 2006; Rotolo et al., 2006), has taken place from the Pliocene (Nameless Bank) to the present-day

time (Ferdinandea and Foerstner volcanoes, Fig. 1, Colantoni et al. 1975; Beccaluva et al. 1981; Calanchi et al. 1989; Peccerillo, 2005).

Seismic activity involves up to 20 km deep hypocentres with $M_L < 3.5$ (Chiarabba et al. 2005; Galea 2007). Earthquakes can occur along N-S trending belt, between the Sciacca offshore and the Lampedusa and Linosa Islands, down to a depth of 60 km, reaching $M_L \geq 5$ (Calò and Parisi, 2016).

3. Materials and Methods

In this work, we used different types of high-resolution data acquired during the ACUSCAL cruise, carried out in 2015 aboard the R/V *Minerva1*, in the framework of the RITMARE Project (CNR IAMC Sez. Capo Granitola, Mazara del Vallo) (Fig. 1b).

Multibeam echosounder coverage of 100 km² of seafloor has been obtained using the Reson SeaBat 7160, which generates 512 beams at a nominal frequency of 44 kHz. Differential Global Positioning Systems (dGPS) by FUGRO SEASTAR provided positional data. The multibeam data were processed using the PDS-2000 software; this included removal of erroneous beams, noise filtering, processing of navigation data and correction for sound velocity. A Digital Terrain Model (DTM) was obtained with a grid size of 5 m.

A grid with 200 km of CHIRP profiles were acquired using a hull-mounted 16 transducer Teledyne/Benthos CHIRP III profiler. This instrument works with frequencies ranging between 2 and 7 kHz, a ping rate between 250 and 750 ms, Tx power between 5 and 7, a pulse length of 10 ms and 30-42 db of gain. The “Communication Technology SWANPRO” software was used to acquire and store the data. The profiles were processed and interpreted using Kingdom and GeoSuite Work software packages. Data processing included Automatic Gain Control, Time Variant Gain, Swell Filter and Mute. The time-depth conversions of the Chirp profiles have been made adopting average velocities derived from lithostratigraphy and sonic log data collected in

the southern and western Sicily offshore. A seismic P-wave velocity of 1600 m/s was used for the Holocene sediments, whereas 1500 m/s was used for seawater (Catalano et al. 2000).

4. Results

4.1 Geomorphological characterisation

In the north-western Sicily Channel there is a triangular morphological high 360 km² wide, comprising the Graham (-7 m), Nerita (-16 m), and Terrible (-20 m) Banks (Fig. 1). We focus on the area comprising the Graham Bank and the seafloor to its southwest.

The study area is a submarine volcanic sector, comprising between 10 and 350 m in depth, characterised by a jagged seafloor morphology, where seamounts, fault escarpments, submarine plain, pockmarks and mounds occur. Its seafloor morphology is irregular due to the occurrence of mounds, ridges, scars, pockmarks, and small escarpments. Seven morphological highs that comprise a cluster of seamounts (Coltelli et al. 2016) have been identified and mapped (M1-M7 in Figs. 2, 3).

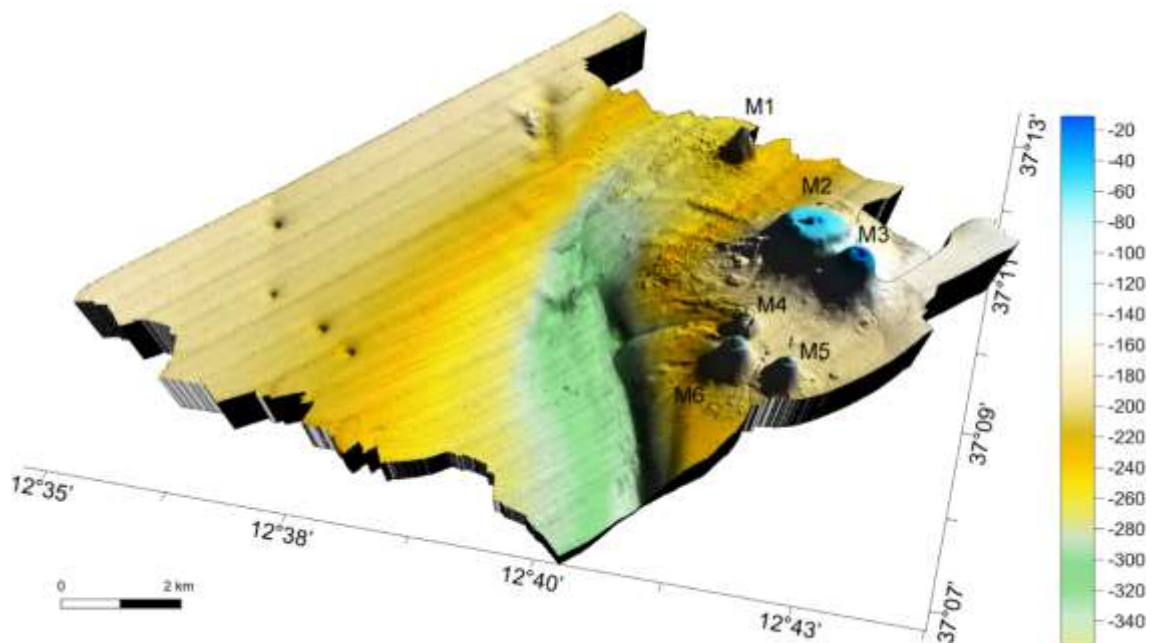


Figure 2 Digital Elevation Model of the study area. The eastern sector is, characterised by several morphostructures: M1-M7 volcanic seamounts. Vertical exaggeration 1:5.

4.1.1 Western sector

The general morphology of the western part is flat and has an average slope gradient of 1.2-1.5° (increasing westward; Figs. 2, 3).

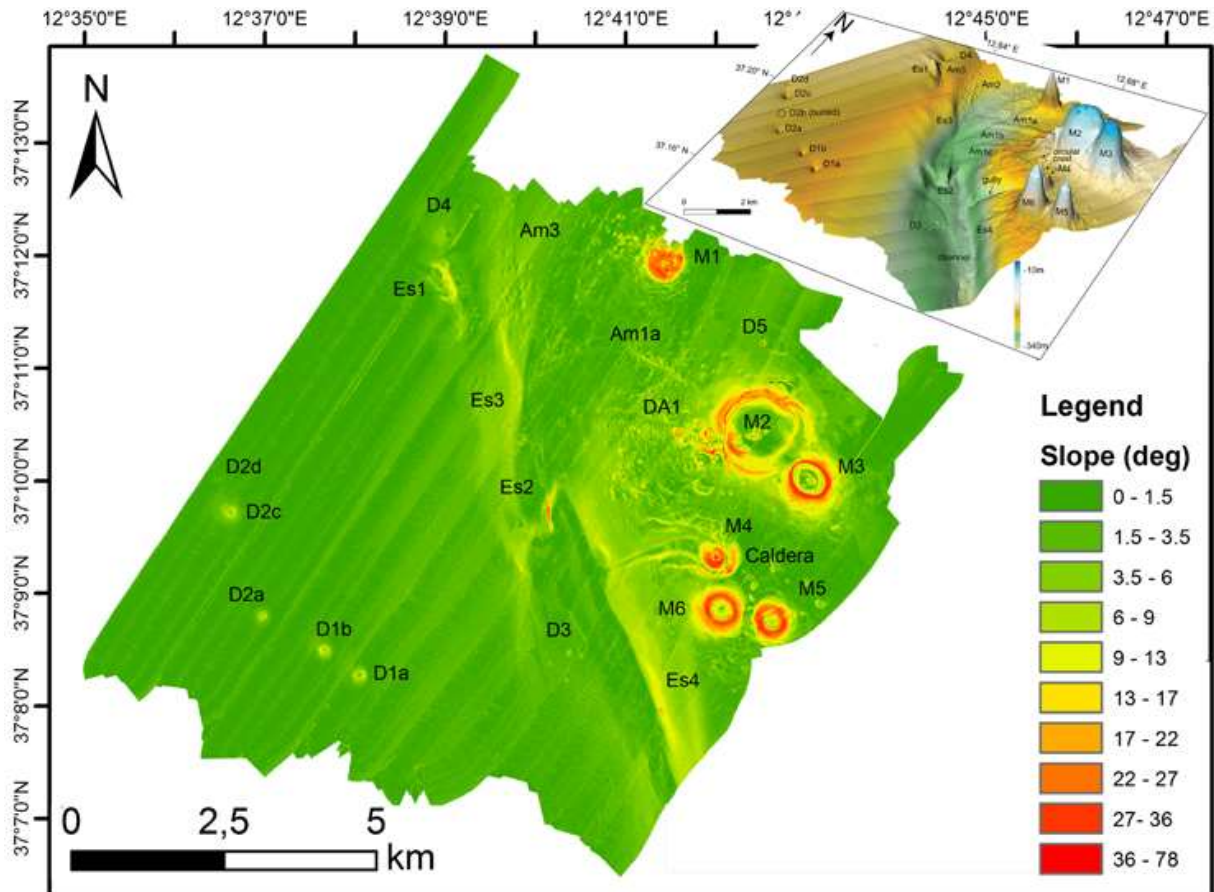


Figure 3 Slope map with the main recognised structures (M1-M7 mounds, Am1-Am3 aligned mounds, Es1-Es4 fault escarpments, D1-D2 aligned, D3 clustered and D4 isolated pockmarks). In Fig. 3b. Digital Elevation Model of the study area.

About 20 sub-circular, negative relief structures, interpreted as fluid escape features (pockmarks), occur at water depths from 195 to 317 m. They have diameters of 25-580 m, depths of 1.3-15 m, and wall slope gradients (of the walls) up to 23°. They are often grouped in clusters that are either aligned NW-SE or NNW-SSE, or occur individually.

A 27 m high, NW-SE -oriented elongate steep escarpment (Es1 in Fig. 3) is located in the northernmost part of the study area.

4.1.2 Central sector

An intervening channel runs, predominantly, in an N-S and NW-SE direction and is bounded, along its SW and NE sides, by sub-vertical fault-escarpment (Es2-3 and Es4 in Fig. 3). It has a length of 10 km, depth of 250-350 m, and width of 0.8-1.5 km (Figs. 2, 3). It has an incised, U-shaped thalweg, moderately concave upwards at depths of up to 310 m.

The channel becomes asymmetrically V-shaped between 310 m and 325 m, and flat in its southernmost side. A concave break in slope separates the channel in two different segments at a depth of about 305 m. In the NW segment, the downslope gradient varies between 1° and 2°, whereas in the SE segment, the gradient is <1° (Figs. 2, 3).

The channel walls have gradients vary between 4° and 7°, forming escarpments about 100 m high. The top of these escarpments is characterised by a convex break in slope at a depth between 220 m and 270 m. In the neighbour of the concave break in slope, a NNW-SSE -oriented elongated steep escarpment, 25 m high, occurs (Es2 in Figs. 3).

4.1.3 Eastern sector

The morphometric analysis of these structures has been conducted to measure all size of these structures that have been renamed as Sicily Channel Volcano: M1-M7 and we measured and tabulated their dimensions in Table 1.

M2 and M3 form a NW-SE oriented elongate structure, which corresponds to the Graham Bank, 3.5 km long and 2.8 km wide (Figs. 2, 3, 4).

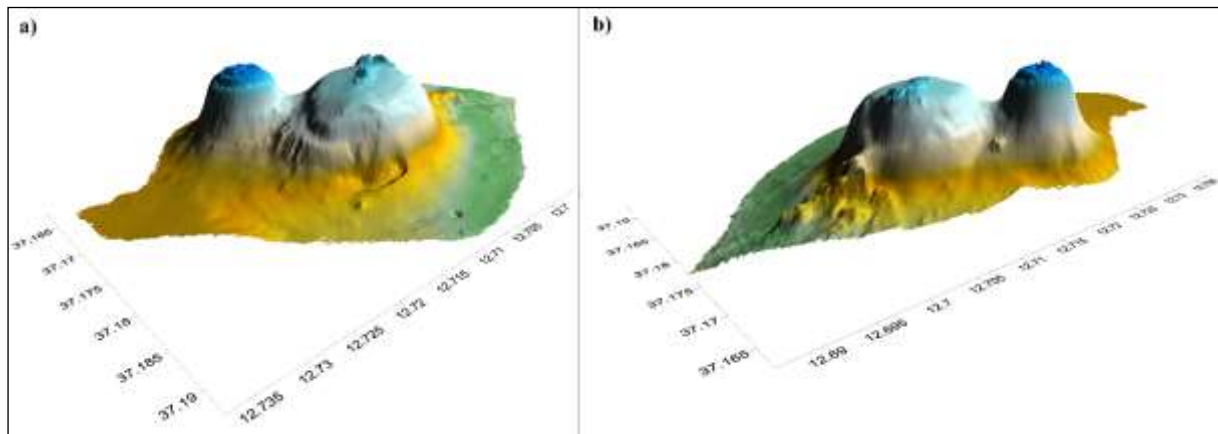


Figure 4 3D Digital Elevation Model of the Graham Bank.

M1 is a small volcanic 115 m high and 812 m wide at the bottom and about 150 m at the top. It rises from a gentle sloping seafloor at 240 m depth and is bounded by strong inclined flanks with 20° of average slope and with maximum gradient of 26° (Figs. 2, 3, 4).

M2, 155 m high and sloping at 14-19°, is the largest one (Figs. 2, 3, 4). Around this structure and at its top there are many smaller mounds (Figs. 2, 3, 4). Along its western flank, the seafloor is extremely indented due to the presence of a large fan shaped body (DA1 in Figs. 3, 4, 5), composed of different NW-SE and NNW-SSE oriented ridges.

DA1 consists of a big heterogeneous deposit with fan shape, which form a chaotic pattern typical of a hummocky sea floor surface. It is hanging 200-250 m below the top of M2. The deposits accumulated over a surface 2D of 2.15 km² and a surface 3D of 2.2 km². Its basal major axis length (E-W elongated) is about 2.2 km and minor axis 2.1 m x 2 km with it has an estimated volume of 0.15 km³ (Figs. 2, 3, 4).

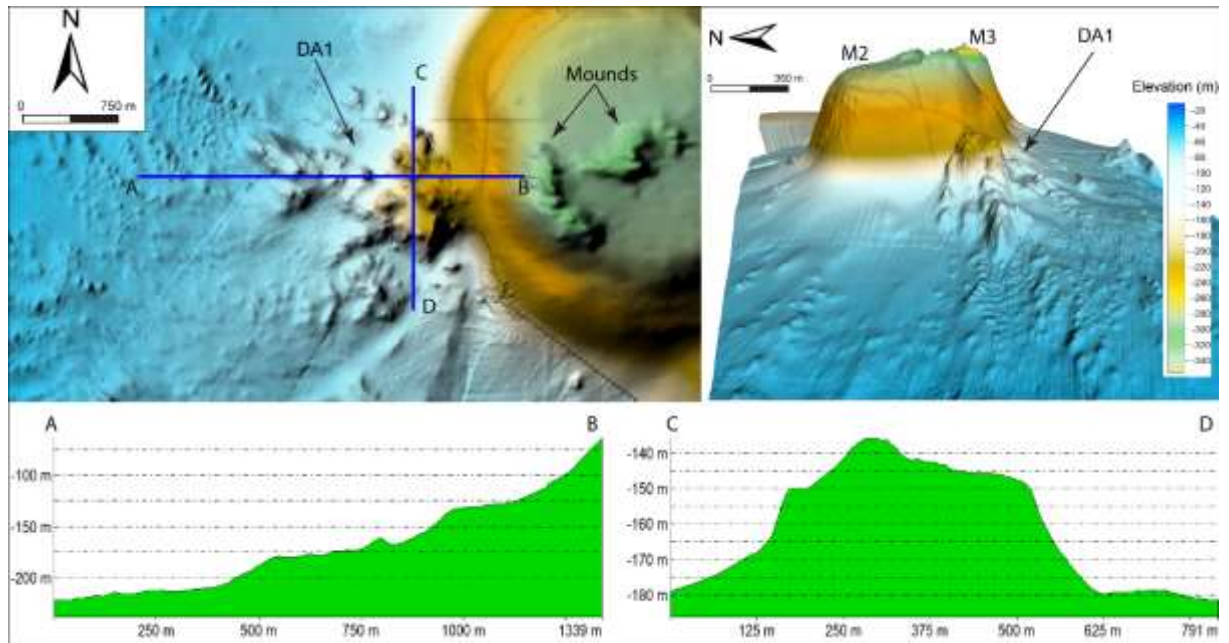


Figure 5 Shaded relief of the Graham Bank composed of M3 showing mounds and a fan shaped body (DA1). In the bottom bathymetric profiles crossing the centre of the DA1.

A small circular depression defined by a relatively well-preserved rim occurs in the north-east of M2 (Figs. 3, 4, 6). Most of this structure rim ranges between 150 and 170 water in depth.

It is elliptic in shape, aligned northwest to southeast and 540×220 m wide, with a surface area of 0.012 km^2 and a volume of 0.0005 km^3 . Into its centre, a small dome-shaped mound, 15 m high, with steep walls sloping at 6° occurs (Figs. 3, 6).

Evidence of active fluid flow system, plumes and pockmark (Fig. 5), were observed in places in proximity of circular negative morphology (Fig. 6).

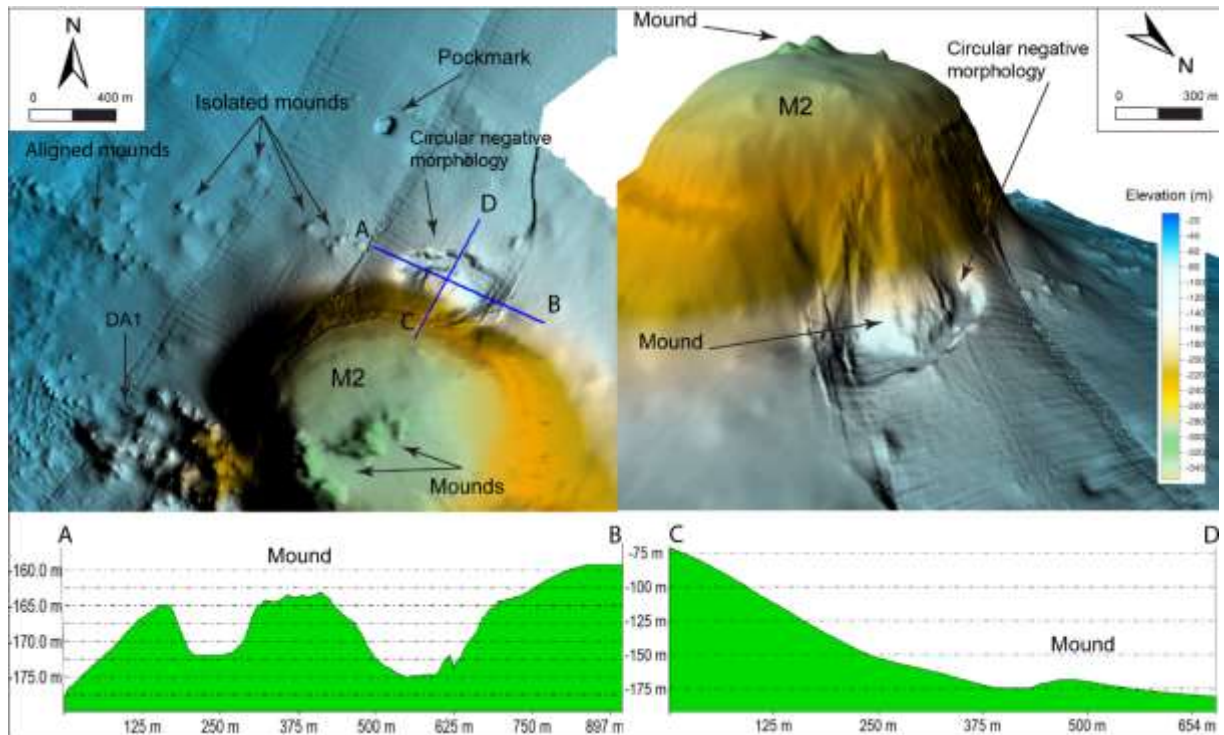


Figure 6 Shaded relief of the Graham Bank composed of M3 showing DA1, mounds, pockmark and the negative morphology. In the bottom bathymetric profiles crossing the centre of negative morphology.

M3 is 148 m high; it is 980 m wide at the bottom and 780 m at the top. It rises from a gently sloping seafloor at 79 m water depth in the NW and at 149 m in the SE and is bordered by inclined flanks and rimmed on the top by a plain surface (Figs. 3, 7). Its northern and southern flanks have slope gradients of 10° . The eastern flank deepens to 148 m, with maximum gradient of 27° , while the NW flank has a slope gradient of $24\text{--}25^\circ$.

Isolated, clustered and aligned mounds are common across the western and south-western flank of the Graham Bank (Figs. 2, 3, 5, 6). The aligned morphologies (oriented about NW-SE and NNW-SSE) are length up to 600 m height between 1.5 m and 10 m (Figs. 2, 3, 5, 6).

The summits of M2 and M3 are characterised by plain surfaces with gradient between 1.4 and 2.3° with maximum width of 300 m that often is incised by numerous aligned small gullies (Figs. 2, 3, 4, 5, 6, and 7).

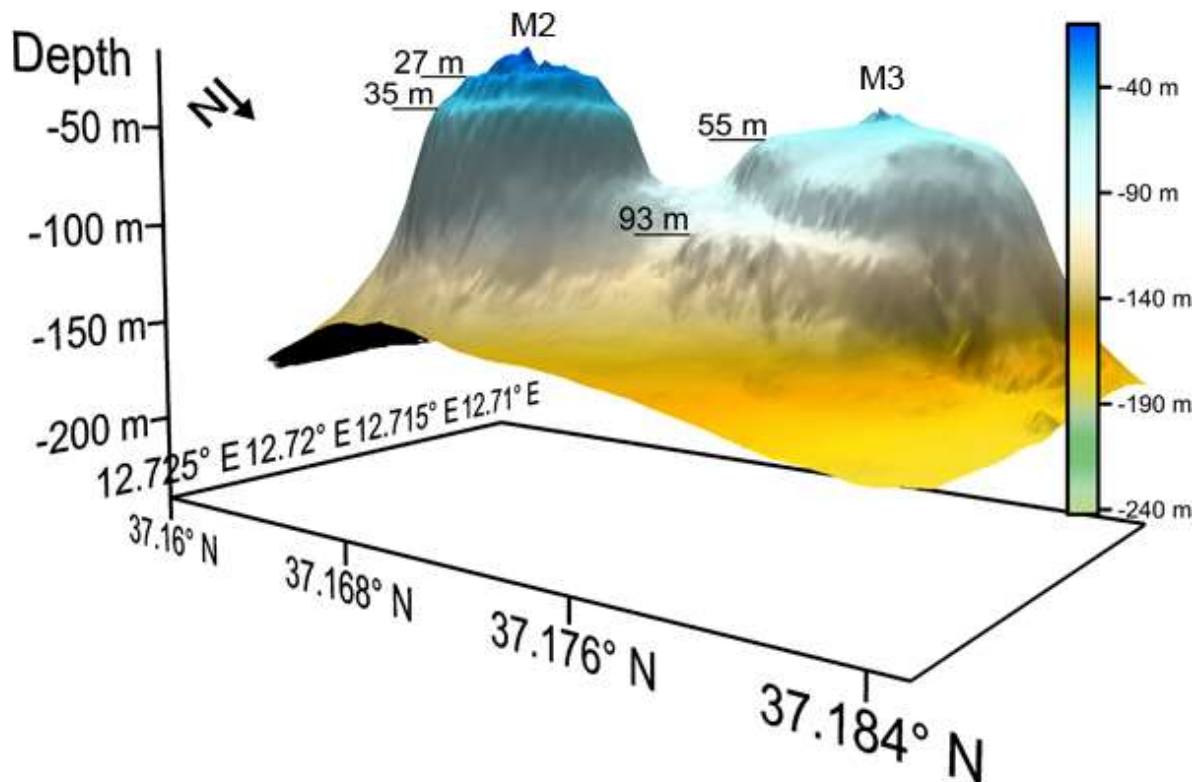


Figure 7 3D view of the Graham bank showing the flat morphologies identified at the top of the volcanic bank (vertical exaggeration 1:7).

At the south of M2, we recognised a prominent saddle with concave form, 80 m high and 1.3 km wide, divides two very distinct volcanoes the Graham Bank (Fig. 8).

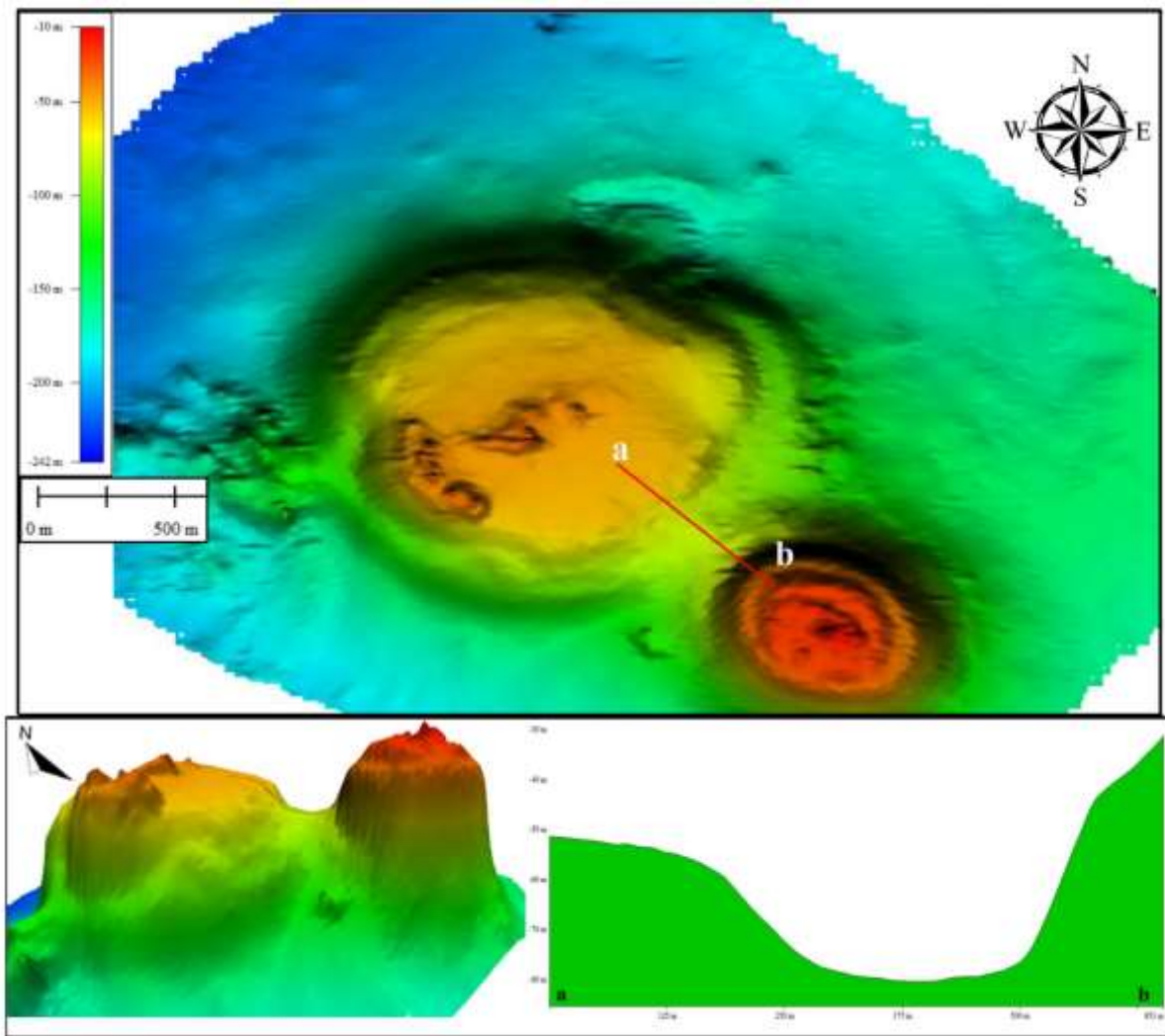


Figure 8 Shaded relief of the Graham Bank composed of M3 showing the saddle. In the bottom bathymetric profiles crossing the centre of the saddle (vertical exaggeration 1:7).

M4 is 123 m high and 500 m wide. It has a typical cone shape and rises from a great sloping seafloor at 230 m depth, and is bordered by very strong inclined flanks with 30° of average slope. It is characterised at the top by a sharp summit at 103 m depth (Figs. 9, 10).

The shaded relief images clearly show the presence around its south-eastern flank the seabed that deepens to 174 m, of a saddle with u-shape in section followed of a high morphology (22 m height) showing a pointed annular shape (Fig. 8).

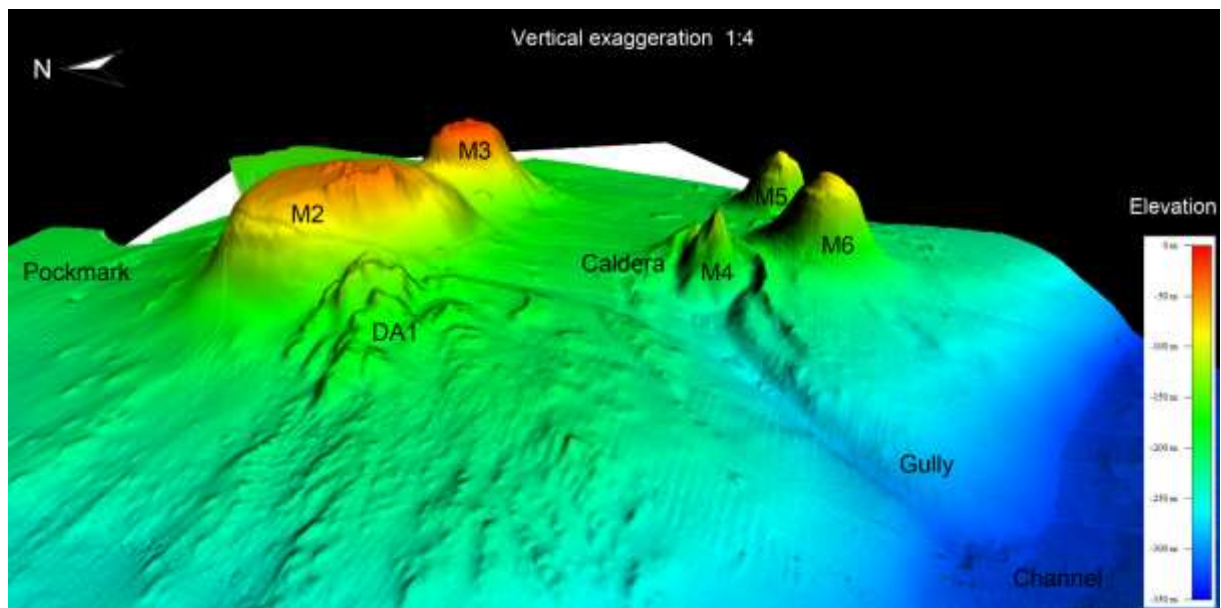


Figure 9 Shaded relief of the Graham Bank showing the main volcanic features.

M5 is a volcano 141 m high and 740 m wide at the bottom and about 350 m at the top. It rises from a gentle sloping seafloor at 210 m depth and is bordered by strong inclined flanks with 22° of average slope. It is rimmed on the top by a small plain surface of about 80 m wide with a slope of 8° (Figs. 9, 10).

M6 is a volcano 117 m high and about 770 m wide at the bottom and about 280 m at the top. It rises from a sloping seafloor at 197 m depth and is bordered by very strong inclined flanks with slopes of about 25° . It is rimmed on top by two small plain surfaces at different depths (97.3 m and 83 m) and are 55 m and 100 m wide respectively, both with slopes of less than 4° .

ID	Lat.	Long.	D (m)	d (m)	Sb (km ²)	St (Km ²)	Pb (km)	Pt (km)	V (Km ³)	H (m)	R (m)	Bt (m)	Bb (m)	bsr (d/D)	ds	flatness	Fs	R/h
M1	37° 12.06522' N	12° 41.50725' E	812	694	0.4483	0.01553	2.517	0.478	0.0169	115	406	124	239	0.854679803	25	0.036023055	62.84	0.28
M2	37° 10.58369' N	12° 42.61890' E	1503	1387	2.012	0.4954	6.271	2.599	0.1652	152.7	751.5	33.3	186	0.922821025	810	0.583994232	69.24	0.21
M3	37° 10.17622' N	12° 43.14215' E	980	780	1.275	0.0965	2.716	1.142	0.0591	148	490	11	159	0.795918367	406	0.520512821	55.95	0.3
M4	37° 9.44090' N	12° 42.21293' E	494	391	0.159	0.04155	1.475	0.736	0.00623	123	247	103	226	0.791497976	126	0.322250639	67.28	0.49
M5	37° 9.00621' N	12° 42.26925' E	960	750	0.4137	0.0887	2.316	1.017	0.02697	141	480	69	210	0.78125	100	0.133333333	53.32	0.29
M6	37° 8.91760' N	12° 42.82876' E	900	760	0.3174	0.0653	2.054	0.931	0.0634	117	450	80	197	0.844444444	90	0.118421053	44.27	0.26
M7	37° 13.03627' N	12° 42.25717' E	850	850	0.5				0.0238	123	425	96	219	1	22	0.025882353		0.29

Table 1 Location and measured and estimated parameters of seven selected volcanic seamounts

4.2. Seismic characteristics

An investigation of the seismic reflection profiles intersecting the study area highlights the presence of several structures organised in different seismic units.

We define three main facies named units A-C.

- The lowermost unit A is an acoustically transparent seismic facies due to poor penetration of the seismic signal. It is mainly detected in the western sector of the study area. It has a discontinuous pattern with the reflector offset by normal faults dipping to the NNE and SSW locally dislocating also the seabed (Fig. 10).
- Unit B overlies facies A and occurs across the eastern sector of the study area. It is an acoustically opaque/transparent seismic facies due to poor penetration of the seismic signal (Fig. 10). It comprises discontinuous, high-amplitude reflectors laterally passing to the facies A.
- Unit C comprises thin layered, high-amplitude and divergent to aggrading reflectors, with good lateral continuity, that alternate with low-amplitude reflectors. The unit (affected by many faults) is characterised by a tabular external shape and maximum thickness of 90 ms TWTT corresponding to 72 m if we assume seismic P-velocity of 1600 m for this facies.

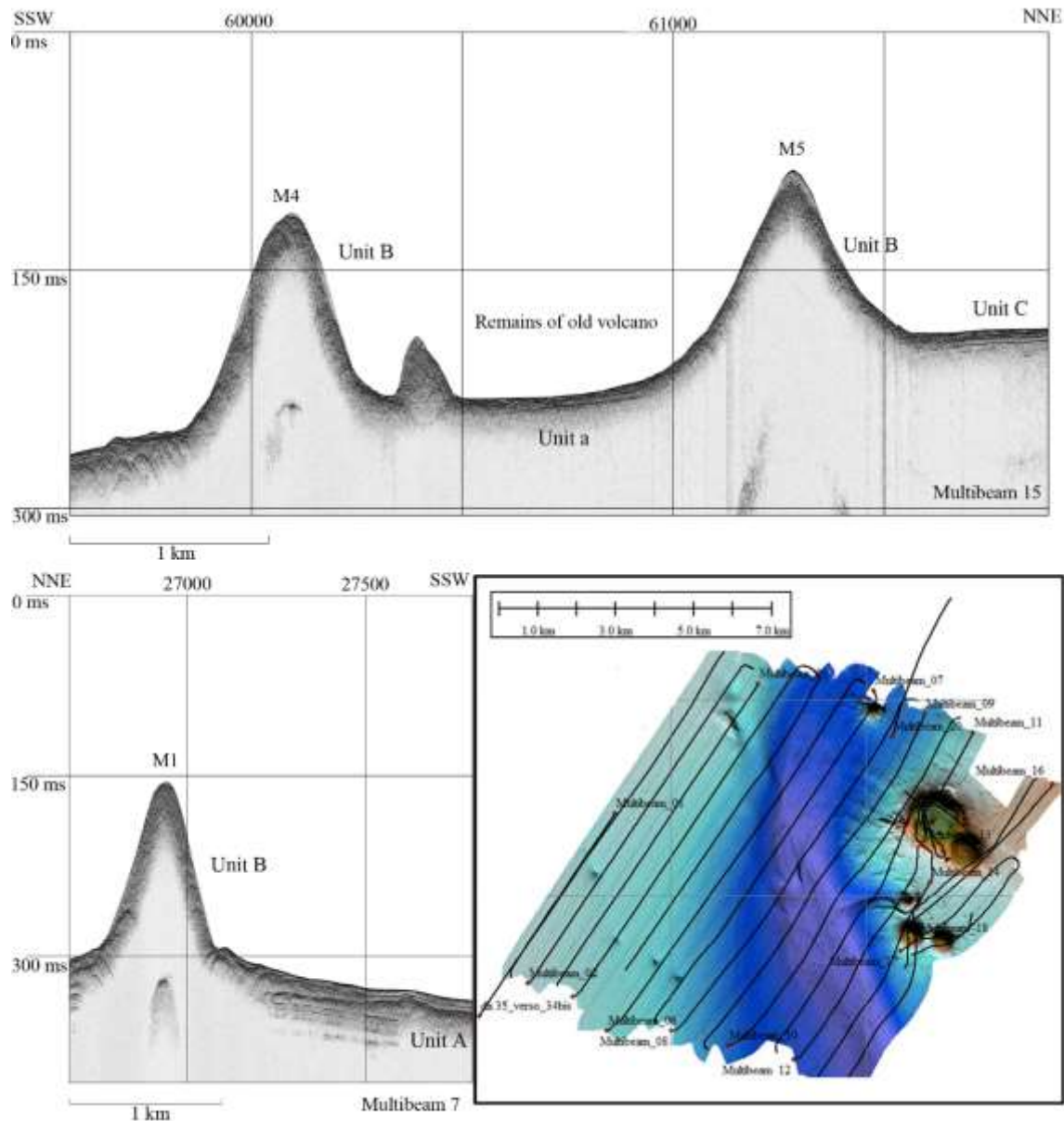


Figure 10 Chirp profiles showing the presence of the volcanic seamount named M1 and M4, M5 located in the north of the study area.

At the north of the studied area mapped, another seamount (123 m high and 860 m wide) occurs (M7 in Fig. 11). It rises from a sloping seafloor at 219 m depth and is bordered by very strong inclined flanks.

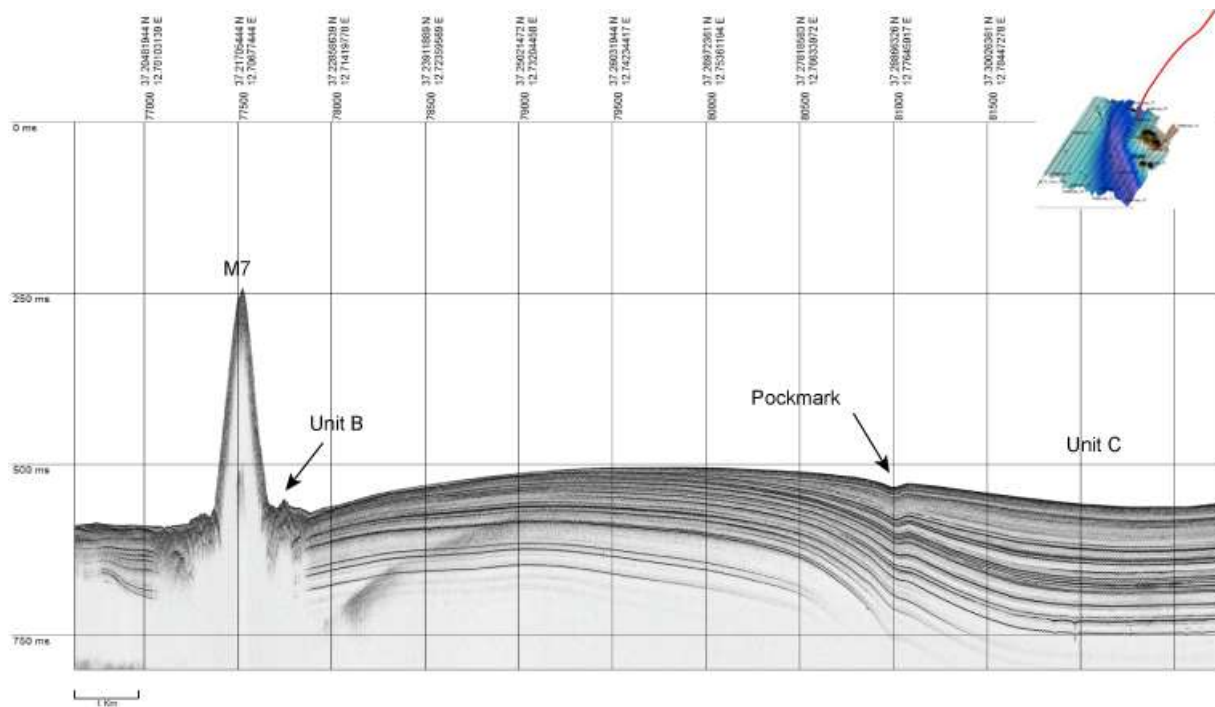


Figure 11 Chirp profile showing the presence of the volcanic seamount named M7 located in the north of the study area.

5 Discussion and conclusions

5.1 Tectonic control

Our study area is clearly affected by recent normal fault systems activity showing topographic and morphological evidence. Our data do provide evidence of the geomorphic response to the occurrence of fault structures. A cluster of seven seamounts with trends about NW-SE and NNW-SSE and a cluster of aligned fluid escape structures such as mounds, pockmarks and plumes (about NW-SE) occur. These structures, which have trends parallel with the main directions of the tectonic setting of the Sicily Channel, display a recent activity of the area.

We therefore propose such alignment of volcanoes NW-SE oriented coincide with these fault systems and that this extensional tectonic regime controlled their genesis and evolution of the Sicily Channel. Furthermore, this inference is also corroborated by the spatial concentration of recent seismic activity along the northern section of the Sicily Channel where there is a multi-layer that corresponds to Mesozoic Carbonate Platform, buried by Plio-Pleistocene deposits, locally

affected by vertical normal faults (Corti et al. 2003, 2006; Civile et al. 2010; Calò and Parisi, 2016).

5.2 Morphological interpretation of the seamounts

We measured and estimated parameters (tabulated in table 1), using a morphometric approach proposed in previous studies which were conducted in different submarine volcanic context such as East Pacific Rise (Scheirer and Mcdonald 1995; Scheirer et al. 1996), Easter Island (Rappaport et al. 1997) and Canary Islands (Romero et al. 2000). This methodology allowed us to infer the origin and evolution of the seamounts bu different cross correlation.

All established cross-correlations in this work, using the main size of the seamounts (Figs. 2, 3) such as height, basal radius, volume, base area, flatness and standard deviation slope, bsr (minimum diater/maximum diameter) that are tabulated in table 1, have been confronted with the calculated cross-correlations of the main seamounts in the world obtaining a good relationship with them (Scheirer and Macdonald, 1995; Scheirer et al., 1996; Rappaport et al., 1997; Romero et al. 2000).

We calculated more parameters compared to Rappaport et al. 1997 because we used a very-high resolution multibeam data. On the base of this quantitative approach, we suggest a possible evolution of the seamounts recognised in the study area.

The first cross correlation that we have established is between base radius and height of the seamounts (Fig. 12). The average value radius/height for the seven recognised seamounts is 0.29, which is similar with the value that were obtained in the Tenerife seamounts (0.22; Romero et al. 2000); in the northern Mid-Atlantic Ridge (0.22: Smith and Cann, 1992) in the Reykjanes Ridge (0.26: Magde and Smith, 1995), in Mid-Atlantic Ridge (Kong et al., 1988), in the Pacific (Abers

et al., 1988; Smith and Jordan, 1988) and in the south-western Indian Ridge (Mendel and Sauter, 1997).

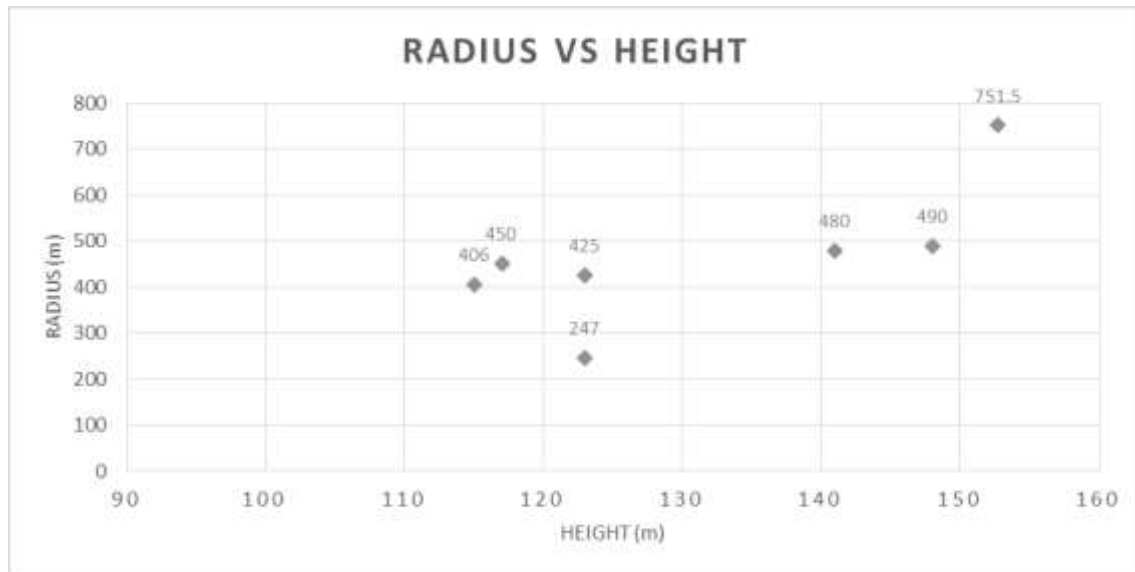


Figure 12 Cross correlation Radius vs height.

Another important established cross correlation is between volume and base diameter that shows a good agreement with other published data (Rappaport et al. 1997; Romero et al. 2000; Fig. 13).

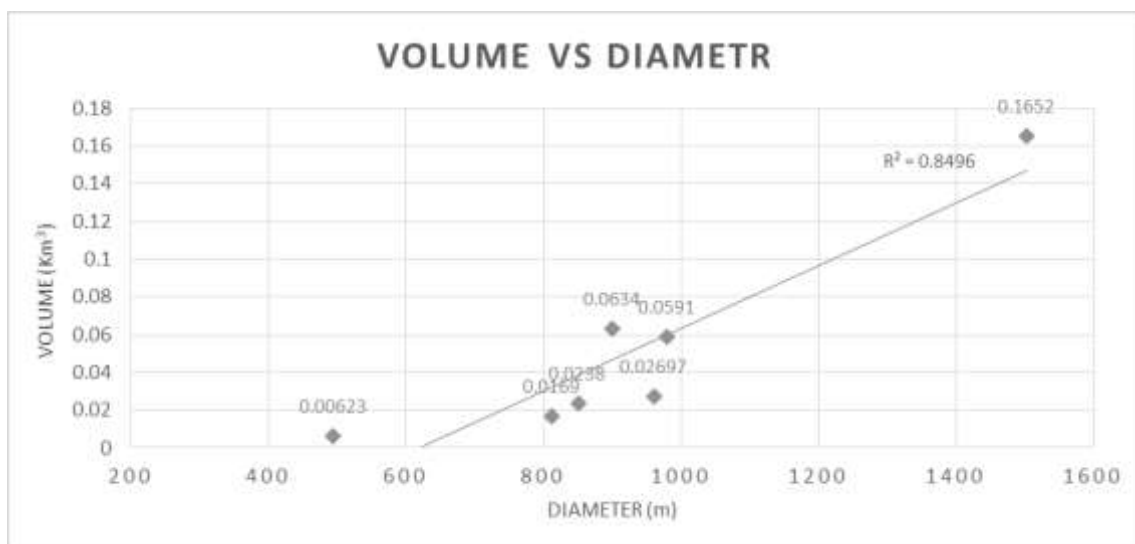


Figure 13 Cross correlation Volume vs basal diameter.

The obtained values allowed us to interpret the recognised positive structures (M1-M7) to be as the volcanic seamounts confirming the universal control of this shape parameter in submarine volcanic environments (Romero et al. 2000).

Furthermore, on the base of the morphology of the volcanic seamounts showing different shapes, we subdivided in three different populations the volcanoes.

The first population (M2, M3, M5, M6 in Figs. 2, 3) is characterised at the top by marine terraces, which were by the sea-level fall of about 115 m during the Last Glacial Maximum (Lambeck and Chappell, 2001), and which were successively remodelled by wave erosion during the subaerial phase linked to its historical submarine eruptions.

M2 and M3 (Fig. 7) show two different marine terrace probably formed during two different cycles of “appear and disappear” of the volcanic islands linked to the local subsidence (mainly thermal and tectonic), which have affected the Graham Bank sector. We suggest that these two subaerial phase are linked to the two important documented submarine eruptions of the Sicily Channel. The first one, in the 1831 that has formed a small island, 65 m above sea level (Colantoni, 1975; Corti et al., 2006), namely Ferdinandea Island and the second eruption documented in 1831 (Colantoni, 1975).

The second population is composed by M1 and M7 (Figs. 2, 3, 11) showing a typical cone shape of the volcanic seamounts. On the base of the cross correlation between the height, basal ratio, aspect ratio and flatness and also considering their shape we suggest that these two volcanoes are the youngest in the study area and also they does not have a subaerial phases.

M4 (Figs. 2, 3, 9) show a very complex shape making a difficult to establish the good cross correlations. Its morphological features and the information that are obtained by cross correlation suggest that it form a third population of seamount. It shows this shape due to a construction

mechanism that took place in two volcanic successive phases. It is surrounded by a positive morphology with a ring shape interpreted as the remains of an older and bigger volcanic edifice, which probably is collapsed forming a caldera in which the actual volcanic cone is grown. M4 is, probably, the oldest seamounts in the study area.

In conclusion, we infer that this cluster of submarine volcanoes were formed by more than one process. In agreement with recent work, that volcanism is not contemporaneous along the entire length of the Sicily Channel (Corti et al. 2003, 2006, Rotolo et al. 2006). These volcanic seamounts are aligned along two volcano-tectonic lines (NW-SE and N-S) which are the trend typical of the Sicily Channel.

The presence of this cluster of alignments volcanic seamounts (NW-SE and N-S) as well as of the cluster of aligned fluid escape structures that occur in the same sector that have trend parallel at the main system faults that affect the Sicily Channel indicates that the growth of the Graham Bank sector had an important development (with submarine and subaerial events) strongly linked to the genesis and evolution of the Sicily Channel.

4.2. Fluid escape structures in the Graham Bank (Sicily Channel, Central Mediterranean) triggered by volcanism and tectonics.

Abstract

The Graham Bank (NW Sicily Channel, Central Mediterranean) is characterised by an uneven seafloor morphology, where morphostructural highs, submarine plains, escarpments, and negative and positive relief features indicate a complex structural setting and the occurrence of seepage fluids. New high-resolution acoustic data (multibeam, Chirp profiles) and multi-channel profiles allowed us to differentiate between two main morphological sectors, and to identify several pockmarks and mounds linked to fluid escape. The eastern sector, corresponding to the volcanic edifice of the Graham Bank, is characterised by rough morphology, several mounds, focused seepage plumes and an acoustic substrate interpreted as generated by magmatic rocks. All these features are related to volcanic activity forming both the Graham Bank and a series of minor cones. The western sector displays a generally flat morphology dominated by Upper Pleistocene-Holocene outer shelf deposits, where mounds and pockmarks with sub-circular and ellipsoidal planform shapes and U-shaped cross-sections are the prevailing features indicating that the fluid migration processes are and/or were active. These two areas are separated by a fault-controlled channel with NW-SE direction, bordered by steep walls forming fault escarpments, and shedding the eroded materials into the adjacent lower slope and deep-water zones. The overall morphostructural setting, and the alignment of the faults with the distribution of both pockmarks and mounds, suggest a tectonic control. The source of fluid is rooted at depth, resulting from tectonic activity involving sub-vertical recent extensional faults developing along, and reactivating, the Cenozoic (both Plio-Quaternary and Messinian) and Mesozoic tectonic systems.

Keywords: Graham Bank, fluid escape, pockmark, mound, seepage plume, active tectonics, submarine volcanic edifice.

1. Introduction

Seepage of fluids is a phenomenon that has been described worldwide, both onshore and offshore. It gives rise to a range of geological, geochemical, thermal, and biological activities (e.g., Hovland and Judd, 1988; Dando and Hovland, 1992; Milkov, 2000; Judd, 2004; Milkov et al., 2004; Jerosch et al., 2007). Fluids expulsion in submarine areas produces a variety of seabed morphologies, including mud volcanoes, diapirs, pockmarks, and cemented sediments, whereas active seepage may be detected by acoustic profiles in the form of hydroacoustic flares or plumes (Canet et al., 2010). The morpho-bathymetric character of seabed features associated with seepage depend on the type of fluid involved and the geological setting in which they occur. Fluid escape can be a result of underlying hydrocarbon gas reservoirs (Bezrodnykh et al., 2013), overpressurised fluids in the subsurface (Kopf, 2002), and deformation of sediments, especially by faulting (Dimitrov, 2002; Dupré et al., 2007).

Fluid- and mud-escape structures occur in various geodynamic scenarios, such as continental shelves, slopes and abyssal plains, in epicontinental seas of passive margins, as well as at rifted margins (Hovland et al., 1985; Robertson, 1996; Sibuet and Olu, 1998; Milkov, 2000; Berndt, 2005; Brothers et al., 2013; Skarke et al., 2014). They also occur in active margins, where compressional stress drive the expulsion and faults provide a conduit (Moore and Vrolijk, 1992; Fernández-Puga et al., 2007; Hensen et al., 2007).

The study of fluid expulsion phenomena is important for a number of reasons. Released gases, such as methane, carbon dioxide, and minor hydrocarbons, can contribute to enhance greenhouse climatic conditions (Milkov, 2000; Etiope and Klusman, 2002; Milkov et al., 2003; Etiope et al., 2004; Sauter et al., 2006; Jerosch et al., 2007). They can influence the climatic changes (Judd et

al., 2002; Kvenvolden and Rogers, 2005) and contribute to the “ocean acidification” (e.g., Larson, 1991; Tejada et al., 2009). Gas seeps also control the location of specific biocenosis, such as coral mounds and chemosynthetic communities, which typically feature symbiotic methane- and sulphur-bacteria (Barry et al., 1996; Canet et al., 2003; Levin, 2005; Campbell, 2006). The latter are able to produce methane-derived authigenic carbonates by means of microbially-mediated chemical reactions as anaerobic oxidation of methane and sulphate reduction (e.g., Aloisi et al., 2000; Canet et al., 2006; Magalhães et al., 2012). These structures provide breeding grounds for fish (MacDonald et al., 1990).

Many examples of fluid escape have been document worldwide, to depths of 3500 m (Milkov, 2000; Kholodov, 2002; Dupré et al., 2007; Law et al., 2010). In the Mediterranean Sea they are well documented in the Strait of Gibraltar, both in its Atlantic (Gulf of Cádiz) and Mediterranean sides (Alboràn Sea), where the pockmarks are related to the venting of overpressure gas-rich fluid entrapped in shallow subsurface reservoirs consisting of coarse-grained contourites, charged by deep-seated fluids migrating upwards along diapir related faults (Medialdea et al., 2009; Leòn et al., 2010; 2014; Somoza et al., 2012).

The Sicily Channel (Fig. 1a), central Mediterranean Sea, is a region where fluid flow and hydrocarbon systems are widespread. Microbial and thermogenic fluid flows, and related fluid escape features (e.g., pockmarks, plumes, pipes, methane anomalies, carbonate crusts, domes and ridges) have been reported, mainly from the Malta Plateau (Max et al., 1993; Holland et al., 2003; 2006; Savini et al., 2009; Micallef et al., 2011; Taviani et al., 2013). Minor examples have been documented from the western Sicily Channel. They occur offshore Pantelleria (Parello et al., 2000) and the Graham Bank, where a fumarole field had already been described (Coltelli et al., 2016). In the latter case, the chemical composition of the seeping fluid is predominantly, CO₂, with minor amounts of N₂ and CH₄ and p.p.m. of He, H₂, CO and C₂₊ alkanes (Coltelli et al., 2016). Onshore,

in the Sciacca area, thermal waters have been related to active degassing of likely mantle-derived fluids (Caracausi et al., 2005).

The aim of this paper is to describe fluid escape structures from the seafloor in the Graham Bank area (Fig. 1b) using high-resolution geophysical and sedimentological data (Fig. 1c), collected during a recent oceanographic cruise in the frame of the CNR-IAMC RITMARE project. Using a multidisciplinary approach (seismo-stratigraphic, structural, and morpho-bathymetric), we propose a model for the origin of the fluids and the mechanism by which they are transferred to the seafloor.

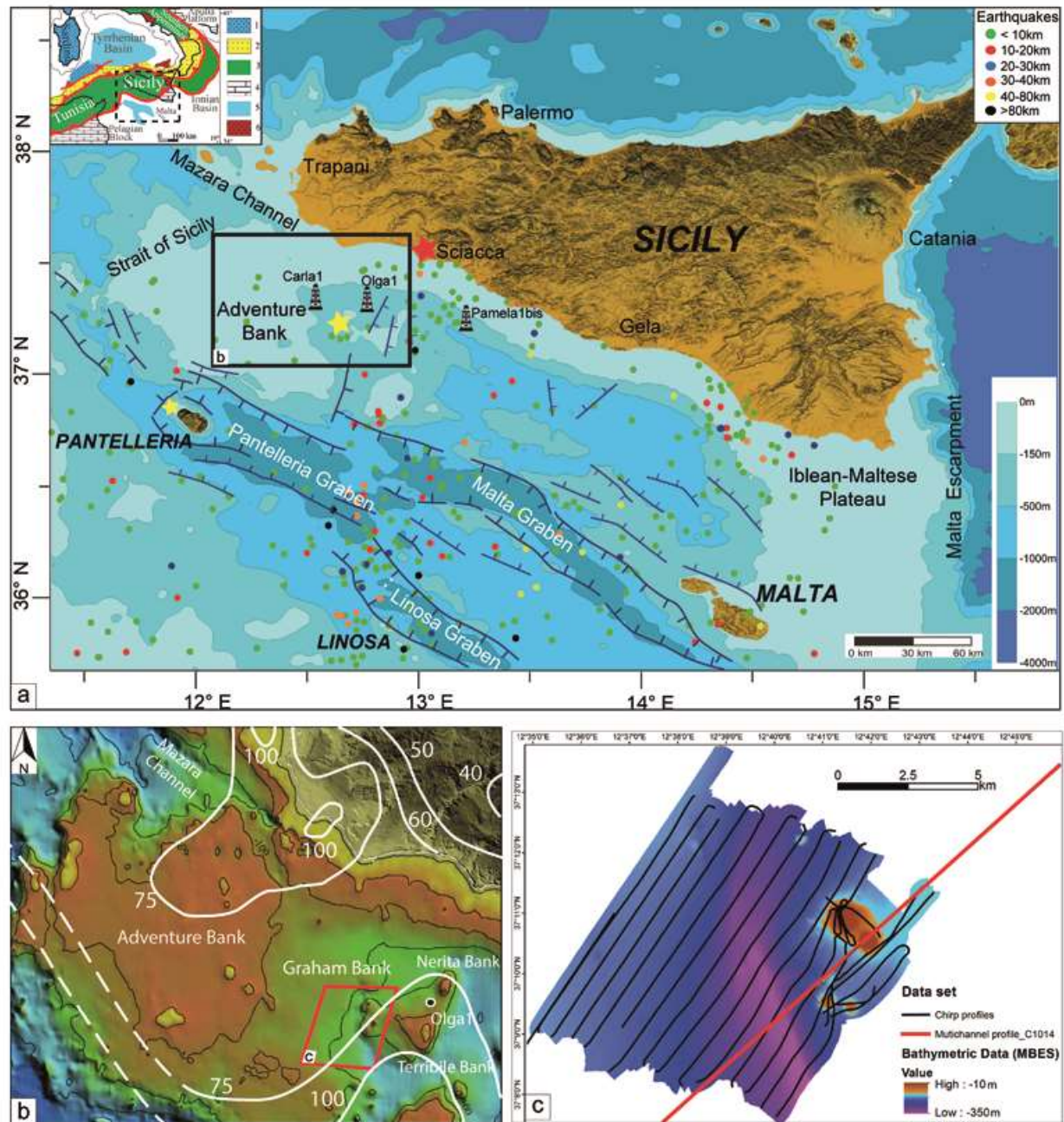


Figure 1 Bathymetric map of the Sicily Channel (Central Mediterranean), showing the main physiography, Plio-Pleistocene graben systems (modified after Catalano et al., 1993), and distribution of earthquake epicentres recorded between 1981 to 2012 in the region (data from ISIDE: Italian seismological instrumental and parametric database, <http://iside.rm.ingv.it>) (a); yellow stars indicate fumarole fields (Conte et al., 2014), red star is thermal water spring (Caracausi et al., 2005). The inset shows the structural setting of central Mediterranean and surrounding areas (modified after Catalano et al., 2013a): 1) Corsica-Sardinia; 2) Kabilyan-Calabrian units; 3) Apennine-Maghrebian units; 4) Foreland; 5) Plio-Quaternary extensional areas; 6) Plio-Quaternary volcanic rocks; b) shaded relief of the Adventure Bank area (bathymetry from Gebco - General bathymetric chart of the oceans); Contour lines represent heat flow values in mW/m^2 (from geothopica.igg.cnr.it). The red box displays the study area; c) morphobathymetric and seismic reflection data set.

2. Geological Setting

The Sicily Channel is located in the central Mediterranean Sea, between the southern coast of Sicily, the eastern coast of Tunisia, and the Malta Escarpment (Fig. 1a). It represents a part of the foreland Sicilian-Maghrebian Fold and Thrust Belt (FTB), which links the African Maghrebides with the Southern Apennines across the Calabrian accretionary wedge (inset in Fig. 1a). It is considered a segment of the Alpine collisional belt, described as a result of both the post-collisional convergence between Africa and Europe (Bonardi et al., 2001), and the roll-back of the subduction hinge of the African-Ionian crust (Casero and Roure, 1994; Catalano et al., 1996; 2000; 2013a; Granath and Casero, 2004; Finetti et al., 2005).

The Sicilian FTB is a roughly S-vergent thin-skinned imbricated wedge that was progressively emplaced from the Miocene. It originated from the piling-up of tectonic bodies due to deformation of the palaeo-geographic domains in the African rifted continental margin that developed during the Mesozoic (Basilone et al., 2016a and references therein). It grows above a northwest dipping regional monocline that consists of Mesozoic carbonate platform deposits covering the stretched African continental crust (Handy et al., 2010; Catalano et al., 2013b). The foreland area, cropping out in south-eastern Sicily (Iblean Plateau) and submerged in the Sicily Channel (Pelagian Block), is the result of the interaction of both the Sicilian-Maghrebian mountain building and the Sicily Channel rifting (Fig. 1a, Argnani, 1990; Catalano et al., 1996; Sulli, 2000; Finetti et al., 2005).

The Pelagian carbonate platform, outcropping in the Sciacca Mountains, Iblean Plateau, Maltese Archipelago, Lampedusa Island, and in the southeastern Tunisian region, represents the main bulk of the Sicily Channel. It consists of 6-7 km thick Meso-Cenozoic carbonate platform and pelagic deposits (Fig. 2), with igneous intercalations (mostly basalts). Neither salt diapirism nor mud volcanoes have been documented. They display lateral facies variations as a result of the syn-sedimentary fault systems active during the Jurassic extensional rifting tectonics (e.g.,

Streppenosa basin, Patacca et al., 1979; Frixia et al., 2000; Basilone et al., 2016b). The carbonate succession is covered by 2-2.5 km of Miocene-Pliocene clastics, evaporites and carbonates (Antonelli et al., 1988; Catalano et al., 1996; Gasparo Morticelli et al., 2015).

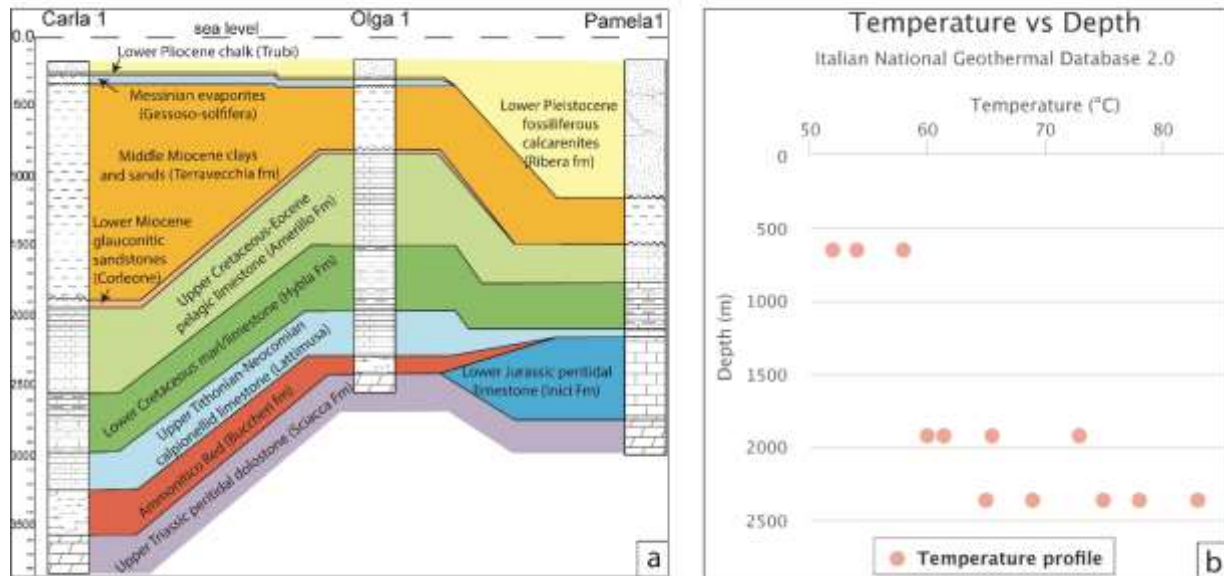


Figure 2 a) Stratigraphic log correlation of some boreholes (ENI) drilled in NW Sicily Channel showing the main stratigraphy of the Meso-Cenozoic carbonates of Iblean foreland (see Fig. 1a for location); b) temperature vs. depth profile of the Olga1 well (see location in Fig. 1b) (from geothopica.igg.cnr.it).

Elongate bathymetric depressions, located in proximity of the Pantelleria, Malta, and Linosa islands (Fig. 1a), are morphological expression of a continental rifting episode affecting the northern African lithosphere since the Neogene (Finetti, 1984; Argnani, 1993). The rifting thinned the continental crust to 15–18 km (Argnani, 1990; Civile et al., 2008) and opened the Pantelleria, Malta and Linosa grabens along NW-SE sub-vertical normal faults (Fig. 1a, Finetti, 1984; Torelli et al., 1991; Catalano et al., 1993; Finetti et al., 2005; Civile et al., 2010). The rifting process was accompanied by widespread subaerial and submarine volcanic activity (e.g. Pantelleria and Linosa volcanic islands, Graham and Nameless banks, Fig. 1a). This volcanism, with alkaline to peralkaline affinity related to anorogenic magmatism (Corti et al., 2006; Rotolo et al., 2006), took place since the Pliocene (Nameless Bank) up to the present day (e.g. Ferdinanda and Foerstner

volcanoes, Fig. 1b, Colantoni et al., 1975; Carapezza et al., 1979; Beccaluva et al., 1981; Calanchi et al., 1989; Peccerillo, 2005).

Seismic activity is associated with 20-80 km deep hypocentres with $M_L > 3$ (Fig. 1a, Chiarabba et al., 2005; Galea, 2007). Earthquakes can occur along a N-S trending belt, between the area offshore Sciacca and the Lampedusa and Linosa Islands (Fig. 1a), and are triggered by extensional to strike-slip focal mechanisms (Calò and Parisi, 2016).

The study area is located in the NW sector of the Sicily Channel (Fig. 1b). The latter is a shallow seafloor (75 to 205 m depth) characterised by an 80 km wide continental shelf, mainly represented by the Adventure Bank, and is separated from the southern coast of Sicily by the “Mazara Channel”. It is linked to the 1300 m deep Pantelleria Graben by a continental slope ranging from 150 to 1000 m and steeping up to 14° (Orru et al., 2003). The Graham Bank is a section of the outer continental shelf to upper slope, where several positive morphologies linked to volcanic activity occur (Fig. 1b, Colantoni, 1975). Heat flow values show relative high isothermal contours located between the Graham, Nerita and Terribile Banks, where a 75 to 100 mW/m^2 flow is recorded ((Fig. 1b, from geothopica.igg.cnr.it)).

In the Sicily Channel, two main water masses occur: the Modified Atlantic Water (MAW), which flows eastward bordering the Adventure Bank, and the saltier and deeper Levantine Intermediate Water (LIW), which flows in the opposite direction (Millot, 1999; Lafuente et al. 2002). The latter is responsible for reshaping of seafloor and contouritic deposition (Marani et al., 1993; Reeder et al., 2002).

3. Data and methods

The data set (Fig. 1c), consisting of single- and multibeam data, and sub-bottom profiles, was collected during an oceanographic cruise (CNR ACUSCAL 2015) carried out aboard the R/V

Minerva1, in the framework of the RITMARE Project (CNR IAMC Sez. Capo Granitola, Mazara del Vallo). An area around the Graham Bank (Fig. 1b) was mapped in detail using a Reson SeaBat 7160 multibeam echosounder system, which generates 512 beams at a nominal frequency of 44 kHz with a depth range of 10-3000 m. Positional data were provided by differential Global Positioning Systems (dGPS) by FUGRO SEASTAR. Bathymetric data were processed using the PDS-2000 software and entailed removal of erroneous beams, noise filtering, calibration and processing of navigation and correction for sound velocity. The resulting Digital Terrain Model (DTM) has a footprint of 5 m. We used Global Mapper and Golden Software Surfer 9 in order to obtain 3D and shaded relief models, bathymetric profiles, and to interpret the morpho-bathymetric data.

About 200 km of high-resolution seismic reflection profiles, spaced at 800 m, were acquired using a hull-mounted 16 transducer Teledyne/Benthos CHIRP III profiler with operating frequencies ranging between 2 and 7 kHz and a ping rate between 250 and 750 ms, Tx power between 5 and 7, pulse length of 10 ms and 30-42 db of gain. The seismic reflection data were recorded by the “Communication Technology SWANPRO” software. The profiles were processed and interpreted using Kingdom and GeoSuite Work software packages. Data processing included Automatic Gain Control, Time Variant Gain, Swell Filter and Mute.

Multichannel seismic reflection profiles (“C and G sectors”, www.ViDEPI.it), with low vertical resolution (10-80 m) and high-penetration power (about 6 s TWTT), were also available in raster format. This entailed merging all files in one seismic profile, geo-referencing them (Datum WGS84, UTM33) using GIS software, and converting to SEG-Y format using a Matlab script (`image2segy`).

4. Results

4.1. Geomorphological characterisation

Overall, the north-western sector of the Sicily Channel forms a 360 km² morphological high, comprising the Graham (7 m), Nerita (16 m), and Terrible (20 m) Banks (Fig. 1b). We focused on an area comprising the Graham Bank and the surrounding sector. It is a ~100 km² submarine area, ranging between 10 and 350 m in water depth, characterised by a complex seafloor morphology that includes topographic highs, submarine plains, escarpments, and negative and positive reliefs (Fig. 3).

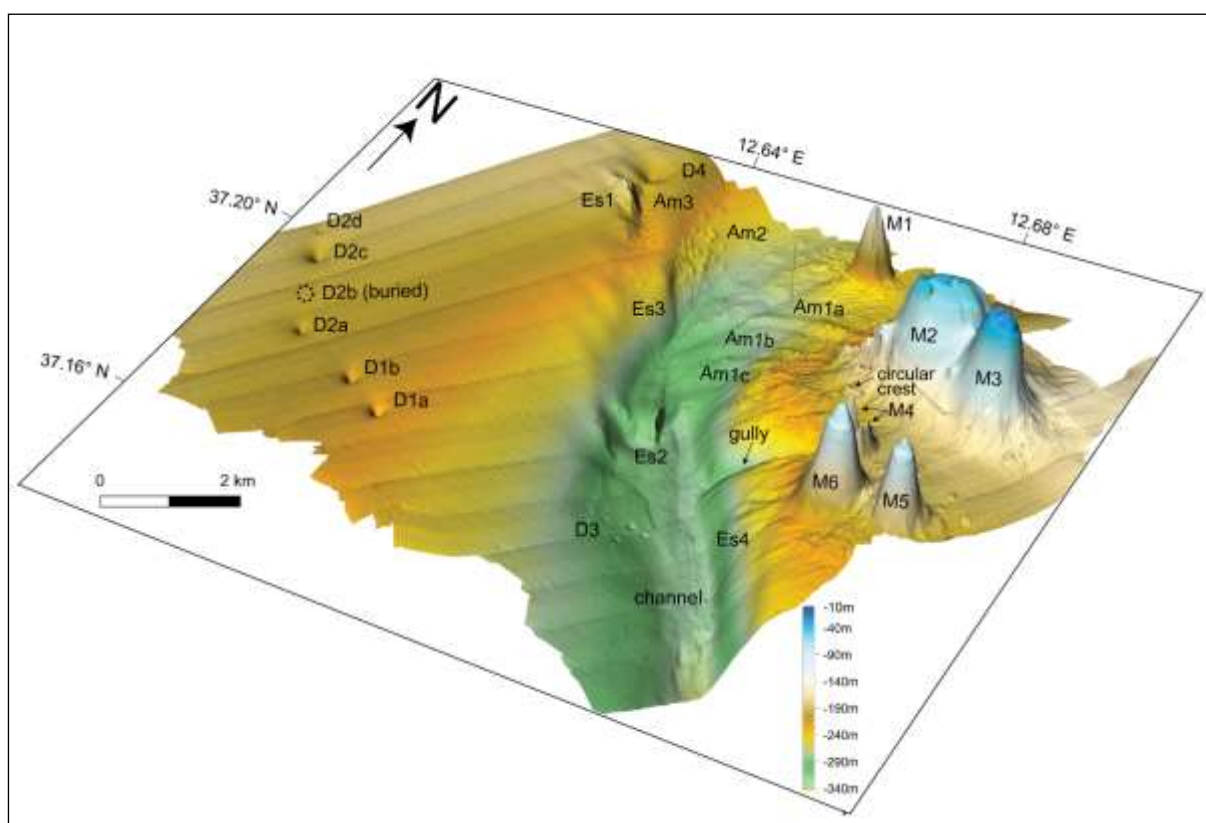


Figure 3 Digital Elevation Model of the study area. Two different sectors are separated by a NW-SE channel, characterised by several morphostructures: M1-M7 mounds, Am1-Am3 aligned mounds, Es1-Es4 fault escarpments, D1-D2 aligned, D3 clustered and D4 isolated pockmarks. Vertical exaggeration 1:8.

Two main sectors are separated by an asymmetric channel (about 12 km² wide) crossing the whole investigated area (Fig. 3).

The eastern sector, corresponding to the volcanic edifices of the Graham Bank, has a rugged morphology and is characterised by several positive structures that comprise a cluster of mounds (M1-M7 in Fig. 3). Two of the mapped mounds form a NW-SE oriented elongate structure, 185

m high, 3.5 km long and 2.8 km wide, corresponding to the Graham Bank (M2 and M3 in Figs. 3, 4).

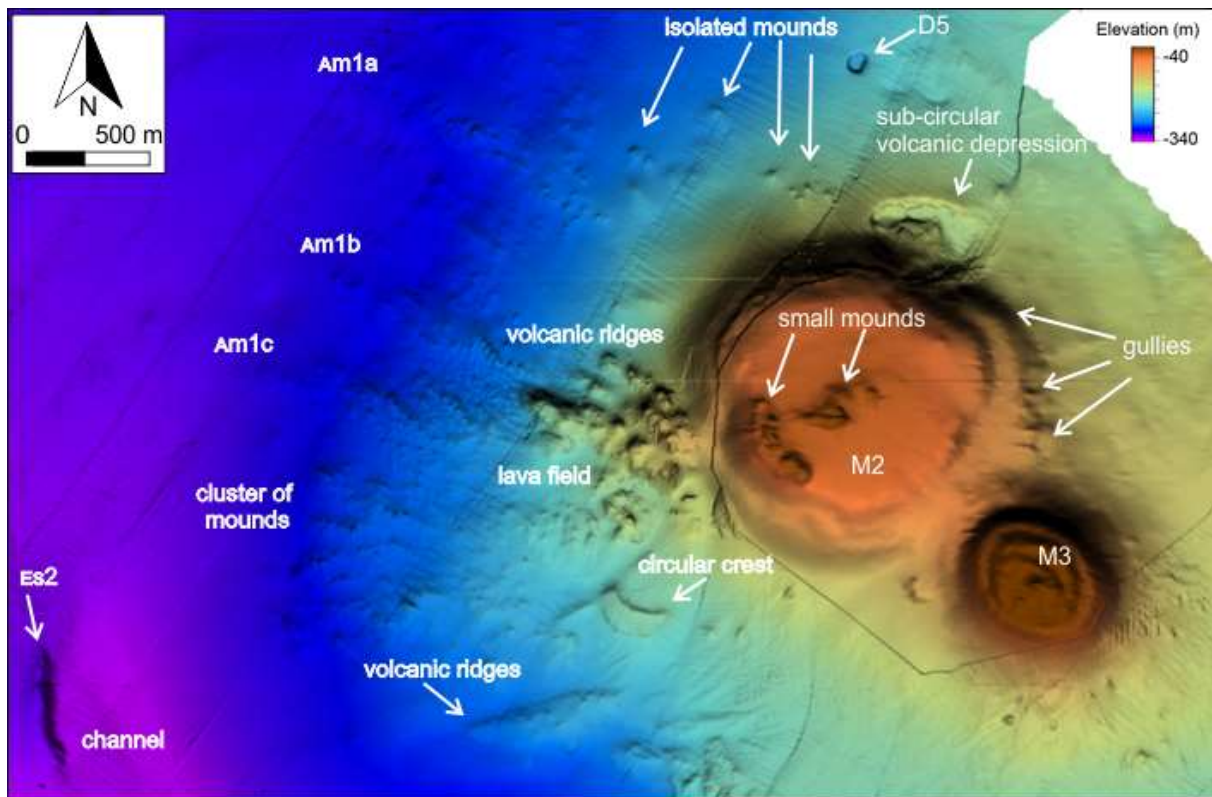


Figure 4 Shaded relief of the Graham Bank in the western sector of the study area, composed of two main isolated mounds (M2 and M3) with related morphostructural forms. Am1a, b, c aligned mounds, D5 isolated pockmark, Es2 fault escarpment.

M2, which is 155 m high and slopes at 14-19°, is the largest one. Around this structure and at its top there are numerous smaller mounds (Fig. 3). M3 is a seamount with a flat surface at the top (i.e., guyot), probably as consequence of relative sea-level changes. At this site, an eruption in 1831 gave rise to a small subaerial volcano (Ferdinanda Island, Colantoni et al. 1975), which submerged soon after due to a fast subsidence. M1 and M4-M7 have similar sizes (about 120 m high, 500 m wide), and similar cone shapes with flanks sloping at 30° (Fig. 3). There are numerous isolated, clustered and aligned mounds on the western and south-western flanks of the Graham Bank (Fig. 4). The NW-SE and NNW-SSE oriented mound ridges, extending as far as 600 m in length and reaching heights of 1.5-10 m, form hummocky surfaces (Figs. 3, 4).

The western sector displays a generally flat morphology, with an average steepness of 1.2-1.5°, and characterised by many negative circular depressions (D1-D5 in Fig. 3) and a 27 m high, NW-SE -oriented steep escarpment (Es1 in Fig. 3).

The depressions, occurring at water-depths ranging between 195 and 317 m, are grouped in two main clusters that are either aligned NW-SE or NNW-SSE, or occur as isolated structures (Fig. 3).

These structures display in cross-section both U and V-shape, and in plan-view variable shape from circular to elongate often with eroded edges and are oriented along a NNW-SSE trend. In this work, in plan-view, the depressions will be defined circular if $L/W=1.0-1.2$, and elliptical if $W/L>1.2$. They can be grouped into three clusters (Table 1).

The depressions are U-shaped in cross-section and sub-circular, ellipsoidal to complex in planar view. They are 1.3-15 m deep, their diameters range from 25 to 580 m, and the slope gradients of their walls are up to 23°.

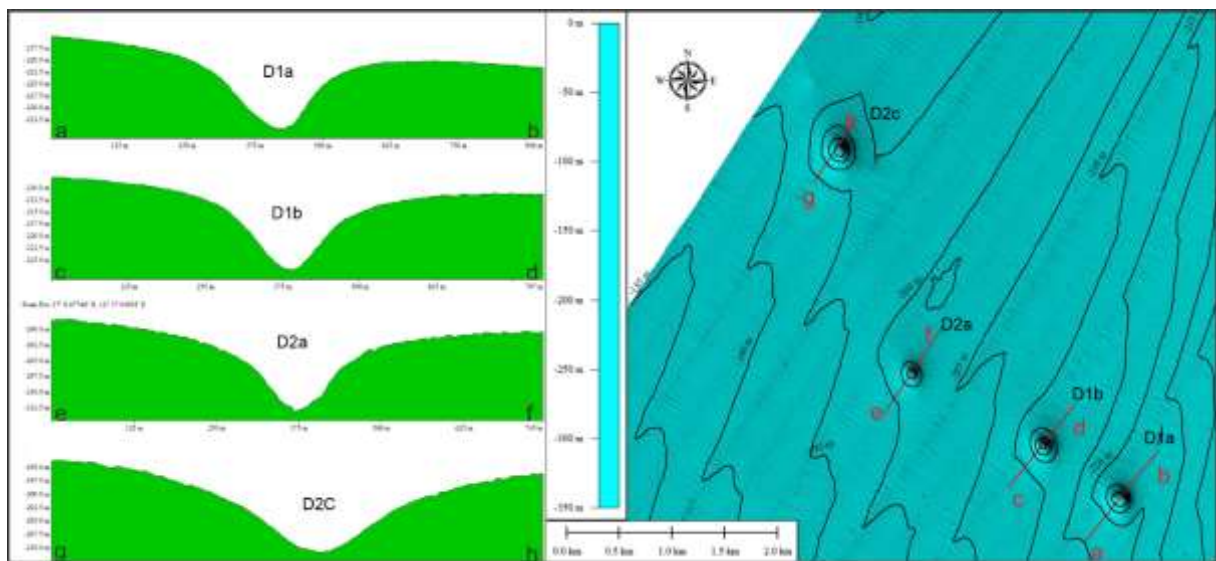


Figure 540 Bathymetric profiles and location map of the array of pockmark located in the western part of the study area.

The D1a (Figs. 3, 5, 6) is elliptical in plan-view, so it results elongated in NW direction, and it displays in cross section a symmetric V shape. Its dimensions are 415 m in the major axis, 298

m in the minor axis, 14.5 m deep where the walls are gently steep, up to 6-9°. Its top lies at 220 m and its bottom lies at 234.5 m. It is 47 km far from the coastline (Southern Sicily) and about 7.7 km from the Graham Bank.

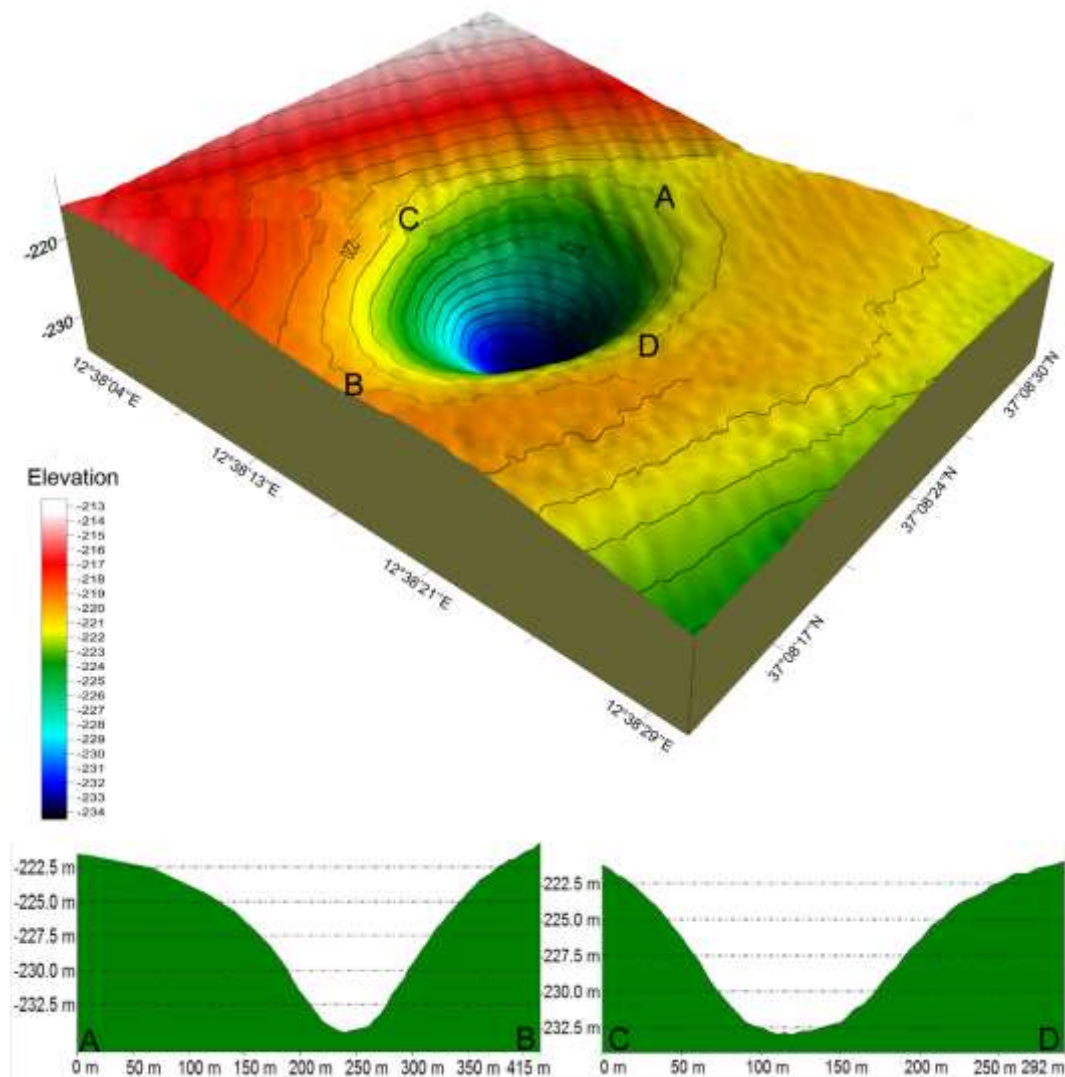


Figure 6 Detail of pockmark D1a in Fig. 38 (above) and bathymetric profiles (below) crossing the centre of the depression.

The D1b (Figs. 3, 5) is elliptical in plan-view and it shows in cross section a symmetric V shape. Its dimensions are 428 m in the major axis, 334 m in the minor axis, 13.5 m deep and display walls inclined up to 7°. Its top lies at 212 m and its bottom lies at 225.5 m.

The D2a (Figs. 3, 5) is elliptical in plan-view and it displays in cross section a symmetric V shape. Its dimensions are 321 m in the major axis, 237 in the minor axis, 10 m deep. Its top lies at 203 m and its bottom lies at 213 m.

The D2c (Figs. 3, 5) is elliptical in plan-view and it displays in cross section a symmetric V shape. Its dimensions are 578 m in major axis, 440 m in minor axis, 17 m deep. The walls of this depression are steep about 6° . Its top lies at 196 m and its bottom lies at 213 m.

The D2d (Figs. 3, 5) is elliptical in plan-view and it displays in cross section a symmetric V shape. Its dimensions are 242 m in major axis, 153 in minor axis, 2 m deep. The depression walls are steep about 6° . Its top lies at 193 m and its bottom lies at 195 m.

The widest depression (D4 in Fig. 3) has an axis of 400 m, depth of about 8 m and wall slope gradient of about 4° . The D4 (Figs. 38) is an isolated structure that occurs in the northern sector. It is the widest in the area and has a diameter of 400 m, depth of about 8 m and the slope of the walls is about 4° . It lies at -210 m depth, 6 km from the Graham Bank.

Another isolated occurs in the north-eastern sector, in the area surrounding the Graham Bank (D5 in Figs. 3, 7). This structure shows the eroded edges. Probably this negative relief have been formed by the coalescence of two minor depressions. As a whole it has an elliptical shape in plan-view, with major axis oriented NE-SW. The short axes measures 85 m while its longest one is 107 m. It is 6.5 m deep and its walls slope at a maximum angle of 20° .

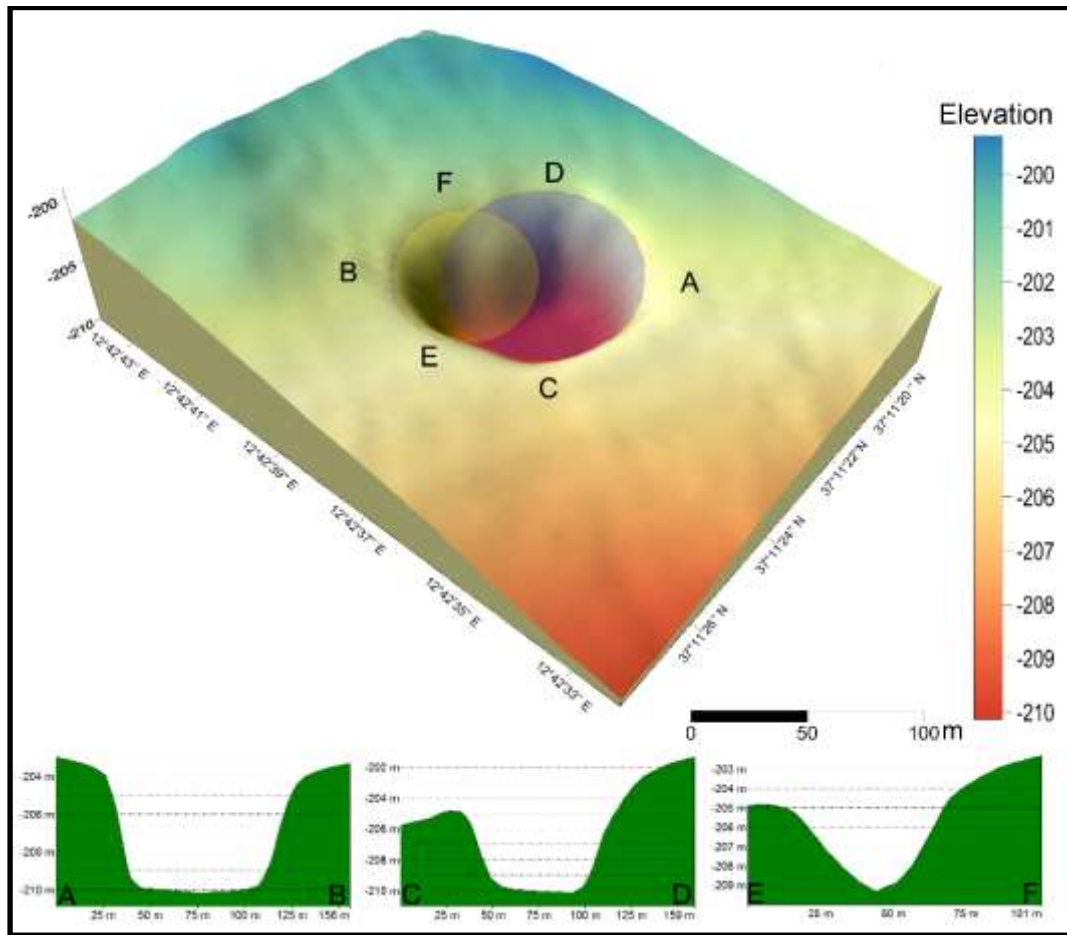


Figure 7 Detail of pockmark D5 (above) and bathymetric profiles (below) crossing the centre of the depression.

The intervening channel runs in an N-S to NW-SE direction and is bounded on both its SW and NE sides by a sub-vertical fault-escarpment (Es2, Es3 and Es4 in Figs. 3, 4, 8, 9, 10). The channel has a length of 10 km, depth of 250-350 m, and a width of 0.8-1.5 km (Fig. 3). It has a U-shaped cross-sectional shape, which becomes V-shaped between 310 m and 325 m depth, and flat in the deepest section. A concave break-in-slope located at a depth of about 305 m separates the moderately concave upwards channel in two different portions. In the NW one, the downslope gradient ranges from 1 to 2° until a depth of 306 m, whereas in the SE one, the gradient is <1° until 350 m. The channel walls have gradients varying from 4 to 7°, forming escarpments about 100 m high, bounded at the top by a convex break in slope at a depth of 220-270 m. A 25 m high, NNW-SSE -oriented elongate steep escarpment occurs (Es2 in Fig. 3).

The smallest sub-circular depressions have an average axis of 70 m and an average depth of 2 m and form a cluster that occurs in the southern part of the study area, along the western flank of the channel, which extends along a NW-SE trend.

ID	Latitude	Longitude	Plan-View	Cross Section	Major Axis (m)	Minor Axis (m)	Mean Axis (m)	Depth	Surface base (km ²)	Perimeter base (m)	Summit depth (m)	Basal depth (m)
D_1	37°08'20,11" N	12°38'16,35" E	Elliptical	V-shape	498	215	356,5	14,5	0,03513	731	220	234,5
D_2	37°08'33,46" N	12°37'51,93" E	Elliptical	V-shape	428	334	381	13,5	0,0428	794	212	225,5
D_3	37°08'50,63" N	12°37'10,47" E	Elliptical	V-shape	321	237	279	10	0,022	595	203	213
D_4	37°09'45,35" N	12°36'47,26" E	Elliptical	V-shape	578	440	509	17	0,0251	615	196	213
D_5	37°10'02,17" N	12°36'37,38" E	Elliptical	V-shape	242	153	197,5	3	0,0084	361	193	196
D_6	37°08'10,33" N	12°41'20,30" E	Elliptical	V-shape	109	99	104	2,2	0,0074	318	188	190,2
D_7	37°08'21,34" N	12°40'34,42" E	Elliptical	V-shape	95	89,3	92,15	2,5	0,0068	308	301	303,5
D_8	37°08'34,11" N	12°40'44,11" E	Circular	V-shape	316	316	316	3,5	0,0061	309	314	317,5
D_9	37°08'35,53" N	12°40'35,86" E	Elliptical	V-shape	165	156	160,5	5	0,0201	535	308	313
D_10	37°08'23,97" N	12°40'23,85" E	Elliptical	V-shape	76	71	73,5	2,7	0,00422	251	298,3	301
D_11	37°08'35,22" N	13°40'20,32" E	Elliptical	V-shape	53,8	58,4	56,1	2,5	0,00212	175	298	300,5
D_12	37°09'17,65" N	12°40'17,89" E	Elliptical	V-shape	87	71	79	1,5	0,0053	281	311	312,5
D_13	37°09'26,09" N	12°39'53,67" E	Elliptical	V-shape	56	52	54	3,5	0,0025	194	279	282,5
D_14	37°08'50,41" N	12°40'57,75" E	Elliptical	V-shape	104,5	96,6	100,55	1,4	0,0079	336	324	325
D_15	37°08'06,04" N	12°41'37,26" E	Elliptical	V-shape	73	72,8	72,9	4,7	0,00402	243,5	316,6	321,3
D_17	37°12'15,30" N	12°39'04,81" E	Elliptical	V-shape	540	520	530	11	0,163	1716	199	210
D_18	37°11'22,69" N	12°42'38,09" E	Elliptical	V-shape	107	85	96	6,5	0,00863	341,35	203,5	210

Table 1. In the tables are tabulated all size of the recognised pockmarks.

4.2 Seismostratigraphic analysis

Based on a wide grid of recently acquired Chirp profiles and from reinterpretation of published multichannel profiles (Fig. 1c), both calibrated with the revised stratigraphic log of the Olga1 exploration well (Fig. 2, www.ViDEPI.it), a seismostratigraphic analysis was performed to reconstruct the tectono-stratigraphic and volcanic setting of the region.

4.2.1 High-resolution data

Three main seismic facies have been recognised by the seismostratigraphic analysis of the Chirp profiles (Figs. 8, 9, 10, 11).

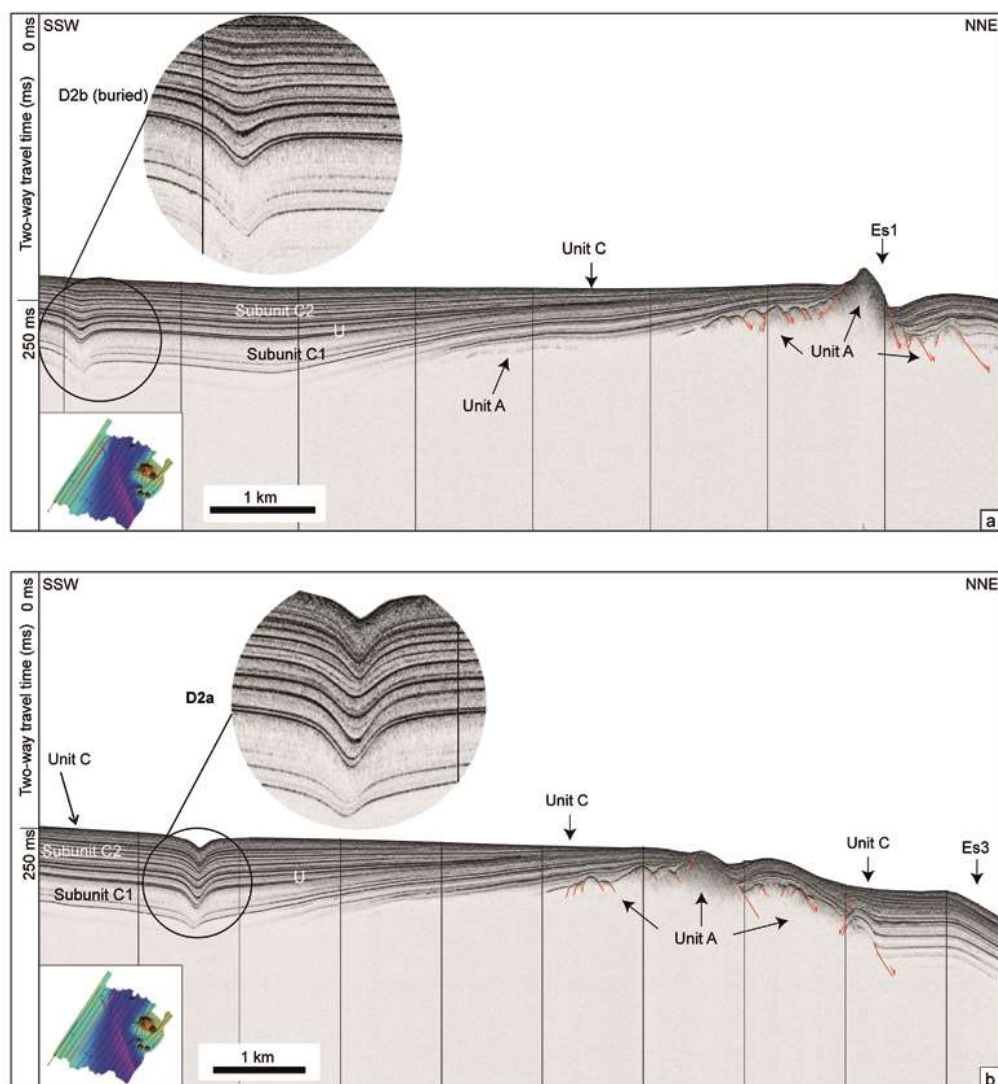


Figure 8 Very high-resolution seismic profiles (Chirp) showing the western sector of the study area and the adjacent channel to NNE. The Unit A (Lower Pleistocene deposits) is affected by extensional faults, corresponding to escarpments (Es1 and Es3 in Fig. 3); the Unit C (Upper Pleistocene to Holocene deposits), subdivided in two sub-units (C1 and C2) separated by an unconformity (U), shows concave upward reflectors forming U-shaped depressions buried (D2b in a) or developed up to the seafloor (D2a in b). The latter correspond to the pockmarks shown in Fig. 3. Location of the seismic profiles is shown in the inset map.

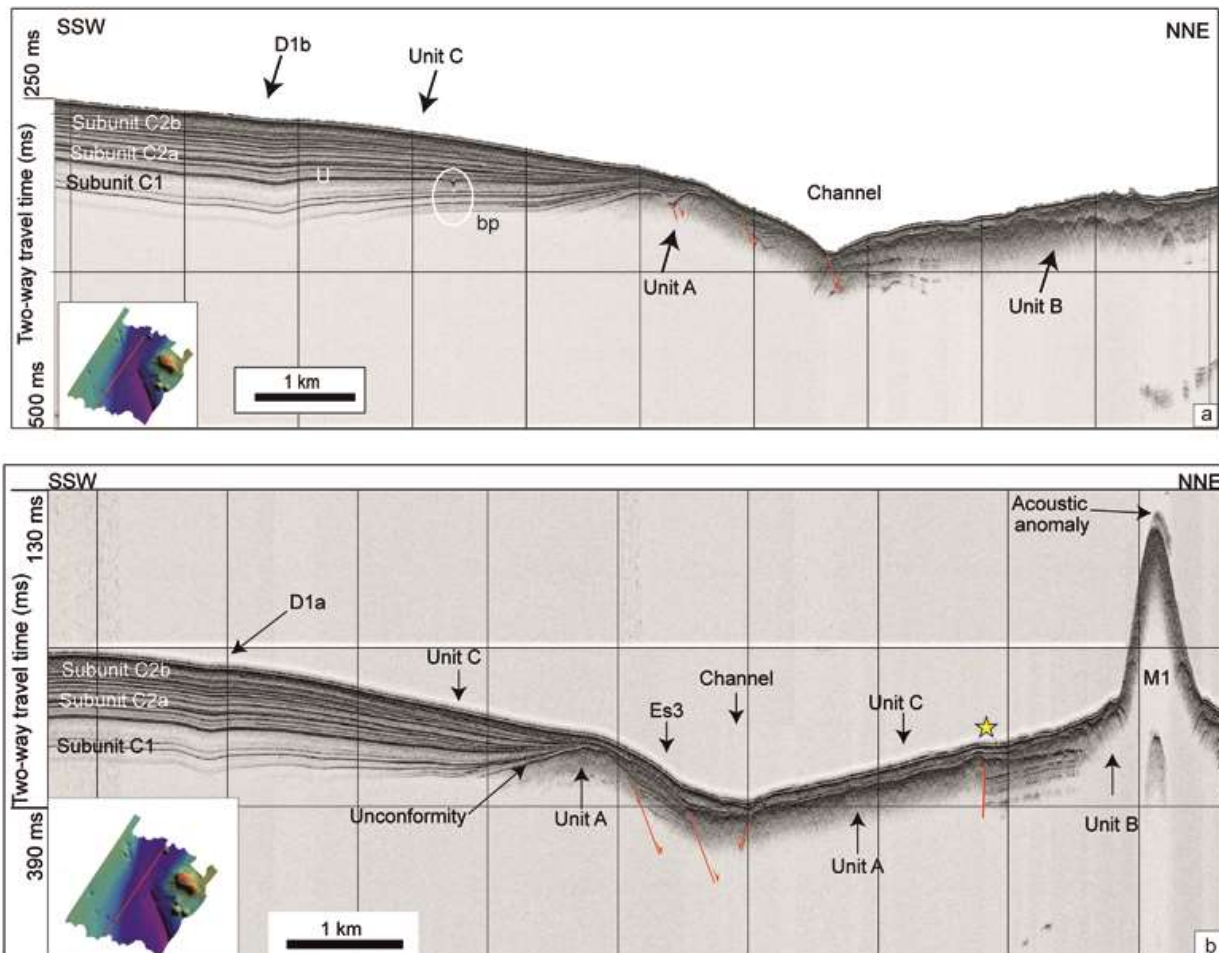


Figure 9 Chirp profiles showing both the western and eastern sectors and the intervening channel. The Unit A, topped by an unconformity, is affected by extensional faults and laterally passes to the Unit B (magmatic substrate); the Unit C shows concave upward reflectors (D1a in b, D1b in a) corresponding to aligned pockmarks (D1a and D1b in Fig. 3). A concave-upward feature (bp) can be observed at the top of the sub-unit C1 just in correspondence of the unconformity (U) separating C1 and C2 sub-units. The upper high amplitude sub-unit C2 can be subdivided in a progradational reflector package (C2a) and an aggradational group of reflectors (C2b). The top of the mound (M1 in b) shows an acoustic anomaly interpreted as a fluid vent. The yellow star indicates the epicentre of the 22-08-2003 earthquake (ML 2.6; depth 5 km) here corresponding to a sub-vertical fault.

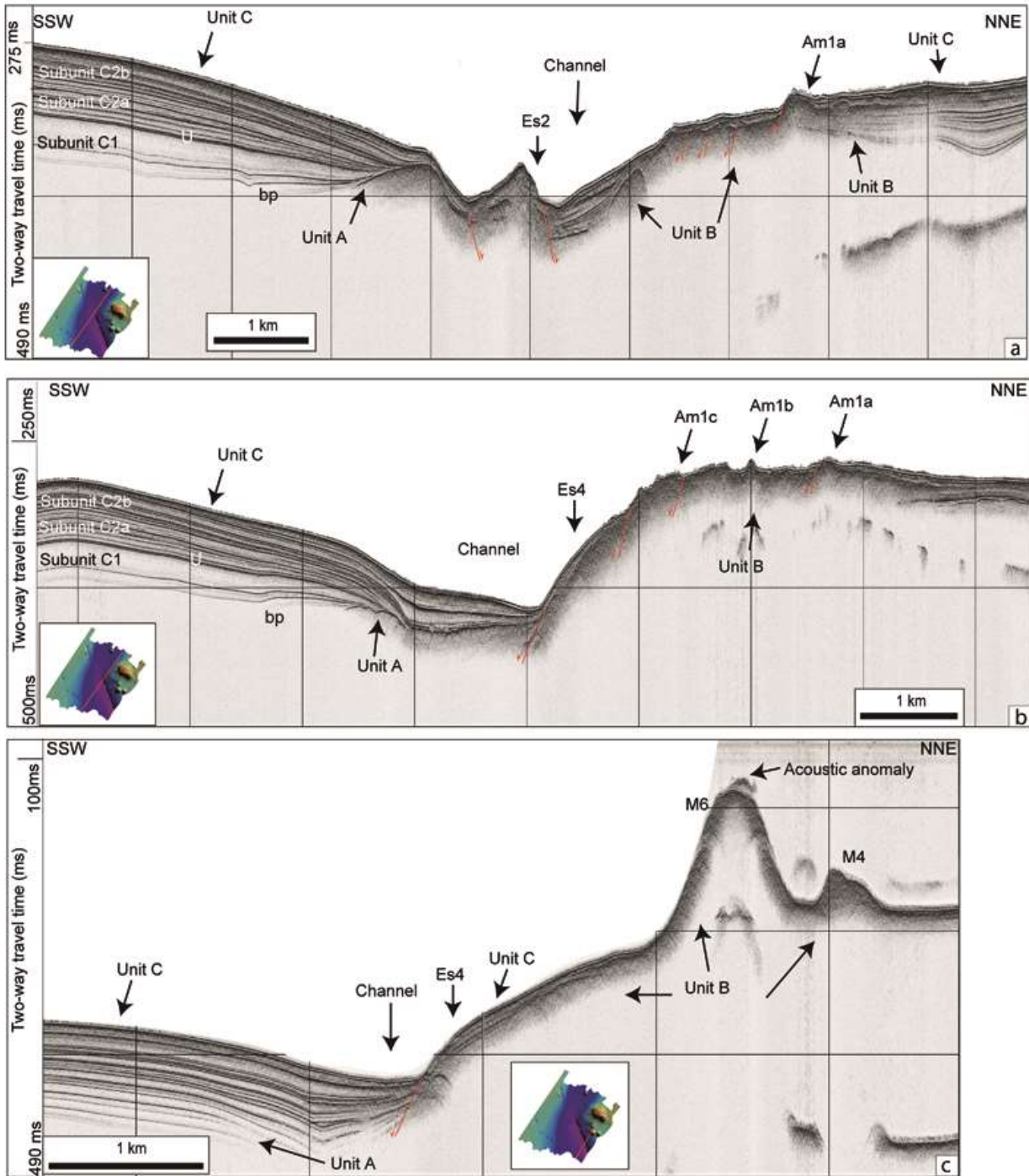


Figure 10 Chirp profiles showing both the western and eastern sectors and the intervening channel in the south-eastern part of the study area. Both Units A and B are affected by extensional faults. The uneven morphology of the seafloor highlights morphostructural features (Es2-Es4, Am1a-c, M4, M6) shown in Fig. 3. The water column at the top of the mound (M6 in b) shows an acoustic anomaly.

- Unit A is an acoustically transparent seismic facies resulting from poor penetration of the seismic signal. It is recognised in the western sector of the study area and is defined at the

- top by a low-amplitude and discontinuous reflector, which is considered the acoustic basement. It has a discontinuous pattern, with the reflector being offset by normal faults dipping to the NNE and locally dislocating the seabed (Figs. 8, 9, 10a).
- Unit B, recognised across the eastern sector of the study area, is an acoustically opaque/transparent seismic facies due to poor penetration of the seismic signal (Figs. 9, 10, 8). It comprises discontinuous reflectors laterally passing to Unit A (Figs. 9, 10).
 - Unit C comprises thin layered, high-amplitude and divergent to convergent reflectors with good lateral continuity, which alternate with low-amplitude reflectors (Figs. 8, 9, 10). The unit is characterised by a tabular external shape and maximum thickness of 90 ms two-way travel time (TWTT); these correspond to 72 m considering a seismic P-velocity of 1600 m/s (see also Catalano et al., 2000). Based on reflectors amplitude, we distinguish between a lower reflection-free sub-unit (C1) and an upper high amplitude sub-unit (C2); the latter can be subdivided in a progradational reflector package (C2a) and an aggradational group of reflectors (C2b). The unit C is affected by faults in the NNE, the largest of which shows a fault escarpment 36 ms TWTT (29 m) high (Es1 and Es2 in Figs. 8a, 10a). Concave upward reflectors form U-shaped depressions up to the seafloor (D2a and D2b in Fig. 8, D1a and D1b in Fig. 9). The latter represent two clusters of sub-circular depressions aligned NNW-SSE and NW-SE, which are well imaged by the bathymetric data set (Fig. 3). A concave-upward feature (bp) can be observed at the top of the sub-unit C1 in correspondence of the unconformity (U) separating C1 and C2 sub-units (Figs. 9, 10). Furthermore, Unit C in the hanging wall of the faults appears slightly folded (Fig. 8a) whilst in the footwall it rests unconformably above Unit A.

Several acoustic anomalies in the water column have been recognised along the study area and particularly in the eastern sector (Figs. 9b, 10c, 11). Two large acoustic anomalies, consisting of

hyperbolic water-column reflections, have been recognised in the northern flank of M2 (in correspondence of a small escarpment) and at the top of M2 (Figs. 3, 4, 11).

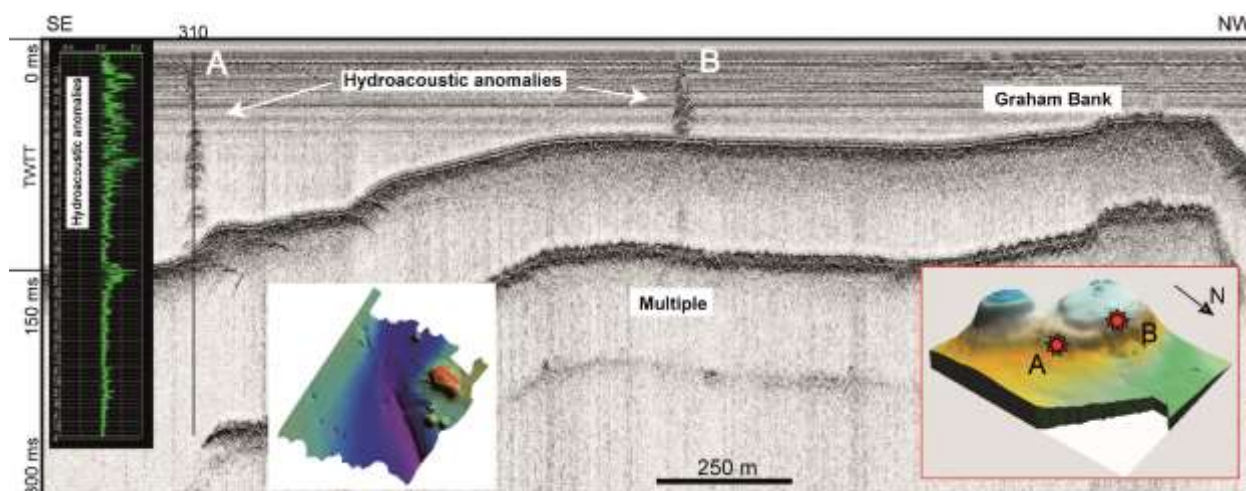


Figure 11 Chirp profile showing in detail the mounds (M2 and M3) composing the Graham Bank. Hydroacoustic anomalies in the water column (A and B) are indicative of fluid escape from the seafloor. They are located at the top of the mounds as shown in the 3-D model (right corner inset). The seismic trace in correspondence of the plume A (left side) shows the amplitude peaks recorded along the water column.

4.2.2 High-penetration data

The interpretation of a multichannel reflection profile crossing the study area (Fig. 1c) evidenced different tectonic structures affecting the Meso-Cenozoic sedimentary succession (Fig. 12). The profile shows thick shallow- and deep-water Meso-Cenozoic carbonates, covered by Miocene clastics, Messinian evaporites and Pliocene-Pleistocene carbonates. In the central portion of the profile, the volcanic edifice of the Graham Bank is visible.

The multi-layered sedimentary succession is crossed by different fault systems involving the seismostratigraphic intervals at different times. In the deep portion of the profile, stepped normal faults dipping NE-wards produce a displacement of about 0.1 s TWTT of the Upper Triassic-Lower Jurassic carbonate platform reflectors (Fig. 12). A similarly trending major fault system, with extensional kinematics, affects the whole Meso-Cenozoic succession (Fig. 12). A mainly NE-ward dipping faults system affects the Miocene sequence, as evidenced by the displacement of the

very high-amplitude and continuous top Messinian reflector. This tectonic activity produced a variable accommodation space that resulted in the strong variation of the Plio-Quaternary deposits thickness. The latter has a mean thickness of 0.3 s TWTT thick (300 m) and is characterised by undeformed medium-amplitude continuous and parallel reflectors. The Plio-Quaternary deposits appear displaced, particularly in the north-eastern sector of the profile, towards the southern Sicily coastal area. Sub-vertical faults bordering the Graham Bank affect the whole Meso-Cenozoic succession up to recent deposits (Fig. 12).

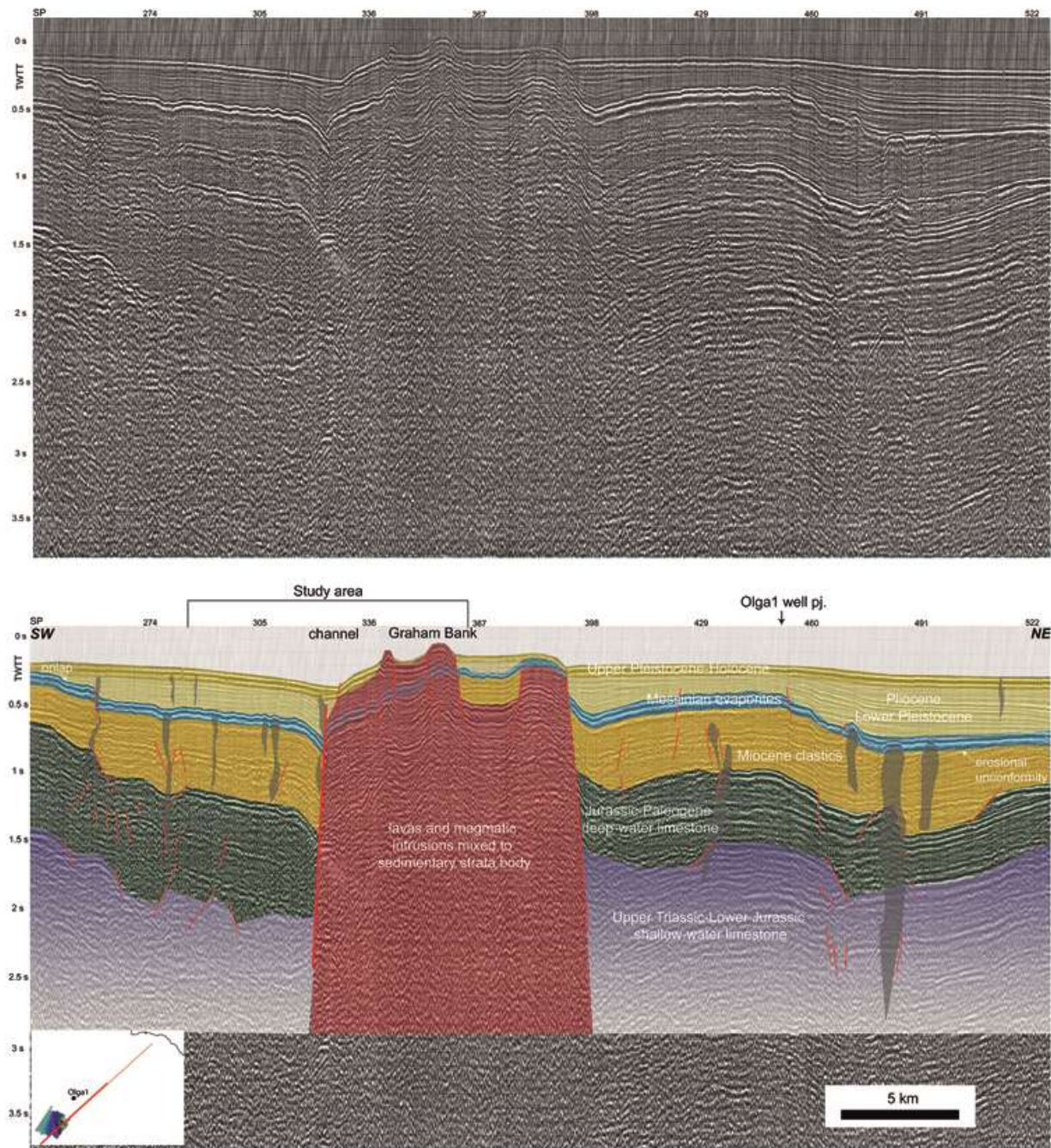


Figure 12 Multichannel seismic profile (un-interpreted up, interpreted down) crossing the Graham Bank. The seismostratigraphic interpretation, calibrated by the Olga1 well (see inset map for location), shows the interaction between the magmatic intrusions and the sedimentary multilayer. The Mesozoic-Quaternary packages are affected by fault systems of different ages and are crossed by fluid ascent (light grey pattern). TWTT: Two-Way Travel Time; SP: Shot Point.

4.3 ISOPACH MAPS

Using the multichannel seismic data associated with the published stratigraphic data and the stratigraphic record of the Agip/Eni well, we generated an isopach map of the Plio-Pleistocene sedimentary body.

The Messinian basement was reconstructed across the north-western Sicily Channel from Multichannel Seismic Profiles data. This surface (Fig. 13) shows a complex morphology of the Sicily Channel during the Messinian where alternating there are high positive relieves and deep basin that are clearly visible.

Furthermore, with the above-mentioned surface map combined with wells data (from ViDEPI), using as Velocity of seismic waves in the sedimentary body equal at:

- 3000 m/s in the Pliocene succession (*Trubi Fm.*);
- 2400 m/s in the Pleistocene succession (*Ribera Fm.*);
- 1600 m/s in the Holocene succession;
- 1500 m/s in the water.

We constructed an isopach map of the Plio-Pleistocene sedimentary sill (Fig. 13b).

The isopach map shows that the accumulation is highest near to southern Sicilian Platform, likely because there were gullies and canyons incising this sector during the Messinian Salinity Crisis. While, the central sector of the Sicily Channel, where the Messinian surface shows the high morphologies appear to be characterised by fewer thicknesses of sediments.

The Holocene basement was interpreted only across the study area, with the CHIRP profile, and we reconstructed the isopach map of Holocene sedimentary fill (Fig. 13b), using as Velocity of seismic waves in the sedimentary body equal at 1600 m/s and 1500 m/s in the water. It shows that the Holocene sediments thicken towards the southern sector of the study area, where the seafloor morphology is flat while in the central sector and in correspondence of the seamounts the

thickness of Holocene is minimal and in many point is zero. In fact, The Holocene is lacking on almost all the Graham Bank, especially where seafloor morphology is irregular.

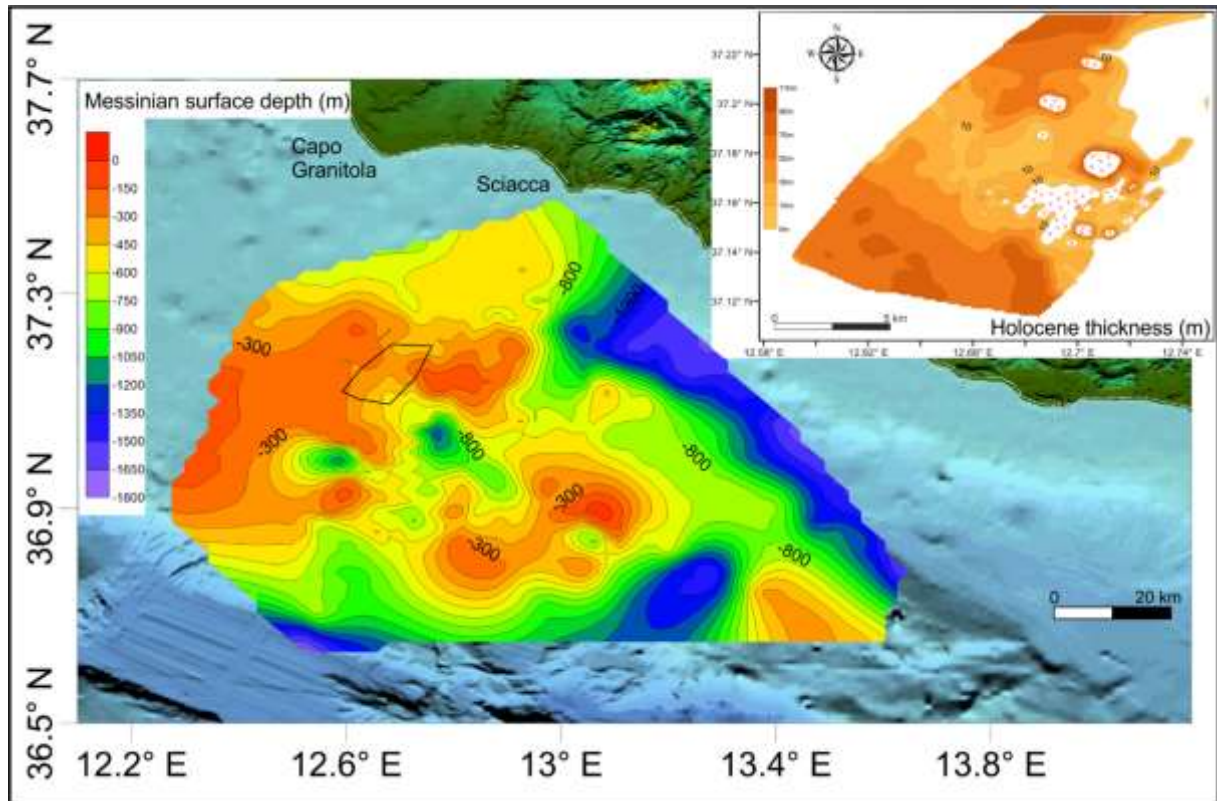


Figure 13 Messinian surface depth obtained using multichannel seismic profiles. The inset shows the Holocene thickness obtained using chirp profiles.

5. Discussion

5.1 Seafloor morphology controlled by tectonic, volcanic and sedimentary processes

Morphobathymetric and seismostratigraphic analysis of the very high-resolution data here described highlight an uneven morphostructural setting of the study area (Figs. 3, 14). The channel, separating the two morphological sectors, in its southernmost tract developed with a SE direction assuming the orientation of the major faults that separate the Graham Bank from the western flat submerged plain (Figs. 3, 9, 10). It displays erosional features, suggesting that it continues into the adjacent lower slope (out of map) where the eroded material is possibly discharged (Gardner et al., 1999).

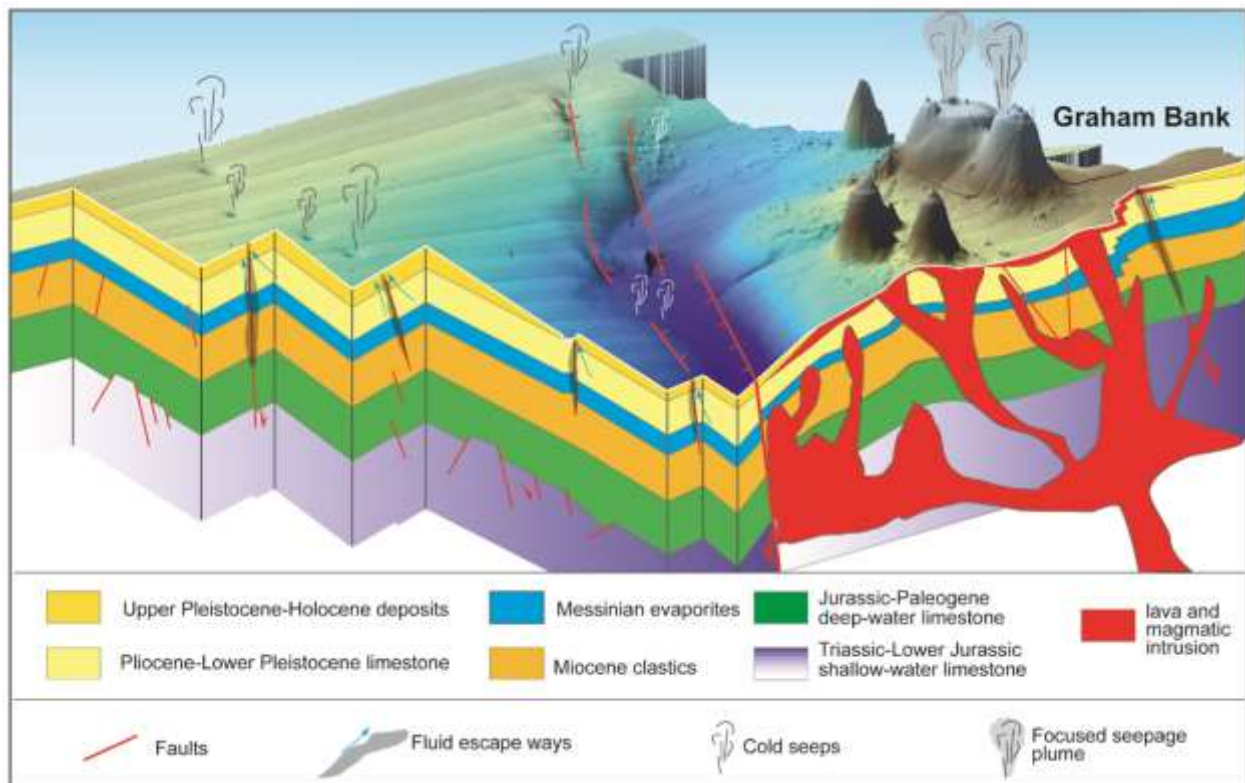


Figure 14 Schematic model of the Graham Bank area, where two different (sedimentary and volcanic respectively) sectors are separated by a fault-controlled NW-SE oriented channel. In the western sector, the sedimentary multilayer is affected by faults that are the pathways for the fluid flow, generating pockmarks in the seafloor. In the eastern sector a deeply rooted volcanic complex is highlighted by mounds and seepage plumes. Along the channel the structural control is shown by fault escarpments being aligned with pockmarks and mounds.

The eastern sector is characterised by magmatic substrate (Unit B in Figs. 9, 10), volcanic mound and a rough morphology related to volcanic products (i.e., lava fields, volcanic ridges, Figs. 3, 4). The M2 mound was an active volcano until the 1831's eruption, product of which comprises the small mound on its flat top (Fig. 4). Similarly, we can hypothesise that the cluster of small mounds above the M3 edifice, which shows a planar seamount morphology, could be related to recent magma activity accompanied by the build-up of coral mounds (Zibrowius and Taviani, 2005). The eastern sector is therefore governed by volcanic processes, while the depositional and erosional features (e.g. local incised valley, Figs. 3, 4) have minor influences in determining the overall morphology.

In contrast, the sector located westward of the channel displays an overall morphology dominated by sedimentary processes whereas the Upper Pleistocene-Holocene multi-layer (Unit C) is affected by deformational features (Figs. 8, 9, 10). Evidence of recent and buried slope failures, the latter occurring during the Quaternary, have been documented on the eastern continental slope of the Sicily Channel (Gela Basin)s (Gardiner et al., 1993; Max et al., 1993; Minisini et al., 2007).

5.2. Fluid escape structures

The several features described as positive and negative reliefs are interpreted here as mounds and pockmarks linked to fluid escape (Hovland et al., 1985; 2002; Judd and Hovland, 2007).

The clusters of depressions, mainly mapped in the western sector of the study area (Fig. 3), are considered as active pockmarks. They display size parameters, shape and seismic attributes comparable with similar features in the central Mediterranean Sea (Micallef et al., 2011). Generally, pockmarks are described as circular erosive structures with variable diameters and depths (Hovland et al., 2002). The pockmarks occur within the stratified hemipelagic Upper Pleistocene-Holocene deposits (Unit C in Figs. 8, 9) and are characterised by continuous high amplitude reflectors with upward concave geometry. This suggests that the pockmarks have a genesis linked to sediments collapse and are rooted deeper than the penetration range of the seismic acquisition system (Figs. 9, 10). Similar features are described from Eivissa and Mallorca Channels (western Mediterranean Sea), where aligned pockmarks are related to submarine volcanism and recent faulting that facilitated the expulsion of hydrothermal gas and water (Acosta et al., 2001; Lastras et al., 2004). In the active fluid flow systems recently described from the Malta Plateau, the methane sources, detected at a number of shallow seep-related seafloor (pockmarks and plumes) and mud-volcanoes, appear to originate from more or less deep reservoirs located close to the Vega oil field (Holland et al., 2006; Savini et al., 2009; Micallef et al., 2011).

Alternatively, the seismic facies and stratal pattern of Unit C (Figs. 8, 9, 10) could suggest the occurrence of a shallow reservoir that act as temporary storage for deeply generated biogenic gas. This interpretation is supported by the high amplitude reflectors alternating with reflection-free bands generated by coarse-to-fine grained sequences. In high energy straits of the Mediterranean they are referred to as high to low energy bottom currents that generate contourite systems (Somoza et al., 2012). In this view, the fine grained deposits (i.e., the reflection-free bands) could represent the seal of a “third migration” geological trap for deeper hydrocarbon gas, with the coarse grained sediments (i.e. the high amplitude reflectors) comprising the reservoir.

This interpretation is confirmed by the aggradational-progradational pattern of the Unit C (Figs. 9, 10) that points out Late Quaternary sea level oscillations, producing variation in the bottom current speed and/or shear stress and responsible for overpressure variations that favoured fluid escape.

Several hydro acoustic anomalies were observed in the water column around the Graham Bank (Figs. 9, 10, 11). Seismic analysis evidenced anomalous amplitude peaks in the water column, which can be attributed to the occurrence of active seepage of fluids from the seabed (Fig. 11, Sauter et al., 2006; Micallef et al., 2011). In this view, their top deflections (Fig. 11) can be considered as due to the NW-oriented oceanographic currents.

5.3. Controlling factors of fluid flow

The mounds, which are widespread in the eastern sector of the mapped area, appear related to submerged volcanic edifices (Figs. 3, 4). Among them, only two of these (M2 and M3, Figs. 3, 4) were already described as active volcanoes (Colantoni, 1975; Coltelli et al., 2016). The occurrence of a magmatic substrate (Unit B), also confirmed by the magnetic and Bouguer anomalies recorded in the area (Lodolo et al., 2012), suggests a volcanic origin of the newly mapped mounds (Figs. 3, 4) and their relationships with recent magmatic activities. The fluids appear to emerge through

faults bordering the Graham Bank (Fig. 11, 12). Furthermore, geochemical data collected in this area (Coltelli et al., 2016) suggest a possible source from hydrocarbons due to the occurrence of CH₄, the abundant CO₂, related to the huge thickness of Meso-Cenozoic carbonates, and the concentration of He, which has a crust-mantle magmatic source. The ³He/⁴He ratio, evaluated in the samples collected in the nearby Sciacca onshore area (Caracausi et al., 2005), supports the idea that a continuous and similar fault system occurs in the SW Sicily and NW Sicily Channel, crossing the whole crust and the upper mantle, down to at least 70 km (Catalano et al., 2000). The hypothesis of a deep origin of fluid is supported also by geophysical data, in particular the alignment of the seismic clusters (Galea, 2007; Calò and Parisi, 2016) and the distribution of volcanic and geothermal regions (Fig. 1b and Lodolo et al., 2012). Vertical distribution of temperatures shows a cold layer between 500 m and 2000 m and a sudden increase of temperature at higher depths (Fig. 2b), suggesting that the fluid escape could represent cold seeps. The latter should rule out that they are hydrothermal vents related to the occurrence of intrusion of volcanic sills, which is different from similar features linked to craters around major volcanic cones and recognised in some oceanic regions (Somoza et al., 2004).

The pockmarks and mounds in the western sector (Fig. 3) developed in a context dominated by tectonic processes. The common orientation of the aligned fluid escape structures reveals an overall geomorphic response to the occurrence of recent NW-SE and NNW-SSE oriented normal faults that cut the Upper Pleistocene-Holocene sedimentary cover (Figs. 3, 8, 9, 10, 11, 14). These faults show the same orientations and kinematics of both the NW-SE Plio-Pleistocene extensional faults system here recognised (Figs. 8, 9, 10) and the structures involving the Miocene strata (Fig. 12), largely described from the NW Sicily Channel (Sulli, 2000; Corti et al., 2006; Civile et al., 2014). These faults, due to their extensional kinematics, favour the migration of fluids from localised gas reservoirs through locally faulted Messinian evaporites (Fig. 12, see also Holland et

al., 2003), suggesting that reactivation of ancient shallow and deep faults has occurred in recent time. Furthermore, among the identified fault systems, the extensional faults cutting the Upper Triassic-Lower Jurassic shallow-water carbonates appear to be conducive to the generation of horst and graben structures, tilted blocks and stepped margin morphologies (Figs. 12, 14). These faults, elsewhere related to the rifting process of the Southern Tethyan continental margin (Bernoulli and Jenkyns, 2009; Basilone, 2009a, b), when reactivated, play an important role in squeezing the fluids originated from deeper hydrocarbon reservoirs subjected to the overpressure at depth (Kopf, 2002; Judd and Hovland, 2007; Etiope et al., 2008). A compressional reactivation related to inversion tectonics has been suggested for the Sicily Channel rift systems (Catalano et al., 1993).

This scenario, where different types of fluid escape structures are distributed in the two main sectors of the study area, implies the presence of two main geological contexts (Fig. 14): the eastern sector (Graham Bank and nearby structures) with volcanic mounds and seepage fluids related to volcanic activity, and the western one, mainly involving aligned pockmarks and mounds where faults are the preferential pathways for the migration of fluids. These volcanic and sedimentary contexts respectively, reflect the occurrence of different fluid migration and escape systems (Fig. 10).

The channel, separating the two different morphological sectors, is the seafloor expression of a deep tectonic structure. Well imaged in the seismic profile as a vertical fault with probably lateral movement (Fig. 12), it separates two different geological settings responsible for the differentiated morphology of the seafloor, and likely acts as barrier to the fluid flows.

6. Conclusions

Two main seafloor sectors of the study area (Graham Bank), separated by a deeply incised channel, can be discerned. The eastern one is characterised by rough morphology, several mounds, focused seepage plumes, and volcanic edifices (Graham Bank and minor cones here mapped). Differently, the western area has a quite flat morphology where the Upper Pleistocene-Holocene deposits are characterised by the occurrence of several aligned pockmarks and mounds, indicating migration of fluid to the seafloor, seeping out through active faults.

Considering the good correlation between orientations of pockmarks, fault escarpments, mounds, channel geometry and the main identified fault systems in the region, this study reveals strong relationships between tectonics, volcanism, migration of fluids, and morphology. Considering the He isotopic ratio of the fluids and that, the fault systems and volcanic activity are rooted at depth, we propose that the fluids originate in the deepest thinned continental crust at the boundary with the mantle. Vertical distribution of temperatures suggests cold seeps through dip-slip faults that dislocated and that favoured the migration of fluids from gas reservoirs at different stratigraphic levels where they are temporary hosted.

In this view, the intervening channel, which is the seafloor expression of a deep tectonic lineament with lateral movement (transtensive fault), may act as a barrier to fluid flow systems and has controlled the morphostructural evolution of the adjacent sectors.

4.3. Submarine Gravity Driven Deposits in the volcanic Graham Bank (central Mediterranean Sea): an interaction among tectonic and volcanic triggering mechanisms

Abstract

We present a geomorphological study based on new very high-resolution dataset (multibeam and CHIRP) of the Graham Bank volcanic area (Sicily Channel) focusing on the gravity driven deposits as well as mass transport deposits (MTDs) and relating them to the interaction of sedimentary-oceanographic, tectonic and volcanic processes affecting the area.

The Graham Bank, making part of the Sicily Strait geographical element, is the SE-ward prolongation of the Adventure Bank. It is a shallow-water area ranging between 10 and 350 m in depth and is the marginal sector of the southern Sicilian continental platform. This sector is linked to the deep-water Pantelleria Graben through an erosive submarine canyon.

The geomorphology of the area comprises two different regions separated by a tectonically-originated NW-SE erosive channel. The first one is a volcanic region, dominated by cones and seamounts, aligned mounds, craters and focused seepages and the other one is a flat sedimentary region characterised by fluid escape structures.

The mapped gravity driven deposits, variously distributed in the area, are: a) soft-sediment depositional structures (SSDSs), including rotational slumps and translational glides, mainly located along the slopes bordering the channel and inside the channel; b) rock falls that are diffused at the foot of the steep fault escarpments and the volcanic cones; c) large debris avalanches that occur at the foot of the main volcanic cones associated with slide scars and rotated blocks.

The main pre-conditioning geomorphological factor which could have induced sediment instability is the steep gradient of the slope, while the deformational forces and trigger mechanisms

are related to the interplay of volcanic activity, including bulging and subsidence, eruptions, focused seepage plumes, tectonics including the NW-SE oriented normal faults and associated earthquakes, fluid escape structures (pockmarks), and sedimentary/oceanographic processes that act with mass-gravity movements and bottom currents mainly influenced by the AIS and the local Adventure Bank Vortex.

Keywords: mass transport deposits, soft-sediment deposition structures, rock falls, debris avalanches, volcanic and tectonics triggers, Sicily Channel.

1. Introduction

Submarine mass movement are one of the geological processes responsible for the transfer of large amounts of sediment onto the deeper parts of a basin (Varnes, 1978; Lowe, 1976; Posamentier and Kolla, 2003). They are driven by gravitational forces, are common on inclined areas of the seafloor, often in situations of rapid deposition of un-lithified or semi-lithified fine grain sediment or fractured rock and play an important role in shaping the seafloor (Gee et al., 2006; Moscardelli et al., 2006; Tripsanas et al., 2008).

Many factors have been suggested as triggers to the initiation of submarine mass movements, examples include sedimentary, tectonic and/or volcanic processes. Sediment loading and rapid burial of cohesive sediment commonly result in overpressuring. This leads to gravitational instability which triggers flowage of sediments (Maltman, 1994; Odonne et al., 2010; Moretti et al., 2001). Thus, where rivers contribute large amounts of sediment to relatively localised areas favoured slope failures on the continental margins (Lee et al., 2007; Gamboa et al., 2010). Present-day channels, canyons and various-scale gravity driven deposits such as turbiditic fan, debris flow, and grain flows are documented mainly from the continental slope and are addressed to the interaction of tectonic and sea level fluctuations (McAdoo et al., 2000; Garziglia et al., 2008, Sulli

et al., 2013; Lo Iacono et al., 2011; 2014).

Passing storm waves, bottom currents and the presence of gas filled cavities within sediments are also capable of reducing the strength of the strata (Molina et al., 1998; Chen and Lee, 2013). When these packages of sediment are subjected to tectonic erosion or seismic strain, such as earthquakes, reduction of pore water pressure occurs and reduces the strength of the strata, inducing slope instability and mass movements (Allen, 1986; Obermeier, 1996; Montenat et al., 2007; Owen et al., 2011). Several types of seafloor volcanic processes are also able to mobilise large quantities of material that are volumetrically important, both in modern and ancient deep-water basins (Posamentier and Kolla, 2003).

The flanks of insular volcanoes and/or seamounts are potential areas where mass movements, with or without the occurrence of catastrophic effects that are able to produce tsunamis, can be active and represent geohazard elements (Chiocci and De Alteriis 2006; Casalbore et al. 2011; Romagnoli et al. 2012).

Examples, showing particular morphologies (lava fields, blocky topography, complex-shaped scars, fan-shaped bulge, hummocky terrains) related to volcanic activities that can triggered MTDs, come from the Hawaii islands (Moore and Moore, 1984; Moore et al., 1994; McMurty et al., 2004), the Canary–Cape Verde Islands (Gee et al., 2001; Masson et al., 2002; 2008; Romero Ruiz et al., 2000; Ward and Day, 2003), Ischia Island (Chiocci and De Alteriis 2006), and Aeolian Islands (Romagnoli et al. 2009; 2013; Casalbore et al. 2011; 2014).

The Graham Bank, located in the north-western Sicily Channel (Central Mediterranean, Fig.1), is a submarine volcanic area (Colantoni, 1975; Coltelli et al., 2016), where sedimentary and tectonic processes interact with volcanism offering variable morphologies and geomorphic elements, including mounds and pockmarks, sedimentary plains, ancient and recent structural lineaments, volcanic highs and erosional channels.

Aim of this work is to describe, using high-resolution seismic data (Chirp profiles) integrated with swath bathymetric data, the submarine mass movements recognised in the sector around the Graham Bank (Fig. 1). We focus on the classification of the several types of these gravity driven deposits suggesting their formation and their triggering mechanisms that include the interaction among volcanic and tectonic activities, which on the whole controlled the morphogenetic evolution of the area during the Quaternary.

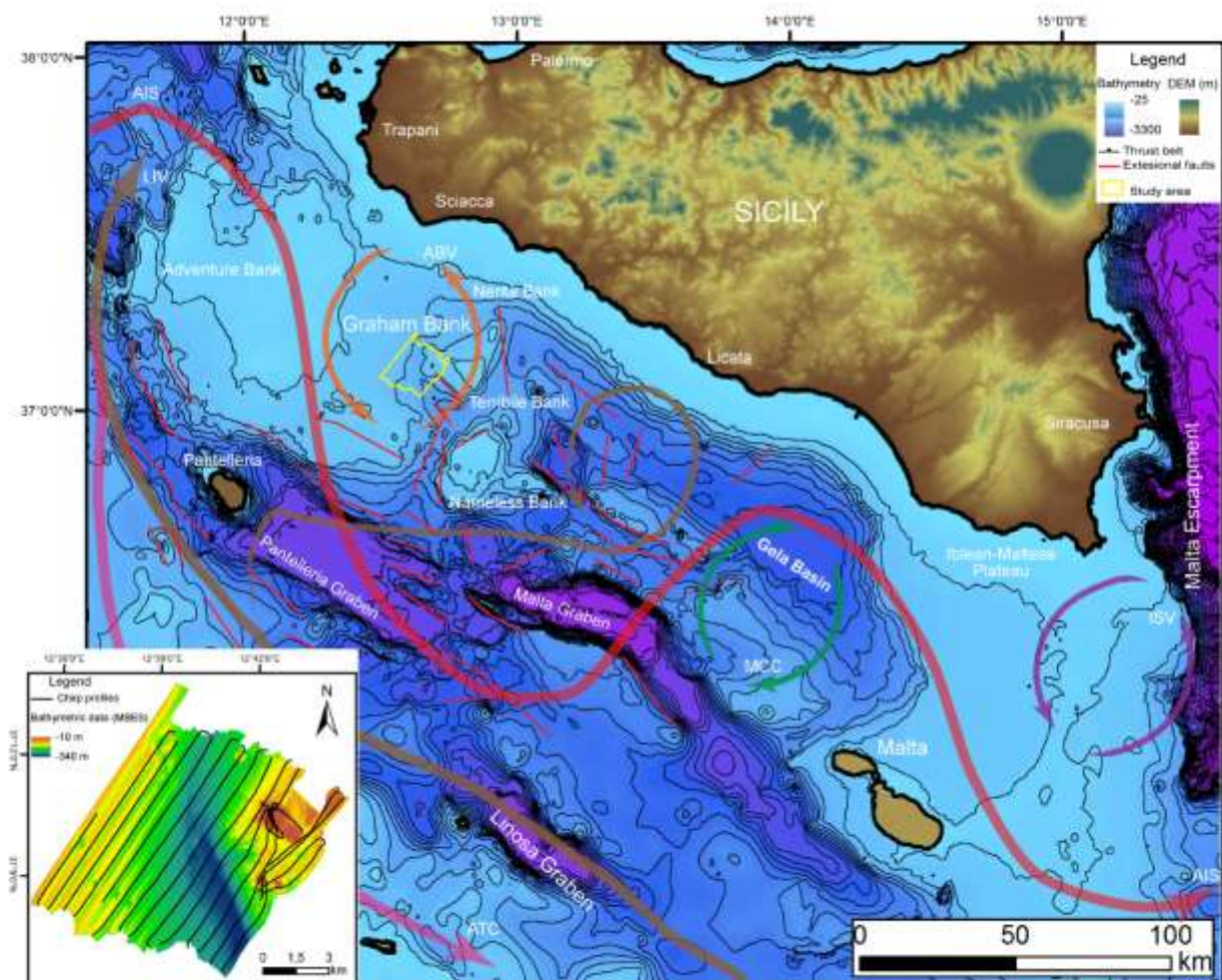


Figure 1 Bathymetric map of the Sicily Channel (Central Mediterranean), showing the main physiography, Plio-Pleistocene graben systems, and distribution of main pathways Main water masses: MAW (Modified Atlantic Water), LIW (Levantine Intermediate Water); AIS (Atlantic Ionian Stream), ATC (Atlantic Tunisian Current); ABV (Adventure Bank Vortex); MCC (Maltese Channel Crest); ISV (Ionian Shelfbreak Vortex); ABV (Adventure Bank Vortex) and in yellow indicated the submarine cables.

2. Regional setting and physiography

2.1. Geological setting

The Sicily Channel (central Mediterranean Sea) is a structural element of the African continent, between the southern coast of Sicily, the northern coast of Africa and the Malta Escarpment (Fig. 1). It is a part of the foreland element of the African compressive margin resulted from the collision between Africa and Europe (Catalano et al., 1996; Granath and Casero, 2004; Finetti et al., 2005).

The Sicilian Fold and Thrust Belt (FTB) originated from the piling-up of tectonic bodies, deriving from the deformation of the paleo-geographic domains developed during the Mesozoic in the African rifted continental margin (Basilone et al., 2016a and reference therein). It grows above a northwest dipping regional monocline consisting of Mesozoic carbonate platform deposits of the Iblean foreland, covering the stretched African continental crust (Handy et al., 2010; Catalano et al., 2013). The foreland area, cropping out in south-eastern Sicily (Iblean-Maltese Plateau) and submerged in the Sicily Channel (Pelagian Block), is the result of the interaction of both the Sicilian-Maghrebian collision and the Sicily Channel rifting (Fig. 1, Argnani, 1990; Sulli, 2000; Finetti et al., 2005).

The present day structural setting of the Sicily Channel is characterised by NW-SE -oriented sub-vertical Neogene-Quaternary normal faults controlled the horst-and-graben structural setting of the “Sicily Channel Rift Zone” (Pantelleria, Malta and Linosa grabens and Adventure Bank, Fig. 1, Torelli et al. 1991; Catalano et al., 1993). The rifting thinned the continental crust to 15–18 km since the Early Pliocene (Argnani 1993; Civile et al. 2008), opened the above-mentioned grabens and produced widespread subaerial and submarine volcanic activity (i.e., Pantelleria and Linosa volcanic islands, Graham and Nameless banks, Fig. 1) with alkaline to peralkaline affinity related to anorogenic magmatism (Corti et al., 2006; Rotolo et al., 2006). Seismic activity involves up to 20 km deep hypocentres with $ML < 3.5$ (Chiarabba et al. 2005; Galea, 2007). Most of

earthquakes occur along N-S trending belt, between the Sciacca offshore and the Lampedusa Island, down to a depth of 60 km, reaching $ML \geq 5$ (Calò and Parisi, 2016).

2.2. Morphology and Oceanography

The Sicily Straits (Fig. 1) is a shallow marine sector characterised by 80 km wide continental shelf, mainly represented by the Adventure Bank. It, entails seafloor ranging from 75 to 205 m in depth, is separated from the southern coast of Sicily by the “Mazara Channel” and is linked to the 1300 m deep “Pantelleria graben” by a continental slope ranging from -150 to -1000 m in depth and steeping up to 14° .

The Graham Bank, the SE-wards prolongation of the Adventure Bank linked with it by intermediate gully (Fig.1), is characterised by a complex geomorphological setting including a volcanic region with several cones and seamounts (Carapezza et al. 1979; Beccaluva et al.1981; Calanchi et al. 1989; Peccerillo, 2005; Lodolo et al. 2012) and a flat continental platform with fluid escape phenomena.

In the last 100 years, the Graham Bank has been affected by numerous volcanic eruptions, up to historical time, when during the 1831 the emergence and rapid disappearance of the Ferdinanda volcanic Island has occurred (see Colantoni, 1975). Heat flow values show relative high isothermal contours located between the Graham, Nerita and Terribile Banks, where a 75 to 100 mW/m² flow is recorded (geothopica.igg.cnr.it).

The Modified Atlantic Water (MAW), which enters through the Sicily Strait and flows eastward interact, immediately S-wards of the study area, with the Levantine Intermediate Water (LIW), which is saltier and deeper (between -200 and -400 m), and which flows in the opposite direction (Fig. 1; Millot, 1999; Lafuente et al. 2002). The MAW when entering the Sicily Channel splits in two sub-currents: the Atlantic Ionian Stream (AIS) and the Atlantic Tunisian Stream

(ATS) (Fig. 1; Sorgente et al., 2003). The AIS flows to the south of the Adventure Bank and proceeds south-eastward while the ATS flows along the African coasts. Around the Adventure Bank and the Maltese Islands, two loop currents called the Adventure bank vortex (Lemursiax & Robinson, 2001; Gabersek et al., 2007), and the Maltese Channel Crest (MCC) are formed.

3. Materials and Methods

In this work we used different types of high-resolution data (Fig. 1 inset) acquired during the ACUSCAL cruise, carried out in 2015 aboard the R/V *Minerva1*, in the framework of the RITMARE Project (CNR IAMC, Sez. Capo Granitola, Mazara del Vallo).

About 200 km of high-resolution seismic reflection profiles, spaced at 800 m, were acquired using a hull-mounted 16 transducer Teledyne/Benthos CHIRP III profiler. This instrument works with frequencies ranging between 2 and 7 kHz, a ping rate between 250 and 750 ms, Tx power between 5 and 7, a pulse length of 10 ms and 30-42 db of gain.

The “Communication Technology SWANPRO” software was used to acquire and store the data. The profiles were processed and interpreted using Kingdom and GeoSuite Work software packages. Data processing included Automatic Gain Control, Time Variant Gain, Swell Filter and Mute. The time-depth conversions of the Chirp profiles have been made adopting average velocities derived from lithostratigraphy and sonic log data collected in the southern and western Sicily offshore.

A seismic P-wave velocity of 1600 m/s was used for the Holocene sediments, whereas 1500 m/s was used for seawater (Catalano et al., 2000).

Multibeam echosounder coverage of 100 km² of seafloor has been obtained using the Reson SeaBat 7160, which generates 512 beams at a nominal frequency of 44 kHz. Positional data were provided by differential Global Positioning Systems (dGPS) by FUGRO SEASTAR.

The multibeam data were processed using the PDS-2000 software and entailed removal of erroneous beams, noise filtering, and calibration and processing of navigation and correction for sound velocity.

A Digital Terrain Model (DTM) was obtained with a grid size of 5 m. We used Global Mapper and Golden Software Surfer 9 in order to obtain 3D and shaded relief models, bathymetric profiles, and to interpret the morpho-bathymetric data.

4. Results

4.1. Geomorphological outline

The study area, a section of the outer continental shelf to upper slope comprising between 10 and 350 m in depth, is characterised by a jagged seafloor morphology where two main geomorphological sectors are separated by an asymmetric channel (about 12 km² wide) crossing the whole investigated area (Fig. 2).

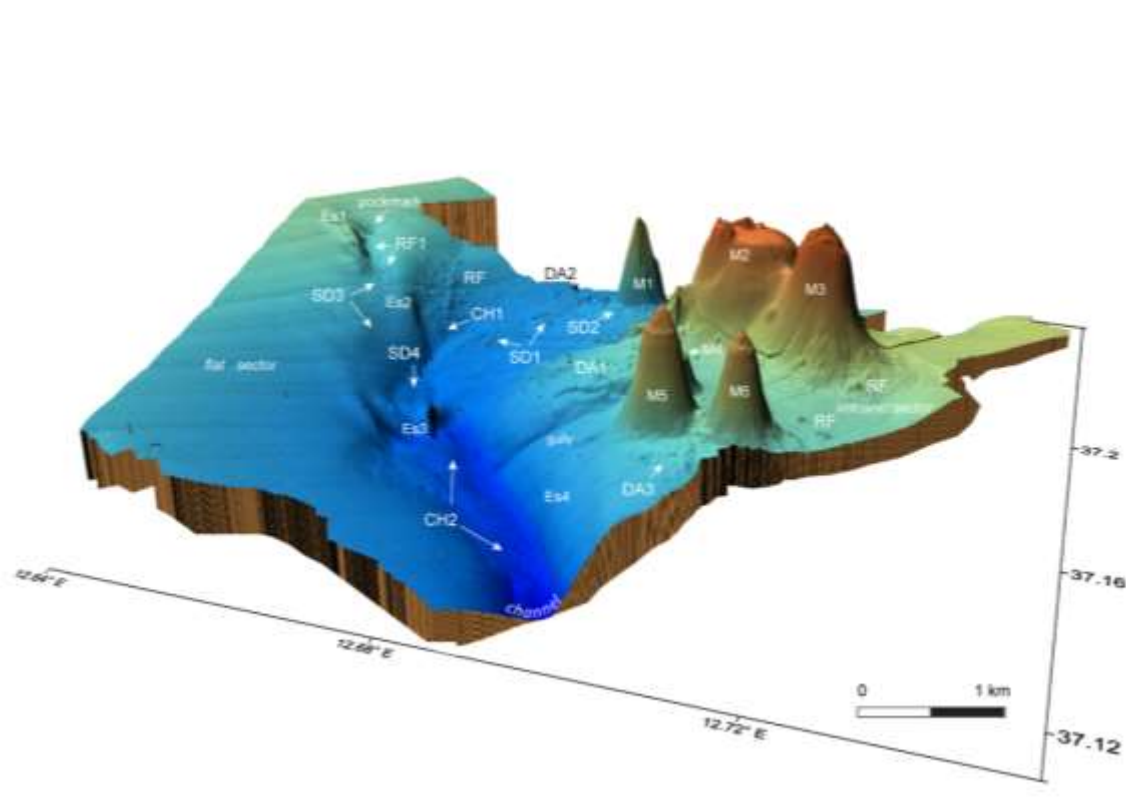


Figure 2 Digital Elevation Model of the study area. A NW-SE channel separates two different sectors (flat and volcanic sectors) that are characterised by several morphostructures: M1-M7 mounds, Es1-Es4 fault escarpments, pockmarks and different types of gravity driven deposits (SD1-SD4), DA1-DA3, CH1-CH2 and RF.

The eastern sector, corresponding to the sector around the volcanic Graham Bank edifice has a rugged morphology, due to the occurrence of aligned mounds, ridges, and a cluster of recent volcanic cones and seamounts with a flat surface at the top (i.e., guyot), as consequence of relative sea-level changes as well as of the subaerial phase during their volcanic eruptions (M1-M7 in Fig. 2).

The largest cones, M2 and M3, form a NW-SE oriented elongated structure with a gradient slope ranging between 19 and 21°, are incised by gullies and slide-scars. The M1, which has similar size and shape with the other cones (M4, M5, M6 in Figs. 2, 3, 4), display flanks sloping at 22°. Adjacent to the main cones, at 150-170 m below sea level, NW-SE elongated elliptic- to circular-shaped crests and craters, defined by a well-preserved rim, are observed.

The western sector displays a flat morphology, with an average steepness of 1.2 to 1.5°, increasing W-ward. It is characterised by pockmarks and NW-SE -oriented elongated steep escarpments (Es1-3 in Fig. 2).

The intervening channel runs, predominantly, in a N-S and NW-SE direction has length of 10 km, depth from -250 m to -350 m, and 0.8-1.5 km width. It is bounded, both in its SW and NE sides, by sub-vertical fault-escarpment (Es2-4 in Fig. 2).

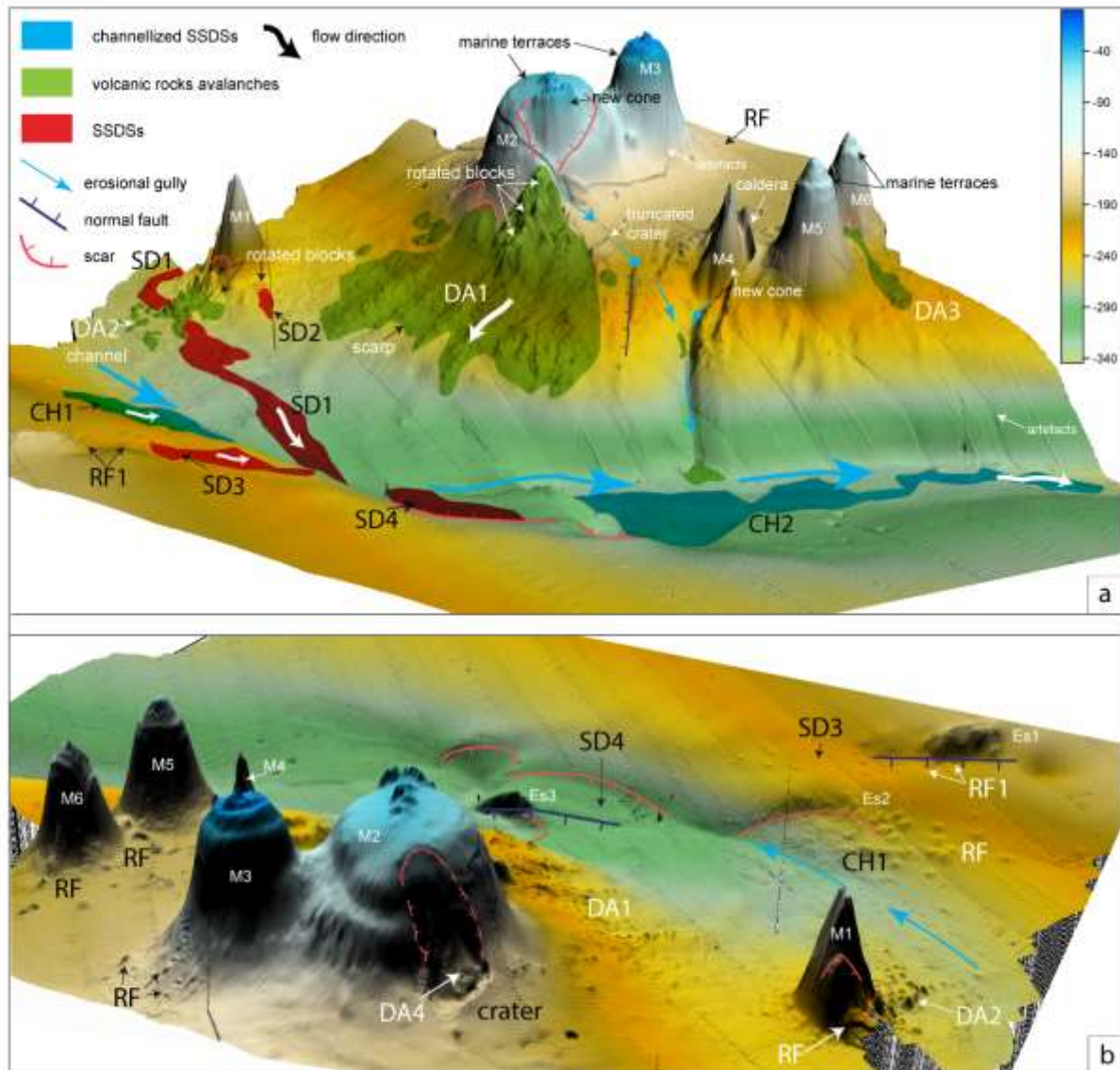


Figure 3 Schematic 3D view of the Graham Bank area, where a fault-controlled NW-SE oriented channel showing the recognised gravity driven deposits separates two different (sedimentary and volcanic respectively) sectors. In the eastern sector seamounts highlight a volcanic context. Along the channel fault escarpments being aligned with pockmarks and mounds show the structural control. (a) Detail of the gravity driven deposits that are subdivided in three main families indicated with different colours. (b) The 3D map show the location of the main scars and normal faults linked to the genesis of the gravity driven deposits.

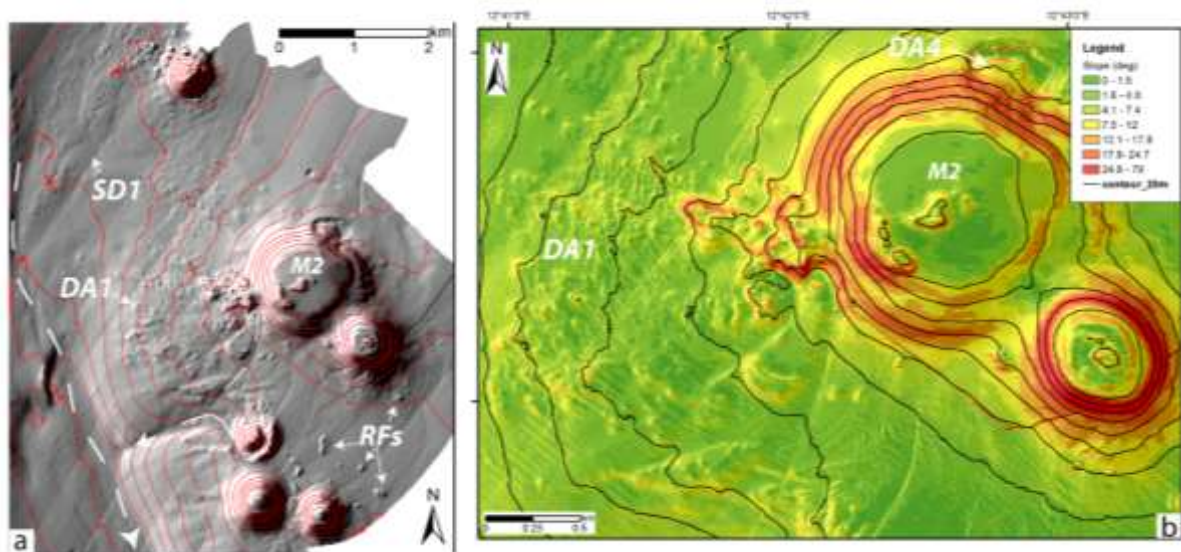


Figure 4 Location map: (a) Regional map illustrating the setting of the Graham Bank sector. White arrow indicate the location of the recognised chaotic deposits. In red are indicated the contours. (b) Slope gradient map of the Graham Bank, illustrating the main landslides.

4.2. Gravity driven deposits

The numerous mapped gravity driven deposits are variously distributed in the previously described morphological sectors, where they occur with different morphology and morphometry (Figs. 2, 3, Tab. 1).

In the eastern volcanic region, they are:

- A large fan-shaped body 2.15 km² wide, highlighted by the extremely indented seafloor forming a chaotic pattern with blocky topography, occurs along the western flank of M2 (DA1 in Figs. 2, 3 and Tab. 1). It, located 65 m below the top of the M2, is associated with a slide scar with a gradient slope of 21° that affect the steep flank of the volcanic cone (Figs. 3a, 4). The scar was activated before an eruption event forming the new cones on the summit of the M2 and after the erosional process forming the marine terrace. At the base of this scar, many rotated blocks are present as well as a remnant of the original volcanic crater occurs scoured from the summit of the M2. It is located immediately south of the M2 and bordered by a post-landslide erosional

- channel starting from the head of the DA1 (Figs. 3a, 4). Various blocks decrease in size toward the toe area, indicating the flow direction towards the channel depression (Fig. 4a). Secondary escarpments, dipping towards the channel, are present in the lower part of the body (Fig. 3a);
- A small fan-shaped body, with an extension of 0.278 km² forming a blocky topography of the seabed, occurs at the base of the western flank of M1 (DA2 in Figs. 2, 3a and Tab. 1). It is associated with a well-defined scar with gradient slope of 26° and rotated blocks accumulated at its base (Figs. 3a, 5);

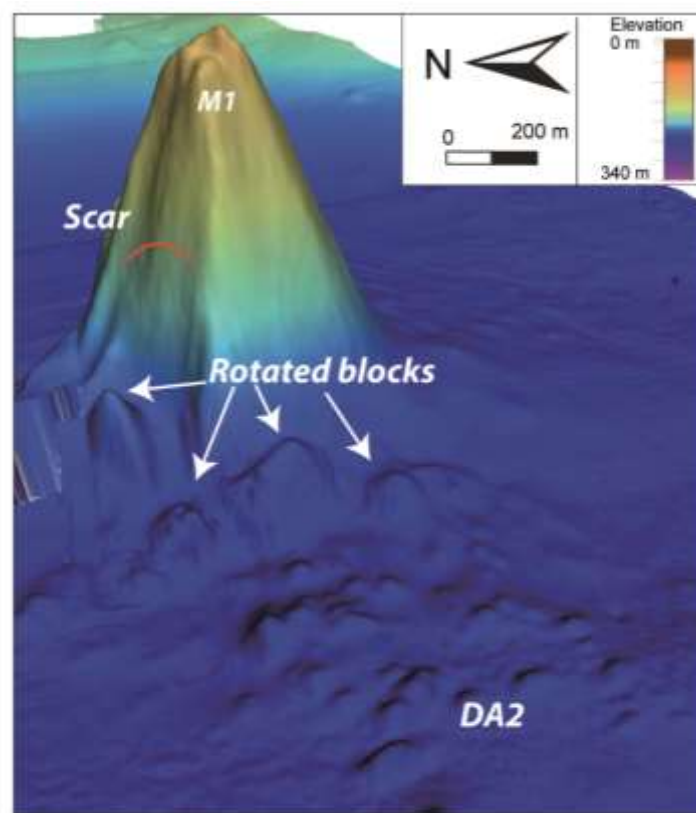


Figure 5 3D Detail of the M1 showing the recognised rotated blocks and the relative scar.

- A small elongated body with lobe shape 0.279 km² wide, characterised by blocky topography and steeped escarpments, occurs at the foot of the volcanic cone M6 where an arcuate scar cuts its SW flank (DA3 in Figs. 2, 3a and Tab 1);

- A mound-shaped body, 0.149 km² wide, is located at the base of the northern side of the M2 volcanic cone (DA4 in Figs. 3b, 4b). It develops from a well-defined scar interesting the whole volcano side starting from its top, where a concave erosional surface carves the flat top of the volcanic cone. The reworked material is preserved in an adjacent sub-circular-shaped volcanic depression;
- Small and isolated bodies with dome shape, locally associated with arcuate scars (e.g. the scar with gradient slope of 26° occurring along the northern side of the M1, Fig. 3b), are mapped at the foot of the volcanic cones (RFs in Figs. 3, 4a);
- An elongated body, 0.897 km² wide, forming a rough surface of the seabed (hummocky topography) occurs immediately at south of M1 (SD1 in Figs. 2, 3a, 4a and Tab. 1). It, on its head, is truncated and covered by the DA2 that is related to more recent instability event;
- A small sub-circular dome-shaped body, 0.0247 km² wide occurs at the foot of the southern flank of M1 (SD2 in Figs. 2, 3a and Tab. 1). It is associated with a small scar with concave shape cutting an adjacent small cone.

In the NE side of the flat morphological sector, immediately adjacent to the main channel, have been mapped:

- A cluster of heterogenic blocks, covering an area of 0.136 km², formed a jagged surface of the seabed. It occurs at the foot of the steep fault escarpment (Es1) in the north-western corner of the flat region (RF1 in Figs. 2, 3b, Tab. 1). It is bordered NW-wards by a large pockmark where the seabed displays a concave-upwards morphology;
- An arcuate-shaped SE-wards elongated body, covering an area of 0.75 km² and characterised by rough seafloor morphology (SD3 in Figs. 2, 3 and Tab. 1), occurs at the foot of the 30 m wide steep fault escarpment (Es1 in Fig. 2) and is prolonged into the main channel.

Along the channel morphological sector have been differentiated:

- An elongated body characterised by a rough seafloor morphology, 0.961 km² wide, occurs in the northernmost portion of the channel starting from the area at the foot of the steep escarpment Es2 (CH1 in Figs. 2, 3 and Tab. 1). In this portion, the channel displays an incised U-shaped thalweg, moderately concave upwards at depths until 310 m, becoming V-shaped with asymmetric flanks between -310 m and -325 m and with a downslope gradient ranging between 1 and 2°. The channelized body CH1 is limited southwards by a concave break forming 20 m high escarpment that separates it from the CH2 channelized body occupying the southernmost portion of the channel (Figs. 2, 3a);
- A fan-shaped body, 0.528 km² wide and partially buried, occurs in the central portion of the channel (SD4 in Figs. 2, 3, Tab. 1), and is associated with an arcuate- and concave NW-SE oriented scar, 1.2 km length (Fig. 3b);
- An elongated body with irregular shape occurs in southernmost sector of the NW-SE oriented channel, covering an area of 2.458 km² (CH2 in Figs. 2, 3, Tab 1). In this portion the channel displays a flat shaped thalweg, with downslope gradient <1° and walls with steepness varying from 4° to 7°, which form elongated steep escarpments 30 (Es3) and 100 m (Es4) high.

ID	Latitude	Longitude	Length (m)	Wigth (m)	Perimeter (km)	Deposit area 2D (km ²) ^a	Deposit area 3D (km ²) ^a	Volume (km ³) ^a	Slope (deg)	Thickness (m) ^b
DA1	37° 10' 22.1443" N	12° 41' 34.6393" E	2100	2000	6.6	2.15	2.2	0.15	21	—
DA2	37° 12' 11.2353" N	12° 41' 11.6538" E	740	540	2.6	0.278	0.283	0.028	23.5	5.2
DA3	37° 08' 40.7177" N	12° 42' 26.4908" E	1200	200	2.7	0.279	0.282	0.027	5.8	6
RF1	37° 11' 51.4507" N	12° 39' 12.2662" E	700	165	1.8	0.136	0.137	0.0011	11	6.4
SD1	37° 11' 53.6259" N	12° 40' 40.1697" E	3600	280	7.9	0.897	0.9	0.022	2	6.3
SD2	37° 11' 52.1719" N	12° 41' 18.8561" E	310	100	0.75	0.0247	0.0248	0.000193	4.8	5.7
SD3	37° 11' 12.2173" N	12° 39' 55.7357" E	2600	280	5.8	0.75	0.76	0.018	2	3.5
SD4	37° 10' 5.2958" N	12° 40' 4.1897" E	1340	617	3.25	0.528	0.529	0.00483	2	9.6
CH1	37° 11' 44.9497" N	12° 39' 50.1878" E	2800	850	6.8	0.961	0.965	0.038	1.5	6.7
CH2	37° 08' 46.2300" N	12° 41' 1.2812" E	4600	500	9.4	2.458	2.46	0.04	2_3	9
DA4	37° 10' 59.2168" N	12° 42' 53.1678" E	545	300	1.65	0.149	0.152	0.000138	12	—

^a values estimated by ArcGIS using the multibeam data

^b values calculated using CHIRP profiles considering a seismic P-velocity of 1600 m.

Table 1 Physical features of the recognised gravity driven deposits.

4.3. Seismostratigraphic analysis

Seismostratigraphic analysis has pointed out the occurrence of three main seismic units (Tab. 2).



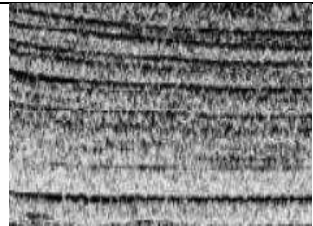

Unit A	Acoustic substrate	It is the oldest facies and shows acoustically transparent reflectors. At the top is bordered by a discontinuous high amplitude reflector. Internally It is affected by normal faults dipping to the NNE and SSW that locally displaced the seabed.	
Unit B	Volcanic context	Facies B overlies facies A. Internally is formed by an acoustically opaque/transparent seismic facies delimited by discontinuous often with high-amplitude reflectors that laterally passing to the facies A.	
Unit C	Holocene sedimentary body	The unit is characterised by a tabular external shape and maximum thickness of 90 ms TWTT and comprises thin-layered showing high-amplitude and divergent to aggrading reflectors, with good lateral continuity, that alternate with low-amplitude reflectors. This regular geometry is interrupted in the western part of the study area only by circular depressions or escarpments while in the NNE edge is affected by faults.	
Unit D	Chaotic Bodies	It is the highest, has been recognised at the top or within Facies C. Internally consists of acoustically transparent and chaotic seismic features where continues reflectors did not have been identified. Externally, it shows chaotic bodies with an irregular-shaped top. This seismic unit is often in unconformity with the shallower facies (Facies C).	

Table 2 Seismic features of the recognised seismic units.

Unit A, which is considered the Lower Pleistocene hardened substrate, has a discontinuous pattern with the reflectors being offset by normal faults dipping to the NNE and SSW. These faults locally affect the seabed forming steep faulted escarpments (Es1-3 in Figs. 2, 3).

Unit B, which is the magmatic substrate of the Graham Bank volcanic region, is an acoustically opaque/transparent seismic facies due to poor penetration of the seismic signal.

Unit C comprises thin layered high-amplitude progradational to aggradational group of reflectors with good lateral continuity alternate with low-amplitude reflectors, representing the

Upper Pleistocene-Holocene multi-layer. It is affected by normal faults in the NNE, the largest of which shows a fault escarpment 36 ms TWTT (29 m) high (Es2 in Figs. 2, 3). The unit in the hanging wall of the faults appears slightly folded, whilst in the footwall it rests unconformably above Unit A (Figs. 6, 7).

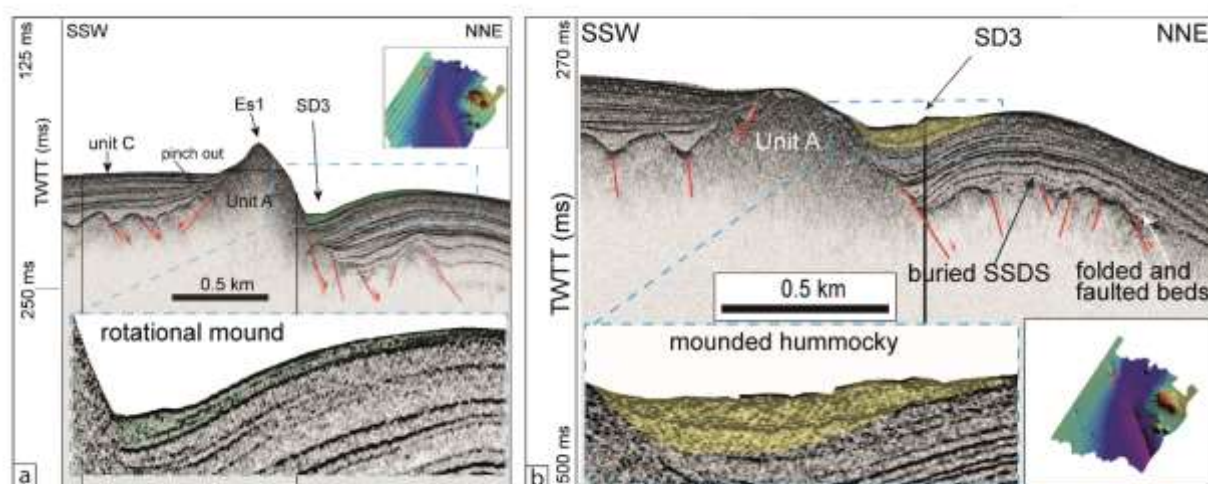


Figure 6 Chirp profile showing the presence of gravity driven deposits (in green and in yellow) in the western sector of the study area. The Unit A is affected by extensional faults, corresponding to escarpments (Es1)

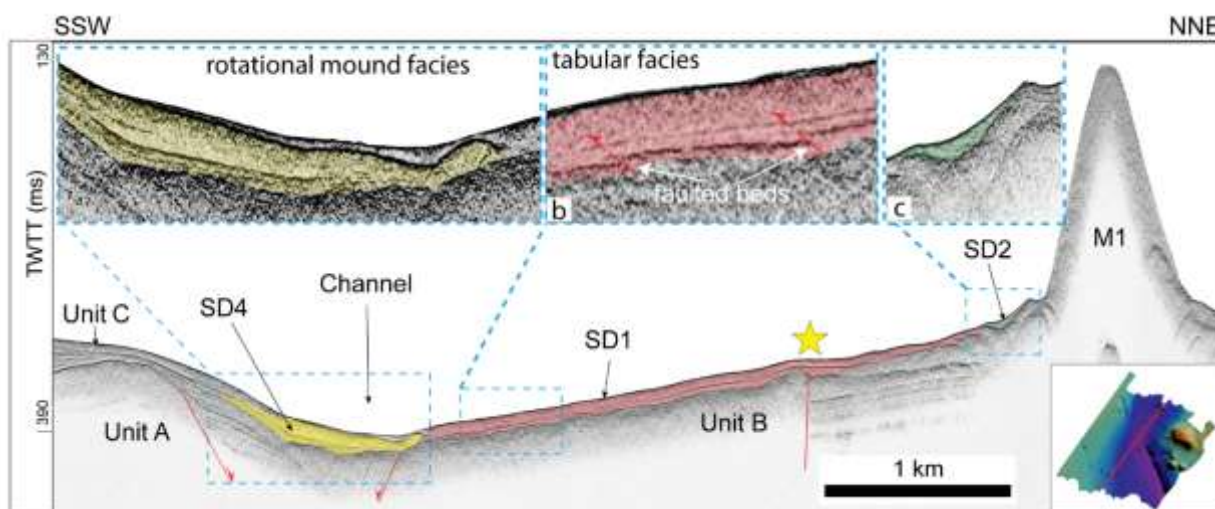


Figure 7 Chirp profile showing the general morphology of the study area. Both unit A and B are affected by extensional faults (in red). The morphology of the seafloor highlights morphostructural features and the chaotic bodies indicated in yellow and in red. The yellow star indicates the epicentre of the 22-08-2003 earthquake (ML 2.6; depth 5 km) here corresponding to a sub-vertical fault.

4.3.1 Seismostratigraphic features of the gravity driven deposits

Some seismic facies, showing sedimentary structures as chaotic beds, truncations stratal discordance, hummocky geometries, faulted and folded beds, have been identified:

- “Mounded-hummocky facies” is a chaotic/opaque seismic facies of continuous high-amplitude reflectors alternating with low-amplitude reflectors characterising bodies with convex shape (Fig. 6b). It laterally, with increase of distance from the broken slope, displays thin low-amplitude and continue reflectors that grades into the unit C. This represents the seismic facies of the elongated chaotic and channelized bodies identified at the base of escarpments where the seabed shows elevated slope (SD3 and CH1-2, Figs. 6a, 6b, 8c). These bodies, with variable thickness, display a basal erosional unconformity generally carved on the top of the unit C (Fig. 6b).

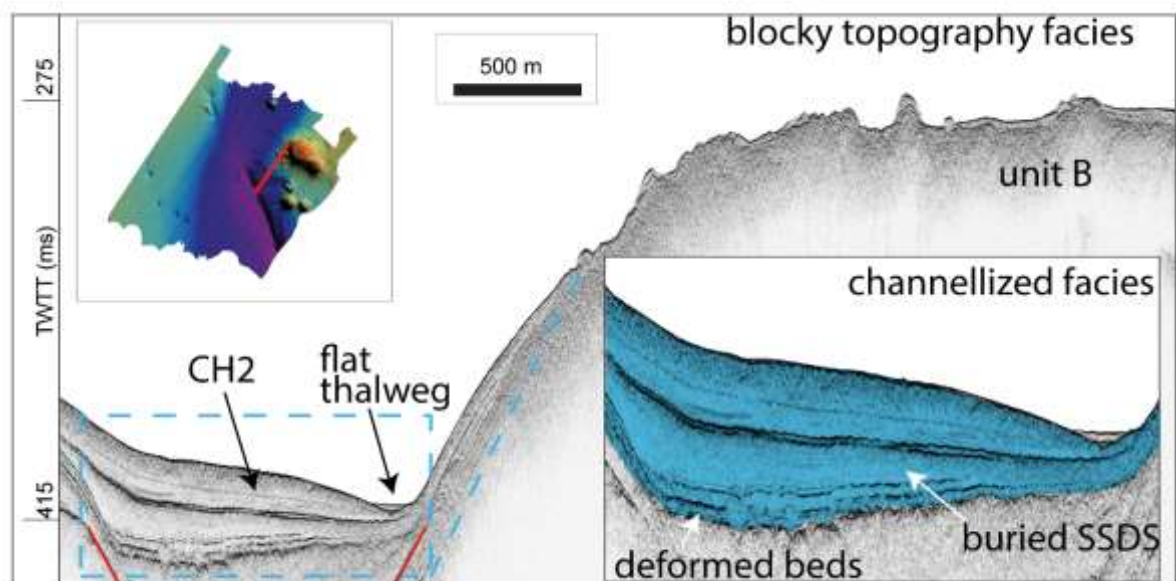


Figure 8 Chirp profiles showing the general morphology of the southern part of the elongated channel. This sector is affected by extensional faults (in red). The morphology of the seafloor in the central sector of the channel highlights shown an elongated chaotic body (in blue).

- “Rotational mound facies” is a chaotic seismic facies characterised by discontinuous very low amplitude reflectors, becoming reflectors-free and/or discontinuous high reflectors with arcuate shape (Figs. 6a, 7a, c). It is topped by very-high amplitude reflector and its basal surface is defined by generally continuous high amplitude reflector that has concave to strongly irregular shape (Fig. 7a). This seismic facies represents large to small chaotic bodies with lobate and circular shape, occurring both in the volcanic region (SD2 in Fig. 7c, and others unnamed bodies in Figs. 2, 3), along the SW side of the channel, where the SD4 has an asymmetric shape with two small moats partially filled and buried (Fig. 7a) as well as of the SD3 body (Fig. 6a).
- “Slide masses facies” is transparent/opaque and in some portion appears with chaotic seismic facies with very low amplitude and discontinuous reflectors, characterised at the top by high-amplitude continuous reflector with planar shape (Fig. 7b). Its basal surface can be a continuous high amplitude weakly irregular reflector in unconformity with unit B (Figs. 7b, 9). It corresponds at the chaotic body SD1 (Figs. 2, 3, 7, 9a) that is affected by normal and reverse faults at its head and toe portions respectively (Fig. 7b, 9a).

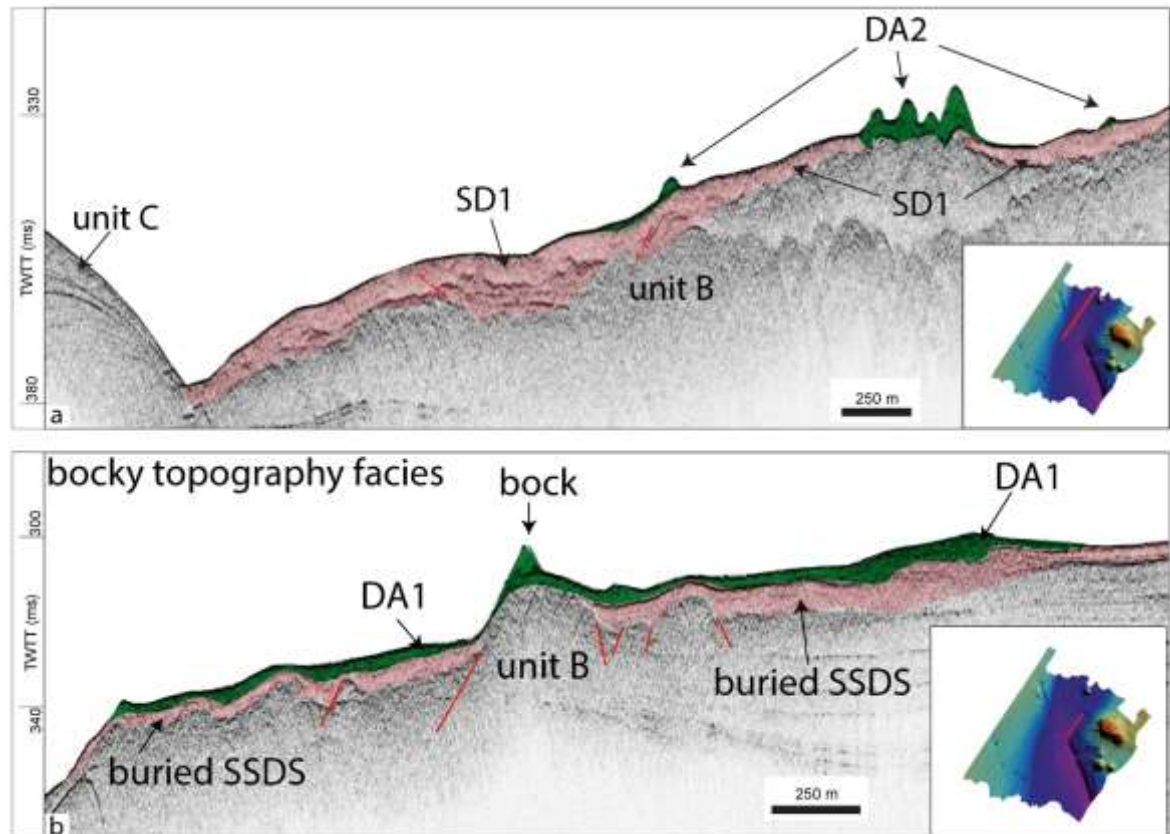


Figure 9 Chirp profiles showing the general morphology of the eastern part of the study area. Unit B is affected by extensional faults (in red). The jagged morphology of the seafloor highlights morphostructural features shown and the chaotic bodies indicated in pink and in green.

- “Blocky topography facies” is a transparent/opaque and in some portion chaotic seismic facies with discontinuous and very low amplitude reflectors, due to the very high reflectivity of the volcanic rocks. It is characterised at the top by high-amplitude continuous reflectors, represent the large chaotic bodies dominating the volcanic region, and localised at the base of the cones (DA1-4 in Figs. 2, 3, 9).

5. Discussion

The numerous chaotic bodies identified and mapped in the study area and surrounding area were considered as submarine gravity driven deposits because they involve various types of rocks and sediments as well as are associated with down-slope sliding of a sediment mass.

A huge spectrum of deposits can fall into the category, including slides, slumps, debris flows and turbidites (Varnes, 1978; Shanmugam, 2000, 2002; Shipp et al., 2004; Moscardelli and Wood, 2008; Posamentier and Martinsen, 2011).

The different types of deposits distinguished on the basis of their geomorphic expression and seismic facies, are below defined and classified. Successively, they are related to different driving forces and triggering mechanisms.

5.1. Types of gravity driven deposits

On the basis of their deformational style, morphology of the deformed structures, internal geometry, lithology of the involved sediments and source areas, the described deposits have been classified in soft-sediment deformation structures (SSDs), comprising rotational (slump) and translational (glide) slides, subaqueous rock falls and debris avalanches.

5.1.1. Soft-sediment deformation structures, SSDs

They develop when primary stratification is deformed by a system of driving forces, such as gravitational instability, overloading, wave-induced stress, and reverse density gradient, while the sediment is temporarily in a weakened state due to the action of a deformation mechanism such as liquefaction or fluidization (Lowe, 1979). The chaotic stratification, as well as folded and faulted beds, disrupted beds, variations in bed thickness, intra-formational truncation surfaces, hummocky stratification features, detected in the elongated and channelized bodies mapped inside the channel (CH1-2) and draping the steep slopes (SD1-4, Figs. 2, 3, 6, 7) indicate that these bodies represent SSDs, as far as they occurred during/after sedimentation and before complete lithification (Leeder, 1987; Owen, 1987; Pratt, 1994; Van Loon, 2009). In detail, the CHs and SD2-4 appear as landslide accumulations originating for rotational sliding of mass-deposits from the channel sides (i.e. slumps). The end-member of the aggrading-prograding reflectors of the Upper

Pleistocene-Holocene semi-consolidated deposits (Unit C, Figs. 6, 7), draping the slopes of the channel, display a weakly deformation (e.g. SD1) suggesting that were affected by translational slide (i.e. glide) processes. Furthermore, the SD1 displays both extensional and compressive features, at the head and the toe of the slide respectively (Fig. 7), confirming their SSDS nature (Alsop and Marco, 2011; Owen and Moretti, 2011; Moretti and Van Loon, 2014; Basilone et al., 2016b).

5.1.2. Rock falls

Rock falls are the product of gravitational movements of the fragmented bedrock or consolidated sediment that fails abruptly from a steep slope producing talus and scree deposits at the base of the slopes. They are characterised by free falling, and often large rock fragments that are transported across steep and moderate angles over short distance (Varnes, 1978; Nardin et al., 1979). The localised dome-shaped bodies mapped along the flanks and at the foot both of submarine volcanic cones and seamounts (dominating the eastern volcanic region, RFs in Figs. 2, 3, 4a) and steep fault escarpments (characterising the walls of the channel, RF1 in Figs. 2, 3) are the poor-sorted angular to sub-angular clasts with variable size including gravels, blocks and mega blocks, displaying the typical characteristics of rock fall deposits (e.g., Edmunde et al., 2006; Micallef et al., 2007).

5.1.3. Debris avalanches

This type of mass movement involves large volumes of failing masses, in which the interacting clasts collide among them and allowing free clast motion (Kessler & Bedard, 2000). Debris avalanches are characterised by high velocities and long run-outs and, usually, originate from deep rotational failures on steep slopes and they disperse to form widespread blocky topography (Mulder and Alexander, 2001; Masson et al., 2002). The study area shows analogies with other volcanic islands, e.g., Canary Islands (Urgeles et al. 1997; Ollier et al., 1998; Masson et al., 2002;

2008), Aeolian Islands (Romagnoli et al., 2009) and the irregular blocky topography of the DA1-4 bodies is interpreted as debris avalanche deposits.

5.2. Driving forces and trigger mechanisms

5.2.1. Tectonic trigger mechanisms

The Graham Bank SSDSs (SDs and CHs in Figs. 2-3, 6-9) developed in unconsolidated sediments through the loss of shear resistance. These require both the action of a driving force (gravitational force) and a reduction in sediment strength (deformation mechanism), usually initiated by a trigger mechanism (Owen et al., 2011). The occurrence of several syn-sedimentary faults, affecting both the sedimentary and volcanic substrate, sealed by the immediately overlying SSDSs (Figs. 6-9) suggests that active tectonics have large influence in activation of these gravity slides. This tectonics, which induced instability of the slope either through the earthquake-induced reduction of sediment shear strength or through the tectonically-induced steepening of the slope is believed the trigger mechanism generating the slump sheets (e.g. Seilacher, 1969; Montenat et al., 2007; Audemard and Michetti, 2011; Mastrogiacomo et al., 2012). A clear example of this genetic relation is offered by the sub-vertical fault correlated with recent earthquake date 08-22-2003 with ML 2.6 and depth 5 km that can be the trigger mechanism of the mobilization of the SD1 glide (Fig. 7). Evidence of slope failures as well as buried and exposed mass transport deposits (Gardiner et al., 1993; Max et al., 1993), occurring during the Quaternary on the eastern continental slope of the Sicily Channel (Gela Basin), have been documented and related to earthquakes trigger (Minisini et al., 2007). In the study case, seismic (sediment-weakening) and tectonic to volcanic (slope-steepening) trigger mechanisms, which presumably were simultaneously active, acted in different ways: tectonic tilting and volcanic expansion (bulging) would increase the magnitude of the driving force system, while associated seismic shocks would reduce sediment stability (e.g. Mastrogiacomo et al., 2012; Masson et al., 2002; 2008).

In the study are tectonic and volcanic processes, which have induced the conformation of the seabed in structural highs and lows and steeped morphology have led to the beginning of SSDSs (both slumps and glides). Similar morpho-structural features and configurations are described from Upper Triassic deep-water carbonates outcropping in Central Sicily where SSDSs are moved along a weakly steep slope towards graben and half-graben, along which the channelized deposits flow towards deepest sector of the basin (Basilone et al., 2016b).

RF1 that is the result of rock falls from the steep fault escarpment (Es1 in Fig. 2) dislocating the Lower Pleistocene lithified deposits (unit A) suggest that in this case the trigger mechanism is related to the tectonics dissecting both the substrate and the seabed with normal faults (Figs. 2, 3).

5.2.2. Volcanic trigger mechanisms

Volcanic processes, similarly to the tectonic activity, have strong influences determining the evolution of the described MTDs on the volcanic region. Thus the RFs and DA1-4, which are rock falls and debris avalanches of volcanic material that is removed from the sides of volcanoes suggest that changes in the slope angle of the volcanic cones, directly controlled by the volcanic activity, including vertical movements (bulging and subsidence), emplacement of volcanic material that is accompanied by magmatic and pore fluid pressurisation (Elsworth and Voight, 1995), produce instability of the flanks of the cones (e.g., Masson et al. 2002; 2008; Gee et al. 2001; Romagnoli et al., 2009; Casalbore et al., 2011).

It is confirmed also by the occurrence of large scars that cut the volcanic cones (Figs., 3, 4, 5). Because these scars cut also the marine terraces characterising the top of the volcanic cones (Figs. 2, 3) that are believed as the product of the sea-level fall related to the last glaciation event (e.g., Chiocci and Orlando, 1996; Casalbore et al., 2016), their formation must be related to a younger volcanic activity event that has built the new cone along the southern side of the M2 edifice (Figs. 3a, 4) possibly formed during the 1831 eruption (see Colantoni, 1975).

5.2.3. Sedimentary/oceanographic trigger mechanisms

The different axial incision observed along the thalweg of the channel (Figs. 2, 3, 7a, 8) demonstrates that active or recent downslope sedimentary fluxes occur (e.g., Baztan et al. 2005; Lo Iacono et al., 2011). Thus, undercutting by deep currents or maybe other erosive bottom current flows could have been responsible of the evolution of the elongated bodies of the channelized SSDSs (CHs in Figs. 2, 3). The occurrence of the strongly oceanographic currents flowing along the study area, where the AIS flows SE-wards along the Adventure Bank producing a loop current, the Adventure bank vortex (Fig. 1, Lemursiax and Robinson, 2001; Gabersek et al., 2007), supports the hypothesis of the influence of bottom currents that rework the channelized SSDSs.

6. Conclusion

A geomorphological study based on new very high-resolution dataset (multibeam and CHIRP) of the Graham Bank volcanic area (Sicily Channel) have pointed out the occurrence of different types of MTDs. They have been classified and relating to specific trigger mechanisms comprising the interaction of sedimentary, tectonic and volcanic processes affecting the area.

The Graham Bank, making part of the Sicily Strait geographical element, is a shallow-water area that comprises a volcanic sector dominated by cones and seamounts, aligned mounds, craters and focused seepages, a flat platform sector characterised by fluid escape structures and NW-SE oriented steep faulted escarpments, and a tectonically-originated erosive channel separating the volcanic region from the sedimentary plain ones.

The mapped MTDs are variously distributed in the area: a) soft-sediment depositional structures, including rotational slumps and translational glides, are mainly located along the channel and the foot steep slopes bordering it; b) rock falls are diffused at the foot of the volcanic cones or of the steep fault escarpments; c) debris avalanches forming fan-shaped bodies are localised at the foot of the volcanic cones and are associated with incised scar and rotated blocks.

Deformational forces and trigger mechanisms are related to the interplay of tectonics, including earthquakes that are able to induce reduction of sediment shear strength and NW-SE oriented normal faults that are able to induce steepening of the slope, volcanic activity, including bulging and subsidence, eruptions, emplacement of magmatic material, pore fluid pressurisation and focused seepage plumes, that induces major flank instability, and sedimentary processes, as gravitational forces, bottom currents influenced by the local Adventure Bank Vortex, that triggers sliding or mass-gravity movements.

Chapter 5

5. SYNTHESIS AND DISCUSSION

This thesis project was focused on the morphological and morphostructural analysis of the tectonically active sector around the Graham Bank (Sicily Channel, central Mediterranean Sea).

The primary data sets that was used is composed of very high-resolution multibeam bathymetry and CHIRP data and multichannel seismic profiles.

The principal topic was the identification and classification of the fluid escape morphologies regarding to the differentiation the main drivers that control the origin and the migration of fluids to the seabed of the study area. This research project for the first time investigated seafloor fluid seepage in a shallow water sector of the north-western Sicily Channel dominated by the coexistence of a compressional regime of Sicilian-Maghrebian Mountain and the extensional regime of Sicily Channel rifting.

The foreland area, cropping out in south-eastern Sicily (Iblean Plateau) and submerged in the Sicily Channel (Pelagian Block), is the result of the interaction of both the Sicilian-Maghrebian mountain building and the Sicily Channel rifting (Fig. 1, Argnani, 1990; Catalano et al., 1996; Sulli, 2000; Finetti et al., 2005).

The Sicily Channel consists of 6-7 km thick Meso-Cenozoic carbonate platform and pelagic deposits, with igneous intercalations (mostly basalts). They display lateral facies variations as a result of the syn-sedimentary fault systems active during the Jurassic extensional rifting tectonics (e.g., Streppenosa basin). The carbonate succession is covered by 2-2.5 km of Miocene-Pliocene clastics, evaporites and carbonates.

The interaction of the two above-mentioned geodynamic processes with the stratigraphic setting have been indispensable to understand and to display the setting and evolution of fluid escape

structures in the Graham Bank region and to reconstruct the origin and the mechanisms of the migration of these fluids to the seafloor.

The morphobathymetric and seismostratigraphic analysis of published and unpublished (new acquisition dataset) data allowed us to recognise and analyse different types of structures with genesis linked to the active geological processes that have dominated, during the Quaternary, the morphological and structural evolution of the Sicily Channel.

The present chapter synthesises the main findings of this study (summarised in the chapter 4). Three main case studies have been conducted within this project and they are summarized in the paragraphs:

- **4.1 Based On The Geomorphology Of The Volcanic Seamounts**
- **4.2 Based On The Fluid Escape Structures**
- **4.3 Based On The Gravity Driven Deposits**

The main case study dealt the seepage sites situated directly at the top of the region of the Graham Bank.

Two main morphological seafloor sectors that are separated by a deeply incised channel with genesis linked to a sub vertical normal fault, which marks the boundary between a sedimentary context and a volcanic.

The eastern sector is characterised by rough morphology, several mounds, focused seepage plumes, and volcanic edifices (Graham Bank and minor cones here mapped). The location of seafloor seepage sites at the top of volcanic submarine bank (eastern part) showed the effective mobilization of gas from the sub-seafloor as focused plumes and mounds (isolated, aligned and clustered).

Differently, the western area has a quite flat morphology where the Upper Pleistocene-Holocene deposits that are characterised by the occurrence of cold seep such as aligned pockmarks and mounds, indicating migration of fluid to the seafloor and seeping out through active faults (calm flux sensu Dimitrov and Woodside, 2003). In many cases, the areal distribution of pockmarks was coincident with a shallow Messinian substrate.

The morphological expression of these structures is still well preserved (that is, not sealed by subsequent deposits to their formation) and do not show evidence of erosion (as normally reported in sever case in literature). This feature allows us to consider their recent genesis.

In the study area, the recent tectonic acts mainly with two main fault systems.

- The first one is extensional/transpressive with trend about NW-SE, characterised in some cases by reversing structures, which creates a morphology of the fund divided the sea, which recognizes an alternation of ups and downs structural.
- The second one is an extensional system oriented NNW-SSE. These two system faults show same trends with the main faults recognized s in the several studies conducted in the Sicilian Channel by various author.

Throughout the study area, both pockmarks, the mounds and plumes are trended approximately NW-SE, parallel to the tectonic trend recognised by seismic profiles that are in according with the main geological works conducted in the Sicily Channel.

The study area hosts fluid escape structures (pockmarks, mounds and active plumes) that have probably a genesis linked to the deep fault systems, which affects the sedimentary multilayer and the volcanic sector. Vertical distribution of temperatures suggests cold seeps through dip-slip faults that dislocated and that favoured the migration of fluids from gas reservoirs at different stratigraphic levels where they are temporary hosted. And also, considering the published geochemical information showing that He isotopic ratio of the fluids, the recognised vertical fault

systems that affects the eastern part of the study area as well as the volcanic activities that are rooted at depth, we hypothesize and suggest that the fluids can be originated in the deepest thinned continental crust at the boundary with the mantle.

Furthermore, the geomorphological study based on the same very high-resolution dataset (multibeam and CHIRP) of the Graham Bank volcanic area have pointed out the occurrence of important submarine mass movement process in the study area highlighting the presence of many gravity driven deposits, which were classified on the base of their features. We however inferred their specific trigger mechanisms considering the interaction of sedimentary, tectonic and volcanic processes affecting the area.

The mapped gravity driven deposits variously distributed in the study area are:

- Soft-sediment depositional structures, including rotational slumps and translational glides, are mainly located along the channel and the foot steep slopes bordering it;
- Rock falls that are diffused at the foot of the volcanic cones or of the steep fault escarpments;
- Debris avalanches forming fan-shaped bodies and that are localised at the foot of the volcanic cones and are often associated with incised scar and rotated blocks.

Deformational forces and trigger mechanisms are related to the tectonics such as earthquakes that are able to induce reduction of sediment shear strength and NW-SE oriented normal faults. These factors induced the genesis of very steep slopes, the volcanic activity that produces bulging and subsidence, eruptions, emplacement of magmatic material. In addition, others causes are the pore fluid pressurisation and focused seepage plumes, which induces major flank instability; and sedimentary processes such as gravitational forces, bottom currents strongly influenced by the local Adventure Bank Vortex.

Furthermore, seven volcanic seamounts have been identified and studied in detail using high-resolution bathymetric and CHIRP data. Main dimensions and associated parameters allowed us a morphometric and morphologic classification on the basis of their shapes.

We infer that this cluster of submarine volcanoes were formed by more than one process. These volcanic seamounts are aligned along two volcano-tectonic lines (NW-SE and N-S) which are the trend typical of the Sicily Channel. In agreement with recent work, that volcanism is not contemporaneous along the entire length of the Sicily Channel (Corti et al. 2003, 2006, Rotolo et al., 2006).

On the base of the presence of seven aligned volcanic seamounts (NW-SE), elongated gravity driven deposits as well as of the cluster of aligned fluid escape structures, which are, parallel at the main system faults that affect the Sicily Channel, we suggest that the growth of the Graham Bank sector had an important and recent development of both with submarine and aerial events.

Furthermore, the combined study of the morpho-structural (using multibeam and seismic data) and seismological data has highlighted a clearly relationship between earthquakes and the recognised tectonic features. We correlated the earthquake of 22/08/2003 earthquake (ML 2.6; depth 5 km) with a sub-vertical fault that affected the central part of the study area.

In conclusion, the geological evolution of the Graham bank is strongly linked to the genesis and evolution of the Sicily Channel reflecting the main features of the geodynamic context of the Sicily Channel.

REFERENCES

- Acosta, J., Munoz, A., Herranz, P., Palomo, C., Ballesteros, M., Vaquero, M. and Uchupi, E., 2001. Pockmarks in the Ibiza Channel and western end of the Balearic Promontory (western Mediterranean) revealed by multibeam mapping. *Geo-Marine Letter* 21, 123–130.
- Allain, V., 2006. Seamount and pelagic fisheries interactions under study. Retrieved from: http://www.spc.int/coastfish/News/Fish_News/116/ValerieAllain_116.pdf.
- Allen, J.R.L., 1986. Earthquake magnitude-frequency, epicentral distance, and soft-sediment deformation in sedimentary basins. *Sedimentary Geology* 46 (1-2), 67-75, doi:10.1016/0037-0738(86)90006-0.
- Aloisi, G., Pierre, C., Rouchy, J.M., Foucher, J.P., Woodside, J., 2000. Methane-related authigenic carbonates of eastern Mediterranean Sea mud volcanoes and their possible relation to gas hydrate destabilisation. *Earth and Planetary Science Letters* 184, 321–338.
- Alsop, G.I., Marco, S., 2011. Soft-sediment deformation within seismogenic slumps of the Dead Sea Basin. *Journal of Structural Geology* 33, 433–457. doi:10.1016/j.jsg.2011.02.003.
- Amelio, M., Martorelli, E. 2008. Seismo-stratigraphic characters of paleocontourites along the Calabro-Tyrrhenian margin (Southern Tyrrhenian Sea). *Marine Geology*, 252 (3-4), 141-149.
- Andresen A. and Bjerrum L. 1967. Slides in subaqueous slopes in loose sand and silt. *Marine Geotechnique*, Adrian F.Richards Ed., University of Illinois Press, 221-239.
- Andresen, K.J. and Huuse, M., 2011. ‘Bulls-eye’ pockmarks and polygonal faulting in the Lower Congo Basin: Relative timing and implications for fluid expulsion during shallow burial. *Marine Geology* 279, 111-127.
- Antonelli, M., Franciosi, R., Pezzi, G., Querci, A., Ronco, G.P., Mezzani, F., 1988. Paleogeographic evolution and structural setting of the northern side of the Sicily channel. *Memorie Società Geologica Italiana* **41**, 141–157.
- Argnani, A., 1990. The strait of Sicily rift zone: foreland deformation related to the evolution of a back-arc basin. *Journal of Geodynamics* 12, 311–331.
- Argnani, A., 1993. Neogene tectonics of the Strait of Sicily, in: Max MD, Colantoni P (Eds.) *Geological development of the Sicilian-Tunisian Platform*. UNESCO Report in marine science 58, 55–60.
- Audemard, M.F.A., Michetti, A.M., 2011. Geological criteria for evaluating seismicity revisited: Forty years of paleoseismic investigations and the natural record of past earthquakes. In: Audemard M.F.A., Michetti, A.M., and McCalpin, J.P., (Eds.), *Geological Criteria for Evaluating Seismicity Revisited: Forty Years of Paleoseismic Investigations and the Natural Record of Past Earthquakes*. Geological Society of America, Special Paper 479, 1–21, doi:10.1130/2011.2479(00).
- Avellone, G., Barchi, M.R., Catalano, R., Gasparo Morticelli, M., Sulli, A. 2010. Interference between shallow and deep-seated structures in the Sicilian fold and thrust belt, Italy. *Journal of the Geological Society*, London, 167, 109-126.

- Barberi, F., Borsi, S., Ferrara, G., and Innocenti, F., 1969. Strontium isotopic composition of some recent basic volcanites of the Southern Tyrrhenian Sea and Sicily Channel. *Contributions to Mineralogy and Petrology*, v. 23, 157–172, doi: 10.1007/BF00375177.
- Barry, J.P., Greene, H.G., Orange, D.L., Baxter, C.H., Robison, B.H., Kochevar, R.E., Nybakken, J.W., Reed, D.L., McHugh, C.M., 1996. Biologic and geologic characteristics of cold seeps in Monterey Bay, California. *Deep-Sea Research I* 43, 1739–1762.
- Basilone, L., Lena G, Gasparo Morticelli M., 2014. Synsedimentary tectonic, soft-sediment deformation and volcanism in the rifted Tethyan margin from the Upper Triassic-Middle Jurassic deep-water carbonates in Central Sicily. *Sedimentary Geology* 308, 63–79. DOI: 10.1016/j.sedgeo.2014.05.002.
- Basilone, L., 2009b. Sequence stratigraphy of a Mesozoic carbonate platform-to-basin system in western Sicily. *Cent. Eur. J. Geosci.*, 1 (3), 251-273, doi: 10.2478/v10085-009-0021-8
- Basilone, G., Guisande, C., Patti, B., Mazzola, S., Cuttitta, A., Bonanno, A., Vergara A. R., Maniero I., 2006. Effect of habitat conditions on reproduction of the European anchovy (*Engraulis encrasicolus*) in the Strait of Sicily. *Fish. Oceanogr.*, 15:4, 271-280.
- Basilone, L., 2009a. Mesozoic tectono-sedimentary evolution of the Rocca Busambra (western Sicily). *Facies* 55, 115–135, doi: 10.1007/s10347-008-0156-2.
- Basilone, L., 2011. Geological Map of the Rocca Busambra-Corleone region (western Sicily, Italy): explanatory notes. *Ital.J.Geosci. (Boll.Soc.Geol.It.)* 130, 42–60.
- Basilone, L., Frixia, A., Trincianti, E., Valenti, V., 2016a. Permian-Cenozoic deep-water carbonate rocks of the Southern Tethyan Domain. The case of Central Sicily. *Ital.J.Geosci. (Boll.Soc.Geol.It.)* 135, 171–198. doi:10.3301/IJG.2015.07
- Basilone, L., Sulli, A., Gasparo Morticelli, M., 2016b. Integrating facies and structural analyses with subsidence history in a Jurassic–Cretaceous intraplateau basin: Outcome for paleogeography of the Panormide Southern Tethyan margin (NW Sicily, Italy). *Sedimentary Geology* 339, 258–272. doi:10.1016/j.sedgeo.2016.03.017.
- Basilone, L., Sulli, A., Gasparo Morticelli, M., 2016c. The relationships between soft-sediment deformation structures and synsedimentary extensional tectonics in upper Triassic deep-water carbonate succession (Southern Tethyan rifted continental margin - Central Sicily). *Sedimentary Geology*. doi:10.1016/j.sedgeo.2016.01.010
- Beccaluva, L., Macciotta, G., Di Girolamo, P., and Savelli, C., 1981. Upper Miocene submarine volcanism in the Strait of Sicily (Banco Senza Nome): *Bulletin of Volcanology*, 44, 573-581.
- Bello, M., Franchino, A. & Merlini, S. 2000. Structural model of eastern Sicily. *Memorie della Società Geologica Italiana*, 55, 61–70.
- Berndt, C., 2005. Focused fluid flow in passive continental margins. *Philosophical Transaction of the Royal Society A* 363, 2855-2871.

- Bernoulli, D., Jenkyns, H.C., 2009. Ancient oceans and continental margins of the Alpine-Mediterranean Tethys: deciphering clues from Mesozoic pelagic sediments and ophiolites. *Sedimentology* 56 (1), 149–190.
- Bezrodnykh, Yu.P., Deliya, S.V., Lavrushin, V.Yu., Yunin, E.A., Poshibaev, V.V., Pokrovskii, B.G., 2013. Gas seeps in the North Caspian water area. *Lithology and Mineral Resources* 48, 373–383.
- Biscontin G., Pestana J.M. and Nadim F. 2004. Seismic triggering of submarine slides in soft cohesive soil deposits. *Marine Geology*, 203: 341-354.
- Boccaletti, M., Cello, G., Tortorici, L., 1987. Transtensional tectonics in the Sicily Channel, *J. Struct. Geol.* 9, 869-876
- Boëly, T., Chabanne, J., Frèon P., 1978. Schémas des cycles migratoires, lieux de concentration et periods de reproduction des principales espèces de poissons pélagiques côtiers dans la zone sénégal-mauritanienne. In: Rapport du groupe de travail ad hoc sur les poissons pélagiques côtiers ouest-africains de la Mauritanie au Libéria (16° N à 5° N), 63-70. COPACE/FAO, PACE series 78/10 fr.
- Bonanno, A., Goncharov, S., Mazzola, S., Popov, S., Cuttitta, A., Patti, B., Basilone, G., Di Nieri, A., Patti, C., Aronica, S., Buscaino, G., 2006. Acoustic evaluation of anchovy larvae distribution in relation to oceanography in the Cape Passero area (Strait of Sicily). *Chemistry and Ecology*, 22 (1), S265-S273.
- Bonardi, G., Cavazza, W., Perrone, V., Rossi S., 2001. Calabria-Peloritani terrane and northern Ionian Sea, in: Vai G.B., Martini I.P. (Eds.), *Anatomy of an Orogen: the Apennines and Adjacent Mediterranean Basins*. Kluwer Academic Publisher, Dordrecht, The Netherlands, pp. 287–306.
- Bonardi, G., de Capoa, P., Di Staso, A., Estévez, A., Martín-Martín, M., Martín-Rojas, I., Perrone, V. and Tent-Manclús, J.E., 2003. Oligocene-to-Early-Miocene depositional and structural evolution of the Calabria-Peloritani Arc southern terrane (Italy) and geodynamic correlations with the Spanish Betics and Morocco Rif. *Geodinamica Acta*, 16, 149-169.
- Borsetti, A. M., Colantoni, P. & Zarudzki E. F. K., 1975. Note strutturali stratigrafiche sul Canale di Sicilia. 67° Congr. Soc. Geol. It., Parma, 27-31.
- Brothers, L.L., Van Dover, C.L., German, C.R., Kaiser, C.L., Yoerger, D., Ruppel, C., Lobecker, E., Skarke, A., Wagner, J.K.S., 2013. Evidence for extensive methane venting on the southeastern U.S. Atlantic margin. *Geology* 41, 807-810.
- Bussmann, I. and Suess, E., 1998. Groundwater seepage in Eckernförde Bay (Western Baltic Sea): Effect on methane and salinity distribution of the water column. *Continental Shelf Research* 18, 1795-1806.
- Calanchi, N., Colantoni, P., Rossi, P.L., Saitta, M., and Serri, G., 1989. The Strait of Sicily continental rift systems: Physiography and petrochemistry of the submarine volcanic centres: *Marine Geology*, v. 87, p. 55–83, doi: 10.1016/0025-3227(89)90145-X.
- Calò, M., Parisi, L., 2016. Evidences of a Lithospheric fault zone in the Sicily Channel (Southern Italy) from instrumental seismicity data. *Geophysical Journal International* 199, 219–225 DOI: 10.1093/gji/ggu249.

- Campbell, K., Farmer, J. and Des Marais, D., 2002. Ancient hydrocarbon seeps from the Mesozoic convergent margin of California: carbonate geochemistry, fluids and palaeoenvironments. *Geofluids* 2, 63-94.
- Campbell, K.A., 2006. Hydrocarbon seep and hydrothermal vent paleoenvironments and paleontology: Past developments and future research directions. *Palaeogeography, Palaeoclimatology, Palaeoecology* 232, 362-407.
- Canary Islands: implications for tectonic controls, and oceanic shield forming processes. *J Volcanol Geotherm Res* 103:105–119.
- Canet, C., Prol-Ledesma, R.M., Dando, P.R., Vázquez-Figueroa, V., Shumilin, E., Birosta, E., Sánchez, A., Robinson, C.J., Camprubí, A., Tauler, E., 2010. Discovery of massive seafloor gas seepage along the Wagner Fault, northern Gulf of California. *Sedim. Geol.* 228, 292–303. doi:10.1016/j.sedgeo.2010.05.004
- Cangemi, M., Di Leonardo, R., Bellanca, A., Cundy, A., Neri, R., Angelone, M., 2010. Geochemistry and mineralogy of sediments and authigenic carbonates from the Malta Plateau, Strait of Sicily (Central Mediterranean): Relationships with mud/fluid release from a mud volcano system. *Chemical Geology* 276, 294-308.
- Caracausi, A., Favara, R., Italiano, F., Nuccio, P.M., Paonita, A., Rizzo, A., 2005. Active geodynamics of the central Mediterranean Sea: Tensional tectonic evidences in western Sicily from mantle-derived helium. *Geophysical Research Letters*, 32 L04312 doi:10.1029/2004GL021608, 2005.
- Carapezza, M., Ferla, P., Nuccio, P.M., Valenza, M., 1979. Caratteri petrologici e geochimici delle vulcaniti dell'Isola "Ferdinandea": *Rendiconti della Società Italiana Mineralogia di e Petrologia*, 35, 377–388.
- Cartwright, J., 2011. Diagenetically induced shear failure of fine-grained sediments and the development of polygonal fault systems. *Marine and Petroleum Geology* 28, 1593-1610.
- Casalbore, D., Falese, F., Martorelli, E., Romagnoli, C., Chiocci, F.L., 2016. Submarine depositional terraces in the Tyrrhenian Sea as a proxy for paleo-sea level reconstruction: Problems and perspective. *Quaternary International* 1–11. doi:10.1016/j.quaint.2016.07.051.
- Casalbore, D., Romagnoli, C., Bosman, A., Chiocci, F.L., 2011. Potential tsunamigenic landslides at Stromboli Volcano (Italy): Insight from marine DEM analysis. *Geomorphology*, Volume 126, Issues 1-2, 1 March 2011, Pages 42-50.
- Casero, P., Roure, F., 1994. Neogene deformation at the Sicilian-North African plate boundary: in Roure, F. (Ed.), *Peri-Tethyan Platforms*, Editions Technip, Paris, p. 27-50.
- Catalano, R. & D'Argenio, B. 1982. Schema Geologico della Sicilia. In: Catalano, R. & D'Argenio, B. (eds) *Guida alla geologia della Sicilia occidentale*. Geological Society of Italy, Memoir, XXIV (Suppl. A), 9-41.
- Catalano, R. & Sulli, A., 2006. Crustal image of the Ionian basin and accretionary wedge. *Bollettino di Geof. Teor. Appl.*, 47, 343-374.
- Catalano, R., & D'Argenio, B., 1978. An essay of palinspastic restoration across western Sicily. *Geologica Romana*, 17, 145-159.

- Catalano, R., Agate, M., Albanese, C., Avellone, G., Basilone, L., Gasparo Morticelli, M., Gugliotta, C., Sulli, A., Valenti, V., Gibilaro, C. & Pierini, S., 2013a. Walking along a crustal profile across the Sicily fold and thrust belt. *Geol.F.Trips of SGI*, 5, no. 2.3, 1-213, doi: 10.3301/GFT.2013.05.
- Catalano, R., Agate, M., Albanese, C., Avellone, G., Basilone, L., Gasparo Morticelli, M., Gugliotta, C., Sulli, A., Valenti, V., Gibilaro, C. & Pierini, S., 2013b. Walking along a crustal profile across the Sicily fold and thrust belt. *Geol.F.Trips of SGI* 5, 1–213. doi: 10.3301/GFT.2013.05.
- Catalano, R., Di Stefano, P., Sulli, A., Vitale, F.P., 1996. Paleogeography and structure of the Central Mediterranean: Sicily and its offshore area. *Tectonophysics*, 260, 291-323.
- Catalano, R., Franchino, A., Merlini, S., Sulli, A., 2000. A crustal section from the Eastern Algerian basin to the Ionian ocean (Central Mediterranean). *Mem. Soc. Geol. It.*, 55, 71-85.
- Catalano, R., Infuso, S., Milia, A., Sulli, A., 1993. The submerged Sicilian-Maghrebian chain along the Sardinia Channel-Sicily straits belt, in Max M.D. & Colantoni P. (Eds.). *Geological development of the Sicilian-Tunisian Platform. Proceedings of international Scientific Meeting held at the University of Urbino, Italy, 4-6 November, 1992. Unesco Report in Marine Science* 58, 43–48.
- Catalano, R., Valenti, V., Albanese, C., Accaino F., Sulli, A., Tinivella, U., Gasparo Morticelli, M., Zanolla C., Giustiniani, M., 2013b. Sicily's fold-thrust belt and slab roll-back: the SIRI.PRO. Seismic crustal transect. *Journal of the Geological Society*, Online First, <http://dx.doi.org/10.1144/0016-76492012-099>.
- Cathles, L.M., Su, Z. and Chen, D., 2010. The physics of gas chimney and pockmark formation, with implications for assessment of seafloor hazards and gas sequestration. *Marine and Petroleum Geology* 27, 82-91.
- Cello, G., 1987. Structure and deformation processes in the Strait of Sicily ‘‘rift zone’’. *Tectonophysics*, 141, 237-247.
- Ceramicola, S., Praeg, D., Wardell, N., Unnithan, V., 2007. Seismic imaging of mud volcanoes on the Calabrian Arc accretionary prism, central Mediterranean Sea. *Eos, Transactions, American Geophysical Union* 88 (52) SUPPL., Abstract V22C-05, Dec 2007.
- Charlou, J.L., Donval, J.P., Zitter, T., Roy, N., Jean-Baptiste, P., Foucher, J.P. and Woodside, J., 2003. Evidence of methane venting and geochemistry of brines on mud volcanoes of the eastern Mediterranean Sea. *Deep Sea Research Part I: Oceanographic Research Papers* 50, 941-958.
- Chen, J., Lee, H.S., 2013. Soft-sediment deformation structures in Cambrian siliciclastic and carbonate storm deposits (Shandong Province, China): Differential liquefaction and fluidization triggered by storm-wave loading. *Sedim. Geol.* 288, 81–94. doi:10.1016/j.sedgeo.2013.02.001.
- Chiarabba, C., Jovane, L. & Di Stefano, R., 2005. A new look to the Italian seismicity: seismotectonic inference, *Tectonophysics* 395, 251–268.
- Chiocci, F. L. and De Alteriis, G. 2006, The Ischia debris avalanche: first clear submarine evidence in the Mediterranean of a volcanic island prehistorical collapse. *Terra Nova*, 18: 202–209. doi:10.1111/j.1365-3121.2006.00680.x.

- Chiocci, F.L., Orlando, L., 1996. Lowstand terraces on Tyrrhenian Sea steep continental slopes. *Marine Geology* 134, 127–14
- Cita, M.B., Ivanov, M.K., Woodside, J.M., 1996. The Mediterranean Ridge Diapiric Belt. *Marine Geology* 132, 1–6.
- Civetta, L., D'Antonio, M., Orsi, G., and Tilton, G.R., 1998. The geochemistry of volcanic rocks from Pantelleria Island, Sicily Channel. Petrogenesis and characteristics of the mantle source region: *Journal of Petrology*, 39, 1453–1491, doi: 10.1093/petrology/39.8.1453.
- Civile, D., Lodolo, E., Accettella, D., Geletti, R., Ben-Avraham, Z., Deponte, M., Facchin, L., 2010. The Pantelleria graben (Sicily Channel, Central Mediterranean): An example of intraplate “passive” rift. *Tectonophysics*, 410, 173-183.
- Civile, D., Lodolo, E., Tortorici, L., Lanzafame, G., Brancolini G., 2008. Relationships between magmatism and tectonics in a continental rift: the Pantelleria Island region (Sicily Channel, Italy). *Marine Geology* 251, 32–46.
- Civile, D., Lodolo, E., Zecchin, M., Ben-Avraham, Z., Baradello, L., Accettella, D., Cova, A., Caffau, M., 2014. The lost Adventure Archipelago (Sicilian Channel, Mediterranean Sea): Morpho-bathymetry and Late Quaternary palaeogeographic evolution. *Global and Planetary Change* 125, 36–47. doi:10.1016/j.gloplacha.2014.12.003
- Claypool, G.E. and Kvenvolden, K.A., 1983. Methane and other Hydrocarbon Gases in Marine Sediment. *Annual Review of Earth and Planetary Sciences* 11, 299-327.
- Colantoni, P., 1975. Note di Geologia Marina sul Canale di Sicilia. *Giornale di Geologia* (2), 40, 1, 181-207.
- Colantoni, P., 1975. Note di Geologia Marina sul Canale di Sicilia. *Giornale di Geologia* (2), 40, 1, 181-207.
- Coltelli M., Cavallaro D., D'Anna G., D'Alessandro A., Grassa F., Mangano G., Patanè D., Gresta S., 2016. Exploring the submarine Graham Bank in the Sicily Channel. *Annals of Geophysics* 59, 2, 2016, S0208; doi:10.4401/ag-6929
- Coltelli M., D'Anna G., Cavallaro D., Grassa F., Mangano G., Azzaro R., D'Alessandro A., Amato A., Gurrieri S., Patanè D., Gresta S., 2013. Ferdinanda 2012: La Campagna oceanografica nell'area del Banco Graham, Canale di Sicilia. *Contributi al Meeting Marino*, 48-52.
- Conte, A.M., Martorelli, E., Calarco, M., Sposato, A., Perinelli, C., Coltelli, M., Chiocci, F.L., 2014. The 1891 submarine eruption offshore Pantelleria Island (Sicily Channel, Italy): Identification of the vent and characterization of products and eruptive style. *Geochemistry, Geophysics, Geosystems* 15, 2555–2574. doi:10.1002/2014GC005238
- Corti, G., Bonini, M., Cloetingh, S., Innocenti, F., Manetti, P., and Sokoutis, D., 2003. Analogue modelling of continental extension. A review focused on the relations between the patterns of deformation and the presence of magma: *Earth-Science Reviews*, 63, 169-247, doi: 10.1016/S0012- 8252(03)00035-7.

- Corti, G., Cuffaro, M., Doglioni, C., Innocenti, F., Manetti P., 2006. Coexisting geodynamic processes in the Sicily Channel. Geological Society of America Special Paper 409, 83-96.
- Coulter S.E. (2005) - Seismic initiation of submarine slope failures using physical modeling in a geotechnical centrifuge. MEng Thesis, Memorial University of Newfoundland.
- Cuttitta, A., Carini, V., Patti, B., Bonanno, A., Basilone, G., Mazzola, S., García Lafuente, J., García, A., Buscaino, G., Aguzzi, L., Rollandi, L., Morizzo, G., Cavalcante C., 2003. Anchovy egg and larval distribution in relation to biological and physical oceanography in the Strait of Sicily. *Hydrobiologia*, 503, 117–120.
- Dan G, Sultan N, Savoye B, (2007) The 1979 Nice harbor catastrophe revisited: trigger mechanism inferred from geotechnical measurements and numerical modelling. *Mar. Geo.* 245:40–64.
- Dando, P.R., Hovland, M., 1992. Environmental effects of submarine seeping natural gas. *Continental Shelf Research* 12, 1197–1207.
- Davis, A.M., 1992. Shallow gas: an overview. *Continental Shelf Research* 12, 1077–1079.
- De Boever, E., Huysmans, M., Muchez, P., Dimitrov, L. and Swennen, R., 2009. Controlling factors on the morphology and spatial distribution of methane-related tubular concretions – Case study of an Early Eocene seep system. *Marine and Petroleum Geology* 26, 1580-1591.
- D'Elia, M., Patti, B., Sulli, A., Tranchida, G., Bonanno, A., Basi Ione, G., Giacalone, G., Fontana, I., Genovese, S., Guisande, C., & Mazzola, S., 2009. Distribution and spatial structure of pelagic fish schools in relation to the nature of the seabed in the Sicily Straits (Central Mediterranean). *Marine Ecology*. ISSN 0173-9565.
- Dimitrov, L. and Woodside, J., 2003. Deep sea pockmark environments in the eastern Mediterranean. *Marine Geology* 195, 263-276.
- Dimitrov, L.I., 2002. Mud volcanoes—the most important pathway for degassing deeply buried sediments. *Earth-Science Reviews* 59, 49–76.
- Ding, F., Spiess, V., Brüning, M., Fekete, N., Keil, H. and Bohrmann, G., 2008. A conceptual model for hydrocarbon accumulation and seepage processes around Chapopote asphalt site, southern Gulf of Mexico: From high resolution seismic point of view. *Journal of Geophysical Research* 113, B08404.
- Doglioni, C., et al. (1999), Orogens and slabs vs. their direction of subduction, *Earth-Science Reviews*, 45, 167-208.
- Dóniz, J., Romero, C., Coello, E., Guillén, C., Sánchez, N., García-Cacho, L. and García, A. 2008. Morphological and statistical characterisation of recent mafic volcanism on Tenerife (Canary Islands, Spain). *J. Volcanol. Geother. Res.* 173 (3-4), 185-195.
- Dower, J., Freeland, H. and Juniper, K. 1992. A strong biological response to oceanic flow past Cobb seamount. *Deep Sea Res.*, 39, 1139-1145.
- Driscoll N W, Weissel J K, Goff J A (2000) Potential for large-scale submarine slope failure and tsunami generation along the US mid-Atlantic coast. *Geology*. 28:407-410.

- Dupré, S., Woodside, J., Foucher, J.P., de Lange, G., Mascle, J., Boetius, A., Mastalerz, V., Stadnitskaia, A., Ondréas, H., Huguen, C., Harmégnies, F., Gontharet, S., Loncke, L., Deville, E., Niemann, H., Omoregie, E., Olu-Le Roy, K., Fiala-Medioni, A., Dählmann, A., Caprais, J.C., Prinzhofer, A., Sibuet, M., Pierre, C., Damsté, J.S., the NAUTINIL Scientific Party, 2007. Seafloor geological studies above active gas chimneys off Egypt (Central Nile Deep Sea Fan). *Deep-Sea Research I* 54, 1146–1172.
- Edmond, J.M., Von Damm, K.L., McDuff, R.E. and Measures, C.I., 1982. Chemistry of hot springs on the East Pacific Rise and their effluent dispersal. *Nature* 297, 187-191.
- Elsworth and Voight, 1995 Dike intrusion as a trigger for large earthquakes and the failure of volcano flanks. *J. Geophys. Res.* 100, 6005–6024.
- Etiopie, G., 2015. *Natural Gas Seepage*. Springer International Publishing.
- Etiopie, G., Feyzullayev, A., Baciú, C.L., 2008. Terrestrial methane seeps and mud volcanoes: a global perspective of gas origin. *Marine and Petroleum Geology* 26 (3), 333–344.
- Etiopie, G., Klusman, R.W., 2002. Geologic emissions of methane to the atmosphere. *Chemosphere* 49, 777–789.
- Faccenna, C., Piromallo, C., Crespo-Blanc, A., Jolivet, L., Rossetti, F., 2004. Lateral slab deformation and the origin of the western Mediterranean arcs. *Tectonics*, 23, TC1012.
- Fader, G.B., 1991. Gas-related sedimentary features from the eastern Canadian continental shelf. *Continental Shelf Research* 11, 1123-1153.
- Falautano, M., Cillari, T., Perzia, P., Vivona, P., Castriota, L., Andaloro, F., 2010. Methodological approach to integrated coastal zone management: a case of study in the Strait of Sicily. *Biol. Mar. Medit.* 17 (1), 145-148.
- Faugeres, J.-C., Stow, D. A. V., Imbert, P., Viana, A. R. & Wynn, R. B. (1999). Seismic features diagnostic of contourite drifts. *Marine Geology*, 162, 1-38.
- Favalli, M., Karátson, D., Mazzuoli, R., Pareschi, M.T., Ventura, G., 2005. Volcanic geomorphology and tectonics of the Aeolian archipelago (Southern Italy) based on integrated DEM data. *Bull Volcanol* (2005) 68: 157–170 DOI 10.1007/s00445-005-0429-3.4.
- Fernández-Puga, M.C., Vázquez, J.T., Somoza, L., Díaz del Rio, V., Medialdea, T., Mata, M.P., León, R., 2007. Gas-related morphologies and diapirism in the Gulf of Cádiz. *Geo-Marine Letters* 27, 213–221.
- Ferruggia, P., Apopei, I., Bonjer, K.P., 1987. Observation on the seismicity of the Sicily Channel. *Mem. Soc. Geol. It.*, 38, 329-340.
- Feseker, T., Foucher, J.P. and Harmégnies, F., 2008. Fluid flow or mud eruptions? Sediment temperature distributions on Håkon Mosby mud volcano, SW Barents Sea slope. *Marine Geology* 247, 194-207.
- Finetti I., Lentini F., Carbone S., Del Ben A., Di Stefano A., Forlin E., Guarnieri P., Pipan M., Prizzon A., 2005. Geological outline of Sicily and Lithospheric Tectono-Dynamics of its Tyrrhenian Margin from new CROP Seismic Data, in: Finetti I.R. (Ed.), *CROP PROJECT: Deep Seismic Exploration of the Central Mediterranean and Central Italy*, Atlases in Geoscience, 1, Elsevier BV.

- Finetti I., Lentini F., Carbone S., Del Ben A., Di Stefano A., Forlin E., Guarnieri P., Pipan M., Prizzon A., 2005. Geological outline of Sicily and Lithospheric Tectono-Dynamics of its Tyrrhenian Margin from new CROP Seismic Data, in: Finetti I.R. (Ed.), CROP PROJECT: Deep Seismic Exploration of the Central Mediterranean and Central Italy, Atlases in Geoscience, 1, Elsevier BV.
- Finetti, I., 1984. Geophysical study of the Sicily Channel Zone. *Bollettino di Geofisica Teorica ed Applicata* 26, 3–28.
- Finetti, I.R, Del Ben, A., 2005. Crustal tectono-stratigraphic setting of the Pelagian foreland from new CROP Seismic data. In: Finetti I.R. (ed) CROP PROJECT: Deep seismic exploration of the central Mediterranean and Italy, Elsevier B.V., 581–595.
- Floodgate, G.D. and Judd, A.G., 1992. The origins of shallow gas. *Continental Shelf Research* 12, 1145-1156.
- Foglini, F., Dalla Valle, G., Micallef, A., Berndt, C., Campiani, E., Trincardi, F., 2011. Seafloor instability and mass wasting processes along the eastern Gela slope, in: Yamada, Y., Kawamura, K., Ikehara, K., Ogawa, Y., Urgeles, R., Mosher, D., Chaytor, J.D., Strasser, M.C. (Eds.), 5th International Symposium on Submarine Mass Movements and their Consequences, Kyoto, Japan.
- Fourniguet J. (1987) - Géodynamique actuelle dans le nord et le nord-est de la France. *Mém.BRGM* 127, 160.
- Frixa, A., Bertamoni, M., Catrullo, D., Trincianti, E., Miuccio, G., 2000. Late Norian-Hettangian paleogeography in the area between wells Noto 1 and Polpo 1 (S-E Sicily). *Mem. Soc. Geol. It.*, 55: 279-284, 6 figg., Roma.
- Gabersek, S., Sorgente, R., Natale, S., Ribotti, A., Olita, A., Astraldi, M., and Borghini, M, 2007. The Sicily Channel Regional Model forecasting system: initial boundary conditions sensitivity and case study evaluation, *Ocean Sci.*, 3, 31–41, 2007, <http://www.ocean-sci.net/3/31/2007/>.
- Galea, P., 2007. Seismic history of the Maltese islands and considerations on seismic risk, *Annales Geophysics* 50, 725–740.
- Gamboa, D., Alves, T., Cartwright, J., Terrinha, P., 2010. MTD distribution on a 'passive' continental margin: The Espirito Santo Basin (SE Brazil) during the Palaeogene. *Marine and Petroleum Geology* 27, 1311–1324. doi:10.1016/j.marpetgeo.2010.05.008
- García Lafuente, J., García, A., Mazzola, S., Quintanilla, L., Delgado, J., Cuttitta, A., Patti, B., 2002. Hydrographic phenomena influencing early life stages of the Sicilian Channel anchovy. *Fish. Oceanogr.*, 11, 31-44.
- Gardiner, W., Grasso, M., Sedgeley, D., 1993. Plio-Pleistocene stratigraphy and recent movements of the Malta platform. In: Max, M.D., Colantoni, P. (Eds.), UNESCO Technical Reports in Marine Science, Urbino, pp. 111–116.
- Gardner, J., Prior, D., Field, M., 1999. Humboldt Slide - a large shear-dominated retrogressive slope failure. *Marine Geology* 154, 323-338.

- Garziglia, S., Migeon, S., Ducassou, E., Loncke, L., Mascle, J., 2008. Mass-transport deposits on the Rosetta province (NW Nile deep-sea turbidite system, Egyptian margin): characteristics, distribution, and potential causal processes. *Marine Geology*, 250, 180–198.
- Gasparo Morticelli M., Valenti V., Catalano R., Sulli A., Agate M., Avellone G., Albanese C., Basilone L., Gugliotta C. 2015. Deep controls on foreland basin system evolution along the Sicilian fold and thrust belt. *Bulletin de la Société géologique de France*, 186, 273–290.
- Gee, M. J. R., A. B. Watts, D. G. Masson, and N. C. Mitchell (2001), Landslides and the evolution of El Hierro in the Canary Islands, *Mar. Geol.*, 177, 271–294, doi:10.1016/S0025-3227(01)00153-0.
- Gee, M.J.R., Gawthorpe, R.L. & Friedmann, S.J. (2006) Triggering and evolution of a Giant Submarine Landslide, Offshore Angola, revealed by 3D seismic stratigraphy and geomorphology. *J. Sediment. Res.*, 76, 9–19.
- Genin, A., and G. W. Boehlert. Dynamics of temperature and chlorophyll structures above a seamount: An oceanic experiment. *Journal of Marine Research* 43, 907-924.
- Giannoulaki, M., Machias, A., Tsimenides, N. 1999. Ambient luminance and vertical migration of the sardine *Sardina pilchardus*. *Marine Ecology Progress Series*, 178, 29-38.
- Granath, J.W., Casero, P. 2004. Tectonic setting of the petroleum systems of Sicily, in *Deformation, Fluid Flow and Reservoir Appraisal in Foreland Fold-and-Thrust Belts*, in: Swennen, R., Roure, F. Granath, J. (Eds.) American Association Petroleum Geology Hedberg Series 1, 391–411.
- Gugliotta, C., Gasparo Morticelli, M., Avellone, G., Agate, M., Barchi, M. R., Albanese, C., Valenti, V., Catalano, R. 2014. Middle Miocene–Early Pliocene wedge-top basins of NW Sicily (Italy): constraints for the tectonic evolution of a ‘non-conventional’ thrust belt, affected by transpression. *Journal of the Geological Society*, London.
- Guliev I.S. (1992) - A review of mud volcanism. Translation of the report by Azerbaijan Academy of Sciences Institute of Geology, 65.
- Haflidason H., Sejrup H.P., Nygård A., Mienert J., Bryn P., Lien R., Forsberg C-F., Berg K. & Masson D. 2004. The Storegga Slide: architecture, geometry and slide development. *Marine Geology* 213,201-234.
- Hampton M.A., Lee H.J. and Locat J. 1996. Submarine landslides. *Reviews of Geophysics*, 34(1): 33-59.
- Handy, M. R., Schmid, S. M., Bousquet, R., Kissling, E., Bernoulli, D., 2010. Reconciling plate-tectonic reconstructions of Alpine Tethys with the geological–geophysical record of spreading and subduction in the Alps. *Earth-Science Reviews* 102, 121-158.
- Harris, R. A., R. J. Archuleta, and S. M. Day (1991), Fault steps and the dynamic rupture process: 2-D numerical simulations of a spontaneously propagating shear fracture, *Geophysics Research Letter* 18, 893.
- Hasiotis T., Papatheodorou G., Kastanos N., Ferentinos G. (1997) - A pockmark field in the Patras Gulf (Greece) and its activation during the 14/7/93 seismic event. *Marine and Petroleum Geology*, 130, 333–344.

- Henry, P., Le Pichon, X., Lallemand, S., Foucher, J.-P., Westbrook, G., Hobart, M., 1990. Mud volcano field seaward of the Barbados accretionary complex: a deep-towed side scan sonar survey. *Journal of Geophysical Research* 95, 8917–8929.
- Hensen, C., Nuzzo, M., Hornibrook, E., Pinheiro, L.M., Bock, B., Magalhães, V.H., Brückmann, W., 2007. Sources of mud volcano fluids in the Gulf of Cadiz—indications for hydrothermal imprint. *Geochimica et Cosmochimica Acta* 71, 1232–1248.
- Hillier, J.K., and Watt, A.B., 2007. Global distribution of seamounts from ship-track bathymetry data. *Geophysical Research Letters*, vol. 34, L13304, doi: 10.029/2007GL029874.
- Ho, S., Cartwright, J.A. and Imbert, P., 2012. Vertical evolution of fluid venting structures in relation to gas flux, in the Neogene-Quaternary of the Lower Congo Basin, Offshore Angola. *Marine Geology* 332–334, 40-55.
- Holland, C.W., Etiope, G., Milkov, A.V., Michelozzi, E., Favali, P., 2003. Mud volcanoes discovered offshore Sicily. *Marine Geology* 199, 1-6.
- Holland, C.W., Weber, T.C., Etiope, G., 2006. Acoustic scattering from mud volcanoes and carbonate mounds. *Journal Acoustical Society of America* 120, 3553-3565.
- Hovland M. 1981. Characteristics of pockmarks in the Norwegian Trench. *Marine Geology* 29, 103-117.
- Hovland M. 1991. Large pockmarks, gas-charged sediments and possible clay diapers in the Skagerrak: *Marine and Petroleum Geology*, 8, 311-316.
- Hovland M., Judd A. G. & King L. H. 1984. Characteristic features of pockmarks on the North Sea Floor and Scotian Shelf. *Sedimentology*, 31, 471-480.
- Hovland M., Judd A.G. 1988. *Seabed Pockmarks and Seepages, Impact on Geology, Biology and the Marine Environment*. Graham & Trotman, London. 293.
- Hovland M., Talbot M., Qvale H., Olaussen S. & Aasberg L. 1987. Methane-related carbonate cements in pockmarks of the North Sea. *J. Sed. Petrol.*, 57, 881-892.
- Hovland, M., Gardner, J.V. and Judd, A.G., 2002. The significance of pockmarks to understanding fluid flow processes and geohazards. *Geofluids* 2, 127–136.
- Hovland, M., Judd, A.G. and Burke Jr, R.A., 1993. The global flux of methane from shallow submarine sediments. *Chemosphere* 26, 559-578.
- Hovland, M., Talbot, M., Olaussen, S., Aasberg, L., 1985. Recently formed methane-derived carbonates from the North Sea floor, in: Thomas, B.M. (Ed.), *Petroleum Geochemistry in Exploration of the Norwegian Shelf*. Graham & Trotman, 263–266.
- Hürliamann, M., Ledesma, A., Martí, J., 2001. Characterisation of a volcanic residual soil and its implications for large landslide phenomena: application to Tenerife, Canary Islands. *Eng. Geol.* 59, 115– 132.
- Hyndman, R.D., and Davis, E.E., 1992. A mechanism for the formation of methane hydrate and seafloor bottom-simulating reflectors by vertical fluid expulsion. *J. Geophys. Res.*, 97:7025–7041
- Imbò, G., 1965. *Catalogue of the active volcanoes of the world, Italy*, 18, Rome, IAVCEI, 72.

- Jerosch, K., Schlüter, M., Foucher, J.P., Allais, A.G., Klages, M., Edy, C., 2007. Spatial distribution of mud flows, chemoautotrophic communities, and biogeochemical habitats at Håkon Mosby Mud Volcano. *Marine Geology* 243, 1–17.
- Judd, A.G. and Hovland, M., 1992. The evidence of shallow gas in marine sediments. *Continental Shelf Research* 12, 1081-1095.
- Judd, A.G., 2004. Natural seabed gas seeps as sources of atmospheric methane. *Environmental Geology* 46, 988–996.
- Judd, A.G., Hovland, M., 2007. *Seabed Fluid Flow: The Impact on Geology, Biology and the Marine Environment*. Cambridge University Press, Cambridge.
- Judd, A.G., Hovland, M., Dimitrov, Kvenvolden, K.A., Rogers, B., 2005. Gaia's breath: Global methane exhalations. *Marine and Petroleum Geology* 22, 579-590.
- Judd, A.G., Hovland, M., Dimitrov, L.I., Garcia-Gil, S., Jukes, V., 2002. The geological methane budget at continental margins and its influence on climate change. *Geofluids* 22, 579-590.
- Judd, A.G., Hovland, M., Dimitrov, L.I., Garcia-Gil, S., Jukes, V., 2002. The geological methane budget at continental margins and its influence on climate change. *Geofluids* 22, 579-590.
- Kelley J.T., Dickson S.M., Belknap D.F., Barnhardt W.A., and Henderson M. (1994) - Giant seabed pockmarks: evidence for gas escape from Belfast Bay, *Maine Geology* 22, 59-62.
- Kennett, J.P. and Stott, L.D., 1990. Proteus and proto Oceanus: ancestral Paleogene oceans as revealed from Antarctic stable isotopic results: ODP Leg 113. In: P.E. Barker and J.P. Kennett, *Proc. ODP Sci. Res.* I 13:865 88.
- Kholodov, V.N., 2002. Mud volcanoes: distribution regularities and genesis (Communication 2. Geological–geochemical peculiarities and formation model). *Lithology and Mineral Resources* 37, 293–309.
- King, L.H. and MacLean, B., 1970. Pockmarks on the Scotian Shelf. *Geological Society of America Bulletin* 81, 3141-3148.
- Kopf, A.J., 2002. Significance of mud volcanism. *Rev. Geophysics* 40 (2).
- Kvenvolden, K.A., 1993. Gas hydrates - geological perspective and global change. *Rev. Geophys.* 31, 173-187.
- Kvenvolden, K.A., Rogers, B., 2005. Gaia's breath: Global methane exhalations. *Marine and Petroleum Geology* 22, 579–590.
- Lafuente, J. G. , García, A. , Mazzola, S. , Quintanilla, L. , Delgado, J. , Cuttita, A. and Patti, B., 2002. Hydrographic phenomena influencing early life stages of the Sicilian Channel anchovy. *Fisheries Oceanography* 11, 31–44. doi:10.1046/j.1365-2419.2002.00186.x
- Laier, T. and Jensen, J., 2007. Shallow gas depth-contour map of the Skagerrak-western Baltic Sea region. *Geo-Marine Letters* 27, 127-141.
- Lanzafame, G., Rossi, P.L., Tranne, C.A., and Lanti, E., 1994. *Carta geologica dell'isola di Linosa*, scale 1:5.000, Firenze, SELCA.

- Larson, R.L., 1991. Geological consequences of superplumes. *Geology* 19, 963–966. doi:10.1130/0091-7613(1991).
- Lastras, G., Canals, M., Urgeles, R., Hughes-Clarke, J.E., Acosta, J., 2004. Shallow slides and pockmark swarms in the Eivissa Channel, western Mediterranean Sea. *Sedimentology* 51, 837–850. doi:10.1111/j.1365-3091.2004.00654.x
- Law, C.S., Nodder, S.D., Mountjoy, J.J., Marriner, A., Orpin, A., Pilditch, C.A., Franz, P., Thompson, K., 2010. Geological, hydrodynamic and biogeochemical variability of a New Zealand deep-water methane cold seep during an integrated three-year time-series study. *Marine Geology* 272, 189–208.
- Le Friant, A., Boudon, G., Deplus, C., Villemant, B., 2003. Large-scale flank collapse events during the activity of Montagne Pelée, Martinique, Lesser Antilles. *J. Geophys. Res.* 108, 2055. doi:10.1029/2001JB001624.
- Le Pichon, X., Foucher, J.-P., Boulegue, J., Henry, P., Lallemand, S., Benedetti, M., Avedik, F., Mariotti, A., 1990. Mud volcano field seaward of the Barbados accretionary complex: a submersible survey. *Journal of Geophysical Research* 95, 8931–8943.
- Lee, H.J., Locat, J., Desgagnes, P., Parsons, J.D., Mcadoo, B.G., Orange, D.L., Puig, P., Wong, F.L., Dartnell, P., Boulanger, E., 2007. Submarine mass movements on continental margins. *IAS Spec. Publ.* 1–62.
- Leeder, M.R., 1987. Sediment deformation structures and the palaeotectonic analysis of sedimentary basins, with a case-study from the Carboniferous of northern England. In: Jones, M.E., Preston, R.M.F. (Eds.), *Deformation of Sediments and Sedimentary Rocks: Geological Society, London, Special Publication*, 29, pp. 137–146.
- Lentini, F., Carbone, S., Catalano, S., 1994. Main structural domains of the central Mediterranean region and their tectonic evolution. *Boll. Geofis. Teor. Appl.* 36, (141–144): 103-125.
- León, R., Somoza, L., Medialdea, T., Gonzalez, FJ, Gimenez-Moreno, CJ, Perez-Lopez, R., 2014. Pockmarks on either side of the Strait of Gibraltar: formation from overpressured shallow contourite gas reservoirs and internal wave action during the last glacial sea-level lowstand?. *Geo-Marine Letters*: 34 (2-3), 131–151. DOI: 10.1007/s00367-014-0358-2.
- León, R., Somoza, L., Medialdea, T., Hernández-Molina, F.J., Vázquez, J.T., Díaz-del-Río, V., González F.J., 2010. Pockmarks, collapses and blind valleys in the Gulf of Cadiz. *Geo-Marine Letters* 30, 3-4, 31-247, doi:10.1007/s00367-009-0169-z.
- Lermusiaux, P.F.J., Robinson, A.R., 2001. Features of dominant mesoscale variability, circulation patterns and dynamics in the Strait of Sicily. *Deep-Sea Res. I* 48, 1953-1997.
- Levin, L.A., 2005. Ecology of cold seep sediments: interactions of fauna with flow, chemistry and microbes. *Oceanography and Marine Biology: Annual Review* 43, 1–46.
- Lewis, B.T.R., Cochrane, G.C., 1990. Relationship between the location of chemosynthetic benthic communities and geologic structure on the Cascadia subduction zone. *Journal of Geophysical Research* 95 (B6), 8783–8793.

- Llanes, P., Herrera, R., Gómez, M., Muñoz, A., Acosta, J., Uchupi, E., Smith, D., 2009. Geological evolution of the volcanic island La Gomera, Canary Islands, from analysis of its geomorphology. *Mar. Geol.* 264, 123–139.
- Lo Iacono, C., Sulli, A., Agate, M., 2014. Submarine canyons of north-western Sicily (Southern Tyrrhenian Sea): Variability in morphology, sedimentary processes and evolution on a tectonically active margin. *Deep-Sea Research Part II: Topical Studies in Oceanography*, 104, 93–105.
- Lo Iacono, C., Sulli, A., Agate, M., Presti, V., Pepe, F., Catalano, R., 2011. Submarine canyon morphologies in the Gulf of Palermo (Southern Tyrrhenian Sea) and possible implications for geo-hazard. *Marine Geophysical Research* 32, 127–138. doi:10.1007/s11001-011-9118-0
- Lodolo, E., Civile, D., Zanolla, C., Geletti, R., 2012. Magnetic signature of the Sicily Channel volcanism. *Marine Geophysics Research* 33, 33–44.
- Lowe, D.R., 1976. Subaqueous liquefied and fluidized sediment flows and their deposits. *Sedimentology* 23, 285–308.
- Lu, S., and G. A. McMechan (2002), Estimation of gas hydrate and free gas saturation, concentration, and distribution from seismic data, *Geophysics*, 67, 582–593.
- Macdonald, I.R., Guinasso, N.L., Ackleson, S.G., Amos, J.F., Duckworth, R., Sassen, R. and Brooks, J.M., 1993. Natural oil slicks in the Gulf of Mexico visible from space. *Journal of Geophysical Research: Oceans* 98, 16351-16364.
- MacDonald, I.R., Guinasso, N.L., Reilly, J.F., Brooks, J.M., Callender, W.R., Gabrielle, S.G., 1990. Gulf of Mexico hydrocarbon seep communities: VI. Patterns in community structure and habitat. *Geo-Marine Letters* 10, 244–252.
- MacDonald, I.R., Guinasso, N.L., Reilly, J.F., Brooks, J.M., Callender, W.R., Gabrielle, S.G., 1990. Gulf of Mexico hydrocarbon seep communities: VI. Patterns in community structure and habitat. *Geo-Marine Letters* 10, 244–252.
- Magalhães, V.H., Pinheiro L.M., Ivanov M.K., Kozlova E., Blinova, V., Kolganova, J., Vasconcelos, C., McKenzie, J., Bernasconi, S.M., Kopf, A.J., Díaz-del-Río, V., González, F.J., Somoza, L., 2012. Formation processes of methane-derived authigenic carbonates from the Gulf of Cadiz. *Sedimentary Geology* 243-244, 155–168.
- Magde, L.S., and Smith, D.K., 1995. Seamount volcanism at the Reykjanes Ridge: Relationship to the Iceland hot spot. *J. Geophys. Res.*, 100, 8449-8468.
- Maltman, A.J. (Ed.), 1994. *The Geological Deformation of Sediments*. Chapman and Hall, London.

- Marani, M., Argnani, A., Roveri, M., Trincardi, F., 1993. Sediment drifts and erosional surfaces in the central Mediterranean: seismic evidence of bottom-current activity, *Sedimentary Geology*, 82, 207–220.
- Maravelias, C. D., 1999. Habitat selection and clustering of a pelagic fish: effect of topography and bathymetry on species dynamics. *Can. J. Fish. Aquat. Sci.*, 56, 437-450.
- Maravelias, C.D., Reid, D.G., Swartzman, G., 2000. Seabed substrate, water depth and zooplankton as determinants of the prespawning spatial aggregation of North Atlantic herring. *Marine Ecology Progress Series* 195, 249-259.
- Marchant, F. L., 1972. Ionian Sea. Carter T.G. et al.: A new bathymetric chart and physiography of the Mediterranean Sea. *The Mediterranean Sea: a natural sedimentation Laboratory* (Stanley D. J. Ed), 14-16, Dowden Hutchinson and Ross, Pennsylvania.
- Martonelli, E., Falcini, F., Salusti, E. & Chiocci, F.L., 2010. Analysis and modeling of contourite Drifts and contour currents off promontories in the Italian Seas (Mediterranean Sea). *Marine Geology* 278, 19-30.
- Martorelli, E., Petroni, G., Chiocci, F.L., Pantelleria Sci, P., 2011. Contourites offshore Pantelleria Island (Sicily Channel, Mediterranean Sea): depositional, erosional and biogenic elements. *Geo-Marine Letters* 31, 481–493.
- Masson D G, Canalis M, Alonso B, Urgeles R, Huhnerbach V, 1998. The Canary Debris Flow: source area, morphology and failure mechanism. *Sedimentology*. 45: 411-432.
- Masson, D. G., Watts, A. B., Gee, M. R. J., Urgeles, R., Mitchell, N. C., Le Bas, T. P. & Canals, M. 2002 Slope failures on the flanks of the western Canary islands. *Earth Sci. Rev.* 57, 1–35. (doi:10.1016/S0012-8252(01)00069-1).
- Masson, D.G., Le Bas, T.P., Grevemeyer, I., Weinrebe, W., 2008. Flank collapse and large-scale landsliding in the Cape Verde Islands, off West Africa. *Geochemistry, Geophysics, Geosystems* 9, n/a–n/a. doi:10.1029/2008GC001983.
- Masson, D.G., Watts, A.B., Gee, M.J.R., Urgeles, R., Mitchell, N.C., Le Bas, T.P., Canals, M., 2002. Slope failures on the flanks of the western Canary Islands. *Earth Sci. Rev.* 57 (1–2), 1–35.
- Mastrogiacomo, G., Moretti, M., Owen, G., Spalluto, L., 2012. Tectonic triggering of slump sheets in the Upper Cretaceous carbonate succession of the Porto Selvaggio area (Salento peninsula, southern Italy): Synsedimentary tectonics in the Apulian Carbonate Platform. *Sedim. Geol.* 269-270, 15–27. doi:10.1016/j.sedgeo.2012.05.001.

- Max, M. D. & Colantoni, P., 1992. Geological development of the Sicilian-Tunisian Platform. *Unesco reports in marine science*, 58.
- Max, M.D., Kristensen, A., Michelozzi, E., 1993. Small scale Plio-Quaternary sequence stratigraphy and shallow geology of the west-central Malta Plateau, in: Max, M.D., Colantoni, P. (Eds.), *Geological Development of the Sicilian-Tunisian Platform*. UNESCO, Urbino, pp. 117-122.
- McAdoo, B.G., Pratson, L.F., Orange, D.L. (2000). Submarine landslide geomorphology, U.S. Continental slope. *Mar. Geol.*, 169, 103–136.
- McGinnis, D.F., Schmidt, M., DelSontro, T., Themann, S., Rovelli, L., Reitz, A. and Linke, P., 2011. Discovery of a natural CO₂ seep in the German North Sea: Implications for shallow dissolved gas and seep detection. *Journal of Geophysical Research: Oceans* 116, C03013.
- McMurtry, G.M., Watts, P., Fryer, G.J., Smith, J.R., Imamura, F. (2004). Giant landslides, Mega-Tsunamis, and Paleo-Sea Level in the Hawaiian Islands. *Mar. Geol.*, 203, 219–233.
- Medialdea, T., Somoza, L., Pinheiro, L.M., Fernández-Puga, M.C., Vázquez, J.T., León, R., Ivanov, M.K., Magalhaes, V., Díaz-del-Río, V., Vegas, R., 2009. Tectonics and mud volcano development in the Gulf of Cádiz. *Marine Geology* 261, 48–63. doi:10.1016/j.margeo.2008.10.007
- Micallef, A., Berndt, C., Debono, G., 2011. Fluid flow systems of the Malta Plateau, Central Mediterranean Sea. *Marine Geology* 284, 74-85.
- Micallef, A., Berndt, C., Masson, D.G., Stow, D.A.V., 2007. A technique for the morphological characterization of submarine landscapes as exemplified by debris flows of the Storegga Slide. *Journal of Geophysical Research* 112, F02001.
- Milkov, A.V., 2000. Worldwide distribution of submarine mud volcanoes and associated gas hydrates. *Marine Geology* 167, 29–42.
- Milkov, A.V., Sassen, R., Apanasovich, T.V., Dadashev, F.G., 2003. Global gas flux from mud volcanoes: a significant source of fossil methane in the atmosphere and the ocean. *Geophysical Research Letters* 30, 1037. doi:10.1029/2002GL016358.
- Milkov, A.V., Vogt, P.R., Crane, K., Lein, A.Y., Sassen, R. and Cherkashev, G.A., 2004. Geological, geochemical, and microbial processes at the hydrate-bearing Håkon Mosby mud volcano: a review. *Chemical Geology* 205, 347-366.
- Millot, C., 1999. Circulation in the Western Mediterranean Sea. *Journal of Marine Systems* 20, 423–442.
- Minisini, D., Trincardi, F., Asioli, A., Canuz, M., Foglini, F., 2007. Morphologic variability of exposed mass-transport deposits on the eastern slope of Gela Basin (Sicily channel). *Basin Research* 19, 217–240.
- Mitchell, N.C., Dade, W.B., Masson, D.G., 2003. Erosion of the submarine flanks of the Canary Islands. *J. Geophys. Res.* 108 (F1), 6002. <http://dx.doi.org/10.1029/2002JF000003>.

- Molcard, A., Gervasio, L., Griffa, A., Gasparini, G.P., Mortier, L., Tamay, M., Özgökmen, T. M., 2002. Numerical investigation of the Sicily Channel dynamics: density currents and water mass advection. *Journal of Marine Systems*, 36, 219- 238.
- Molina, J.M., Alfaro, P., Moretti, M., Soria, J.M., 1998. Soft-sediment deformation structures induced by cyclic stress of storm waves in tempestites (Miocene, Guadalquivir Basin, Spain). *Terra Nova* 10, 145–150.
- Montenat, C., Barrier, P., Ott d’Estevou, O., Hibsich, C., 2007. Seismites: an attempt at critical analysis and classification. *Sedim. Geol.* 196, 5-30.
- Moore G. W. 1961. Coastal sedimentation in northwestern Alaska: U.S. Geological Survey Report TEI-779, 43–65.
- Moore, J. G., and G. W. Moore 1984, Deposit from a giant wave on the island of Lanai, Hawaii, *Science*, 226, 1312– 1315, doi:10.1126/science.226.4680.1312.
- Moore, J. G., W. R. Normark, and R. T. Holcomb 1994. Giant Hawaiian landslides, *Annu. Rev. Earth Planet. Sci.*, 22, 119–144, doi:10.1146/annurev.ea.22.050194.001003.
- Moore, J.C., Vrolijk, P., 1992. Fluids in accretionary prisms. *Reviews in Geophysics* 30, 113–135.
- Moore, J.G., Clague, D.A., Holcomb, R.T., Lipman, P.W., Normark, W.R., Torresan, M.E., 1989. Prodigious submarine landslides on the Hawaiian Ridge. *J. Geophys. Res.* 94, 17465–17484.
- Morelli, C., Gantar, G. & Pisani, M., 1975. Bathymetry, gravity and magnetism in the Strait of Sicily and the Ionian Sea. *Boll. Geof. Teor. ed Appl.*, XVII, 65, 39-58, Trieste.
- Moretti, M., Soria, J. M., Alfaro, P., Walsh, N., 2001. Asymmetrical soft-sediment deformation structures triggered by rapid sedimentation in turbiditic deposits. *Facies*, 44: 283-294.
- Moretti, M., Van Loon, A.J.T., 2014. Restrictions to the application of “diagnostic” criteria for recognizing ancient seismites. *Journal of Palaeogeography* 3, 162–173. doi:10.3724/SP.J.1261.2014.00050.
- Moscardelli, L., Wood, L., 2008. New classification system for mass transport complexes in offshore Trinidad. *Basin Res* 20, 73–98. doi:10.1111/j.1365-2117.2007.00340.x .
- Moscardelli, L., Wood, L. & Mann, P. 2006. Mass-transport complexes and associated processes in the Offshore Area of Trinidad and Venezuela. *AAPG Bull.*, 90, 1059–1088.
- Mulder, T., Alexander, J., 2001. The physical character of subaqueous sedimentary density flows and their deposits. *Sedimentology* 48, 269–299.
- Nardin, T.R., Hein, F.J., Gorsline, D.S. & Edwards, B.D. (1979) A review of mass movement processes, sediment, and acoustic characteristics and contrasts in slope and base-of- slope systems versus canyon-fan-basin floor systems. *Spec. Publ. SEPM*, 27, 61–73.
- Obermeier, S.F., 1996. Using liquefaction-induced features for paleoseismic analysis. In: McCalpin, J.P. (Ed.), *Paleoseismology*. *Int. Geophys. Ser.* 62, 331–396.
- Odonne, F., Callot, P., Debroas, E.-J., Sempere, T., Hoareau, G., Maillard, A., 2011. Soft-sediment deformation from submarine sliding: favourable conditions and triggering mechanisms in examples from the Eocene

- Sobrarbe delta (Ainsa, Spanish Pyrenees) and the mid-Cretaceous Ayabacas Formation (Andes of Peru). *Sedimentary Geology*, 235, 249-263.
- Oehler, J.F., Lénat, J.F., Labazuy, P., 2008. Growth and collapse of the Reunion Island volcanoes. *Bull. Volcanol.* 70, 717–742.
- Ollier, G., P. Cochonat, J. F. Lenat, and P. Labazuy (1998), Deep-sea volcanoclastic sedimentary systems: An example from La Fournaise volcano, Reunion Island, Indian Ocean, *Sedimentology*, 45, 293 – 330, doi:10.1046/j.1365-3091.1998.0152e.x.
- Orrù, P., Melegari, G., Badalini, M., 1993. Geomorphological observations of the seabed between Cape Bon and Cape Feto (Strait of Sicily). Geological development of the Sicilian-Tunisian Platform, *Unesco reports in marine science*, (ed. By M.D. Max and Colantoni), 58, 153-160.
- Owen, G., 1987. Deformation processes in unconsolidated sands. In: *Deformation of Sediments and Sedimentary Rocks* (M.E. Jones and R.M.F. Preston, eds). *Geol. Soc. Spec. Pub.* 29, 11–24.
- Owen, G., Moretti, M., 2011. Identifying triggers for liquefaction-induced soft-sediment deformation in sands. *Sedimentary Geology*, 235, 141-147.
- Papatheodorou G., and Ferentinos G. 1997. Submarine and coastal sediment failure, triggered by the 1995, Ms=6.1R, Aegion earthquake, Gulf of Corinth, Greece. *Mar. Geol.*, 137, 287-304.
- Parello F., Allard P., D'Alessandro W., Federico C., Jean-Baptiste P., Catani. O., 2000. Isotope geochemistry of Pantelleria volcanic fluids, Sicily Channel rift: a mantle volatile end-member for volcanism in southern Europe. *Earth and Planetary Science Letters* 180, 325-339.
- Patacca, E., Scandone, P., Giunta, G., Liguori, V., 1979. Mesozoic paleotectonic evolution of the Ragusa zone (Southeastern Sicily). *Geologica Romana*, 18, 331–369.
- Patti, B., Bonanno, A., Basilone, G., Goncharov, S., Mazzola, S., Buscaino, G., Cuttitta A., García Lafuente, J., García, A., Palombo, G., Cosimi, G., 2004. Interannual fluctuations in acoustic biomass estimates and in landings of small pelagic fish populations in relation to hydrology in the Strait of Sicily. *Chem. Ecol.*, 20, 365-375.
- Paull C. K., Ussler III W., and Borowski W.S. (1995) - Methane-rich plumes on the Carolina continental rise: associations with gas hydrates. *Geology* 23, 89-92.
- Peccerillo, A., 2005. Plio-Quaternary volcanism in Italy. *Petrology, Geochemistry, Geodynamics*. Springer, Heidelberg, 365 pp.
- Pennino, V., Sulli, A., Caracausi, A., Grassa, F., Interbartolo, F., 2014. Fluid escape structures in the north Sicily continental margin. *Marine and Petroleum Geology* 55, 202–213. doi:10.1016/j.marpetgeo.2014.02.007
- Perez-Garcia, C., Feseker, T., Mienert, J. and Berndt, C., 2009. The Håkon Mosby mud volcano: 330000 years of focused fluid flow activity at the SW Barents Sea slope. *Marine Geology* 262, 105-115.
- Pilcher R., Argent J. (2007) - Mega-pockmarks and linear pockmark trains on the West African continental margin. *Marine Geology*, 244, 15–32.

- Posamentier, H., Martinsen, O.J., 2011. The character and genesis of submarine mass-transport deposits: insights from outcrop and 3D seismic data, in: Shipp, C., Weimer, P., Posamentier, H. (Eds.), Mass-transport deposits in deepwater settings. SEPM Special Publication 96, pp. 7-38.
- Posamentier, H.W. & Kolla, V. 2003. Seismic geomorphology and stratigraphy of depositional elements in deep-water settings. *J. Sediment. Res.*, 73, 367–388.
- Pratt, B. R., 1994. Seismites in the Mesoproterozoic Altyn Formation (Belt Supergroup), Montana: A test for tectonic control of peri-tidal carbonate cyclicity. *Geology*, 22, 1091-1094.
- Prior, M.K., 2005. A scatterer map for the Malta Plateau. *IEEE Journal of Oceanic Engineering* 30, 676-690.
- Prosperini, N., Perugini, D., Poli, G., and Manetti, P., 2000. Magmatic enclaves distribution within the Khaggiar lava dome (Pantelleria, Italy). Implication for magma chamber dynamics and eruption: *Acta Vulcanologica*, 12, 37-47.
- Rappaport, Y., Naar, D.F., Barton, C.C., Liu, Z.J., and Hey, R.N., 1997. Morphology and distribution of seamounts surrounding Easter Island. *J. Geophys. Res.*, 102, 24713-24728.
- Rebesco, M., Stow, D.A.V., (2001). Seismic expression of contourites and related deposits: a preface. *Mar. Geophys. Res.* 22, 303–308.
- Reeburgh, W.S., 2007. Oceanic methane biogeochemistry. *Chemical Reviews* 107, 486–513.
- Reeder, M.S., Rothwell, G., Stow, D.A.V., 2002. The Sicilian gateway: anatomy of the deep-water connection between East and West Mediterranean basins. In: Stow, D. A. V., Pudsey, C. J., Howe, J. A., Faugeres, J.-C. & Viana, A. R. (eds) *Deep-Water Contourite Systems: Modern Drifts and Ancient Series, Seismic and Sedimentary Characteristics*. Geological Society, London, *Memoirs*, 22, 171-189.
- Reid, D.G. & Maravelias, C.D., 2001. "Relationships between herring school distribution and seabed substrate derived from RoxAnn", *ICES J MAR*, 58(6), 1161-1173.
- Reuther, C.D., Eisbacher, G.H., 1985. Pantelleria rift-crustal extension in a convergent intraplate setting. *Geol Rundsch*, 74, 585-597.
- Ribera d'Alcal'a, M., Civitarese, G., Conversano, F., and Lavezza, R., 2003. Nutrient fluxes and ratios hint at overlooked processes in the Mediterranean sea, *J. Geophys. Res.*, 108, 8106, doi:10.1029/2002JC001250.
- Rise L., Sættem J., Fanavoll S., Thorsnes T., Ottesen D. & Bøe R. (1999) - Sea-bed pockmarks related to fluid migration from Mesozoic bedrock strata in the Skagerrak offshore Norway, *Mar. Pet. Geol.*, 16, 619-631.
- Robertson, A., 1996. Mud volcanism on the Mediterranean Ridge: initial results of Ocean Drilling Program Leg 160. *Geology* 24, 239–242.
- Romagnoli, C., Casalbore, D. & Chiocci, F. L. 2012. La Fossa caldera breaching and submarine erosion (Vulcano island, Italy). *Marine Geology*, 303–306, 87–98.
- Romagnoli, C., Casalbore, D., Bosman, A., Braga, R., Chiocci, F.L., 2013. Submarine structure of Vulcano volcano (Aeolian Islands) revealed by high-resolution bathymetry and seismo-acoustic data. *Marine Geology* 338, 30–45. doi:10.1016/j.margeo.2012.12.002.

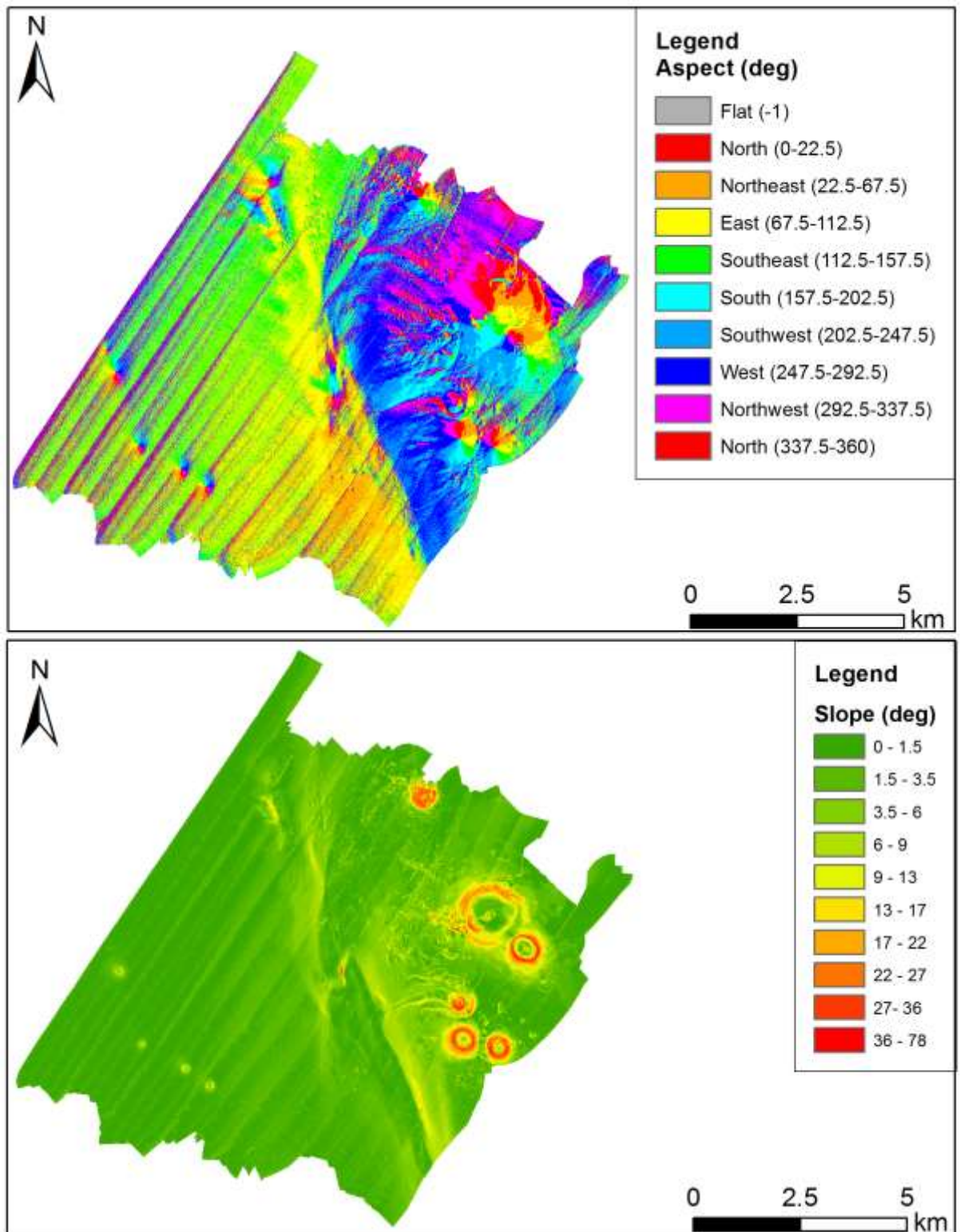
- Romagnoli, C., Kokelaar, P., Casalbore, D., Chiocci, F.L., 2009. Lateral collapses and active sedimentary processes on the northwestern flank of Stromboli volcano, Italy. *Marine Geology* 265, 101–119. doi:10.1016/j.margeo.2009.06.013.
- Romero Ruiz, C., García-Cacho, L., Araña, V., Yanes Luque, A., Felpeto, A., 2000. Submarine volcanism surrounding Tenerife, Canary Islands: implications for tectonic controls, and oceanic shield forming processes. *J Volcanol Geotherm Res* 103:105–119.
- Rotolo, S.G., Castorina, F., Cellura, D., Pompilio, M., 2006. Petrology and geochemistry of submarine volcanism in the Sicily Channel Rift. *Journal of Geology* 114, 355–365.
- Roure, F., Howell, D.G., Muller, C., Moretti, I., 1990. Late Cenozoic subduction complex of Sicily. *Journal of Structural Geology*, 12, 259–266.
- Sahling, H., Bohrmann, G., Spiess, V., Bialas, J., Breitzke, M., Ivanov, M., Kasten, S., Krastel, S. and Schneider, R., 2008a. Pockmarks in the Northern Congo Fan area, SW Africa: Complex seafloor features shaped by fluid flow. *Marine Geology* 249, 206-225.
- Sauter, E.J., Muyakshin, S.I., Charlou, J.L., Schlüter, M., Boetius, A., Jerosch, K., Damm, E., Foucher, J.P., Klages, M., 2006. Methane discharge from a deep-sea submarine mud volcano into the upper water column by gas hydrate-coated methane bubbles. *Earth and Planetary Science Letters* 243, 354–365.
- Sautkin, A., Talukder, A.R., Comas, M.C., Soto, J.I., Alekseev, A., 2003. Mud volcanoes in the Alboran Sea: evidence from micropaleontological and geophysical data. *Marine Geology* 195, 237–261.
- Savini, A., Malinverno, E., Etiope, G., Tessarolo, C., Corselli, C., 2009. Shallow seep-related seafloor features along the Malta Plateau (Sicily channel – Mediterranean Sea): Morphologies and geo-environmental control of their distribution. *Marine and Petroleum Geology* 26, 1831-1848.
- Scarascia, S., Cassinini, R., Lozej, A., Nebulosi, A., 2000. A seismic and gravimetric model of crustal structures across the Sicily Channel Rift Zone: *Bollettino della Società Geologica Italiana*, 119, 213-222.
- Schroeder, I. D., W. J. Sydeman, N. Sarkar, S. A. Thompson, S. J. Bograd, and F. B. Schwing, 2009. Winter preconditioning of seabird phenology in the California Current, Smith, WHF., Sandwell, DT., 1997. Global sea floor topography from satellite altimetry and ship depth soundings. *Science*, 277, 1956-1962.
- Schubel J. R. (1974) - Gas bubbles and the acoustically impenetrable, or turbid, character of some estuarine sediments. In: Kaplan IR (Ed.), *Natural Gases in Marine Sediments*. New York: Plenum Press, 275-298.
- Seilacher, A., 1969. Fault-graded beds interpreted as seismites. *Sedimentology* 13, 155–159.
- Shanmugam, G. 2000. A 50 years of the turbidite paradigm (1950s-1990s); deep-water processes and facies models; a critical perspective. *Mar. Petrol. Geol.*, 17, 285–342.
- Shanmugam, G. 2002. Ten turbidite myths. *Earth-Sci. Rev.*, 58, 311–341.
- Shepard, F.P., 1954. Nomenclature based on sand-silt-clay ratios: *J. Sediment Petrol.*, 24, 151.

- Shipp, C., Nott, J.A., Newlin, J.A. 2004. Physical characteristics and impact of mass transport complexes on deepwater jetted conductors and suction anchor piles. In: Annual Offshore Technology Conference, Houston, Texas.
- Sibuet, M. and Olu, K., 1998. Biogeography, biodiversity and fluid dependence of deep-sea coldseep communities at active and passive margins. *Deep Sea Research Part II: Topical Studies in Oceanography* 45, 517-567.
- Siebert L, Glicken H, Ui T, (1987) Volcanic hazards from Bezymiannyand Bandai-type eruptions. *Bulletin of Volcanology*. 49:435-459.
- Skarke, A., Ruppel, C., Kodis, M., Brothers, D., Lobecker, E., 2014. Widespread methane leakage from the sea floor on the northern US Atlantic margin. *Nature Geosci* 7, 657-661.
- Skempton A.W. & Hutchinson J.N. 1969. Stability of natural slopes. *Proc. 7th Int. Conf. Soil Mech. and Found. Eng.*, Mexico, 4, 291-340.
- Sloan, E.D., 2003. Fundamental principles and applications of natural gas hydrates. *Nature* 426, 353-363.
- Smith, W. H. F. & Sandwell D.T., 1997. Global Sea Floor Topography from Satellite Altimetry and Ship Depth Soundings. *Science*, 277, 1956-1962.
- Solheim, A., Elverhøi, A., 1985. pockmark field in the Central Barents Sea; gas from a petrogenic source? *Polar Research* 3, 11-19.
- Somoza, L., Martínez-Frías, J., Smellie, J.L., Rey, J., Maestro, A., 2004. Evidence for hydrothermal venting and sediment volcanism discharged after recent short-lived volcanic eruptions at Deception Island, Bransfield Strait, Antarctica. *Marine Geology* 203, 119–140. doi:10.1016/S0025-3227(03)00285-8.
- Somoza, L., Medialdea T., León, R., Ercilla, G., Vázquez, J.T., Farran, M., Hernández-Molina, J., González, F.J., Juan, C., Fernández-Puga, M.C., 2012. Structure of mud volcano systems and pockmarks in the region of the Ceuta Contourite Depositional System (Western Alborán Sea). *Marine Geology* 332 (334), 4–26.
- Sorgente R., Drago A.F., Ribotti A., 2003. Seasonal variability in the Central Mediterranean Sea circulation. *Annales Geophysicae*, 21, 299-322.
- Sorgente, R., Drago, A.F., Ribotti, A., 2003. Seasonal variability in the Central Mediterranean Sea circulation. *Ann. Geophys.* 21, 299e322.
- Stegmann, S., Sultan, N., Kopf, A., Apprioual, R. and Pelleau, P., 2011. Hydrogeology and its effect on slope stability along the coastal aquifer of Nice, France. *Marine Geology* 280, 168-181.
- Stow, D.A.V., Kahler, G., Reeder, M., (2002b). Fossil contourites: type example from an Oligocene palaeoslope system, Cyprus. In: Stow, D.A.V., Pudsey, C.J., Howe, J.A., Faugères, J.-C., Viana, A.R. (Eds.), *Deep-water Contourite Systems: Modern Drifts and Ancient Series, Seismic and Sedimentary Characteristics*. Geological Society, London, *Memoir*, 22, pp. 443–455.
- Suess, E., 2010. Marine Cold Seeps, in: Timmis, K.N. (Ed.), *Handbook of Hydrocarbon and Lipid*.

- Sulli A., Agate M., Lo Iacono C., Lo Presti V., Pennino V., Polizzi S. 2013. Submarine Slope Failures along the Northern Sicilian Continental Margin (Southern Tyrrhenian Sea) and Possible Implications for Geo-hazard. *Landslide Science and Practice*, 5, 41-48.3
- Sulli, A., 2000. Structural framework and crustal characteristics of the Sardinia Channel Alpine transect in the central Mediterranean. *Tectonophysics*, 324, 321-336.
- Sulli, A., Agate, M., Iacono, C.L., Lo Presti V., Pennino, V., Polizzi, S., 2013. Submarine slope failures along the northern sicilian continental margin (Southern Tyrrhenian Sea) and possible implications for geo-hazard. In: Margottini C., Canuti P., Sassa K. (Eds.), *Landslide Science and Practice*, 5, Complex Environment, 41-48, Springer-Verlag Berlin, Heidelberg.
- Talukder, A.R., 2012. Review of submarine cold seep plumbing systems: leakage to seepage and venting. *Terra Nova* 24, 255-272.
- Taviani, M., Angeletti, L., Ceregato, A., Fogliini, F., Frogliola, C., Trincardi, F., 2013. The Gela Basin pockmark field in the Strait of Sicily (Mediterranean Sea): Chemosymbiotic faunal and carbonate signatures of postglacial to modern cold seepage. *Biogeosciences* 10, 4653-4671.
- Tejada, M.L.G., Suzuki, K., Kuroda, J., Coccioni, R., Mahoney, J.J., Ohkouchi, N., Sakamoto, T., Tatsumi, Y., 2009. Ontong Java Plateau eruption as a trigger for the early Aptian oceanic anoxic event. *Geology* 37, 855–858. doi:10.1130/G25763A.1
- Thakur, N. K., Rajput, S. (2011) *Exploration of Gas Hydrates, Geophysical Techniques*. :Springer.
- Tonarelli, B., Turgutcan, F., Max, M. D., Akal, T., 1993. Shallow sediment composition at four localities on the Sicilian-Tunisian Platform. *Geological development of the Sicilian-Tunisian Platform, Unesco report in marine science*, (ed. By M.D. Max and Colantoni), 58, (ed. By M.D. Max and P. Colantoni), 123-128.
- Torelli, L., Zitellini, N., Argnani, A., Brancolini, G., De Cillia, C., Peis, D., Tricart, P., 1991. Sezione geologica crostale dall'avampaese pelagiano al bacino di retroarco tirrenico (Mediterraneo centrale). *Memorie Società Geologica Italiana* 47, 385–399.
- Tricart, P., Torelli, L., Argnani, A., Rekhiss, F. & Zitellini, N., 1994. Extensional collapse related to compressional uplift in the Alpine Chain off northern Tunisia (Central Mediterranean). *Tectonophysics*, 238: 317-329.
- Tripanas, E.K., Piper, D.J.W., Jenner, K.A., Bryant, W.R., 2008. Submarine mass-transport facies: new perspectives on flow processes from cores on the eastern North American margin. *Sedimentology* 55, 97–136, doi:10.1111/j.1365-3091.2007.00894.x.
- Urgeles R, Canals M, Baraza J, Alonso B, Masson D G, (1997) The most recent megaslides on the Canary Islands: the El Golfo Debris Avalanche and the Canary Debris Flow, west El Hierro Island. *J. Geophys. Res.* 102:20305-20323.
- Urgeles, R., Canals, M., Baraza, J., Alonso, B. & Masson, D. G. 1997 The most recent megaslides on the Canary islands: the El Golfo Debris avalanche and the Canary Debris flow. *J. Geophys. Res.* 102, 305–323, (doi:10.1029/97JB00649).

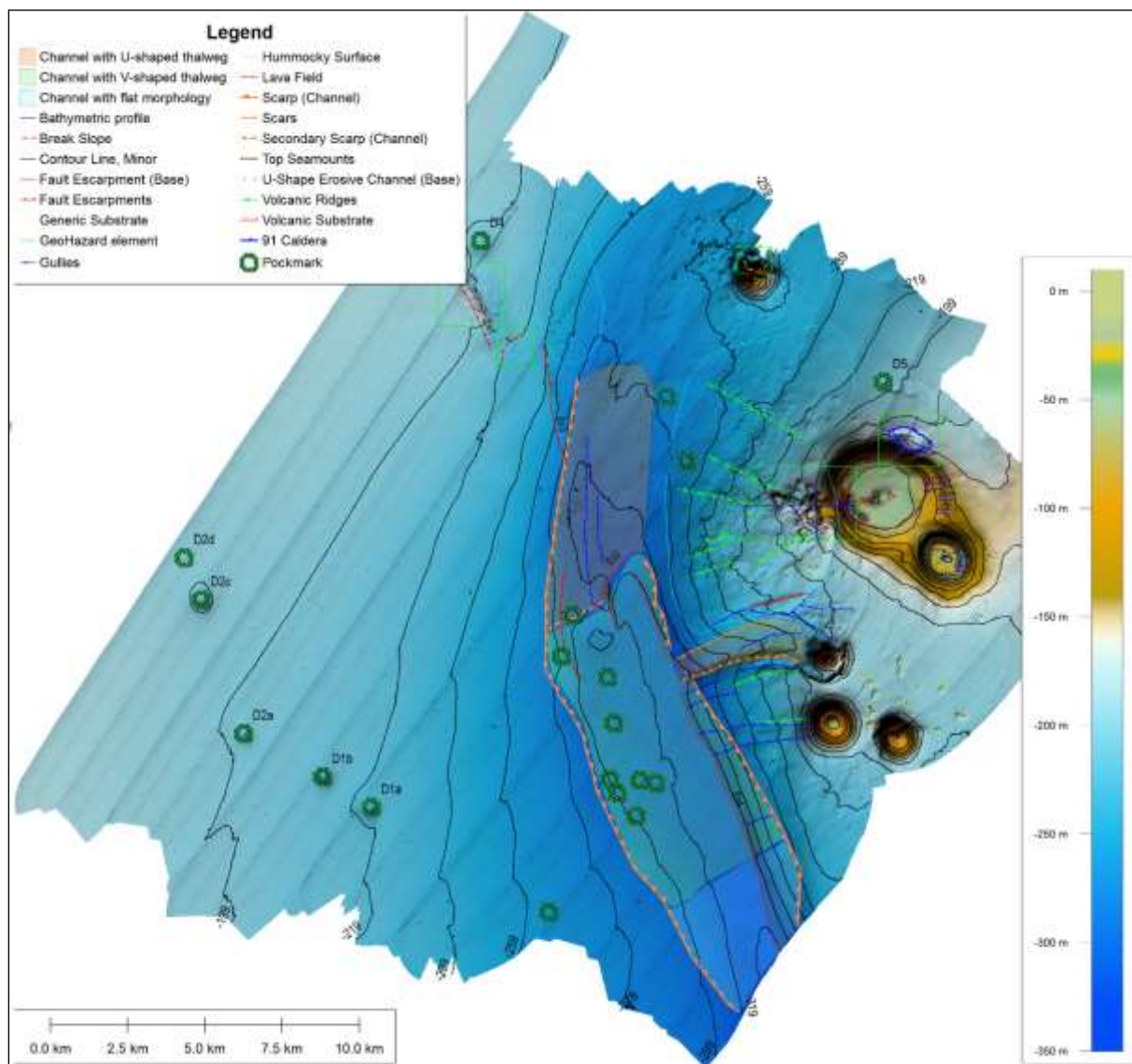
- Van Dover, C.L., Aharon, P., Bernhard, J.M., Caylor, E., Doerries, M., Flickinger, W., Gilhooly, W., Goffredi, S.K., Knick, K.E., Macko, S.A., Rapoport, S., Raulfs, E.C., Ruppel, C., Salerno, J.L., Seitz, R.D., Sen Gupta, B.K., Shank, T., Turnipseed, M. and Vrijenhoek, R., 2003. Blake Ridge methane seeps: characterization of a soft-sediment, chemosynthetically based ecosystem. *Deep Sea Research Part I: Oceanographic Research Papers* 50, 281-300.
- Van Loon, A. J., 2009. Soft-sediment deformation structures in siliciclastic sediments: An overview. *Geologos*, 15, 3-55.
- Varnes D.J. 1958. Landslide types and processes in Eckel E.B., ed., *Landslides and Engineering Practice*, Highway Research Board Special Report 29, NAS-NRC Publication 544, Washington, D.C., 20 - 47.
- Varnes DJ 1978. Slope movement types and processes. In: Schuster RL, Krizek RJ (eds) *Landslides, analysis and control*, special report 176: Transportation research board, National Academy of Sciences, Washington, DC., pp. 11–33
- Villari, L., 1974. The Island of Pantelleria. *Bulletin of Volcanology*, v. 38, 680–724.
- Wagner-Friedrichs, M., Krastel, S., Spiess, V., Ivanov, M., Bohrmann, G. and Meisner, L., 2008. Three-dimensional seismic investigations of the Sevastopol mud volcano in correlation to gas/fluid migration pathways and indications for gas hydrate occurrences in the Sorokin Trough (Black Sea). *Geochemistry, Geophysics, Geosystems* 9, Q05012.
- Ward, S. N., and S. J. Day 2003, Ritter Island Volcano— Lateral collapse and the tsunami of 1888, *Geophys. J. Int.*, 154, 891–902, doi:10.1046/j.1365-246X.2003.02016.x..
- Washington, H.S., 1909. The submarine eruption of 1831 and 1891 near Pantelleria. *Am J Sci* 27, 131–150.
- Wessels M., Bussmann I., Schloemer S., Schlu ¨ter M., Boder V. 2010), Distribution, morphology, and formation of pockmarks in Lake Constance, Germany. *Limnology Oceanography* 55 (6), 2623–2633 doi:10.4319/lo.2010.55.6.2623
- Whiticar M.J. and Werner F. (1981) - Pockmarks: Submarine vents of natural gas or freshwater seeps *Geo-Marine Letters*, 1, 193-199.
- Wood, W. and C. Ruppel, 2000, Seismic and thermal investigations of hydrate bearing sediments on the Blake Ridge Crest: A synthesis of ODP Leg 164 results, *Proc. Ocean Drilling Program, Final Reports*, 164, 253-264.
- Wright, I.C., Worthington, T.J., Gamble, J.A., 2006. Newmultibeammapping and geochemistry of the 30°–35°S sector, and overview, of southern Kermadec arc volcanism. *J. Volcanol. Geotherm. Res.* 149, 263–296.
- Zibrowius, H., Taviani, M., 2005. Remarkable sessile fauna associated with deep coral and other calcareous substrates in the Strait of Sicily, Mediterranean Sea, in: Freiwald, A., Roberts, J.M. (Eds.), *Cold-Water Corals and Ecosystems*. Springer-Verlag Berlin Heidelberg, pp. 807–819. doi:10.1007/3-540-27673-4_42.

ATTACHMENT 1



Attachment 1 Aspect and Slope maps of the Graham Bank sector

ATTACHMENT 2



Attachment 1 Geomorphological map of the Graham Bank sector showing the main morphologies.